Understanding the mechanisms regulating SCFA mediated release of anorectic gut hormones

A thesis submitted to Imperial College London for the degree of Doctor of Philosophy

Natarin Caengprasath

Section of Investigative Medicine
Division of Diabetes, Endocrinology and Metabolism

Imperial College London

January 2019

Table of Contents

STATEMENT OF ORIGINALITY **5**

ABSTRACT **6**

DECLARATION OF CONTRIBUTORS: **7**

ACKNOWLEDGMENTS **8**

LIST OF FIGURES **10**

LIST OF TABLES **11**

LIST OF ABBREVIATIONS **12**

CHAPTER 1: INTRODUCTION **18**

1.1 OBESITY 19
1.1.1 Epidemic 19
1.1.2 Current treatment options 19
1.2 APPETITE 21
1.2.1 Regulation of appetite 22
1.2.2 Central regulation of appetite 22
1.2.3 Peripheral regulation of appetite: Satiety hormones 24
1.2.4 Peripheral obesity targets 30
1.2.5 Gut hormone secretion by enteroendocrine cells 32
1.3 SHORT CHAIN FATTY ACIDS 35
1.3.1 The production of SCFAs by gut microbiota 35
1.3.2 SCFA absorption and metabolism 36
1.4 G PROTEIN COUPLED RECEPTORS 37
1.4.1 Structure and classification 37
1.4.2 Activation 39
1.4.3 Signalling pathways 42
1.4.4 Regulation of GPCR signalling 43
1.4.5 Multiplicity in GPCR signalling and activity 54
1.4.6 Endosomal trafficking and intracellular signalling 62
1.5 APPL1 67
1.5.1 The endosomal pathway 67
1.5.2 APPL1 structure and its interacting proteins 68
1.5.3 APPL1 in trafficking 70
1.5.4 APPL1 in signalling 71
1.5.5 Therapeutic implications of APPL1 73
1.6 FFA2/3 74
1.6.1 Relevance of SCFAs as signalling molecules 74
1.6.2 Identification of SCFAs receptors 74
1.6.3 SCFA receptors: FFA2 and FFA3 76
1.7 SUMMARY AND GENERAL AIMS 83

CHAPTER 2: MATERIALS AND METHODS **85**

2.1 MATERIALS 86
2.1.1 Primary antibodies 86
2.1.2 Secondary antibodies 86
2.1.3 Plasmids 87
2.1.4 Primers and siRNAs 88

2.1.5 Inhibitors and activators 88
2.1.6 Chemical reagents 89
2.1.7 Kits 91
2.1.8 Cell culture reagents 91
2.1.9 Miscellaneous 92
2.1.10 Buffers and solutions 93
2.2 Molecular Biology methods 95
2.2.1 Preparation of chemically competent cells 95
2.2.2 Transformation of bacteria by heat shock and purification of plasmid DNA 95
2.2.3 Cloning 96
2.2.4 Quantitative Real-Time PCR (q-RT-PCR) 99
2.3 Intestinal Organoids 101
2.3.1 Intestinal crypts 101
2.3.2 Intestinal colonic and ileum organoid culture 102
2.4 Cell culture 104
2.4.1 Transfections of plasmids DNA or siRNA 105
2.4.2 Generation of FLAG-FFA2 and SEP-FFA2 stable HEK 293 106
2.5 Western Blot Analysis 106
2.5.1 Protein extraction 106
2.5.2 Protein concentration 107
2.5.3 SDS polyacrylamide gel electrophoresis 107
2.5.4 Protein transfer to nitrocellulose membranes 107
2.5.5 Stripping membranes 108
2.6 Cell signalling assays 108
2.6.1 Ligand preparation 108
2.6.2 Calcium mobilisation 109
2.6.3 cAMP accumulation 109
2.6.4 IP1 accumulation 110
2.6.5 MAPK 111
2.7 Measurement of GLP-1 and PYY secretion using a radioimmunoassay 111
2.7.1 GLP-1 and PYY secretion 111
2.7.2 Radioimmunoassay (RIA) 112
2.8 Phosphokinase array 113
2.9 Microscopy 114
2.9.1 Fixed sample preparation 114
2.9.2 Confocal microscopy 115
2.9.2.1 Quantification of co-localisation 115
2.9.3 Total Internal Reflection-Fluorescence Microscopy (TIR-FM) 115
2.9.3.1 Quantitation single vesicle recycling events from TIRF movies 116
2.10 Flow cytometry 116
2.11 Statistical analysis 116

CHAPTER 3: INVESTIGATING FFA2 SIGNALLING PROFILES IN ENTEROENDOCRINE CELLS AND COLONIC ORGANOIDS 117

3.1 Introduction 118
3.2 Results 119
3.2.1 Expression of FFA2 mRNA in enteroendocrine L cells 119
3.2.2 SCFAs activates $G\alpha_{i/o}$ signalling in enteroendocrine cells 121
3.2.3 SCFA inhibits forskolin stimulated cAMP in HEK 293 transiently expressing FLAG FFA2 123
3.2.4 SCFAs activate $G\alpha_{i/o}$ signalling in mouse colonic crypts and organoids 124

3.2.5 SCFAs are unable to mediate $G\alpha_{q/11}$ signalling in enteroendocrine cells....127
3.2.6 SCFAs are unable to mediate $G\alpha_{q/11}$ despite absence of FFA3....130
3.2.7 SCFAs are able to activate $G\alpha_{q/11}$ signalling in HEK 293 cells expressing FFA2....136
3.3 DISCUSSION....138

CHAPTER 4: FFA2 INTERNALISATION IS CRITICAL FOR FFA2 MEDIATED SIGNALLING....143

4.1 INTRODUCTION....144
4.2 RESULTS....146
4.2.1 FFA2 is localised at the plasma membrane and at intracellular compartments....146
4.2.2 FFA2 ligand induced internalisation is β-arrestin dependent....149
4.2.3 Constitutive and ligand-induced internalisation of FFA2 is dynamin-dependent....152
4.2.4 Differential requirement of FFA2 internalisation for FFA2 mediated signalling....156
4.2.5 The C-terminal tail of FFA2 is essential for optimal cell surface expression....161
4.2.6 FFA2 is sorted to the recycling pathway....163
4.2.7 Distinct modes of SEP-FFA2 recycling....168
4.3 DISCUSSION....170

CHAPTER 5: INVOLVEMENT OF THE VEE IN FFA2 TRAFFICKING AND SIGNALLING....177

5.1 INTRODUCTION....178
5.2 RESULTS....180
5.2.1 FFA2 internalises into small, VEE-like endosomes....180
5.2.2 FFA2 co-localises with endosomes positive for APPL1....182
5.2.3 APPL1 is essential for FFA2 recycling via the VEE....186
5.2.4 APPL1 knockdown may re-route FFA2 to the EE....188
5.2.5 FFA2 recycling is not driven by the PKA phosphorylation of APPL1 on S410....190
5.2.6 APPL1 negatively regulates cAMP signalling of VEE-targeted FFA2....192
5.2.7 FFA2 co-localises with $G\alpha_i$ in the VEEs....194
5.3 DISCUSSION....195

CHAPTER 6: ENDOSOMAL SIGNALLING REGULATES PROPIONATE-MEDIATED GUT HORMONE RELEASE IN ENTEROENDOCRINE CELLS....200

6.1 INTRODUCTION....201
6.2 RESULTS....202
6.2.1 Propionate induced GLP-1 release is mediated via $G\alpha_i$ but not $G\alpha_{q/11}$....202
6.2.2 Propionate induced GLP-1 release is dynamin dependent....205
6.2.3 Does APPL1 regulate propionate-induced GLP-1 secretion?....207
6.2.3 A phospho-kinase array reveals propionate induced p38 activation may require receptor internalisation....207
6.2.4 p38 does not regulate FFA2 recycling....213
6.2.5 p38 may regulate propionate-induced GLP-1 release....215
6.3 DISCUSSION....216

CHAPTER 7: GENERAL DISCUSSION AND FUTURE PERSPECTIVES....223

REFERENCES....234

Statement of originality

The copyright of this thesis rests with the author and is made available under a Creative Commons Attribution Non-Commercial No Derivatives licence. Researchers are free to copy, distribute or transmit the thesis on the condition that they attribute it, do not use it for commercial purposes and do not alter, transform or build upon it. For any reuse or redistribution, researchers must make clear to others the licence terms of this work.

Abstract

Obesity is a fast-growing epidemic that poses a major challenge to the public health. There is a current lack of safe and effective anti-obesity treatment options, therefore an improved treatment option is critical. Short chain fatty acids (SCFAs), produced in the colon via fermentation of non-digestible carbohydrates by gut microbiota, activates FFA2 and FFA3, G-protein coupled receptors (GPCRs) that stimulate the release of anorectic gut hormones GLP-1 and PYY. However, the underlying molecular mechanisms stimulating their release are poorly understood. A fundamental mechanism controlling the signalling capacity of GPCRs is via receptor trafficking to diverse cellular compartments such as early endosomes (EE), or very early endosomes (VEE). A subpopulation of VEEs contains the adaptor protein APPL1, essential for driving receptor recycling from the VEE and regulating endosomal G protein signalling. I therefore characterised the signalling pathways exerted by SCFAs in intestinal enteroendocrine cells and colonic organoids and elucidated the trafficking properties of FFA2 that regulate anorectic gut hormone release. In enteroendocrine cells, SCFAs are unable to elicit $G\alpha_{q/11}$-signalling but robustly activates $G\alpha_{i/o}$ signalling which is important for propionate induced GLP-1 secretion. FFA2 undergoes both constitutive and ligand induced internalisation. Following ligand-induced internalisation, FFA2 traffics to the VEE to activate $G\alpha_{i}$ endosomal signalling that is regulated by APPL1. In addition, by employing high resolution single vesicle imaging, I unveiled propionate-induced FFA2 recycling is APPL1 dependent. I also examined the dependence of receptor internalisation and found that receptor internalisation is critical only for propionate induced- $G\alpha_{i/o}$ signalling, p38 activation and GLP-1 release, while $G\alpha_{q/11}$ signalling occurs from the plasma membrane. Together these findings suggest an important spatial requirement for propionate-mediated activity and uncovers novel mechanisms regulating the release of anorectic gut hormone, GLP-1.

Declaration of contributors:

The work presented in this thesis was performed by the author. All collaboration and assistance are declared below.

Chapter 3:

Culturing of intestinal organoids were carried out by Dr Noemi Gonzalez Abuin

Chapter 6:

Radioimmunoassay were performed under supervision of Professor Kevin Murphy.

Acknowledgments

First and foremost, I would like to express my sincere gratitude to my supervisors, Professor Gary Frost, Dr. Aylin Hanyaloglu and Professor Ed Tate, for their guidance and continuous support throughout my PhD. Not only have they helped me develop my cell biology and academic skill set, they have also been a great source of encouragement and motivation. I am incredibly grateful for the time they have invested in me and I feel extremely lucky to have had the opportunity to work under the guidance of the people whom I greatly respect.

I would like to thank Noemi Gonzalez-Abuin who has been there for me every step of the way, especially when I first started my PhD. Thank you for teaching me the ropes of growing intestinal organoids and lending me your ear when science just wasn't agreeing with me. I would definitely miss the long hours we spent together in primary discussing about science, what's going in the world or just life in general.

I am extremely grateful to Paul Bech in helping me with the GLP-1 RIAs. For his expertise and most importantly for his patience even after having to explain things to me multiple times.

My thanks go out to all past and current members of the AH lab, for being such lovely people and making my time here so enjoyable. For all the times they took out of their day to help and guide me, special thanks go out to Silvia Sposini, Camila West, Layi Oduwole, Lisa Owens Abbigail Walker, Niamh Sayers and Anthony Okolo. Thank you for supplying constant support, entertainment, laughs, cakes, support, trips to the pub and most importantly friendship. Thank you to all the members of the 2nd floor lab as well, for all the fun times we had. It has been a great pleasure to share a lab with such amazing people. I would also like to thank Pushpa and Simon, for their excellent support in the lab that made my experiments go smoothly.

Finally, I'd like to thank my loving family for their unconditional love and unwavering support. My parents, who taught me the value of an education and how to work hard. My sister, who

is always busy with work but never forgets to order me delicious takeaway. Without them, I wouldn’t have been able to achieve what I have today.

List of figures

Figure 1.1 Schematic diagram of appetite regulated by peripheral and central sites. 24
Figure 1.2 Enteroendocrine gut hormone secretion by glucose and nutrients sensing. 34
Figure 1.3 Schematic representation and crystal structures of GPCRs. 38
Figure 1.4 Activation of heterotrimeric G protein by a GCPR. 41
Figure 1.5 Signalling pathways induced by GPCR activation. 43
Figure 1.6 Regulation of GPCR trafficking. 54
Figure 1.7 Dimerisation of GPCRs. 59
Figure 1.8. Schematic representation of APPL1 domains and interacting domains. 70
Figure 1.9 FFA2/3 signalling 79
Figure 2.1 Intestinal organoids culture 103
Figure 3.1 FFA2/3 expression in STC-1 cells, colonic crypts and organoids. 120
Figure 3.2 Localisation of GLP-1 and PYY in mouse colonic-crypts and intestinal organoids. 120
Figure 3.3 SCFA inhibits forskolin induced cAMP in a Gαi/o manner. 122
Figure 3.4 SCFAs inhibits forskolin induced cAMP via FFA2. 124
Figure 3.5 SCFAs inhibit forskolin induced cAMP in a $G\alpha_i$ manner via FFA2 in mouse colonic-crypts and organoids 126
Figure 3.5 SCFAs are unable to induce intracellular calcium mobilisation. 129
Figure 3.6 SCFAs are unable to elicit Gαq/11 signalling in STC-1 cells that are depleted of FFA3. 132
Figure 3.7 SCFAs are unable to induce intracellular calcium in the colon. 136
Figure 3.8 FFA2 induced intracellular calcium mobilisation occurs may be partially regulated by and $G\alpha_{q/11}$. 137
Figure 4.1 Surface and intracellular localisation of FFA2. 149
Figure 4.2 FFA2 ligand induced internalisation is β-arrestin dependent. 152
Figure 4.3 Dynamin inhibition blocks constitutive and ligand induced internalisation of FFA2. 156
Figure 4.4 Intracellular levels of cAMP pre-treated either with DMSO or Dyngo-4a 158
Figure 4.5 FFA2 internalisation is required for $G\alpha_i$ mediated cAMP but not $G\alpha_{q/11}$. 161
Figure 4.6 The C-terminus of FFA2 is important for its cell surface expression. 163
Figure 4.7 Visualisation of SEP-FFA2 165
Figure 4.8 SEP-FFA2 induces SCFA-mediated inhibition of forskolin induced cAMP in a similar manner as FLAG-FFA2. 166
Figure 4.9 FFA2 undergoes ligand-induced trafficking to the recycling pathway. 167
Figure 4.10 FFA2 delivered to the plasma member are not newly synthesized receptors but are recycled ones. 168
Figure 4.11 Characterisation of SEP-FFA2 recycling modes. 170
Figure 5.1 FFA2 and β2AR are sorted to distinct endosomes 181
Figure 5.2 FFA2 co-localises poorly with EEA1. 183
Figure 5.3 FFA2 co-localises with APPL1. 185
Figure 5.4. APPL1 is required for FFA2 recycling from the VEE. 187
Figure 5.5 APPL1 depletion re-routes FFA2 to EEs. 189
Figure 5.6 FFA2-APPL1 recycling is not regulated by PKA phosphorylation of S410. 191

Figure 5.7. APPL1 negatively regulates propionate induced inhibition of forskolin induced cAMP. 193
Figure 5.8 FFA2 activates Gαi from the VEEs. 195
Figure 6.1 Propionate stimulates GLP-1 release from STC-1 cells....202
Figure 6.2 Propionate induced GLP-1 is dependent on Gαi and not Gαq/11. 204
Figure 6.4 Propionate induced GLP-1 requires receptor internalisation. (....206
Figure 6.5 Effect of APPL1 depletion on propionate-induced GLP-1....207
Figure 6.6 legend overleaf 210
Figure 6.6. Phospho-kinase array data reveals kinases that may require propionate induced internalisation in enteroendocrine cells. 211
Figure 6.8 Propionate activates p38. 213
Figure 6.9 FFA2 recycling is not regulated by the phosphorylation of p38. 214
Figure 6.10 Propionate induced GLP-1 is partially regulated by p38 215
Figure 7.1 Proposed model for APPL1-dependent regulation of FFA2 endosomal signalling and the release of anorectic gut hormones in enteroendocrine cells. 233

List of Tables

Table 1.1. Components of complete medium for intestinal organoid culture....103
Table 3.1. pEC50 values SCFA mediated inhibition of forskolin induced cAMP. 123

List of abbreviations

β-ARR	β-Arrestin
β1AR	β1 adrenergic receptor
β2AR	β2 adrenergic receptor
%	Percentage
°C	Degree Celsius
5-HT2c	Serotonin 2c-receptor
a.u	Arbitrary unit
AC	Adenylyl cyclase
AD	Alzheimer's disease
AdipoR	Adiponectin receptor
AgRP	Agouti-related peptide
ALIX	ALG-interacting protein X
AMPK	5' adenosine monophosphate-activated protein kinase
AP	Adaptor protein
APEX	*Ascorbic* acid peroxidase
APPL1	Adaptor protein containing PH domain, PTB domain and Leucine zipper motif
ARC	Arcuate nucleus
BAR	Bin-N-terminal Bin–Amphiphysin–Rvs
BBB	Blood brain barrier
bp	Base pairs
BRET	Bioluminescence resonance energy transfer
BSA	Bovine serum albumin
Ca^{2+}	Calcium ions
cAMP	Cyclic adenosine monophosphate
CART	Cocaine-and amphetamine-related transcript
CaSR	Calcium sensing receptor
CB1	Cannabinoid receptor
CCK	Cholecystokinin
CCK-1R	Cholecystokinin receptor 1

CCPs	Clathrin coated pits
CDE	Clathrin dependent endocytosis
CIE	Clathrin independent endocytosis
CXCR4	Chemokine receptor 4
D2R	Dopamine D2 receptor
DAF	Diacylglycerol
DOR	δ-opioid receptor
DPPIV	Dipeptidyl peptidase IV
DS	Down syndrome
DTT	Dithiothreitol
ECL	Extracellular loop
EE	Early endosome
EEA1	Early endosome antigen 1
EECs	Enteroendocrine cells
eGFP	Enhanced green fluorescent protein
EGFR	Epidermal growth factor receptor
ER	Endoplasm reticulum
ERK	Extracellular-signal-regulated kinase
ESCRT	Endosomal sorting complex required for transport
FACS	Fluorescence-activated cell sorting
FEME	Fast endophilin mediated endocytosis
FFA	Free fatty acid
FFA1	Free fatty acid receptor 1
FFA2	Free fatty acid receptor 2
FFA3	Free fatty acid receptor 3
FFA4	Free fatty acid receptor 4
FPR1	N-formyl peptide receptor 1
FSHR	Follicle stimulating hormone receptor
FSK	Forskolin
g	Gravity force

GAPDH	Glyceraldehyde-3 phosphate dehydrogenase
GASP-1	GPCR associated sorting protein-1
GCGR	Glucagon receptor
GDI	Guanine nucleotide dissociation inhibitor
GDP	Guanosine diphosphate
GEF	Guanine nucleotide exchange factor
GFP	Green fluorescent protein
GHS-R	Growth hormone secretagogue receptor
GI	Gastrointestinal
GIPC	$G\alpha_i$-interacting protein C terminus
GLP-1	Glucagon-like Peptide 1
GLP-1R	Glucagon-like Peptide 1 receptor
GLUT2	Glucose transporter 2
GOAT	Ghelin-Oacyl transferase
GPCR	G protein-coupled receptor
GPR6A	G protein-coupled receptor family C group 6 subtype A
GRK	G protein-coupled receptor kinase
GTP	Guanosine triphosphate
HCO_3-	Bicarbonate
Hrs	Hepatocyte growth factor regulated tyrosine kinase substrate
IBS	Irritable bowel syndrome
ICL	Intracellular loop
ILVs	Intraluminal vesicles
IP3	Inositol-14,5- trisphosphate
IR	Insulin receptor
Iso	Isoproterenol
KO	Knockout
L	Litre
LCFA	Long chain fatty acid
Lep R	Leptin receptor

LHA	Lateral hypothalamic area
LHR	Luteinizing hormone receptor
LPA1	Lysophosphatidic acid receptor 1
MAPK	Mitogen-activated protein kinase
MCFA	Medium chain fatty acid
MCH	Melanin-concentration hormone
MCT1	Monocarboxylate transporter
mGluR5	Metabotropic glutamate receptor 5
MOR	Mu-opioid receptors
MT_1	Melatonin type 1 receptor
MVBs	Multivesicular bodies
NaCl	Sodium chloride
NAM	Negative allosteric modulator
Nb	Nanobody
NDC	Non-digestible carbohydrates
NK1R	Neurokinin-1 receptor
NPY	Neuropeptide Y
NTS	Nucleuses of the solitary tract
OEA	Oleoylethanolamide
OXM	Oxyntomodulin
PAM	Positive allosteric modulator
PAR-1	Protease-activated receptor-1
PAR-2	Protease-activated receptor-2
PDZ	Postsynaptic 95/disc large/zonula occuldents-1
PH	Pleckstrin homology
PIP_2	Phosphatidylinositol-4,5-bisphosphate
PIs	Phosphoinositides
PKA	Protein kinase A
PKC	Protein kinase C
PLC	Phospholipase C

POMC	Pro-opiomelanocortin
PTB	Phospho-tyrosine binding
PTH	Parathyroid hormone
PTHR	Parathyroid hormone receptor
PTMs	Post-translational modifications
Ptx	Pertussis toxin
PVN	Paraventricular nucleus
PYY	Peptide tyrosine tyrosine
qPCR	Quantitate polymerase chain reaction
RGS	Regulators of G-proteins signalling
RYGB	Roux-en-Y bypass
S1P1	Sphingosine-1-phosphater receptor
SAM	Silent allosteric modulator
SCFA	Short chain fatty acid
SDS	Sodium dodecyl sulphate
SDS-PAGE	SDS- polyacrylamide gel electrophoresis
SEM	Standard error mean
SEP	Superecliptic phluorin
SGLT1	Sodium/glucose co-transporter 1
siRNA	Small interfering RNA
SMCT1	Sodium-dependent monocarboxylate transporter 1
SNAC	Sodium N-[8-(2-hydroxybenzoyl) amino] caprylate
SNX	Sorting nexin
SNX27	Sorting nexin 27
TCA	Tricarboxylic acid
TGN	Trans Golgi network
TIR-FM	Total internal reflected-fluorescence microscopy
TM	Transmembrane
TSHR	Thyroid-stimulating hormone receptor
v/v	Volume/volume

V_2R	Vasopressin type 2 receptor
VEE	Very early endosome
w/v	Weight/volume
WT	Wild type
Y2	Y receptor type 2
YFP	Yellow fluorescent protein
µ	Micro
µM	Micromolar
µm	Micron

Chapter 1:

Introduction

1.1 Obesity

1.1.1 Epidemic

Obesity is a condition characterised by abnormal or excessive fat accumulation that reduces health and longevity, resulting mainly from an energy imbalance between calorie intake and energy expenditure (Nguyen and El-Serag, 2010). With 29% of the world's population obese, obesity is being acknowledge as one of the biggest and rapidly growing public health issues in the developed and developing world (World Health Organisation, 2018). According to the World Health Organisation, globally, there were approximately 650 million people obese in 2010 and the number is expected to reach 4 billion by 2030 (World Health Organisation, 2018; Finucane et al., 2011). Despite signs of stabilisation in some populations, no country has had success in decreasing the proportion of the population that is obese. In 2016 there were ~ 27% of UK adults classified as obese and this number may increase to more than 50% by 2050 (Organisation for Economic Co-operation and Development, 2017). Due to the dysregulation of metabolic and cardiovascular functions that are the consequences of increase adiposity, obesity is an independent risk factor for other diseases including type II diabetes, cardiovascular disease and certain forms of cancer. As a result of obesity-associated illness, an obese person requires more prescription medications and therefore, places a substantial burden on health care resources. For example, in the UK, it has been reported that the estimated direct economic cost of obesity is £5.1 billion each year or 9% of total health care expenditures of the National Health System, a figure projected to double by 2050 (Kopelman, 2007). These trends outline the vital need for research aimed at preventing and treating obesity and its associated comorbidities.

1.1.2 Current treatment options

Current strategies available for the treatment of obesity include intervention of lifestyle changes, pharmacological intervention and bariatric surgery. Among these, bariatric surgical procedures such Roux-en-Y bypass (RYGB) or gastric banding is currently the most effective anti-obesity treatment that results in sustained weight loss, and will double by 2035 (Keaver

et al., 2018). For the remaining of the overweight population, the only options available are thus lifestyle and/or pharmalogical interventions.

Lifestyle changes forms the basis of all weight-loss programmes, however, majority of studies in behavioural treatment have revealed that weight loss from lifestyle changes alone is restricted to only 3-10% of bodyweight, and most people regain at least a certain amount weight after a year (MacLean et al., 2015). The failure of life style changes to sustain weight loss is mainly due to biological changes that increase the chances of weight regain. These changes include, reduction in energy expenditure (Galgani and Ravussin, 2008) changes in hunger and satiety leading an increase in food intake (Polidori et al., 2016), changes to insulin sensitivity and adipocyte levels that increase fat storage. Long-term studies proposed that changes are most likely permanent as the body tends to gain weight gradually over time (Polidori et al., 2016; Sumithran et al., 2011). In fact, the longer a person remains at reduced weight, the further their body is from a persevered weight, resulting to a more rapid weight regain. In addition, to biological changes, failure of compliance is another significant reason of failure of lifestyle changes to produce long-lasting weight loss. Thus, a growing body of evidence from clinical trials have suggested that anti-obesity pharmalogical interventions should be prescribed in combination with recommended life style changes. The UK National Institute for Health and Care Excellence guidelines has suggested that only after dietary, exercise, and behavioural approaches have been started and evaluated, and a target weight loss has not been reached or a plateau has been reached" (Stegenga et al., 2014). Despite this suggestion, the prescription of anti-obesity drugs still remains strikingly low, however this may be due to the limited efficacy of the currently available drugs, leading to low successful treatment rates (Dansinger et al., 2005).

The only pharmalogical treatment for obesity currently licensed in the UK is Orlistat (Xenical® and Alli®). Orlistat is a gastric and lipase inhibitor that acts centrally within the gastrointestinal (GI) tract to reduce fat absorption from the gut by ~30% (Borgstrom, 1988). As Orlistat does exert its effect systemically, no adverse side-effects are associated with it, although flatulence, bloating, abdominal pain, diarrhoea and dyspepsia are common (Bray and Greenway, 2007). Overall weight reduction with Orlistat is modest (~3kg at 12 months),

though it has been reported that it is able to sufficiently reduce blood pressure and glycaemia, low-density-lipoprotein (LDL) cholesterol, and therefore reduces cardiovascular risks (Broom et al., 2002; Torgerson et al., 2004).

Recently, two new pharmacological treatments have been approved in the United States, Qsymia® and Lorcaserin (Belviq®). Both of which, however, have limitations. Qsymia, originally approved to treat patients with seizures and prevent migraines, is a combination of the anticonvulsant Topiramate, a weak carbonic anhydrase inhibitor, and the appetite suppressant Phentermine, an amphetamine derivative. Weight loss for patients treated with Qsymia reported by the SEQUEL study is up to 7% weight loss compared to placebo over 108 weeks of treatment in combination with lifestyle modification (Garvey et al., 2012). The various adverse effects of Qsymia, however has burdened its development. The main concern was the risk of oral clefts in infants that were exposed to Qsymia in utero. Women of child bearing age, patients with glaucoma, patients with thyroid problems and patients taking monamine oxidase were therefore not permitted to be prescribe Qsymia. Lorcaserin is a centrally-acting selective serotonin 2c (5-HT2c) receptor agonist. Lorcaserin efficacy in weight loss was lower than Qysmia, with only 3% weight loss (Smith et al., 2010). However, it was recently demonstrated that Lorcaserin in combination with Phentermine in a 12-week clinical trial, patients administered this combination achieved a 7.2% weight loss (Smith et al., 2017), making this drug combination superior than any other drug alone. Though the long-term side effects of this combination have yet to be reported. Neither of these drugs have been approved for use in Europe. It is thus unlikely that either will be able to act as saviour for the obesity epidemic and therefore novel treatment strategies are required. One approach may be to take advantage of the endogenous systems that regulate energy homeostasis.

1.2 Appetite

Food intake is driven by the sensation of hunger or the “physiological drive to eat” (Whitney and Rolfes, 1996). During food intake, hunger subsides until satiation, the process that leads to termination of eating. Post food intake, satiety, the feeling of repletion, results to the increase in fullness and decline in hunger (Blundell et al., 2010). Appetite, the “psychological

desire to eat or an interest in food", is the result of these feelings and other externals cues consisting of food palatability, memory and psychological aspects, to name a few (Erlanson-Albertsson, 2005). Physiologically, food intake is a highly complex and tightly regulated process. Accumulating evidence in the past decade has highlighted the importance of the peripheral and central regulation of food intake in order to maintain energy homeostasis (Murphy and Bloom, 2006) and food palatability as well as the reward pathways stimulated by the consumption of high-fat, high-sugar goods are part of a hedonic food behaviour which ultimately leads to excessive energy intake over expenditure, and over time, obesity (Hopkins et al., 2016).

1.2.1 Regulation of appetite

The regulation appetite is a complex interplay that exist between the central nervous system (CNS) and the activity of numerous peripheral organs involved in energy homeostasis (Figure 1.1). Energy homeostasis are interconnected processes that are incorporated by the brain to maintain energy stores at appropriate levels in a given environmental conditions. These processes involve the regulation of nutrient levels in key storage organs such as glycogen in the liver, fat storage levels in adipose tissue, as well as the blood glucose levels. In order to achieve this, the brain receives continuous signals of energy stores and fluxes from critical organs, food that is consumed and absorbed, and basal and certain energy needs of tissues. Signals are then relayed to the brain to regulate tissues involved in energy homeostasis such as the liver, skeletal muscle and the secretion of metabolically active hormones, primarily through the autonomic nervous system (Gardiner et al., 2008).

1.2.2 Central regulation of appetite

Upon food intake, digested nutrients trigger the secretion of several gastrointestinal hormones which activates tension gastric mechanoreceptors located along the wall of the proximal stomach and chemoreceptors and luminal mechanoreceptors from the small intestine. Stimulation of these receptors and the release gastrointestinal hormones activates vagal afferent nerves, which transmit signals to the brain, specifically to the brainstem (Date

et al., 2002), (Abbott et al., 2005). These signals then activate neurons within neurons of the nucleuses of the solitary tract (NTS) and the NTS, in turn, relays information to the hypothalamus where it activates the arcuate nucleus (ARC) (Faipoux et al., 2008; Gil et al., 2011). The ARC is a key hypothalamic area involved in the regulation of appetite and comprises of two interconnected groups of "first-order" neurons synthesising neuropeptide-Y (NPY)- and agouti-related peptide (AgRP), which enhances food intake, and the anorexigenics substances pro-opiomelanocortin (POMC)- and cocaine-and amphetamine-related transcript (CART). These neurons project on to 'second-order' neurons, located in part of the paraventricular nucleus (PVN), where anorexigenic substances such as oxytocin are secreted and in part of the lateral hypothalamic area (LHA) where orexigenic molecules such as melanin-concentration hormone (MCH) are released (Valassi et al., 2008). When adiposity signals such as leptin and insulin circulate the blood and enter the ARC via blood brain barrier (BBB), anorexigenic hormones are released and activate a catabolic circuit. Conversely orexigenic hormones activate the anabolic pathway and occurs when adiposity signal levels are low in the brain, thus indicating to replenish fuel stores (Valassi et al., 2008). Together these neurotransmitters act to regulate appetite and require a delicate balance between two neuronal populations.

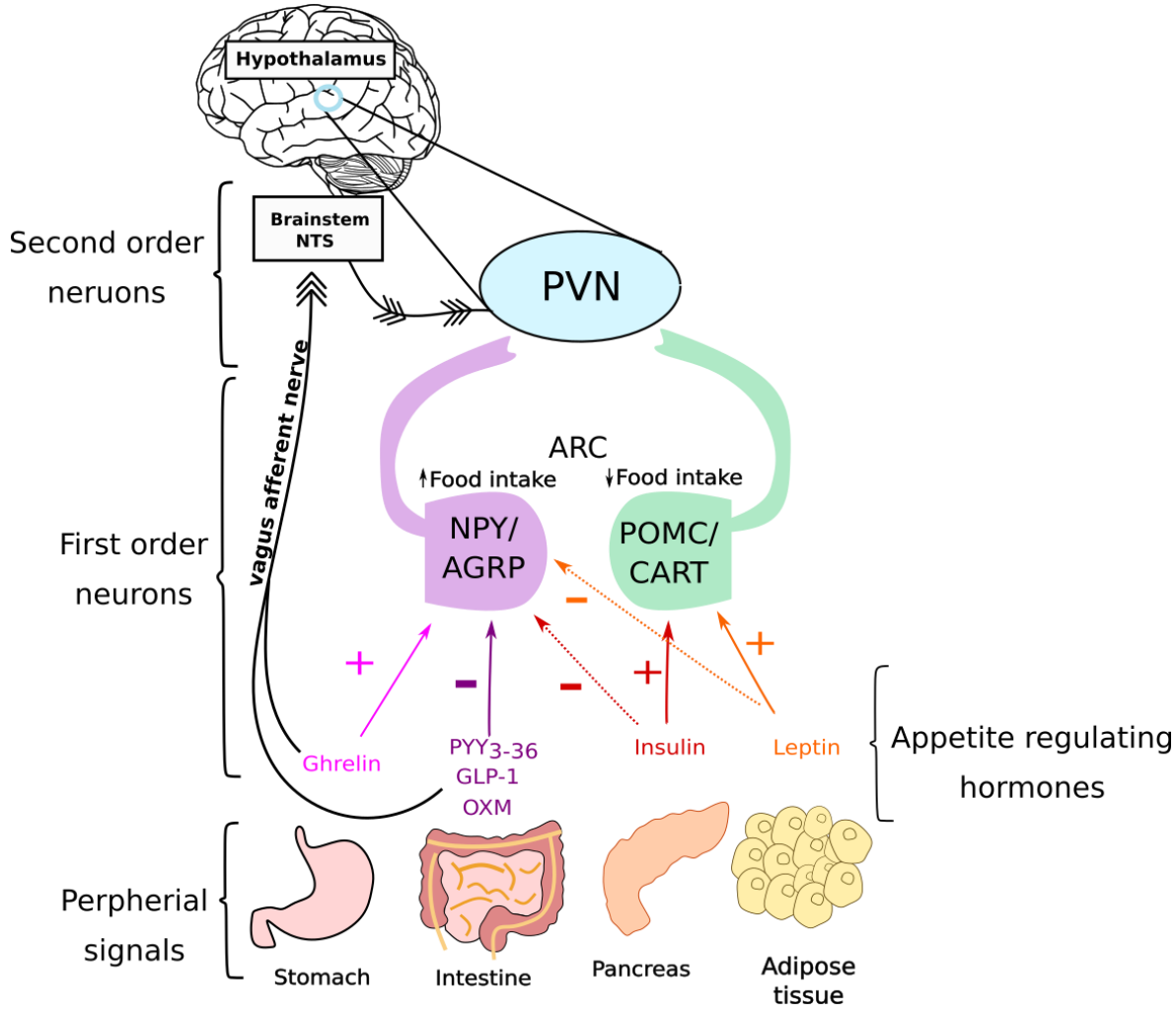


Figure 1.1 Schematic diagram of appetite regulated by peripheral and central sites. Appetite regulating hormones secreted from the stomach (ghrelin), intestine (GLP-1, PYY3-36, OXM), pancreas (insulin) and adipose tissue (leptin). These hormones regulate food intake via three sites: the vagus nerve, brainstem and hypothalamus. Within the hypothalamic arcuate nucleus (ARC) are two critical neuronal populations that integrate appetite regulating hormone energy homeostasis signals to the paraventricular nucleus (PVN), the neuropeptide Y/agouti-related protein (NPY/AGRP) and proopiomelanocortin/cocaine-and amphetamine-regulated transcript (CART)-producing neurons. Further connections between the hypothalamic nucleus tractus solitarius (NTS) and higher brain centres can also impact food intake regulation. GLP-1, glucagon-like peptide-1; PYY3-36, Peptide YY3-36. + indicate orexigenic signals and – indicate anorectic signals.

1.2.3 Peripheral regulation of appetite: Satiety hormones

As outlined above there are several hormones involved in the regulation of appetite and energy homeostasis. Hormones regulating appetite can be divided into either short-term episodic hormones that are responsible to short term fluctuations of fasting and feeding

cycles such as gastrointestinal peptide hormones, or long-term tonic hormones, such as leptin and insulin that are secreted in proportion to fat stores. Functions of these hormones will be discussed below.

1.2.3.1 Adiposity signals

Leptin

Leptin is an adipocyte-derived hormone (adipokine) of the ob gene (Camp et al., 2016). It has multiple roles in the body, but mainly maintains long-term regulation on adiposity and controls adaptive metabolic changes in response to nutritional needs (Dardeno et al., 2010). Plasma leptins levels are proportionate to the body's adiposity levels. Circulating leptin is transported across the BBB and binds the leptin receptor (Ob-R or Lep-R) to mediates its effects (Wang et al., 2014). The Lep-R is widely expressed within in the hypothalamus but in high levels in the ARC and LHA. Leptin signalling directly activates anorectic POMC neurons and antagonises orexigenic ArRP/NPY neurons resulting in decreased food intake and increased energy expenditure (Camp et al., 2016).

Insulin

Insulin is a hormone produced by pancreatic β-cells, is essential for the regulation of both peripheral and central pathways in maintaining glucose homeostasis and provides energy to various tissues and organs. Circulating insulin rises rapidly post prandially, and like leptin, circulating levels reflect fat mass (Woods et al., 2003). The hormone crosses the BBB and enters the CNS via its receptor, insulin receptor (IR)-mediated transport, where supposedly acts as an anorexigenic signal (Burford et al., 2013). The exact mechanism of how insulin suppresses food intake is still not clear, however administration of insulin into the 3rd ventricle of the brain of fasted rats decreased expression levels of NPY and increased expression of POMC in the ARC and reduced food intake (Schwartz et al., 1992), (Sipols et al., 1995).

1.2.3.2 Gut hormones

The GI tract contains a number of specialised enteroendocrine cells (EECs), able to secrete a range of gut hormones. These gut hormones are responsible for the endocrine signalling within the gut-brain axis and has been demonstrated to influence appetite in rodent models and in humans when administered at physiological concentrations (Batterham et al., 2002), (Gantz et al., 2007). They are released upon stimulation by gastric distention, luminal nutrient composition and neuronal signals (Cummings and Overduin, 2007).

Ghrelin

Ghrelin is a 28-amino acid peptide that is the only peripherally circulating peptide that stimulates the NPY/AgRP orexigenic pathway (Wynne et al., 2005). It is secreted from X/A-like endocrine cells in the stomach and proximal small intestine (Date et al., 2000). Further to its role in stimulating food intake, ghrelin also modulates gastrointestinal motility, lipid and glucose metabolism, cardiac function, immune function, blood pressure, cell proliferation and adipogenesis (Levin et al., 2006). Ghrelin was discovered as the endogenous ligand of the growth hormone secretagogue receptor (GHS-R) and stimulates the release of growth hormone through the type 1a receptor in the hypothalamus (Wynne et al., 2005). However, ghrelin's growth hormone effects are independent of the orexigenic effects. For ghrelin to exert its orexigenic effects, ghrelin must undergo acylation with n-octanoic acid through the ghelin-Oacyl transferase (GOAT) enzyme producing acylated ghrelin and its by-product of degradation, desacylated ghrelin (Yang et al., 2008). Acylated ghrelin, the more abundant form, is thus orexigenic, whereas desacylated ghrelin may have distinct biological function (Delhanty et al., 2012). It has been proposed that ghrelin mediates its effect via stimulation of the NPY/ArRP pathways and inhibition the POMC neurons in the ARC, with the GHS-R also expressed on NPY neurons suggesting that ghrelin may mediate its orexigenic action via both the ARC and NTS.

As an orexigenic hormone, much effort has been put into exploring ghrelin as an anti-obesity treatment. Post-prandial, obese individuals are unable to supress ghrelin levels (le Roux et al.,

2005). Thus, pharmalogical interventions to reduce ghrelin signalling were explored, for instance GHS-R antagonists, RNA-Spiegelmers, ghrelin antibodies have been explored. However, none of these were able to produce promising clinical data (Vizcarra et al., 2007). An additional strategy is to target the enzyme required for the acylation of ghrelin. GOAT inhibitors were able to reduce food intake, body weight and fat mass in overweight mice (Barnett et al., 2010).

Cholecystokinin

Cholecystokinin (CKK) is the first gut hormone to be identified to influence food intake. It is released from mucosal enteroendocrine I-cells in the proximal intestine (Buchan, 1978) and is mainly secreted in response to fats and proteins. Following secretion, CKK signals via its receptor, CCK-1R (or CCK_A) in the vagal nerve as its anorexigenic effects were impaired upon vagotomy (Smith et al., 1981). CKK can also signal via its other receptor, CCK-2R (or CCK_B), but signals primarily via CCK-1R to mediates its anorexigenic actions. CCK-1R can also be found in the pancreas, gallbladder and pylorus and specific brain regions and further to its action on the vagal nerve, CCK via CCK-1R can also stimulate pancreatic growth and enzyme release, gallbladder contraction and bile secretion, stimulation of somatostatin and slow gastric emptying (Moran and Kinzig, 2004; Suzuki et al., 2011).

CCK first demonstrated its anorexigenic effects in Otsuka Long-Evans Tokushima Fatty rats, which lacks CCK-1R were hyperphagic and obese (Moran et al., 1998). Subsequently, CCK-1R antagonists was reported to cause an increase in food intake in rodents and humans (Bi and Moran, 2002). However, chronic administration of CCK failed to reduce food intake, although it appeared that CCK was more important for satiation rather than satiety, with acute CKK administration caused a reduction in food intake, but a concomitant increase in meal frequency (Beglinger et al., 2001). Therefore, CCK therapeutic potential may be limited. However, it has been reported that CCK could positively modulate the effects of leptin (Matson et al., 2000), and thus a combination approach involving the CCK model may be a more suitable option for the treatment of obesity.

Glucagon-like Peptide 1

Glucagon-like Peptide 1 (GLP-1) is an anorectic gut hormone that is formed by the post-translation enzymatic cleavage of the pre-proglucagon precursor (Dhanvantari et al., 2001). It is release from enteroendocrine L-cells in response to nutrients, especially carbohydrates, fatty acids and proteins (Herrmann et al., 1995). GLP-1 exist in two biological forms; GLP_{7-36} and $GLP\text{-}1_{7-37}$, the latter is the most abundant circulating form, however both are equally potent to the GLP-1 receptor (GLP-1R) (Orskov et al., 1994). Its biological functions include well characterised incretin effects to enhance insulin secretion, supresses glucagon secretion, delays gastric emptying, has trophic effects in pancreatic cells and initiates satiety (Buhmann et al., 2014). These effects of GLP-1 are mediated by GLP-1R, that is expressed in numerous hypothalamic nucleic including the ARC and PVN, as well as in the brainstem and peripheral nervous systems, pancreatic cells, heart, kidney and GI tract.

Though GLP-1 exert many effects that are metabolically relevant, they are often brief as GLP-1 has a half-life of only 1 – 2 minutes and is rapidly degraded and inactivated via the catalytic function of dipeptidyl peptidase IV (DPPIV) (Deacon, 2004). Only ~10% of gut-derived GLP-1 reaches the systemic circulation, suggesting GLP-1 acts in a paracrine manner. Nonetheless, its incretin actions have formed the foundation of many anti-diabetic drug such as exenatide and liraglutide. Exenatide and liraglutide are long-acting GLP-1 analogues that are both able to stimulate insulin secretion in a glucose-dependent manner, decrease appetite and induce weight loss to a similar extent (Madsbad, 2009). However, the tolerance levels to liraglutide by patients were much better than exenatide, making it a more attractive treatment option for weight management (Buse et al., 2009). Accordingly, it has been approved for clinical use in Europe in 2009 and in the USA in 2010 as a treatment for type II diabetes and also is currently undergoing phase III clinical trials as an anti-obesity drug (Murphy et al., 2017).

Recently however, side effects of GLP-1 analogues have raised concerns and has consequently delayed their development as anti-obesity treatments (Al Tulaihi and Alhabib, 2017). Side effects include an increase incidence of acute pancreatitis in patients treated with either

exenatide or liraglutide compared to other treatments of type II diabetes. In addition, patients treated with liraglutide also experienced nausea, dyspepsia and diarrhea (Mehta et al., 2017).

Oxyntomodulin

Oxyntomodulin (OXM), like GLP-1, is secreted from enteroendocrine L-cells in response to food intake and a product of pre-proglucagon precursor that is able to reduce food intake in animal models and in humans (Liu et al., 2010). No specific OXM receptor has been identified, however OXM exerts its effect mainly via the GLP-1R, though at a 50-fold lower affinity than GLP-1, and has a weak affinity to the glucagon receptor (GCGR) (Kosinski et al., 2012). Though it has a lower affinity than GLP-1, OXM has been reported to have more potent anorectic effects on acute food intake studies and able to reduce body weight at doses similar to GLP-1 (Dakin et al., 2004). Signalling via GCGR, OXM also stimulates energy expenditure and suppresses ghrelin (Wynne et al., 2006), unlike GLP-1. In mouse models, the anorectic effects of OXM, but not GLP-1, are blocked by the GLP-1R antagonist exendin$_{9\text{-}39}$, injected directly in the ARC and is absent in GLP-1R knockout models (Baggio et al., 2004). In addition, magnetic resonance imaging revealed the neuronal pattern of activation post OXM administration differs from GLP-1 (Parkinson et al., 2009), suggesting OXM may mediates its effect through distinct mechanisms.

Due to its dual effects of reduced food intake and increased energy expenditure, OXM is also considered as a viable target for anti-obesity and diabetes drug development programs. In addition, OXM is thought to have the lowest incidence of treatment associated nausea than other gut hormone peptides (Parkinson et al., 2009). However, like GLP-1, OXM is susceptible to rapid degradation via DDP-IV and therefore OXM analogues have been developed. Correspondingly, the OXM analogue OAP-189 is currently in phase I/II trials for safety and tolerability (Kairupan et al., 2016).

Peptide YY

Peptide Tyrosine Tyrosine (PYY), a 36-amino acid peptide, is a member pancreatic polypeptide (PP)-fold family that is secreted from enteroendocrine L cells in response to nutrients (Adrian et al., 1985). PYY has been reported to be able to influence appetite and food intake in many animal and human studies. PYY circulates in two forms: the full length PYY_{1-36} and the truncated form, PYY_{3-36}, produced by the enzymatic cleavage of PYY_{1-36} via DDP-IV. Intriguingly, PYY_{3-36}, is the main isoform found in circulation and has been widely accepted as an anorexigenic hormone that suppresses appetite and food intake in lean and obese animals and humans (Chelikani et al., 2005; Reidelberger et al., 2008). PYY_{3-36} exerts its effect via direct activation of Y receptor type 2 (Y2) found pre-synaptically on NPY neurons within the ARC, resulting in the downregulation of NPY expression and increase in POMC neuronal activity, thus promoting satiety (Batterham et al., 2002). This was further supported by the demonstration that administration of PYY_{3-36} to the ARC reduced food intake in rats, this was not observed in mice lacking Y2 (Batterham et al., 2002). PYY_{3-36} anorexigenic effects is not limited to the ARC, as peripherally administrated of PYY_{3-36} to Y2 receptors on vagal afferent fibres were able to induce a reduction of food intake, reduction of food intake was abolished by vagotomy (Abbott et al., 2005).

The employment of PYY_{3-36} as a treatment of obesity is restricted due to its rapid degradation and increased incidents of nausea following high concentrations. Thus, PYY_{3-36} analogues have been developed and are currently in the early pre-clinical phases for obesity treatments (Nishizawa et al., 2017).

1.2.4 Peripheral obesity targets

1.2.4.1 Gut hormone synergism therapies

Due to the several limitations (i.e. adverse side effects) of using single gut hormones in the treatment of obesity, new research has investigated the idea of using a combination of specific gut hormones to mimic the physiological control of appetite and to ultimately achieve

benefits in metabolism and weight regulation without adverse events (McGavigan and Murphy, 2012). The combined infusion of OXM and PYY_{3-36} at doses that does not cause nausea, is able to significantly reduce food intake in overweight or obese humans (Field et al., 2010), emphasising the fact that though these hormones functions via distinct mechanism can be simultaneously exploited. Another promising combination is GLP-1_{7-36} and PYY $_{3-36}$, orally administered using sodium N-[8-(2-hydroxybenzoyl) amino] caprylate (SNAC) delivery technology, was able to mimic the endogenous secretion of the hormones and also exert an anorectic effect to a greater extent than either of the two peptides alone (Steinert et al., 2010). Most recently, a triple agonism of GLP-1_{7-36}, OXM and PYY_{3-36} have demonstrated to be the most promising in combining gut hormone for the treatment of obesity (Tan et al., 2017). The combination of the three gut hormones mimics the elevated post-prandial secretion levels of GLP-1_{7-36}, OXM and PYY_{3-36} in patients who have undergone RYGB, as secretion is triggered by direct and rapid exposure of jejunal L-cells to nutrients from the bypass (Falken et al., 2011; Hope et al., 2018). The release of these three hormones led to the additive effect of reduced food intake (via all three hormones) and enhanced insulin secretion (via GLP-1 and OXM) (Korner et al., 2009) at doses of each individual hormone calibrated to be sub-anorectic for 10 hours led to a significant reduction in food intake in healthy individuals (Tan et al., 2017). In addition, no issues with nausea were observed (Tan et al., 2017). Further studies of the GOP infusion to be administered chronically and in individuals that are diabetic or obese are currently ongoing (Hope et al., 2018). Therefore, a combination of gut hormones to recapitulate endogenous hormone secretion and anorectic effects is an attractive strategy for the treatment of obesity.

1.2.4.2 Nutrient sensing systems as a target

Another field that has recently gained a lot of interest is the study of nutrient sensing receptors. Various nutrient sensing receptors are found within the GI tract are localised to enteroendocrine L-cells in the distal small intestine and colon. Stimulation of the nutrient receptors such as free fatty acid receptors in immortalised cells lines and primary L-cell cultures haves been demonstrated to cause anorectic gut hormone release (Psichas et al., 2015). Thus, by directly targeting nutrient sensing receptors to stimulate the release of

endogenous anorectic gut hormones may be an effective long-term treatment for weight regulation and obesity.

1.2.5 Gut hormone secretion by enteroendocrine cells

Enteroendocrine cells (EECs) accounts for less than 1% of intestinal epithelial cells, however they constitute the largest and most diversified endocrine organ in the body. They are dispersed throughout the GI tract and are made of more than 10 cell types that produce distinctive epithelia hormones. Enteroendocrine cells have been described to have a distinct cone-shape morphology with one extremity adjacent to the basal lamina with peptide hormone-filled secretory granules and the other holding microvilli on apical pole reaching the gut lumen. This allows them to sense the contents of the intestinal lumen and in turn secrete gut hormones which regulate appetite and energy homeostasis.

Specific cell-surface markers of EECs are limited, thus making these cells a challenge to study (Nagatake et al., 2014). However, with the development of elegant tools allowing to isolate and characterise these previously elusive cell population, the understanding of EECs have significantly evolved. Traditionally, EECs were categorised according to the hormone they secrete. By this classification at least 12 different enteroendocrine cell types were identified, they each express and release a hormone from a single peptide hormone precursor except for the GLP-1/PYY and the ghrelin/motilin cells. More recently, this identification of EECs has been redefined as there is more overlap than previously appreciated. For example, L cells in the colon and upper small intestine share less in common, though considered the same cell type, than the previously thought distinct cell subtypes of the upper small intestine L cells and K cells (Habib et al., 2012). Using transgenic expression of fluorescent markers under gut-hormones promoters, analysis of enteroendocrine cells and profiles of their contents can be carried using fluorescence-activated cell sorting (FACS) analysis and immunofluorescence. Using intestinal tissue from transgenic mice that expressed yellow fluorescent protein (YFP) Venus driven by the proglucagon promoter, it has revealed that cell populations that express mRNA for gut hormones found in certain enteroendocrine cell types, CCK, are in fact found in another enteroendocrine cell type than previously thought (Habib et al., 2012). In the colon,

the majority of the Venus-expressing colonic L cells were shown to express GLP-1 and PYY, as expected. In the small intestine however, most Venus-expressing cells also expressed CKK, approximately 10% cells contained gastric inhibitory peptide and only about 20% were positive of PYY (Habib et al., 2012). Using small intestine tissue from transgenic mice expressing enhanced green fluorescent protein (eGFP) under the CKK promoter also produced a similar pattern of enteroendocrine cell expression (Egerod et al., 2012). Thus, it is evident that enteroendocrine cells and their secretion of gut hormones are not as restrained as previously thought and is dependent on their location along the GI tract and specific to the different luminal factors that they are exposed to.

1.2.5.1 Mechanisms of gut hormone secretion from enteroendocrine cells

Gut hormone secretion from EECs is triggered mostly by nutrient sensing but to a lesser extent, can also be triggered in response to glucose, particularly for GLP-1. For glucose stimulated gut hormone secretion, multiple mechanism has been proposed but the most supported is via sodium/glucose co-transporter 1 (SGLT1), which uses the sodium electrochemical gradient produced by the Na^+/K^+ ATPase pump that allows glucose entry across the apical membrane and into the cells (Dyer et al., 1997). In addition, glucose transporters localised to the basolateral membrane, such as glucose transporter 2 (GLUT2) allows passive diffusion of glucose into the cell (Stumpel et al., 2001). Once glucose enters the cell, the cell membrane undergoes depolarisation and calcium is able to enter the cell via voltage-gated channels, leading to the exocytosis of gut GLP-1 containing vesicles (Reimann et al., 2008) (Figure 1.2 A). Following meal consumption, nutrients are sensed by a variety of G-protein coupled receptor (GPCRs) and are specialised to the nutrient that they can sense, and therefore, stimulate the release of different gut hormones, for example, medium and long chain fatty acids (MCFA and LCFA) are sensed by free fatty acid receptor 1 (FFA1) and stimulate the release of CCK and GLP-1, respectively (Edfalk et al., 2008). Once the nutrient sensing GPCRs are activated by their respective nutrients, there are generally two mechanisms that regulate the release of gut hormone secretion, raised intracellular calcium and cyclic adenosine monophosphate (cAMP) (Figure 1.2B). Increased intracellular calcium via GPCRs coupled to $G\alpha_{q/11}$ G protein triggers calcium release from intracellular calcium

stores and depolarises the cell membrane resulting exocytosis of hormone secretion (Spreckley and Murphy, 2015). Raised intracellular cAMP via GPCRs coupled to $G\alpha_s$ G protein leads to the modulation of adenosine triphosphate (ATP)-sensitive potassium channel which then depolarises the cell membrane and triggers the release the gut hormone secretion (Simpson et al., 2007). Furthermore, protein kinase A (PKA), a second messenger downstream kinase of cAMP is a known enhancer of proglucagon gene expression, thus also enhances the secretion of GLP-1 (Drucker et al., 1987). In addition to nutrients, non-nutrient GPCRs can also stimulate the release of gut hormones, such as GPR119 that activates $G\alpha_s$ upon binding to oleoylethanolamide (OEA) to stimulate the release of GLP-1 (Hansen et al., 2011).

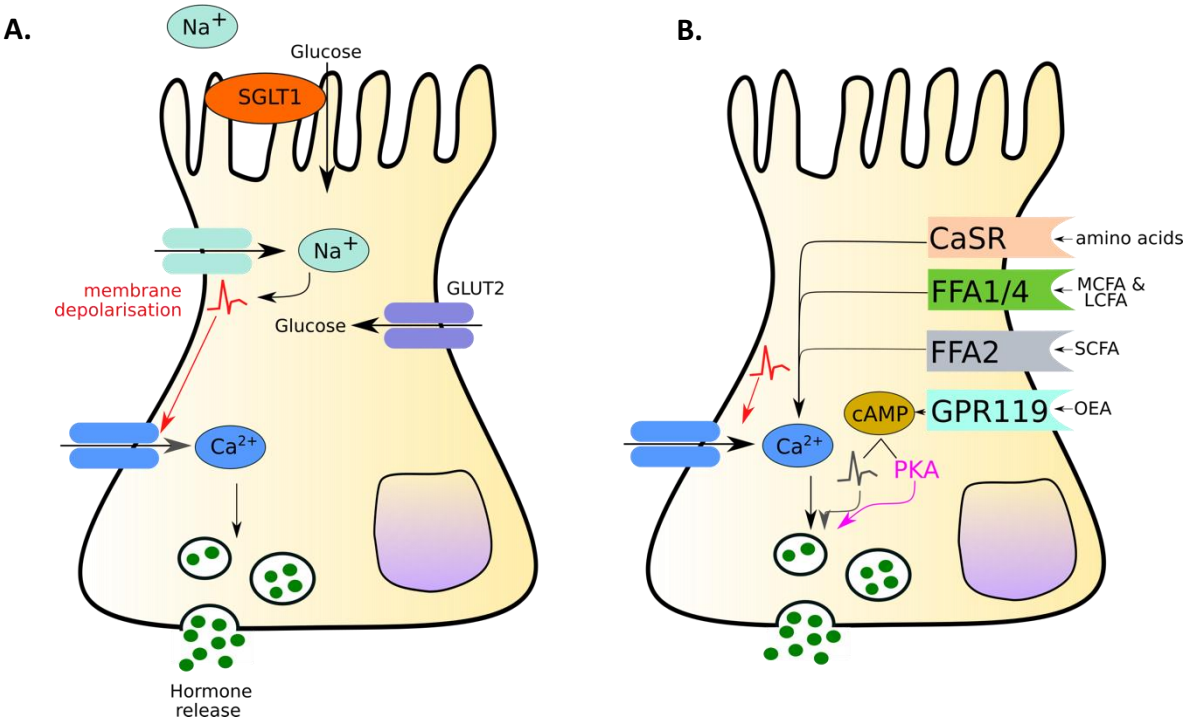


Figure 1.2 Enteroendocrine gut hormone secretion by glucose and nutrients sensing. (A) Glucose sensing by EECs is via Na^+-coupled glucose uptake by SGLT1 and passive diffusion by GLUT2, which produces small currents that trigger depolarisation and voltage gated Ca^{2+} entry, leading to the exocytosis of gut hormone secretion. (B) There are several GPCRs that senses nutrients in EECs. Fatty acids activate FFA1/4 (MCFA and LCFA) and FFA2 (SCFA) and amino acids activate calcium sensing receptor (CaSR) and G-protein coupled receptor family C group 6 subtype A (GPR6A) leads to an increase in intracellular calcium. Activation of GPR119 by oleoylethanolamide (OEA) stimulates gut hormone secretion via an increase in intracellular cAMP. SCFA, short chain fatty acids.

1.3 Short chain fatty acids

Short chain fatty acids (SCFAs), the major end products of gut microbial fermentation of dietary fibres, have been reported to exert many physiological functions including the regulation of appetite. The mechanisms of these functions are not completely understood and currently the subject of intensive research.

1.3.1 The production of SCFAs by gut microbiota

The GI tract is a highly complex ecosystem that harbours over one hundred trillion (10^{14}) bacteria of more than 1,000 different bacterial species (Li et al., 2014). However, most of the bacteria (>90%) belong to the Bacteroidetes (gram-negative) and Firmicutes (gram-positive phyla. The species and quantities of gut bacteria varies along the GI tract and is most enriched and diverse in the colon. Gut bacteria is also highly variable over time and across the human population, however humans share an underlying 'core microbiome' (Turnbaugh and Gordon, 2009). The core microbiome itself, however can be influence by a number of factors such as genetics, lifestyle, medical interventions (antibiotics, vaccinations and hygiene) and most importantly, diet (Burokas et al., 2015; Lankelma et al., 2015). A growing body of evidence have suggested that the consumption of dietary fibre can enhance the diversification of the gut microbiome that can inturn exert beneficial effects on body weight, food intake, glucose homeostasis, insulin sensitivity and anti-inflammatory properties (Kieffer et al., 2016).

Dietary fibres or non-digestible carbohydrates (NDC) are carbohydrate polymers with ten or more monomeric units that escape digestion and absorption in the small intestine and reach the caecum where they are fermented (Cummings and Macfarlane, 1997). Fermentation of NDCs is carried out by the resident anaerobic colonic microbiota that consists of a wide range of hydrolytic enzymes that hydrolyses the large macromolecular structures of NDCs into oligosaccharides and then monosaccharides, which are then used as energy sources for Ruminococcaeceae, Clostridiaceae, and Lachnospiraceae, specific microbiome of NDCS, to ferment these components into short chain fatty acids (SCFAs) as well as other carboxylic acids and gases (CO_2, H_2 and CH_4) (Poeker et al., 2018). The concentrations of these SCFAs in

the lumen are in the range of 70 – 130mmol/L and are in the approximate molar ratio of 60% acetate, 25% propionate and 15% butyrate (McNeil et al., 1979). However, the total concentrations of SCFAs is highly variable depending on amount and type of NDC, the diversity of microbiome and the gut transit time (Macfarlane and Macfarlane, 2003). Moreover, other factors can impact the microbial fermentation of SCFA such as luminal contents, stress, health state and mucous production (Cho et al., 2012).

1.3.2 SCFA absorption and metabolism

Following the production of SCFAs, approximately 95% of acetate, propionate and butyrate is absorbed by colonocytes and transported across the apical membrane. This can occur via four mechanisms. One mechanism is via bicarbonate (HCO_3^-)-coupled, an anion exchange between bicarbonate and SCFAs ions (von Engelhardt et al., 1998) . The second is through the monocarboxylate transporter (MCT1) which transport SCFAs in H^+-dependent electroneutral manner and is expressed along the entire length of the large intestine and is localised in the apical membrane (Takebe et al., 2005). Thirdly, via the sodium-coupled monocarboxylate transporter (SMCT1), is electrogenic and dependent on sodium ions with a Na^+ substrate stoichiometry of 2:1 (Gupta et al., 2006). The fourth mechanism is via passive diffusion of protonated SCFA.

Once absorbed, SCFAs are metabolised by different organs. Butyrate is utilised by colonocytes as their preferred fuel source (Scheppach, 1994). Acetate and propionate both enter the portal vein and are mainly taken up and metabolised by the liver (Bloemen et al., 2009). Acetate is used as an energy source and a substrate for the synthesis of cholesterol, long-chain fatty acids, glutamine and glutamate (den Besten et al., 2013). Propionate undergoes conversion into propionyl-CoA followed by succinyl-CoA, which enters the tricarboxylic acid (TCA) cycle and is converted into oxaloacetate, the precursor of gluconeogenesis (Bloemen et al., 2010). SCFAs that escape liver metabolism can be then metabolised by other tissues such as adipose tissue and muscle (Robertson et al., 2005). Due to the rapid metabolism by the liver, the concentrations of circulating SCFAs are relatively low with acetate: 200$\mu molL^{-1}$,

propionate: 4-5µmolL^{-1} for and butyrate: 1- 3µmolL^{-1}) (Pouteau et al., 2003; Wolever et al., 1989). However, it has been demonstrated that dietary supplementation of fermentable carbohydrates can the double the fasting plasma SCFAs concentration in mice and humans.

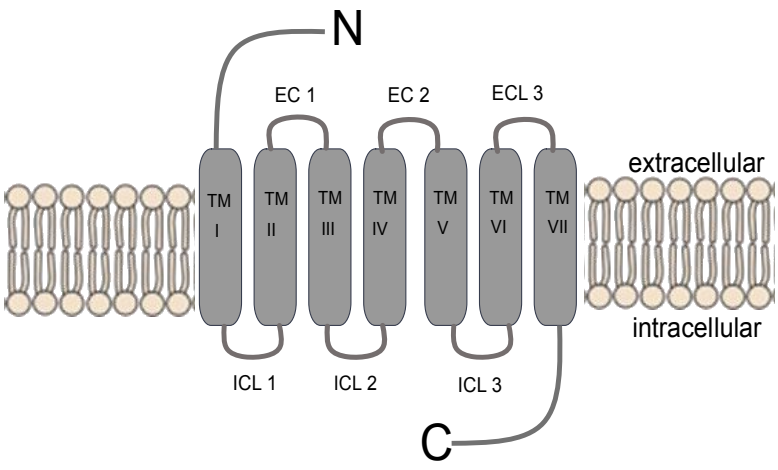
1.4 G protein coupled receptors

G protein coupled receptors (GPCRs) constitute the largest and most diversified family of proteins in the human genome, consisting of > 800 members. They are diverse in both their functions and the ligands they bind, regulating an array of physiological processes from metabolism, secretion, electrical activity, shape and motility of most cells in response to neurotransmitters, hormones, ions and sensory stimuli (Stevens et al., 2013). These processes are mediated by various extracellular stimuli including hormones, neurotransmitters, chemokines, metabolites, ions, nucleotides and amino acids. As such, GPCRs are the most successful group of drug targets and account for ~34% of approved drugs on the market today (Hauser et al., 2017).

1.4.1 Structure and classification

GPCRs are characterised by their common seven hydrophobic transmembrane (TM)-spanning domains, interspersed by an extracellular amino terminus and an intracellular carboxyl terminus. The extracellular terminus and TM domains are essential for ligand binding, whilst the intracellular domain interacts with cytosolic signalling proteins.

A.



B.

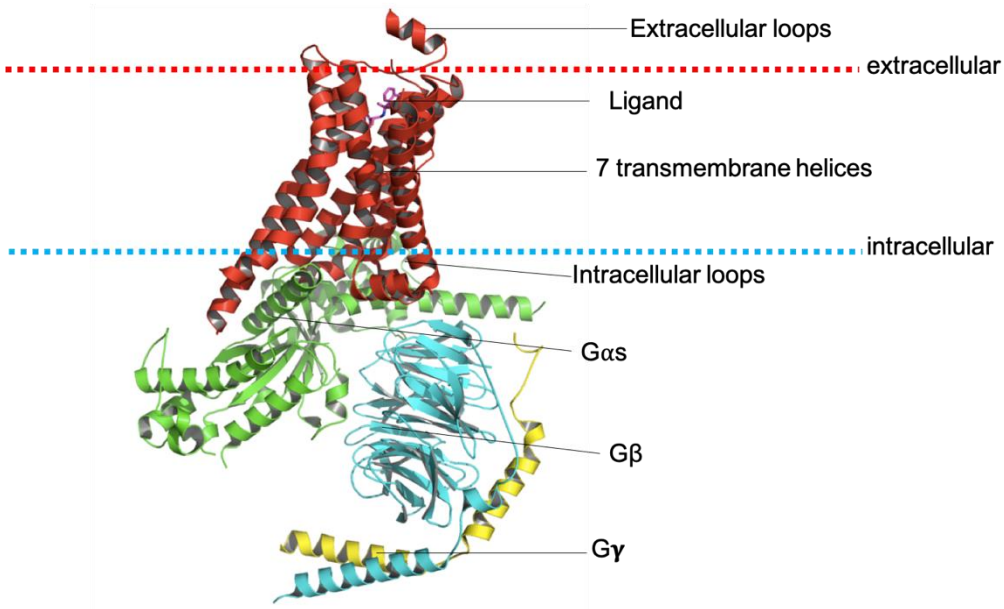


Figure 1.3 Schematic representation and crystal structures of GPCRs. (A) Diagram of the general structure of GPCR. The seven transmembrane helices (TMs), are shown in grey, numbered I - VII and connected by alternating intracellular loops (ICL1-3) and extracellular loops (ECL1-3). The GPCR is embedded in the membrane with the extracellular N-terminus connected to TM I and intracellular C-terminus connected to TM VII. (B) Crystal structure of human β2 adrenoreceptor in complex with Gαs subunit (with βγ). The membrane divides the receptor in the extracellular part (N-terminus), transmembrane helices, and the intracellular part. Adapted from (Rasmussen et al., 2011).

GPCRs based on their sequence homology can be classified into three large classes (Class A-C) and three subclasses (D-F). Class A comprises the largest group of GPCRs and accounts for ~80% of the GPCR genes. These receptors are also known as the 'rhodopsin-like family' and are characterized by several highly conserved amino acids and a disulphide bridge that connects the first and second extracellular loops. Receptors of odorants, mostly amine neurotransmitters (dopamine, serotonin, endocannabinoids) and many neuropeptides belong to this family. Class B receptors, also called 'secretin receptor family', include approximately 70 receptors for peptides such as secretin, glucagon, calcitonin and parathyroid hormone. These receptors are characterized by the presence of a relatively large extracellular domain for ligand binding and contain a network of three disulphide bonds, defining a globular domain structure. The smallest class, class C, are characterised by the extremely long N-terminus with approximately 600 residues to which ligands bind. Receptors of this family include metabotropic glutamate receptors, gamma-aminobutyric acid type B receptors and calcium sensing receptors, the cyclic adenosine monophosphate (cAMP) receptors (Class E) and frizzled/smoothened receptors (Class F) (Kobilka, 2007). The amino acid sequences of these GPCRs contain seven proportions of hydrophobic residues grouped into seven domains, in a manner reminiscent of Class A and B GPCRs. The fungal pheromone receptors are used by organisms for chemical communication (Nakagawa et al., 2005). The frizzled/smoothened receptors are necessary for Wnt binding and mediation of hedgehog signalling, a key regular for animal development (Dann et al., 2001). The cAMP receptors are involved in coordinating aggregation of individual cells and regulate the expression of a large number of growth and development regulated genes (Raisley et al., 2004).

1.4.2 Activation

Understanding how GPCRs translates the extracellular binding of a ligand into conformational changes of its intracellular portion to elicit the interaction of intracellular binding partners and achieve highly specific cellular outcomes has not only been a long-standing research interest for the understanding of GPCR biology but also has translational significance due to its importance on the future of ligand discovery and targeting of specific GPCR signalling pathways. A critical scientific advance that has certainly increased the understanding of this

process is the availability of high-resolution crystal GPCR structures (Figure 1.3 B). In the last five years, there has been an increased number of GPCR crystal structures available and most strikingly has revealed that GPCRs are highly flexible and exist in multiple distinct conformations, including, inactive, active and intermediate states (Dror et al., 2011), redefining the canonical two state receptor model, that assumes GPCRs exists either in inactive (R) or active (R*) states (Samama et al., 1993). In fact, the complexity of conformational changes upon ligand binding and the activation of distinct signalling processes emanating from receptor activation are more complicated than originally appreciated and such distinct conformational changes is due to pharmalogically distinct ligands that are able to evoke distinct receptor conformations (Kenakin, 2013). As such, GPCRs ligands can be categorised into two broad classes: orthosteric, where ligands bind to a ligand-binding pocket within a cavity formed by the transmembrane helices; and allosteric, which bind through a large amino terminal region that forms a distinct domain (Park et al., 2008). Within the orthosteric ligands, ligands can be subcategorised into the following: full agonists, which fully activate and stabilises R*; partial agonist, activates the receptor in varying degrees, has some affinity for both R and R* and thus are less effective in shifting the equilibrium toward R*; neutral antagonist which binds but does not activate the receptor. Inverse agonist decreases basal activity of the receptor by stabilising R and therefore does not activate the receptor and have no intrinsic agonist activity but when they bind to the receptor, they can either inhibit the binding affinity and/or efficacy of the orthosteric agonist (Kobilka, 2007). Among allosteric modulators are positive allosteric modulators (PAMs) that do not always exert an intrinsic efficacy but when they bind to the receptor, enhance the affinity and/or efficacy of the orthosteric ligand and silent allosteric modulators (SAMs) or neutral allosteric modulators (NAMs) bind to the receptor, however, has no effect on the orthosteric agonist affinity or efficacy. SAMs, can however, act as a competitive antagonist at the allosteric site and blocks PAM and NAM activity. Therefore, SAMs can be utilised as an effective tool to characterise the presumed PAM or NAM effects are receptor-mediated (Burford et al., 2013).

After ligand binding, the receptor undergoes substantial conformational changes in both the transmembrane bundle and intracellular domains. Once stabilised in the active conformation form, translocation and binding of heterotrimeric G proteins proteins to the receptor's

intracellular domain is enabled, which in turn regulates intracellular signalling cascades. Heterotrimeric G proteins consist of three subunits: Gα (45 kDA), Gβ (35 kDA) and Gγ (15 kDA). In the inactive state, the Gα subunit is associated with the Gβγ complex and guanosine diphosphate (GDP), resulting to the exchange of GDP with guanosine triphosphate (GTP) in the Gα subunit (Malbon, 2005). Once the GTP replaces GDP the G-protein is activated, resulting in the dissociation of the α subunit and the βγ complex as well as from the receptor. Therefore, allowing both the α subunit and βγ complex to independently interact and modulate the activity of their downstream target proteins, passing the signal to different types of second messengers. Following this, the α subunit hydrolyzes the GTP to GDP facilitated by the binding of regulators of G-proteins signalling (RGS), and rendering the α subunit inactive, allowing it to re-associate to the βγ complex, and thus reunites the G protein in an inactive state (Figure 1.4).

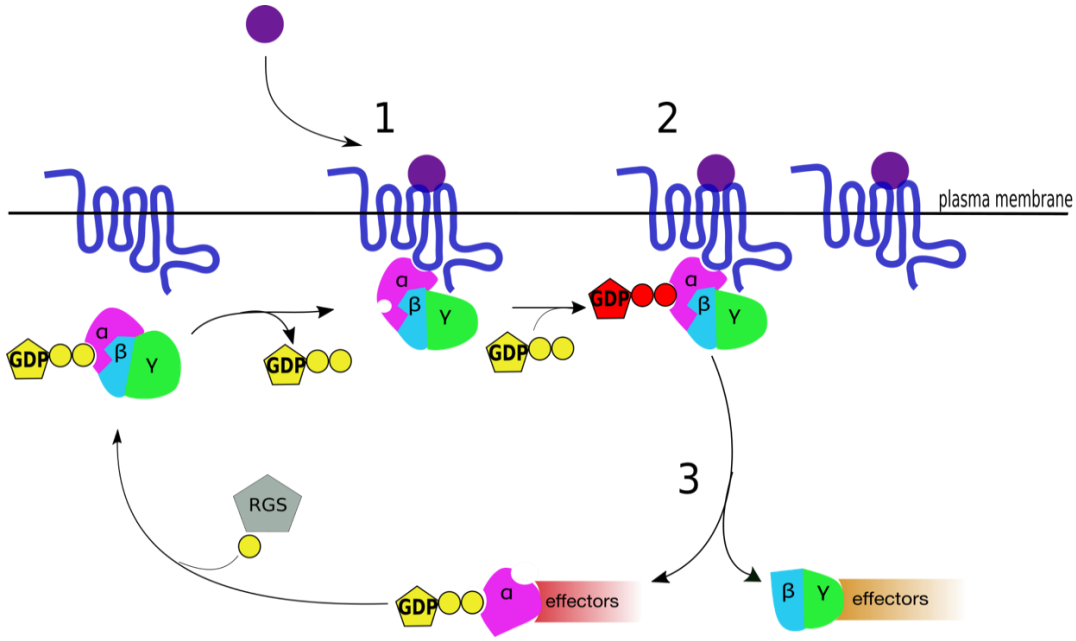


Figure 1.4 Activation of heterotrimeric G protein by a GCPR. In an inactive conformation, the Gβγ heterotrimer is associated with the GPCR and the Gα subunit is associated with GPD. Upon receptor activation (1), the receptor undergoes conformation change and acts as a guanine exchange factor (GEF) for the α subunit, promoting the exchange of GDP for GTP (2). Upon GTP binding, the Gα subunit dissociates from the Gβγ and are detached from the receptor and then start signal transduction through cellular effects (3). The signal is terminated by the intrinsic ability of Gα subunits to hydrolyse GTP, and this activity is accelerated by regulator of G protein signalling RGS domain, thus re-associates Gα with βγ and are retuned to basal state (4).

1.4.3 Signalling pathways

Based on sequence similarity, there are four main classes of Gα subunits that have been identified (Neves et al., 2002) (Figure 1.5). The $G\alpha_s$ and $G\alpha_i$ subunits couple to adenylyl cyclase (AC) and act to stimulate or inhibit AC, respectively. AC regulates levels of intracellular production of cyclic 3', 5-adenosine monophosphate (cAMP) as the activation of AC catalyses the conversion of ATP to cAMP within the cell. cAMP then activates cAMP-dependent kinases, specifically protein kinase A (PKA). The $G\alpha_{q/11}$ subunits activate phospholipase C β (PLC β) which hydrolyses phosphatidylinositol 4,5-bisphosphate (PIP_2) to generate inositol-14,5-trisphosphate (IP3) and diacylglycerol (DAG). IP3 regulates the release of calcium from intracellular stores and DAG activates protein kinase C (PKC). The $G\alpha_{12/13}$ subunits activates Rho guanine nucleotide exchange factors (Rho-GEFs), which in turn activate small cytosolic Rho-GTPase (Schmidt and Hall, 2002; Siehler, 2007). The Rho-GTPase can activates numerous proteins such as Rho-kinase that are essential for the regulation of actin cytoskeletal remodeling in cells (Amano et al., 2010).

The Gβγ heterodimer subunit, in addition to functioning as a guanine nucleotide dissociation inhibitor (GDI) for Gα, has been shown to facilitate the regulation of a variety of downstream effectors such as PLC, K^+ and Ca^{2+} channels, and ACs (Smrcka, 2008; Khan et al., 2013), these are known to modulate mitogen-activated protein kinase (MAPK) pathways, (Yamauchi et al., 1997; Kiyono et al., 1999; Welch et al., 2002). Interestingly, it has recently been demonstrated that the Gβγ can facilitate inter-receptor crosstalk from one receptor by initiating the signalling of another receptor, without physical interaction of the two receptors (Jean-Alphonse et al., 2017).

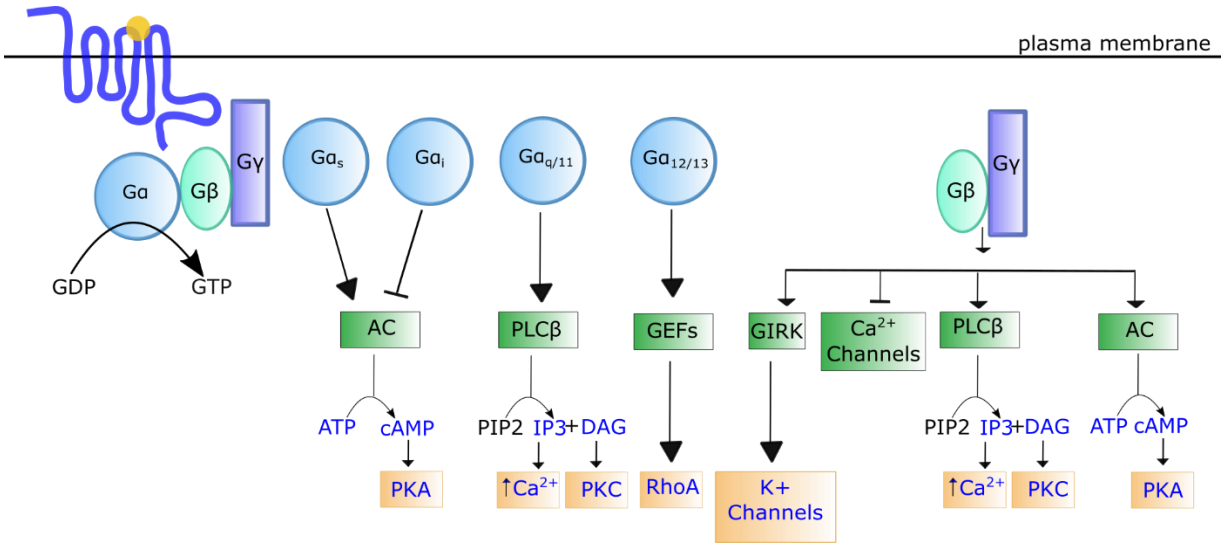


Figure 1.5 Signalling pathways induced by GPCR activation. Activation of GPCRs promotes an active conformational state. This conformational rearrangement leads to the guanosine nucleotide exchange in the Gα subunit that results in the recruitment of heterotrimeric G protein and dissociation of Gα from the Gβγ subunits. There are four main Gα classes (blue circles): stimulatory Gα ($G\alpha_s$) activates AC and converts ATP into cAMP; inhibitory Gα ($G\alpha_i$), inhibits cAMP production; $G\alpha_{q/11}$ activates PLC-β that hydrolyses PIP2 and generates DAG and IP3 which activate PKC and releases Ca^{2+} from intracellular stores; $G\alpha_{12/13}$ activates members of the Rho families of GTPases. The Gβγ subunits are also able to activate various signalling pathways. Second messengers are in green boxes and orange boxes represent proteins activated further downstream.

1.4.4 Regulation of GPCR signalling

1.4.4.1 Desensitisation and internalisation

The activation of GPCRs leads to several desensitisation mechanisms whereby receptor response to a repeated or continuous stimulation is reduced. These mechanisms involve the termination of activated receptor responses and are carried out by kinases and arrestin adaptor proteins (Krupnick and Benovic, 1998; Tobin et al., 2008). Mechanisms of desensitisation are therefore dependent on both the GCPR amino acid sequence and the expression of various cytoplasmic mediators.

1.4.4.2 Heterologous desensitisation by effector kinases

In heterologous desensitisation, second messenger dependent protein kinases (PKA or PKC) phosphorylate receptors independent of agonist occupancy and also the activation of one

type of receptor leading to the desensitisation of other receptors. Phosphorylation occurs on serine and threonine residues at consensus sites in the intracellular loops and C-terminal tail, resulting in disruption to the G-protein binding site and thus uncouples the receptor form G-protein-mediated response (Gainetdinov et al., 2004; Tobin et al., 2008). In addition, phosphorylation by alternative kinases such as Ca^{2+}/calmodulin-dependent protein kinase II (CaMKII) or casein kinases-induced phosphorylation has also been reported to be involved in heterologous desensitization (Yang et al., 2017).

1.4.4.3 Homologous desensitisation by arrestins

Homologous desensitisation is the desensitisation of agonist-bound, activated receptors, and occurs more rapidly than heterologous desensitisation. This desensitisation process involves G protein-coupled receptor kinases (GRKs) and arrestin adaptor proteins (Gainetdinov et al., 2004). The GRK family consist of 7 individual members that are able to generate distinct phosphorylation patterns or 'phosphorylation barcodes' on the GPCR (Butcher et al., 2011; Nobles et al., 2011). GRK 2, 3, 5 and 6 are widely expressed and are the prominent members of the GRK family. GRKs phosphorylate agonist-occupied receptors intracellular domains and C-terminal tails at distinct serine and threonine residues (Bouvier et al., 1988; Huttenrauch et al., 2005), which then induces the binding of arrestin adaptor proteins to the GRK-phosphorylated receptor (Lohse et al., 1992). The arrestin adaptor protein family consist of four proteins: visual arrestin and cone arrestin, that are expressed only in the retina; and arrestin-2 and -3, the non-visual arrestins that are also known as β-arrestin -1 and -2, are ubiquitously expressed (Perry and Lefkowitz, 2002; Lefkowitz and Shenoy, 2005) and thus are responsible for homologous desensitisation of most non-visual GPCRs (Luttrell and Lefkowitz, 2002). The binding of arrestins sterically inhibits further G protein binding, and thus, terminates signalling (Perry and Lefkowitz, 2002). Though most activated GPCRs are phosphorylated prior to β-arrestin binding, receptors such as protease-activated receptor (PAR)-1 and leukotriene B4 receptors bind to β-arrestin independent of receptor phosphorylation (Chen et al., 2004; Jala et al., 2005). Additionally, although identified for their role in arresting signalling, it is now widely appreciated that in addition to G protein signal termination, β-arrestins themselves are able initiate discrete G protein-independent

signalling via scaffolding components of MAP kinase such ERK1/2 (Shukla et al., 2014). However, there is current controversy if the activation of ERK1/2 MAPK distinctively requires β-arrestins but instead is still initiated via G protein activation (Grundmann et al., 2018; Gurevich and Gurevich, 2018a; Gurevich and Gurevich, 2018b). Furthermore, a recent study has identified the possibility of β-arrestins able to sustain G protein signalling via formation of 'megaplexes' that consist of the receptor bound to β-arrestin for receptors that exhibit prolonged arrestin associations as determined by the C-terminal tail serine/threonine phosphorylation sites (Thomsen et al., 2016). This megaplex is distinct from the arrestin conformations of the arrestin-mediated desensitisation that occurs from the plasma membrane (Cahill et al., 2017; Kumari et al., 2017).

Another key role of β-arrestin is to function as an endocytic adaptor protein to target receptors for internalisation via clathrin-coated pits. Following the binding of β-arrestin to the phosphorylated receptor, receptor-bound β-arrestin internalises into clathrin-coated pits (CCPs) via the interaction of both the heavy chain of clathrin and adaptor protein AP-2. Once GPCRs have accumulated in CCPs, the scission of clathrin-coasted vesicles from the plasma membrane is mediated by large GTPase dynamin and receptor is internalised into endosomes. This mechanism is a requisite for clathrin-dependent internalisation for many, but not all, GPCRs (van Koppen and Jakobs, 2004). For example, clathrin-dependent internalisation of the 5-hydroxytryptamine 2A receptor and M1 muscarinic acetylcholine receptor does not require β-arrestin but was dependent on dynamin (Bhatnagar et al., 2001; Uwada et al., 2014). While classically it was thought that GRKs and β-arrestin only have roles in rapid desensitisation, accumulating evidence indicate that they also have roles in the spatial-temporal regulation of GPCR signalling. For example, within the CCP, are distinct populations of CCPs where different GPCRs can be organised into distinct subset of CCPs that can determine the post-endocytic fate of the receptor to a recycling or lysosomal pathway (Mundell et al., 2006). Such sorting is dictated by the means of kinase-dependent internalisation that the receptor utilises, GRK-dependent phosphorylation directs receptors to the recycling pathway and phosphorylation by second messenger kinases such as PKC directs receptors to lysosomal sorting (Mundell et al., 2006). In addition to post-internalisation sorting decisions, there is evidence that CCPs

themselves may function as signalling platforms particularly for receptors that spend an extended amount of time in CCPs (West and Hanyaloglu, 2015). It was demonstrated that the receptor's residency time within the CCP prior to their removal from the plasma membrane could induce specific signalling pathways. This was demonstrated for the cannabinoid 1 receptor (CB1) where specific ligands resulted in specific residency times that CB1 remained in CCPs (Flores-Otero et al., 2014). Ligands that induced longer dwell times of the receptor led to a sustained ERK1/2 activation mediated by β-arrestins whereas ligands that elicited shorter dwell times activated mainly G protein signalling. Signalling dwell times are mediated by specific phosphorylation patterns or barcodes that are a result of specific conformations induced by differential interactions with β-arrestins (transient or prolonged). The extended dwell times provide the required time for all the signalling scaffolds to effectively be recruited to β-arrestins and thus activate signalling (Flores-Otero et al., 2014). For the β1 adrenergic receptor (β1AR) however, a specific dwell time was not required for a sustained β-arrestin-mediated ERK1/2 activation. The β1AR internalises much slower and not as efficiently to CCPs as its closely related receptor, β2AR, however, it robustly recruits β-arrestin to CCPs catalytically via its core once internalised (Eichel et al., 2016; Eichel et al., 2018). This CCP-β-arrestin complex elicited sustained ERK1/2 activation in the absence of receptor via arrestins adopting a specific conformation, demonstrating that a receptor-arrestin complex is not essential for arrestin mediated signalling (Eichel et al., 2016; Eichel et al., 2018). There is also evidence that the receptor themselves could regulate their residency time within the CCPs. For the β2AR, interaction with scaffold proteins such as postsynaptic density 95/dis large/zonula occludens-1 (PDZ) proteins, causes the receptor to be tethered to the cortical actin which delays the recruitment of dynamin, resulting in the receptor spending a prolonged amount of time in CCPs. For the MOR, which does not interact with PDZ proteins, it regulates its residency time in CCPs via receptor ubiquitination (Henry et al., 2012). Though AP-2 and β-arrestins are the core components in initiating CCP endocytosis, a variety of other endocytic machinery that functions as biochemical 'checkpoints' are required for proper internalisation (Henry et al., 2012).

In addition to CME, several GPCRs are also able to internalise by mechanisms that does not require clathrin. One mechanism that GPCRs such as the muscarinic receptor 4 utilises for their internalisaition is via fast endophilin mediated endocytosis (FEME) (Boucrot et al., 2015). FEME takes places by the formation of tubule-vesicular carriers at the plasma membrane within seconds of receptor activation (Boucrot et al., 2015). Instead of clathrin or AP2, internalisation via this mechanism utilises endophilin but still requires dynamin for pit scission. The significance of receptors internalising via this pathway is still unknown, however, an increasing amount GPCRs have demonstrated to utilise this pathway for its internalisation.

1.4.4.4 GPCR endocytic sorting to the recycling pathway

Once internalised, GPCRs are sorted within the endocytic pathway where their intracellular fate is dictated. The sorting of receptors to the recycling pathway to return back to the plasma membrane results in resensitisation of receptor responsiveness and for many years bulk recycling from passive diffusion into endosome tubules was thought to be sufficient to explain receptor recycling, however, accumulating evidence have now demonstrated that the recycling GPCRs undergo regulated recycling (Cao et al., 1999; Gardner et al., 2007; Hanyaloglu and von Zastrow, 2008). GPCR regulated recycling necessitates specific sequences or 'recycling sequences' in the C-terminal tail of the receptor. Majority of these sequences are tyrosine- and dileucine-based motifs or motifs PDZ-ligands that are harboured by many GPCRs (Hanyaloglu and von Zastrow, 2008). Tyrosine-and dileucine-based targeting motifs interact with clathrin adaptor protein complexes (AP-1 and 2) to regulate GPCR recycling via initiation of clathrin-mediated endocytosis, followed by trafficking to the trans Golgi network (TGN) and endosomes which then they are returned back to cell surface (Pandey, 2009). PDZ proteins are conserved cytoplasmic adaptor proteins that function as scaffolding structures to mediate the assembly of multiprotein signalling complexes by interacting with their respective PDZ ligand at the C-terminal tail of receptors. There are currently three classes of PDZ ligands (class I, II, and III) based on their amino acid sequence (Sheng and Sala, 2001). Among the three, class I PDZ ligands are the most characterized and found most commonly to interact with GPCRs (Trejo, 2005; Camp et al., 2016). The discovery that a specific sequence in the C-terminal tail of the β2AR was necessary and sufficient to regulate recycling of this

receptor (Hall et al., 1998; Cao et al., 1999), led to a redefining of how GPCR recycling is regulated. Subsequently, similar recycling sequences was identified for other receptors, such as the β1AR and κ-opioid receptor (Gardner et al., 2007). Receptors that are unable to bind to their PDZ proteins not only impairs their recycling abilities but also reroutes receptor to a lysosomal degradative pathway or, conversely, if a recycling sequence is transplanted onto a receptor that typically undergoes degradation to the lysosome such as the delta-opioid receptor, can result in rapid recycling of the receptor back to the plasma membrane (Gage et al., 2001; Gage et al., 2005). In addition, further PDZ recycling ligands were recently identified for the β2AR, such as sorting nexin 27 (SNX27) (Lauffer et al., 2010). SNX27 facilitates sorting β2AR into actin stabilised, retromer tubules (Puthenveedu et al., 2010). Similarly, SNX27 is also involved in regulating recycling of the β1AR and Somatostatin receptor type 5 (Lauffer et al., 2010; Temkin et al., 2011; Nakagawa and Asahi, 2013; Bauch et al., 2014). Following this, an abundant of GPCRs have demonstrated to contain recycling sequences in their C-terminal tail, though not all confer to PDZ binding ligands but rather novel amino acid motifs that are specific to the receptor or a requirement of an additional 'barcode' for receptor recycling, suggests that GPCR regulated recycling is a highly regulated and complex process that diversifies not only recycling but also G-protein coupling and desensitisation (Romero et al., 2011; Bahouth and Nooh, 2017).

Further to PDZ domain binding proteins, there is a variety of additional core proteins known to be involved in regulating receptor recycling. The EE-localised adaptor protein hepatocyte growth factor regulated tyrosine kinase substrate (Hrs), a protein involved in sorting cargo to the degradative pathway, has also been identified as a protein to be involved in recycling for the β2AR, calcitonin-like receptor, MOR and protease activated receptor 2 (PAR-2) and cellular depletion of Hrs led to receptors to be retained in the EE (Bache et al., 2003; Hanyaloglu et al., 2005). Additionally, β-arrestin both directly and indirectly have been implicated to have a role in receptor recycling. For some GPCRs, the duration of interaction with β-arrestins determines their post-endocytic fate. Class A GPCRs, such as β2AR, transiently interacts with β-arrestin and undergoes rapid recycling. In contrast, class B GPCRs, such as the vasopressin type 2 receptor (V2R), show a much stronger and more prolonged interaction with β-arrestin, following migration to CCPs, receptor and β-arrestin remain

bound in a complex on the surface of CCVs, and as a result, recycles back to the plasma membrane much slowly than class A receptors (Shenoy, 2007; Ranjan et al., 2016). Additionally, for the N-formyl peptide receptor 1 (FPR1), agonist induced-internalisation was unaltered in the absence of β-arrestins, however recycling was impaired and resulted in the accumulation of FPR1 in Rab-11 perinuclear endosomal compartment (Vines et al., 2003; Wagener et al., 2009). This is in contrast to its closely related receptor, FPR2, that required interaction with β-arrestin mediated internalisation for rapid recycling (Thompson et al., 2014). Another endocytic regulator that has been recently identified to facilitate receptor recycling is the retromer complex. The retromer complex is a peripheral membrane protein complex that has a primary role within endosomes to sort membrane cargo to the TGN (Seaman et al., 1998), however, recently an additional role in trafficking of GPCRs from endosomes to the plasma membrane have been described (Temkin et al., 2011). Through the interaction with SNX27 and the major endosomal polymerization-promoting complex known as Wiskott-Aldrich syndrome protein and scar homolog (WASH), the retromer complex forms a major sorting platform on early endosomes (EEs) where receptors such as PTHR and β2AR are sorted to the recycling pathway and/or are organised into specific endosomal tubules that facilitate PDZ-dependent recycling (Temkin et al., 2011; Seaman, 2012; McGarvey et al., 2016). Other core endocytic proteins that regulate recycling are the Rab GTPases. Rab GTases are the largest branch of the Ras-related GTPase superfamily and are involved in almost all aspects of vesicle-mediated endocytosis and exocytosis. They can modulate receptor recycling as well as degradation via association with specific amino acid residues within the receptor's C-terminal. Specifically, Rab4 is known to facilitate rapid recycling and thus, the overexpression of a Rab4 mutant further promoted the resensitisation of some GPCRs, for example the angiotensin II type 1 receptor (Li et al., 2008). In contrast, Rab11, regulates slow recycling of receptors from perinuclear endosomes and the TGN to the plasma membrane (Zerial and McBride, 2001). However, a small number of receptors have demonstrated the ability to efficiently recycle to the plasma membrane from Rab11 positive endosomes, such as the FPR2 (Thompson et al., 2014). Further, from Rab9 positive endosomes, a compartment that regulates the sorting of receptors to the endolysosomal pathway, the delta opioid receptor was able to recycle back to the plasma membrane (Charfi et al., 2018). Recently, it has been demonstrated that receptor's own intracellular signalling cascade can also regulate

receptor recycling. PKA phosphorylation of the β2AR C-terminal tail initiated by activation of receptor's $G\alpha_s$-cAMP pathway restricted the receptor to enter the sequence-dependent recycling tubule and instead the receptor entered the bulk tubule for recycling (Vistein and Puthenveedu, 2013). Conversely, inhibition of PKA phosphorylation for the luteinizing hormone receptor (LHR) and β1AR impaired the receptors ability to recycle (Sposini et al., 2017; Bahouth and Nooh, 2017). Such regulated GPCR recycling have been demonstrated to be essential for various physiological functions, for instance mutations to the recycling sequence of the β2AR not only disrupted receptor's recycling but also increased myocardial contractility due to hyperadrenergic stress (Xiang and Kobilka, 2003). For the FPR1, β-arrestin mediated recycling is essential in the suppression of anti-apoptotic signalling (Wagener et al., 2009).

The diversity in number of binding proteins and recycling sequences in mediating receptor recycling suggest that multiple endosomal compartments for receptor recycling may exist. Studies from the LHR demonstrated that through the interaction with the receptor's PDZ ligand with the PDZ protein $G\alpha_i$-interacting protein C terminus (GIPC), facilitates recycling by routing the LHR to very early endosomes (VEE), an endosomal compartment morphologically and biochemically distinct from the EE (Jean-Alphonse et al., 2014). This interaction was essential as disabling LHR's interaction with GIPC re-routed the receptor to EEs and as a result inhibited receptor recycling (Jean-Alphonse et al., 2014). In a similar manner, mutation to the PDZ ligand of the P2Y purinergic receptor 1 re-routed the receptor from a Rab5-positive compartment thereby perturbing its recycling and instead accumulating in the TGN (Cunningham et al., 2013). These studies and together with the findings that depict the various pathways and molecules that a GPCR traverses and associates with to regulate recycling may suggest that these mechanisms, portrayed only to facilitate receptor resensitisation is inadequate but instead may be represent sites involved in additional functions that enable specific cellular outcomes as the receptor travels through the endocytic pathway.

1.4.4.5 GPCR endocytic sorting to the degradation pathway

The targeting of internalised GPCRs to the degradative pathway results in long-term attenuation of receptor signalling and an overall decrease in receptor protein levels (Figure 1.6). Proteolytic degradation is critical for the turnover of receptors and central to cellular adaptations to chronic stimulation, including those observed in drug tachyphylaxis or tolerance (Tappe-Theodor et al., 2007; Hanyaloglu and von Zastrow, 2008). Once internalised into EEs, GPCRs are sorted the degradative pathway and targeted to Rab7-positive endosomes where receptors invaginate into intraluminal vesicles (ILV) to form multivesicular bodies (MVBs). MVBs then fuse with lysosomes and degrade the receptor (Katzmann et al., 2002; Marchese et al., 2008). This process is regulated primarily by ubiquitination as well as a number of well-characterised protein-protein interactions between endocytic machinery and targeting motifs encoded in the C-terminal tail of receptors. Many GPCRs, such as the chemokine receptor 4 (CXCR4) and muscarinic acetylcholine receptor M2, contain lysosomal sorting signals in their C-terminal tails and ICLs that correspond to lysine residues that ubiquitin covalently attaches to (Krudewig et al., 2000; Bonifacino and Traub, 2003; Marchese and Trejo, 2013). These signals mediate lysosomal targeting by binding to adaptor protein complexes, such as the endosomal sorting complex required for transport (ESCRT) machinery. The ESCRT machinery consist of four subcomplexes, ESCRT-0, -I, -II and -III. ESCRT subcomplexes with numerous accessory proteins and act sequentially to sort ubiquitinated cargo, ESCRT-0, -I and -II are responsible for capturing and retaining ubiquitinated cargo from the EEs resulting in involution to IVLS in MVBs before degradation in the lysosome. ESCRT-III via ATPase vacuolar protein sorting 4 (VSP4) disassembles and recycles ESCRT complexes to promote additional rounds of MVB sorting (Wegner et al., 2011). Ubiquitination-dependent sorting of GPCRs via ESCRT have been demonstrated for a selection of GPCRs; among these are the CXCR4, neurokinin-1 receptor (NK1R), PAR- 1 and 2, β2AR and sphingosine-1-phosphater receptor (S1PR) are ubiquitinated via ubiquitin ligases (E3) and sorted for lysosomal degradation upon agonist stimulation (Marchese and Benovic; Cottrell et al., 2006; Grimsey et al., 2018; Alonso and Friedman, 2013; Alvarez et al., 2010). Impairing ubiquitination of these receptors impaired their lysosomal sorting and degradation and disruptions of the ESCRT component also blocked their lysosomal sorting (Marchese and

Benovic, 2001; Jacob et al., 2005; Cottrell et al., 2006; Hasdemir et al., 2009). Intriguingly, for the β2AR and CXCR4, ubiquitination by E3 ubiquitin ligase was only effective only when β-arrestins were present as an adaptor for ligase recruitment (Shenoy et al., 2001).

Though ubiquitination plays a key role in GPCR lysosomal degradation, there are a subset of GPCRs that sort to lysosomes in a ubiquitin-independent manner, such as the calcitonin-like receptor and δ opioid receptor (DOR). These receptors still however, require an ESCRT-0 complex component for their lysosomal sorting, demonstrating that ubiquitination is not a requirement for GPCRs to enter the ESCRT pathway (Tanowitz and von Zastrow, 2003; Henry et al., 2011; Raiborg and Stenmark, 2009; Hislop and von Zastrow, 2011). Conversely, PAR-1 undergoes ubiquitination upon activation and subsequent trafficking to lysosomes, however degradation is independent of receptor ubiquitination and ESCRT-0 and -I complexes but interacts with an ESCRT-III interacting protein, ALG-2 interacting protein X (ALIX), and arrestin domain-containing protein 3 (ARRDC3) resulting in the recruitment E3 ligase to ubiquitinate of ALIX instead (Wolfe et al., 2007; Petaja-Repo et al., 2001; Dores et al., 2015; Dores et al., 2016), however, regulation by ARRDCs of these receptors have yet been reported. In addition to ubiquitin and ESCRT mediated lysosomal targeting, a subset of GPCRs have been demonstrated to interact with GPCR associated sorting protein-1 (GASP-1) at their C-terminal tail for degradation (Henry et al., 2011; Hislop and von Zastrow, 2011; Dores and Trejo, 2015). GASP-1 has been demonstrated to regulate the degradation of DOR, Dopamine D2 receptor (D2R), bradykinin 1 receptor, CB1, and non-recycling mutant of the β-adrenergic receptor (Whistler et al., 2002; Bartlett et al., 2005; Martini et al., 2007). For the CB1, in addition to GASP-1, also interacts with Beclin 2, which functions as an additional lysosomal degradation mediator. Disruption to Beclin-2 via heterozygous knockout in mice caused increased levels of CB1R in the brain, elevated food intake, weight, insulin resistance and defective autophagy and homozygous knockout mice resulted in decreased embryonic viability (He et al., 2013), highlighting the significance of receptor turnover via proteolytic degradation for cellular adaptations.

Like GPCR recycling, recent evidence has demonstrated that lysosomal sorting can also be regulated by the receptor's own signalling cascades. For example, the degradation of the D2R

is mediated by the phosphorylation of the second messenger PKC in addition to GASP-1 (Cho et al., 2010). Similarly, dopamine D3 receptor degradation, is also mediated by PKC via phosphorylation of specific residues at the receptor's C-terminal tail (Zhang et al., 2016). As other heterotrimeric G protein subunits are implicated to regulate membrane trafficking processes, the $G\alpha_s$ subunit has also been demonstrated to regulate lysosomal degradation via association with GASP-1, dysbindin and Hrs (ESCRT) at the EE, in addition to that of signalling (Rosciglione et al., 2014). Depletion of $G\alpha_s$ impaired the degradation for a selected number of GPCRs such as CXCR4, DOR and the angiotensin 1A receptor as receptors were unable to traffic to IVLs and therefore were retained mainly in the EEs (Rosciglione et al., 2014). Interestingly, $G\alpha_s$ has also been demonstrated to bind to ubiquitin to regulate the lysosomal sorting of other membrane receptors, such as the epidermal growth factor receptor (EGFR) (Li et al., 2017). Binding $G\alpha_s$ to ubiquitin was via a ubiquitin-interacting motif (UIM) in the N-terminal extremity of $G\alpha_s$. Mutation of this UIM prevented the interaction $G\alpha_s$ to Hrs, delaying the sorting of EGFR in ILVS of MVBs and subsequent lysosomal degradation (Li et al., 2017). Overall, the endocytic sorting of GPCRs to the lysosomal degradation pathway, like the endocytic sorting of GPCRs to the recycling pathway, is a complex and tightly regulated process that requires core components to fundamentally and locally tailor the endocytic pathway to the needs of GPCRs that are targeted to this pathway.

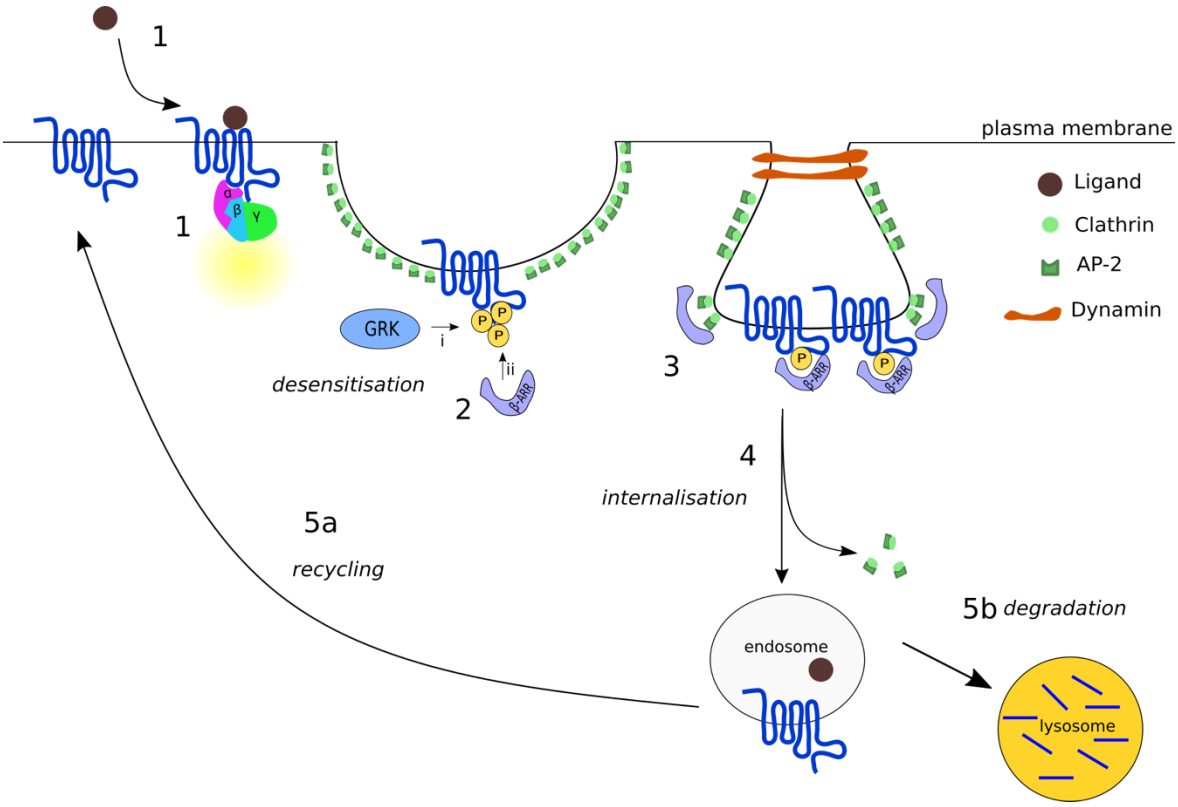


Figure 1.6 Regulation of GPCR trafficking. Ligand binding to the receptor leads to receptor activation, G protein coupling and signal transduction (1). Following G protein dissociation, receptors are phosphorylated (P) by GPCR kinases (GRKs) (2i), leading to the recruitment of β-arrestins (β-ARR) (2ii). β-ARR then interacts with clathrin and adaptor protein 2 (AP2) to target the receptor/arrestin complexes to clathrin coated pits (CCPs) (3). Dynamin, a GTPase, mediates the scission of the CCPs from the plasma membrane, forming clathrin-coated vesicles that then un-coats and fuses to endosomes where the receptor is internalised (4). The receptor is then dephosphorylated before returning to the plasma membrane (5a) or degraded to lysosomes (5b).

1.4.5 Multiplicity in GPCR signalling and activity

The ultimate function of GPCRs is to encode extracellular signals via its coupling to distinct heterotrimeric G proteins. However, as an individual cell can express a variety of GPCRs, understanding how such limited number of directed and regulated signalling pathways that produce distinct responses in different cell types can occur is a long-standing question. Different forms of GPCR signalling can take place in multiple ways and at different levels. GPCRs coupled to multiple G proteins can preferentially activate one signalling pathway over another; can interact with each other or with other types to receptors to form a macromolecular complex; undergo modifications that modulate receptor structure and

function; targeted to distinct endosomal location via the tight regulation of membrane trafficking. Each of these mechanisms will be discussed in dedicated subparagraphs.

1.4.5.1 Biased signalling

It has become increasingly appreciated that GPCRs are able to activate ensembles of signalling pathways organised as integrated networks (Kenakin, 2017). For example, certain GPCRs can couple to multiple G protein subtypes but preferentially activate a particular pathway, whereas others activate non-G protein signalling effectors via direct interaction with specific protein-protein interaction domains, redefining the classical GPCR signalling paradigm that GPCRs only signal through linear second-messenger-dependent cascades. Traditionally, receptors were thought to reside on the plasma membrane in an inactive confirmation and when binding to a specific ligand, conformation of the receptor changes to an active state which then allows the receptor to couple to its cognate G proteins and activate signalling pathways. Once activated, receptors would then undergo desensitisation by GRKs and β-arrestins, which were only limited to their ability to terminate G protein signalling, until accumulating evidence have now shown that they are able to induce an intracellular signalling independent of classical G protein signalling, such as ERK1/2 MAP kinases cascades (Daaka et al., 1998). Though increasing the complexity of GPCR signalling, such signalling has expanded the conceptuality of GPCR activation, in which GPCRs exist in multiple distinct active confirmations where each agonist-induced conformation confers distinct downstream effects. In this respect, certain agonists can induce differential receptor conformation which activates a distinct subset of signalling events, causing bias signalling. Biased signalling allows the receptor to be selectively activated in a manner that produces a biased response, as opposed to the simple activation by balanced agonists. Activation of β2AR with the β-blocker, propranolol and carvediolol, was an early example of an agonist with signalling bias. Propranolol and carvediolol are inverse agonists of β2AR, decreasing $G\alpha_s$-cAMP production, however was able to activate ERK1/2 via a G protein independent pathway (Azzi et al., 2003; Thanawala et al., 2014). The muscarinic M3 receptors (M3 mAChR), activated by different agonist, induced distinct patterns of phosphorylation or phosphorylation 'barcodes', resulting in different signalling outcomes (Butcher et al., 2011). Thus, in addition to distinct receptor

conformation by different agonist, different barcodes could explain for biased signalling (Butcher et al., 2011). Furthermore, agonist bias can also regulate post-endocytic sorting for some receptors. For instance, DOR when activated by two different tolerance DOR agonist, DPDPE and SNC-80, elicited different recycling profiles as result of distinct receptor conformations through different interactions with β-arrestin (Audet et al., 2012). SNC-80 induced internalisation led to sustained interaction with β-arrestin via its Gβγ subunit, which targeted DOR for degradation and generated acute analgesic tolerance in mice (Audet et al., 2012). Whilst, DPDPE internalisation led to a transient interaction with β-arrestins, allowing the receptor to efficiently recycle back to the plasma membrane and thereby producing less analgesic tolerance (Audet et al., 2012), demonstrating agonist-induced receptor trafficking bias. Similarly, activation of the glucagon-like peptide-1 receptor (GLP-1R) with exendin-phe1, an analog of exendin-4 led to a distinct conformation of the receptor that induced transient interactions with β-arrestins, resulting in rapid recycling, less receptor degradation and enhanced insulin secretion in beta cells compared to the unmodified exdenin-4 (Jones et al., 2018).

As GPCRs are the most important class of current drug targets, the complexity that biased signalling brings gives rise to an additional mechanism that can fine-tune cellular effects to desirable outcomes and thereby a therapeutically relevant target. An increasing number of drug developmental programs have now shifted from a simple agonist/antagonist method in targeting drugs, to a continuum of signal-tuning via biased agonists, and indeed, oliceridine, a bias agonist for the MOR, has already undergone phase 3 clinical trials (Ok et al., 2018).

1.4.5.2 Receptor homo-and-heterodimerisation

Conventionally, GPCRs were considered to exist and couple to G proteins primarily as monomeric entities. However, it has now become accepted that GPCRs have the capacity to form homodimers, heterodimers and oligomers and, importantly that these have significant relevant cellular outcomes (Jonas and Hanyaloglu, 2017). GPCRs have been found to form both homodimer and heterodimers with other GPCRs as early as during their protein synthesis, sorting at the level of ER and up to post-internalisation after signalling (Terrillon et

al., 2003; Milligan, 2004). One of the earliest reports of a GPCR dimer was that of rhodopsin dimers in mouse optic disc via atomic force microscopy (Fotiadis et al., 2004). An increasing number of GPCR dimers have been identified since then, not only among homogenous populations of receptors (i.e homo/oligomerisation) but also between two distinct kinds of receptors (i.e heterodimer/oligomerization). Through the use of resonance energy transfer approaches such as bioluminescence- and fluorescence resonance energy transfer (BRET and FRET, respectively), a technique that allows sensitive monitoring of distances between two proteins on a nanometre scale, demonstrated the presence GPCR dimerisation in intact cells in real time (Szidonya et al., 2008; Cottet et al., 2012; Lohse et al., 2012). This application revealed dimers are able to form constitutively or in response to ligand, and even when constitutive dimers are formed, ligand stimulation may induce the rearrangement into a dimeric form (Angers et al., 2002; Kroeger et al., 2001). Numerous significant cellular outcomes have been proposed for receptor homo- and heter-dimer/oligomers. As receptor dimerisation can occur as early as during the receptor's biosynthesis pathway, dimerisation has been demonstrated to be important for protein-folding, and correct transport of receptor from the endoplasm reticulum (ER) to the plasma membrane (Angers et al., 2002; Milligan, 2007). For example, full functionality of the metabotropic $GABA_B$ receptors was only achieved when both receptor's subtypes, $GABA_B$ R1 and $GABA_B$ R2, are both expressed. Interaction of both receptor's subtypes was also critical for signalling, specifically, $GABA_B$ R1 for ligand binding and $GABA_B$ R2 for G-protein coupling (Fritschy and Mohler, 1995). Furthermore, dimerisation can modulate receptor allosterism. During receptor dimerisation, the allosteric effects can be mediated by one receptor acting on the other, and therefore produce different downstream signalling from activation of the individual receptor alone (Gurevich and Gurevich, 2008). For instance, the thyrotropin receptor (TSHR) exhibits negative cooperativity when in homodimers, whereby ligand binding of one protomer reduces the ligand binding of the protomer (Allen et al., 2011). In a similar manner, hetero-dimerisation can induce changes in the pharmacology between two distinct GPCRs, whereby the heteromer complex alters the ligand affinity in one of the GPCRs or may modulate downstream signalling effects of one receptor while a ligand binds to the other receptor. This has been demonstrated for opioid and chemokine receptors (Dalrymple et al., 2008). Additionally, heterodimerisation can alter G protein coupling preference and specificity of co-expressed pairs of GPCRs. When two

receptors interact at the plasma membrane, coupling to its respective G protein subunit may be altered by the receptor's allosteric changes, causing a 'switch' in G protein coupling (Ferre et al., 2009). For example, the heterodimerization between DOR and MOR induces coupling to $G\alpha_z$ instead of their cognate, $G\alpha_i$ (Fan et al., 2005). Heterodimerisation of dopamine receptor 1 and 2 (D1 and D2) results in $G\alpha_{q/11}$ -mediated Ca^{2+} release, though D1 and D2 receptor signals via $G\alpha_s$ and $G\alpha_{i,}$ respectively (Lee et al., 2004). Also notably, the heterodimerisation of the CB1 and D2 switches CB1 coupling from $G\alpha_i$ to $G\alpha_s$ upon interaction with D2 (Kearn et al., 2005). In addition to modulation to signalling, hetero-dimerisation can also regulate receptor trafficking. For instance, DOR undergoes robust ligand-induced internalisation, whereas the κ-opioid receptor does not, however, when the two receptors interact, DOR is unable to internalised upon ligand stimulation (Jordan and Devi, 1999). Dimerisation can therefore expand pharmacological profiles and increase the diversity of signalling to fine-tune cellular outcomes (Smith and Milligan, 2010) (Figure 1.7). Majority of research on receptor dimerisation has been conducted in heterologous cell systems, however, new and emerging technological tools have recently become available for a more complete understanding of receptor dimerisation in native tissues (Gomes et al., 2016). To assess of receptor dimerisation in native tissues, it is important that receptor heterodimerisation must meet the following the criteria: both subunits of the receptors heterocomplex must be co-immunolocalised within the same cellular and subcellular compartment; physical interaction between both subunits should be documented in native tissue and the heteromer disruption should cause of loss of heteromer-specific functions (Gomes et al., 2016). Thus, with a fuller understanding of its significance *in vivo*, receptor dimerisation may become an attractive target for pharmacalogical intervention.

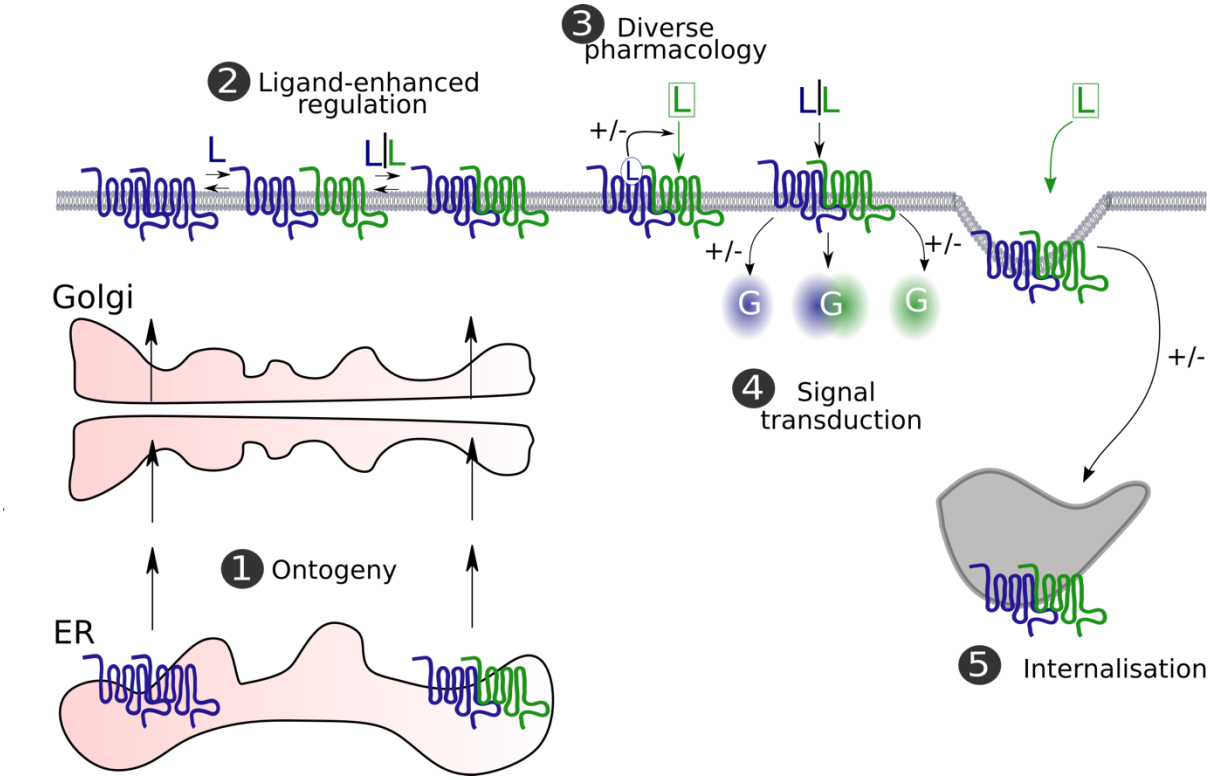


Figure 1.7 Dimerisation of GPCRs. GPCRs dimerisation can impact all aspects of GPCR function, signalling and trafficking. GPCR dimerisation can facilitate receptor maturation and correct transport from the endoplasm reticulum (ER) to the plasma memebrane (1). At the plasma membrane, specific ligand binding can regulate heterodimersation (2) and ligand allostery can either promote (+) or suppress (-) signalling (3) as well as alter G-protein coupling selectivity (4). Heterodimerisation can lead to the co-internalisation of two receptors after the stimulation of only one receptor (5). Alternatively, if one receptor internalises poorly, within in a heterodimer, can inhibit the internalisaiton of the complex. G, G protein; L, ligand; + increase, - decrease.

1.4.5.3 Post-translational modifications of GPCRs

Post-translational modifications (PTMs) are chemical changes to proteins that can take place after protein translation. Modifications can occur in a wide variety of types and primarily occur in the form of proteolytic cleavage events or covalent modifications at specific target sequences within a consensus sequence. Such modifications add diversification and are important to the regulation of GPCR function. The best characterised PTMs for GPCRs are phosphorylation, glycosylation, palmitoylation and ubiquitination.

Glycosylation

Glycosylation is the attachment of oligosaccharides to proteins during their biosynthesis in the endoplasmic reticulum (ER) and the Golgi apparatus (Dong et al., 2007). Glycosylation is important for various functions including, protein folding, protection form proteolysis, secretion, surface expression and intramolecular trafficking (Dong et al., 2007). Several forms of glycosylation can take place; however, N-glycosylation are the most common for GPCRs and occurs by targeting the asparagine residues in the extracellular part of the GPCRs at the consensus sequence NxS/T. This post-translational modification is important to ensure correct folding, surface expression, ligand recognition, signalling, dimerisation (Michineau et al., 2006).

Palmitoylation

Palmitoylation of GPCRs occurs by covalent attachment of palmitic acid, a 16 carbon saturated fatty acid, on one or more cysteine resides in the C-terminal tail of receptors (Goddard and Watts, 2012). The thioester bond that links the palmitate to the cysteine is cleavable and therefore the palmitoylation state of receptor can be used to regulate its activity and for some receptors can determine the formation of a fourth ICL, which can modulate receptor signalling by regulating G protein coupling and thus can produce different cellular outcomes to the same ligand. Palmitoylation can influence all aspects of GPCR function and signalling. Up to three palmitate groups can be found on a receptor's C terminal tail and each exerting distinct conformation, which may be selective to certain G protein interactions (Goddard and Watts, 2012). In addition, palmitoylation can influence the phosphorylation state of the receptor, by regulating desensitisation and internalisation and can also modulate internalisation independent of phosphorylation (Tobin and Wheatley, 2004). Furthermore, palmitate binding in the ER can ensure correct processing and trafficking of receptors to the plasma membrane and may target GPCRs to lipid rafts. However, not all palmitoylated receptors are associated with lipid rafts and not all lipid raft-associated GPCRs undergo palmitoylation (Chini and Parenti, 2009).

Ubiquitination

Ubiquitination is an enzymatic process that mediates the covalent, yet reversible, addition of ubiquitin, a highly conserved polypeptide of 76 amino acids to lysine residues at the C-terminal tail GPCRs. Ubiquitination is catalysed by three different enzymes that act in tandem: E1, a ubiquitin-activating enzyme, E2, a ubiquitin-carrying enzyme; and E3, a ubiquitin ligase (Kennedy and Marchese, 2015). A substantial number of GPCRs have been reported to be ubiquitinated and generally ubiquitination functions as an essential tag for post-endocytic sorting of internalised GPCRs to lysosomes (Bonifacino and Traub, 2003). Depending on the receptor, ubiquitination is not always required for lysosomal sorting, whilst for others, ubiquitination of the receptors facilitates their proteasomal degradation (Alonso and Friedman, 2013). Ubiquitination can be counteracted by deubiquitinating enzymes that deconjugate ubiquitin-modified proteins and therefore rescue receptors from degradation which they are then recycled back to the plasma membrane (Reyes-Turcu et al., 2009). In addition to directing GPCRs for degradation, ubiquitination has recently been demonstrated to be involved in vital downstream cellular functions for the PAR-1, a receptor regulated by ubiquitin. Ubiquitinated PAR-1 initiats the assembly of signalosomes by recruiting transforming growth factor β-activated kinase 1 binding proteins TAB1-TAB2 and resulted in the activation of p38 MAP kinase. The TAB1-TAB2 p38 signalling is essential for activated PAR1-mediated endothelial barrier permeability *in vitro* and vascular leakage *in vivo* (Grimsey et al., 2015; Grimsey et al., 2018).

Phosphorylation

Phosphorylation of proteins involves the addition of a phosphate group on serine, threonine or tyrosine residues mediated by protein kinases that transfer a phosphate from ATP to the protein (Zheng et al., 2013). Phosphorylation of GPCRs is part of the normal cycle of receptor activation and subsequent desensitisation that occur by the phosphorylation of residues contained in the third ICL and C-terminal tail of the receptor (Tobin et al., 2008). In general, phosphorylation is initiated by the combined action of GPCR kinases (GRKs) and β-arrestins

or by second messenger kinases, PKA and PKC that results in the internalisaiton of the receptor and termination of receptor signalling (Tobin et al., 2008).

PTMs of GPCRs dynamically affect almost all aspects of GPCR function and signalling, impacting not only ligand binding, receptor expression, intracellular trafficking but also impacts their adaptor proteins, thus, adding another layer of complexity to GPCR regulation.

1.4.5.4 Membrane trafficking

In addition to the different mechanisms that regulate GPCR signalling at the plasma membrane by post-translational modifications, GPCRs are extensively regulated by membrane trafficking in the endocytic pathway (Jean-Alphonse and Hanyaloglu, 2011). Once activated, GPCRs are uncoupled from their G proteins and internalised into lipid vesicles called endosomes. Once in endosomes, receptors are either recycled back to the plasma membrane for resensitisation or are degraded and delivered to lysosomes for proteolytic degradation. Recycling occurs by rapid desensitisation to prevent over stimulation; resensitisation prevents ligand resistance and degradations results in signal termination (Hanyaloglu and von Zastrow, 2008). This traditional model has now been redefined as several recent findings demonstrate that internalisation does not result in signal termination and that GPCRs are able to sustain or perform distinct signalling activities from endosomes (Eichel and von Zastrow, 2018). Membrane trafficking is a tightly regulated complex system that involves distinct endosomes and other intracellular compartments that function as both sorting and signalling platforms and requires specific endocytic machinery for efficient trafficking.

1.4.6 Endosomal trafficking and intracellular signalling

1.4.6.1 Endosomal signalling

Extensive investigations have revealed several mechanisms that modulate GPCR signalling following agonist occupancy, including agonist-elicited receptor desensitization, endocytosis and resensitisation (or degradation). However, there is now growing evidence that endocytic trafficking and signalling are not separate mechanisms and they work together in regulating

the correct temporal and spatial signalling outcomes. Spatiotemporal compartmentalisation of signalling can occur through various mechanisms that include (but are not restricted to) regulatory mechanisms that control the location and duration of receptor activation and signalling.

1.4.6.2 Signalling from the EE

Initial evidence that GPCRs are able to signal from endosomes was substantiated by studies demonstrating that β-arrestins functions as scaffolds to facilitate activation of MAPK signalling cascades on endosomes. The activation of angiotensin receptor subtype 1a (AT1aR), PAR-2, V2R, and substance P receptor (NK-1) resulted in the endosomal accumulation of receptor β-arrestins-MAP-ERK complex (DeFea et al., 2000; Luttrell et al., 2001; Tohgo et al., 2003). This complex mediated a 'second wave' of GPCR signalling occurring from endosomes that is distinct from G protein-dependent signalling at the plasma membrane.

Conventionally, GPCR-G protein signalling has been thought to occur exclusively at the plasma membrane and endosomal signalling occurs mostly through non-G protein mechanisms. However, sustained G protein signalling following GPCR endocytosis has been demonstrated for several GPCRs, suggesting G protein signalling can occur at the endosome. Both for the thyroid-stimulating hormone receptor (TSHR) and PTHR, internalisation is required for a sustained or persistent $G\alpha_s$ signalling from an endosomal compartment. The TSHR was found in an endosome-associated pre-Golgi compartment in close association with the $G\alpha_s$ subunit and adenylyl cyclase (Calebiro and Godbole, 2018), the internalisation of the PTHR occurred in association with parathyroid hormone and $G\alpha_s$, as an active ternary complex (Ferrandon et al., 2009). Among others, endosomal signalling has now been reported GLP-1R and CXCR4 (Girada et al., 2017). Comparably, a similar complex or a 'megaplex' was involved in sustained cAMP signalling by the V2R (Thomsen et al., 2016). Though, these studies provide mechanistic insight in sustained G protein signalling from internalised GPCRs, it was work using a GFP-tagged nanobody biosensor that provided direct evidence of an activated GPCR and its activated cognate G proteins occur in endosomes. The GFP-tagged nanobody that specifically recognises the activated, nucleotide free, form of $G\alpha_s$ (Nb37), showed that the β2AR $G\alpha_s$

signalling occurs in two temporally and spatially separate waves. First from the plasma membrane before internalization and then from endosomes after ligand induced endocytosis. Both waves of signalling led to a sustained cAMP accumulation (Irannejad et al., 2013). This work was direct evidence of spatially resolved endosomal G protein signalling and suggests that GPCRs indeed can initiate a second wave of signalling from the endosome. Interestingly, a subsequent study from this work showed that plasma membrane and endosomal G protein signalling activate distinct transcriptional profiles of downstream gene targets (Tsvetanova and von Zastrow). This suggests that endosomal GPCR-G protein activation exhibits a spatial control over the specificity of downstream cellular responses. Together, this shows that the endosomes not only function as sorting stations to direct receptors to their respective recycling or degradative fates, but they also regulate diverse intracellular signalling pathways at the EE following agonist activation.

1.4.6.3 Signalling from other endosomal and subcellular compartments

The EE was traditionally thought to be the first and primary platform that internalised cargo are first sorted to distinct cellular fates. However, the recently reported VEE, an endosomal compartment biochemically and morphologically distinct from the EE which certain GPCRs such as the LHR, β1AR and the follicle stimulating hormone receptor (FSHR) internalize to for their post-endocytic sorting (Jean-Alphonse et al., 2014), is shown to play an important role in direct spatial-temporal control of receptor signalling. The VEE is smaller than EE and lacks typical EE markers. However, the adaptor protein containing Pleckstrin homology (PH) domain, phospho-tyrosine binding (PTB) domain and leucine zipper motif (APPL1) is expressed in VEE subpopulations (Jean-Alphonse et al., 2014; Sposini et al., 2017). For the LHR, LH induced activation led to a sustained temporal profile of ERK signalling that required internalisation via the correct endosomal compartment, the VEE (Jean-Alphonse et al., 2014). In addition, a follow up study from this work showed that APPL1 negatively regulates LHR mediated cAMP production from the VEEs and that this indeed occurs within the endomembranes as the endosomal $G\alpha_s$ was acutely activated by LHR, and that Nb37 localizes to a subpopulation of LHR endosomes that also exhibits APPL1 co-localization (Sposini et al., 2017). The VEE therefore is an endosomal compartment that internalized receptors can be

sorted to distinct endocytic pathways and it tightly regulates spatially encoded signalling. Involvement of the VEE in the signalling of other GPCRs remains to be determined.

Late endosomes, or MVBs, may also be considered as GPCR signalling platform particularly for the CB1R and the Wnt activated frizzled receptor. Native CB1R not only interacts with $G\alpha_i$ in late endosomes but can also signal from this compartment to stimulate ERK phosphorylation (Rozenfeld and Devi, 2007). For the frizzled receptor when activated by Wnt proteins redistributes glycogen synthase kinase 3 from the cytosol into MVBs which leads to a sustained Wnt signalling and stabilizing β-catenin to activate gene transcription at the nucleus (Taelman et al., 2010). Endocytic inhibitors reduced this Wnt/β-catenin signalling, thereby demonstrating a role of MVB signalling (Koval et al., 2016).

A subset of GPCRs have shown to additionally or preferentially be localised to various intracellular compartment membranes such as the nucleus, mitochondria, endoplasmic reticulum and TGN where they can elicit distinct signalling responses. Among them, the metabotropic glutamate receptor 5 (mGluR5) can be found at the nuclear membrane as a functional receptor able to mediate sustained calcium signalling (O'Malley et al., 2003). The melatonin type 1 receptor (MT_1) found in the mitochondrial membranes activates $G\alpha_i$ signalling to mediate the inhibition of stress-induced cytochrome c release and capase activation resulting in protective effects against hypoxic-ischemic injury (Suofu et al., 2017) activated by FTY720, a synthetic S1PR agonist, elicited persistent $G\alpha_i$ signalling in the TGN (Mullershausen et al., 2009). Recently, the β1AR, which poorly internalizes to the EE, showed it can stimulate Gαs-mediated cAMP signalling from the TGN (Irannejad et al., 2017).

1.4.6.4 Physiological significance of intracellular and endosomal signalling

Although a growing number of GPCRs are able to signal from endosomes, the mechanisms and outcomes of endosomal signalling are incompletely understood, and its relevance to complex pathophysiological processes *in vivo* has recently been a subject of intense research. However, numerous studies have provided insights of the impact that endosomal signalling has in physiological and pathophysiological processes.

The importance of endosomal signalling in physiology was first highlighted when internalisation dependent sustained endosomal signalling to cAMP was required to ensure normal actin rearrangement in thyroid follicles and phosphorylation of vasodilator-stimulated phosphoprotein (VASP) (Calebiro et al., 2009). Another example is the duration of the PTH-induced calcaemic and phosphate responses in mice that are dependent of the PTH ligands, was related to the duration of cAMP signalling and the ability of certain ligands to stimulate cAMP from internalized PTHRs. The opposing antiatriuretic and antidiuretic actions of vasopressin and oxytocin, both activators of the V2R, were due to the different profiles of cAMP signalling exerted by the two hormones, with vasopressin producing an endosomal persistent cAMP production, which promotes the translocation of aquaporin water channels and epithelial sodium channels from intracellular vesicles to the apical membrane of collecting duct cells to increase renal water and sodium reabsorption. While oxytocin causing a short cAMP signal, limited only to the plasma membrane (Feinstein et al., 2011). Later, this model was extended to the β2AR, where the expression of cAMP-dependent genes and endosomal cAMP production was triggered by internalization of the receptor (Tsvetanova and von Zastrow, 2014). Endosomal signalling of β2AR to cAMP markedly increases the transcription of cAMP dependent genes, such as phosphoenolpyruvate carboxykinase 1, the gene encoding phosphoenolpyruvate carboxykinase 1 that determines the rate of gluconeogenesis, whilst plasma-membrane localised cAMP had no effect on this parameter (Tsvetanova and von Zastrow, 2014). In fact, endosomal signalling is crucial for transcription of cAMP dependent genes as distinct ligands of β2AR with differing binding affinities was able to elicit endosomal signalling and produced identical integrated response of gene transcription (Tsvetanova et al., 2017). Endosomal signalling acted as an ultrasensitive or molecular checkpoint that transforms the diversity at the upstream ligand-receptor interface into a stereotyped cell response to ensure biological signal fidelity, despite diverse ligand input (Tsvetanova et al., 2017).

Endosomal signalling may also have a role in regulating human disorders. The CaSR undergoes adaptor protein-2 (AP2)-clathrin-mediated internalisation to elicit sustained endosomal $G\alpha_{q/11}$ to maintain normal calcium homeostasis and synthesis of parathyroid hormone (PTH) (Gorvin et al., 2018). Mutations of AP2 caused by the sigma subunit of AP2 contributes to

increased surface expression of CaSR, reduced sustained $G\alpha_{q/11}$ signalling and sensitivity of CaSR to extracellular calcium causing hypercalcemia (Gorvin et al., 2018). Conversely, endosomal signalling by the PAR-2 is shown to be strongly implicated in irritable bowel syndrome (IBS) pain. The IBS pain mediated by hyperexcitability of nociceptors in colonic mucosa cells is dependent of PAR-2 activators and related to the duration of ERK responses in correspondence with the ability of activators to stimulate ERK from the internalized PAR-2 (Jimenez-Vargas et al., 2018). In which, a cholesterol-conjugated antagonist of PAR-2 prevented the capacity of proteases release from colonic mucosa that caused sustained hyperexcitability of nociceptors. Demonstrating that endosomally targeted antagonist to PAR-2 could represent a treatment for IBS pain (Jimenez-Vargas et al., 2018).

Together these studies highlight the importance of spatially directed G protein signalling and how the fine-tuning of cellular mechanisms in which they govern signalling outcomes has led to novel understanding of disease processes and in some cases, new therapies. Nonetheless, the understanding of the relative contributions of between plasma membrane and endosomal signalling to regulate complex pathophysiological processes is still incomplete and requires further investigations.

1.5 APPL1

1.5.1 The endosomal pathway

The endosomal pathway comprises of various endosomal compartments each of which have specific roles. The endosomal compartments differ in their biochemical composition, cellular location and morphology, and are regulated by different members of the Rab family of small GTPases and phosphoinositides, both of which functions as molecular tags (Behnia and Munro, 2005). Upon endocytosis, endocytic vesicles are generated from the plasma membrane, which then fuse with pre-existing EEs or undergo vesicles maturation to form new endosomes. During maturation of endosomes, the vesicles undergoes dramatic changes of major protein and lipid remodelling, and concurrent changes in the endosomal luminal mileu which ultimately forms EEs that transition into late endosomes (Huotari and Helenius, 2011).

Particularly, the V-ATPase, a multi-subunit proton pump, is essential for the acidification of EEs and late endosomes to pH values of ~7 and ~5 respectively, which allows many endo-lysosome functions, such as dissociation of receptor-ligand, protease activity and transport. Additionally, this transition mechanism is mediated by the recruitment of GTPase Rab5 which is achieved in coordination with GEF and the lipid composition of the endosome membrane that contains phosphoinositides (PIs) (Woodman, 2000). PIs then facilitates the specific incorporation of binding protein, phosphatidylinositol 4-kinase III α, which consecutively phosphorylates PIs into PtdIns(4) P and PtdIns(4,5) P2, resulting in PtdIns(3)P (Christoforidis et al., 1999), PDZ-binding proteins and arrestins which can also mediate protein sorting, vesicle budding, tethering and fusion, and cytoskeletal translocation (Rink et al., 2005). Thus, via regulation of Rabs that subsequently facilitates the recruitment of scaffolding proteins and effector proteins generates specific signalling microdomains within in the endosomal membrane.

1.5.2 APPL1 structure and its interacting proteins

APPL is a 709-amino acid adaptor protein found only in eukaryotes and is highly conserved in different species (Schenck et al., 2008). In the human genome there are two APPL isoforms, APPL1 and APPL2. They share 52% identity and 72% similarity in amino acid sequence and the same domain organisation (Li et al., 2007). Among the two, APPL1 is the most studied and for this reason, APPL1 will only be referred to, unless otherwise stated. APPL1 has been reported to be expressed in a number of cell lines including HEK 293 and HeLa cells and in a variety of tissues and organs (Mao et al., 2006). APPL1 is found in the heart, brain, ovary, pancreas, skeletal muscle, spleen (mice), brain marrow, gall bladder, GI tract, adipose tissue, and female breasts (Mitsuuchi et al., 1999; Rashid et al., 2009).

APPL1 mediates its function through several of its binding domains that permits it to interact with a variety of protein and membrane components. APPL1 domains include of N-terminal Bin–Amphiphysin–Rvs (BAR), also known as a Leucin-zipper motif; a central Pleckstrin homology (PH); a between PH and PTB (BPP); and a C-terminal phospho-tyrosine binding (PTB) domain (Mitsuuchi et al., 1999; Erdmann et al., 2007). The PTB domain functions as

adaptors or molecular scaffolds that can bind to tyrosine-phosphorylated proteins (Li et al., 2007).

APPL1 was originally identified through its association with Ser/Thr kinase Akt2 and subsequently was shown to interact with various transmembrane proteins of different classes, including the tumour suppressor deleted in colorectal cancer (DCC) and as a result APPL1 is also known as DIC13α (Mitsuuchi et al., 1999). To date, APPL1 is reported to interact with a variety of unique proteins including Rab proteins, receptors such as EGFR, N-methyl-D-aspartate (NMDA) receptor, FSHR, insulin receptor, adiponectin receptor, androgen receptor, kinases and phosphatases like PKC, PKA, PtdIns(3)P kinase (PI3K) and OculoCerebroRenal Syndrome of Lowe (OCRL), and PDZ ligands such as GIPC (Diggins and Webb, 2017). APPL1 does not binds to all of these proteins simultaneously but may interact with a subset of these proteins in a cell type dependent manner to mediate specific signalling pathways. Therefore, APPL1 functions as an adaptor protein that integrates different signalling and trafficking pathways to regulate many cellular processes (Diggins and Webb, 2017) (Figure 1.8).

Through its binding domains, APPL1 is subjected to numerous post-translational modifications (Liu et al., 2017). Among these, phosphorylation and ubiquitination are the most common (Gant-Branum et al., 2010). Phosphorylation of Ser410 by PKA regulates the binding of OCRL to APPL1 (Erdmann et al., 2007) and phosphorylation at Ser430 is implicated in ER stress (Liu et al., 2012). Phosphorylation at Tyr315 and 326 is involved in AKT mediated cell migration (Broussard et al., 2012). APPL1 undergoes ubiquitination at its lysine residues located within the BAR domain, ubiquitination at lysine160 enhances insulin stimulation, membrane localisation of APPL1 and membrane recruitment of and activation of AKT (Pilecka et al., 2011). Significance of other post-translational modifications have yet to be delineated.

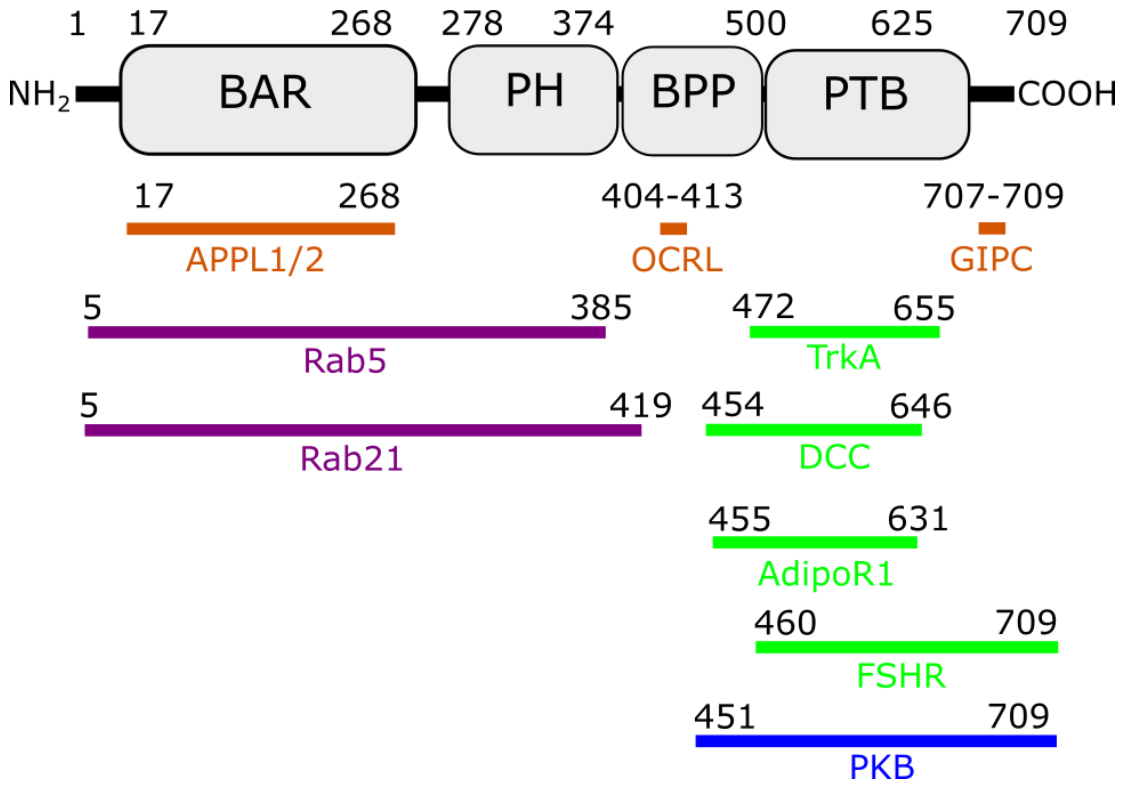


Figure 1.8. Schematic representation of APPL1 domains and interacting domains. Domains and interacting protein binding sites of APPL1. BAR, Bin/amphiphysin/Rvs domain; BPP, region between PH and PTB domains; PH; pleckstrin homology; PTB, phosphotyrosine binding. Numbers correspond to amino acid residues. Numbering of APPL1 domains based on Li et al. (Li et al., 2007). Interacting proteins are labelled as: orange, involved in trafficking and signalling; purple, trafficking; blue, signalling; green, receptors.

1.5.3 APPL1 in trafficking

APPL1 was first identified to be localised in the cytoplasm but predominately underneath the plasma membrane that may mark a transient and very early compartment (Miaczynska et al., 2004; Zoncu et al., 2009). Subsequently, imaging of endosomal compartments via multifocal plane, confocal, TIR-FM and structured illumination has uncovered that APPL1 may mark two distinct endosomal compartments. The first compartment, APPL1 positive endosomes that are highly motile tubulovesicular transport carriers that traffics cargo and fuses to EEs via interaction with Rab5. During this fusion APPL1 is lost and other Rab5-competing effectors are bound, WD Repeat and FYVE Domain Containing 2 (WDFY2) and early endosome antigen

1 (EEA1) (Gan et al., 2013). Similarly, incoming FcRN-loaded vesicles, that partially colocalises with APPL1/Rab4/SNX4, also causes the dissociation of APPL1, and binds to EEs (Gan et al., 2013). The second compartment are APPL1-positive intermediate vesicles that serve as precursors of EEs post endocytic formation of vesicles (Miaczynska et al., 2004). However, recent evidence has demonstrated that a subset of APPL1 endosomes are in fact distinct from the EE compartment and are very stable endosomes that can sort cargo to the recycling pathway without prior sorting from the classic EEs (Kalaidzidis et al., 2015). Indeed, this has recently been demonstrated for a subset of GPCRs, whereby depletion of APPL1 impaired the recycling of the LHR, FSHR and β1AR (Sposini et al., 2017). Additionally, cargo that is trafficked to EEs does not always require transiting to APPL1 endosomes as an intermediate step as demonstrated for the EGFR, which traffics to EEs via an ESCRT-0-positive compartment through an APPL1-independent route (Flores-Rodriguez et al., 2015), suggesting that they are alternative routes of endosomal maturation. In support of this, mathematic models have opposed the hypothesis of the obligatory mechanism of APPL1 endosome maturation into EEA1-positives one along the endocytic route (Kalaidzidis et al., 2015).

Although much progress has been made to delineate the APPL1 compartment, further studies will be needed to define the exact endosomal compartment that APPL1 marks. Either of the compartments proposed above are likely as APPL1 endosomes are very heterogenous and thus can regulate cell specific cellular processes, making them an attractive protein to further investigate.

1.5.4 APPL1 in signalling

Due to the specific positioning of the BAR-PH and PTB domain, APPL1 is able to interact with proteins involved different trafficking and signalling processes. In many signalling pathways APPL1 functions as a positive regulator, for example, it regulates AKT signalling to mediate cell survival (Schenck et al., 2008), enhances leptin signalling to promote leptin-induced proliferation and migration of cancer cells (Ding et al., 2016), promotes transcription of Wnt/β-catenin signalling target genes via forming of a complex with tumour repressor Reptin in complex with HDAC1 to relieve translational repression (Rashid et al., 2009), forms a

complex with NMDARs and PI3K/Akt via PDZ ligand binding at the C-terminal of NMDARs in rat cortical neurons to protect neurons against starvation-induced apoptosis (Wang et al., 2013), essentially interacts with GIPC for nerve growth receptor TrkA-induced ERK1/2 MAPK activation (Lin et al., 2006), interacts with Rab5 to stabilises EGFR expression levels and thereby, propagating EGFR signalling (Lee et al., 2011).

In contrast to positively regulating signalling specificity, APPL1 also negatively regulates signalling, particularly when localisation to the APPL1 endosomal compartment is essential. As an example, the lysophosphatidic acid receptor 1 (LPA1) binds with GIPC to traffic to APPL1 endosomes where its AKT signalling is initiated and is then trafficked to EEs that terminates the APPL1-AKT signalling (Varsano et al., 2012). This initial LPA1 endosomal localisation to APPL1 was essential as depletion of GIPC prolonged APPL1 induced AKT signalling by delaying the LPA1 trafficking to EEs, whereas depletion of APPL1 inhibited AKT signalling (Varsano et al., 2012), suggesting APPL1 indirectly negatively regulations AKT signalling and functions as a biochemical checkpoint for efficient LPA1 trafficking and signalling. More recently, APPL1 was also found to negatively regulate signalling for another GPCR, the LHR (Sposini et al., 2017). LHR endosomal cAMP signalling was enhanced when APPL1 was depleted, suggesting APPL1 regulates essential endosomal signalling (Sposini et al., 2017).

A further role of APPL1 is its ability to facilitate cross-talk between multiple signalling pathways. This has been demonstrated when APPL1 simultaneously interacted with the transforming growth factor β-activated (TAK) member TAK1 and the MAPK member mitogen-activated protein kinase kinase 3 to mediate p38 activation and regulate specific adiponectin signalling (Xin et al., 2011). Additionally, APPL1 also facilitates the cross-talk of the adiponectin and insulin signalling pathway. Stimulation with either insulin or adiponectin resulted in the recruitment of a pre-formed complex of APPL1 and insulin receptor substrate 1/2 that interacted with effectors of both the adiponectin and insulin signalling pathways to transduce signalling through PI3K, AKT and MAPK pathways to supress gluconeogenesis and promote lipogenesis and glucose uptake, thereby sensitising insulin signalling (Ryu et al., 2014). Together these highlights the ability of APPL1 to integrate and direct signals that regulate high complex and spatiotemporally regulated cellular processes.

1.5.5 Therapeutic implications of APPL1

The best characterised role of APPL1 is the regulation of insulin sensitivity. APPL1 protein levels were found to be supressed in both diabetic and overweight mice and in mice that lacked APPL1, experienced glucose intolerance from insulin resistance and impaired glucose-stimulated insulin secretion (Wang et al., 2013; Ryu et al., 2014; Cheng et al., 2012). Similarly, in lean mice that lacked APPL1 resulted in insulin resistance and hyperglycaemia (Cheng et al., 2009). In contrast, overexpression of APPL1 protects against obesity-induced deleterious impacts on glucose homeostasis and endothelial and cardiac functions, and alleviates hyperglycaemia, glucose intolerance and insulin sensitivity in diabetic mice (Wang et al., 2013; Cheng et al., 2009). APPL1 also promotes glucose-stimulated insulin secretion by promoting the AKT-dependent expression soluble *N*-ethylmaleimide-sensitive factor fusion protein in mice pancreatic β cells (Cheng et al., 2012). In addition, APPL1 preserves pancreatic β cell mass from apoptosis and inflammation by supressing the transcript nuclear factor-inducible nitric oxide synthase-nitric oxide axis in type 1 diabetes mice (Jiang et al., 2017). Moreover, a growing body of evidence has found mutations or genetic variations of APPL1 and 2 genes that are associated with ectopic adiposity, coronary artery disease, non-alcoholic fatty liver disease and familial onset of diabetes (Liu et al., 2017).

Furthermore, APPL1 has been implicated to be involved in Alzheimer's disease (AD) and Down syndrome (DS). In AD and DS, elevated levels of β-amyloid precursor protein (APP) and its cleaved products (APP-βCTF) recruits APPL1 to Rab5-positive endosomes; APPL1 then stabilises the active form of Rab5, leading to accelerated endocytic uptake, abnormal enlargement of endosomes and dysregulated axonal transport of Rab5 endosomes (Kim et al., 2016). Thus, APPL1 is an essential adaptor that links APP-βCTF to overactivation of Rab5 and to endosomal impairment in AD and DS.

1.6 FFA2/3

1.6.1 Relevance of SCFAs as signalling molecules

Metabolites are well known for their role in regulating a multitude of physiological processes; they function as crucial energy substrates and intracellular signalling molecules that act on enzymes such as histone deacetylases (HDACs) (Hinnebusch et al., 2002) and nuclear hormone receptors including peroxisome proliferator-activated receptors (PPARs) (Alex et al., 2013) and farnesoid X receptor (Mazuy et al., 2015). However recent research has uncovered that metabolites are also able to act as extracellular signalling molecules for a group of metabolite-sensing GPCRs found in many tissues that are involved metabolic regulation. One particular group of signalling molecules that has received a significant amount of attention as ligands for GPCRs are free fatty acids (FFAs). Fatty acids are categorised based upon by their carbon chain length. Short chain fatty acids (SCFAs) contain up to 6 carbons, medium chain fatty acids (MCFAs) have 7-12 carbons and long chain fatty acids (LCFAs) contain more than 12 carbons. Fatty acids have long been appreciated for their therapeutic potentials, especially for polyunsaturated fats such as omega-3 for prevention of neurological disorders and benefits towards metabolic and inflammatory health (Zivkovic et al., 2011). However, only recently have SCFAs become the interest of intensive research for its therapeutic potential, particularly for metabolic disorders. SCFAs are produced through fermentation of non-digestible carbohydrates (NDC) by the gut microbiome and also in response to alcohol consumption through ethanol metabolism in the liver (den Besten et al., 2013). In contrast, MCFAs and LCFAs are obtained primarily from dietary fats or synthesised *de novo* in the liver. Targeting the gut microbiome composition and signalling in general has been highlighted as a novel approach to treat metabolic and inflammatory disorders and understanding the underlying mechanisms how SCFAs exert their effects present a potential strategy.

1.6.2 Identification of SCFAs receptors

To develop successful therapeutic targets of FFAs, understanding how FFAs exert their physiological role is critical. The deorphanisation of GCPRs that can be activated by FFAs approximately 15 years ago uncovered that FFAs in addition to functioning as energy sources,

are also extracellular signalling molecules for GPCRs, making the FFA receptor family an attractive potential drug target. The FFA receptor family consist of four members: FFA1 (previously known as GPR40), FFA2 (previously known as GPR43), FFA3 (previously known as GPR41) and FFA4 (previously known as GPR120) (Davenport et al., 2013). FFA1 was the first to be deorphanised and responds to MFCAs and LCFAs. FFA2 and FFA3 are closely related and both exhibiting responsiveness to SCFAs with a preference for chain lengths of C2-C5. FFA4 responds to an FFA profile very similar to FFA1. FFA1-3 share relatively high sequence identity of 35-40% and tandemly located on chromosomal 19q131.1 in the human genome (Sawzdargo et al., 1997; Costanzi et al., 2008), whereas FFA4 is structurally distant (Hirasawa et al., 2005). Intriguingly, this genomic location also encodes GPR42, which shares 98% amino acid homology with FFA3, but its function remains largely unknown and is therefore considered a pseudogene. However, one study demonstrates that GPR42 is expressed in humans and may share a different pharmalogical profile in terms of SCFA preferences (Puhl et al., 2015). Thus, GPR42 may play a physiological role, but due to limited findings, this remains to be confirmed.

In addition to the FFA receptor family, there are three other receptors that have been reported to also respond to fatty acids: GPR84, OR51E2 and GPR109A (Milligan et al., 2017). GPR84 is reported to respond to MCFAs with preference to capric acid, a 10-carbon chain fatty acid), however as MCFAs are not the dominant ligands that GPR84 responds to, GPR84 thus remains an orphan GPCR (Wang et al., 2006; Mahmud et al., 2017). Olfr78 is a murine olfactory receptor (OR51E2 in human) found to be expressed in the kidney (Pluznick et al., 2013) and on PYY-secreting enteroendocrine cells (Fleischer et al., 2015). In response to SCFAs, Olfr78 has been demonstrated to positively modulate blood pressure (Pluznick et al., 2013). Although olfactory receptors are generally not considered as drug targets, it is intriguing that an olfactory receptor beyond their role in sensory function can also regulate peripheral functions in responses to SCFAs, however additional research is required to understand the function of this receptor. GPR109A has recently been deorphanised as a receptor for hydroxycarboxylic acids and is therefore also known as the HCA_2 receptor, however it also responds to C4-C8 fatty acids but at a lower potency than to its endogenous ligand β-hydroxybutyrate (Taggart et al., 2005). GPR109A has been demonstrated to regulate

lipolysis in adipocytes (Offermanns et al., 2011) and can mediate anti-inflammatory effects in immune cells and the colon (Graff et al., 2016). Additionally, another receptor GPR119, though responsive to 2-monoacylglycerols and oleoylethanolamides and is therefore not a true FFA receptor but is reported to act in concert with the FFA receptor family to stimulate the release of gut hormones following lipid consumption (Overton et al., 2008). Although the physiological function of these receptors is not yet fully understood, their expression in many cell types that are involved in metabolic regulation such as the GI system and immune cells makes them a prime target further studies.

1.6.3 SCFA receptors: FFA2 and FFA3

1.6.3.1 Pharmacology

Both FFA2 and FFA3 exhibit 43% amino acid sequence identity and are conserved across several mammalian species (Brown et al., 2003; Le Poul et al., 2003; Wang et al., 2010), thus, it not surprising that they also share overlapping ligand selectivity profiles. There is consensus that the shorter the carbon chain length of the SCFA, the higher the potency at FFA2 and vice versa for FFA3 (Priyadarshini et al., 2018). Correspondingly, FFA2 equally binds to acetate (C2) and propionate (C3) followed by butyrate (C4). Formate (C1) and pentanoate (C5) can also activate FFA2 but to a lesser extent and hexanoate (C6) shows no activity to FFA2 (Hudson et al., 2011). For FFA3, C3, C4 and C5 shows highest and equal potency, while binds to C2 and C6 to a lesser extent (Hudson et al., 2011) (Figure 1.9 A). As SCFAs can act on both FFA2 and FFA3 with varying degrees, there is also marked interspecies differences between SCFA binding for both receptors. C2 is 20-fold more selective at human FFA2 than at human FFA3. C3 is 12-fold more selective at mouse FFA3 while binds at a similar potency to human orthologs (Schmidt et al., 2011).

1.6.3.4 Signalling

Though SCFAs can activate both FFA2 and FFA3, they differ significantly in terms of signalling. During the deorpahnisation of FFA2, a range of G protein subtype chimeras were employed and revealed that FFA2 is a promiscuous receptor and couples to multiple members of the

$G\alpha_{q/11}$ and $G\alpha_{i/o}$ G protein families (Brown et al., 2003). FFA2 coupling to both $G\alpha_{q/11}$ and $G\alpha_{i}$ is now well established as a variety of functional assays for measuring, for instance, $G\alpha_{q/11}$-dependent Ca^{2+} release or $G\alpha_{i}$-coupled [^{35}S]-GTPγS incorporation are consistently employed (Hudson et al., 2013). Upon activation, FFA2 recruits β-arrestin 2 for its internalisation and signals dephosphorylation of NFκB, however it is not yet confirmed if whether this leads to desensitisation or if it can also activate G protein-independent signalling (Lee et al., 2013; Hudson et al., 2012a; Grundmann et al., 2018). Activation of FFA2 also results in phosphorylation of ERK1/2 MAPK (Hudson et al., 2012a; Grundmann et al., 2018). In contrast, FFA3 has a distinct signalling profile, as FFA3 only couples $G\alpha_{i}$ (Brown et al., 2003). Additionally, it is not likely that FFA3 recruits arrestins, as siRNA knock-down of β-arrestin in a mouse neuroblastoma cell did not attenuate propionate induced response (Kimura et al., 2011) (Figure 1.9 B).

Additionally, it has been recently reported that human FFA2 and FFA3 are able to undergo heterodimerisation (Ang et al., 2018), adding another level of dexterity to the signalling of SCFA receptors. Heterodimerisation of FFA2-FFA3 both *in vivo* and *in vitro* settings exhibited distinct signalling with significant enhancement of Ca^{2+}mobilisation above what was observed for FFA2 alone; enhancement of β-arrestin 2 recruitment and; reduced $G\alpha_{i/o}$ signalling (Ang et al., 2018). However, a limitation of these finding is the selective tissue range used in this study, where only macrophages and monocytes exhibited heteromers but not in colonic epithelial cells. The physiological relevance of the FFA2-FFA3 heteromer and its existence in other tissues warrants further clarification.

To further add complexity to the signalling mechanisms of the SCFAs receptors, FFA2 and its ligands are also able to elicit distinct signalling pathways. Ligand bias occurs when a ligand preferentially activates one signalling pathway over the other. Multiple synthetic allosteric ligands of FFA2 have been reported to selectively activate the $G\alpha_{q/11}$, $G\alpha_{i/o}$, or β-arrestin pathway (Bolognini et al., 2016b). One of the first selective ligands of FFA2, 4-chloro-α-(1-methylethyl)-N-2-thiazolylbenzeneacetamide (4-CMTB) was initially reported to be able to activate $G\alpha_{q/11}$, $G\alpha_{i/o}$ as well as β-arrestin pathways (Lee et al., 2008; Wang et al., 2010; Smith et al., 2011). However, in islets isolated from both WT and FFA2 knockout mice used in

glucose-stimulated insulin secretion (GSIS) studies, 4-CMTB displayed bias for $G\alpha_{i/o}$ over $G\alpha_{q/11}$ (Priyadarshini et al., 2015). Furthermore, in *in vitro* 4-CMTB was unable to induce intracellular calcium mobilisation in a mouse β cell line (Priyadarshini et al., 2015). Though these finding may suggest biased agonism specifically for 4-CMTB, SCFAs also display a certain level of signalling bias especially across different species orthologs. For instance, though the human FFA2 preferentially binds to acetate, acetate was unable to induce an intracellular calcium response in CHO cells overexpressing human FFA2 (Schofield et al., 2018). Furthermore, acetate had no net effect on GSIS in humans isIets despite being able to activate both $G\alpha_{i/o}$ and $G\alpha_{q/11}$ pathways (Priyadarshini et al., 2015). In contrast, in a mouse β cell line, acetate robustly induced intracellular calcium mobilisation and also enhanced GSIS in mouse islets via $G\alpha_{q/11}$ (McNelis et al., 2015). Therefore, the use of SCFAs and synthetic ligands of these receptors as mean to understand FFA2 and FFA3 functions and to specifically dissect specific physiological roles to each receptor remains a challenge. To overcome this, concomitant use of receptor knockout (KO) models are commonly employed to confirm receptor-dependent effects. However, usage of KO models has limitations and caution must be taken when interpreting results. The pharmacology of the remaining receptor may be modified through the loss of the other receptor through redundancy and functional compensation and a couple of studies have observed an altered expression of one receptor when the other was knocked down (Zaibi et al., 2010; Bjursell et al., 2011). Thus, designing of selective tools or perhaps merely a more in depth understanding of the mechanisms, such as membrane trafficking, that regulate such signalling pathways is crucial to understand how specificity in receptor signalling pathways are achieved.

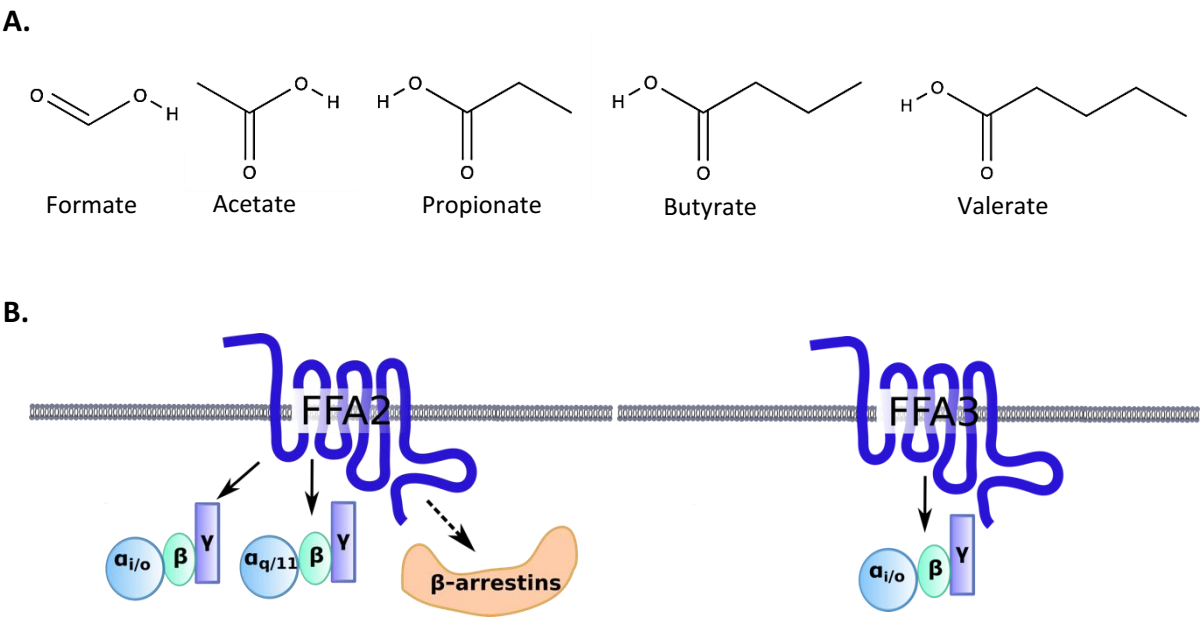


Figure 1.9 FFA2/3 signalling. Fatty acids with carbon chain length from 1 to 5 (A) can bind to FFA2 or FFA3 (B) to activate GPCR signalling. Chemical structures of short chain fatty acids (SCFAs) (A). Activation of FFA2 results in signalling through $G\alpha_{i/o}$ and $G\alpha_{q/11}$ G proteins. Limited studies suggest that FFA2 can also activate the β-arrestin pathway (dotted lines). Whereas, FFA3 only signals through $G\alpha_{i/o}$ G proteins (B).

1.6.3.5 Therapeutic implications of FFA2/3

Due to the widespread distribution of SCFAs in the body after entering the systemic circulation and their ability to act in an autocrine and paracrine manner in tissues that regulate metabolic processes does not make it surprising that FFA2 and FFA3 are expressed in a variety range of peripheral tissues. Both receptors are expressed in the gut epithelium with the highest levels found in enteroendocrine cells (Karaki et al., 2006; Nohr et al., 2013), which also express a variety of other metabolite sensing GPCRs that regulate the stimulation of gut hormone secretion that affect satiety and gut motility. FFA2 and FFA3 are also found to be co-expressed in the pancreatic β cells where they are known to regulate insulin secretion (Priyadarshini et al., 2015). FFA2, but less so FFA3, are also co-expressed in adipose tissues (Hong et al., 2005; Kimura et al., 2013a). In innate immune system cells including monocytes and granulocytes, FFA2 is highly expressed (Le Poul et al., 2003), highlighting a

potential relationship between metabolic regulation and immune response. Finally, in the sympathetic nerve ganglia only FFA3 was found to expressed where it plays a role in energy expenditure (Kimura et al., 2011). The physiological functions of FFA2 and FFA3 in these tissues and how they may be targeted therapeutically will be described below.

In the GI tract, both SCFAs and its receptors are found at high levels, suggesting a strong involvement of FFA2 and FFA3 in the regulation of GI processes. The direct role of FFA2 in stimulating the release of anorectic gut hormones GLP-1 and PPY was first demonstrated when acetate- and propionate- induced secretion of GLP-1 from colonic cultures was impaired in colonic cultures of FFA2 KO mice (Tolhurst et al., 2012). Conversely, cultures from FFA3 KO mice retained the ability of acetate and propionate to stimulate the release GLP-1, indicating the release of GLP-1 from colonic cultures to be a FFA2-dependent effect. In *in vivo* this was further confirmed by the infusion of propionate stimulated the increase the levels GLP-1 and PPY. This effect was attenuated by FFA2 deletion (Psichas et al., 2015). Further, through dietary supplementation of the fermentable carbohydrate, inulin, satiety levels in mice were augmented as result of an increase of PYY-producing cells and increasing PYY release, which was not observed in FFA2 KO mice (Brooks et al., 2017). Another peptide, an orexigenic hormone, ghrelin, one study demonstrated that acetate and propionate via FFA2 in ghrelin cells inhibited the release of ghrelin (Engelstoft et al., 2013). The ability of SCFAs and their receptors to regulate satiety are of great value for the treatment and prevention of obesity and indeed, inulin-propionate ester, a modified form of propionate which is chemically bound by an ester bond to inulin, is already in the early stages of human clinical trials (Chambers et al., 2015). However, the exact molecular mechanisms of SCFAs in regulating the release of GLP-1 and PPY still remained uncharacterised.

With somewhat success in identifying SCFAs and their receptors as potential targets to regulate satiety, similar efforts have consequently been made to identify a role of SCFA receptors in the treatment and prevention of diabetes. Complete elucidation of SCFAs and their role in this process has, however, been complicated by conflicting results from several studies. SCFAs treatment was shown to both enhance (Priyadarshini et al., 2015) and inhibit (Tang et al., 2015) glucose-stimulated insulin secretion GSIS. Disparity in the regulation of

GSIS could be due the preferential activation of FFA2 or FFA3 by stimulation with acetate or propionate (Bolognini et al., 2016b) and the diverse effects of $G_{q/11}$ versus $G_{\alpha/i}$ signalling in islets enhancing or inhibiting insulin secretion, respectively (Milligan et al., 2017). However, in the study of Tang et al., 2015 in FFA2 and FFA3 KO mice maintained on a high-fat diet improved their insulin secretory response, increased insulin secretion and improved glucose tolerance. Suggesting that under diet-induced obese and diabetic conditions, FFA2 and FFA3 may function as negative regulators of insulin secretion while reducing the risk of hypoglycaemia in healthy individuals (Tang et al., 2015). Similarly, in another study, via a $G_{q/11}$ FFA2 biased agonist, increased in β-cell proliferation in *in vitro* and *ex vivo* proliferation assays, which was not obverse in FFA2 KO mice (Villa et al., 2016). Together these studies suggest that FFA2 via specific signalling pathways may have a role in diabetes, however further studies are warranted to clarify this. Additionally, FFA2 may also have a role in regulating gestational diabetes. During pregnancy, FFA2 KO mice developed fasting hyperglycaemia, impaired glucose tolerance and diminished gestational expansion of β-cell (Fuller et al., 2015; Fuller et al., 2016).

The first role to be attributed to FFA2 and FFA3 was involved in neutrophil chemotaxis where in mice lacking FFA2 showed exacerbated inflammation in models of inflammatory colitis, arthritis and allergic airway asthma (Le Poul et al., 2003; Nilsson et al., 2003), (Maslowski et al., 2009). FFA2 protective effects in sodium sulphate (DSS)-induced colitis was further confirmed but also required GPR109A (Macia et al., 2015). A further suggested role of FFA2 and anti-inflammatory mechanisms in the gut was demonstrated when FFA2 was found to be expressed in intestinal Treg cells which decreases the response of inflammation-promoting immune cells (Smith et al., 2013). In fact, FFA2 mediated the expansion and enhanced the activity of Treg cells induced by SCFAs, which resulted in ameliorated colitis (Smith et al., 2013). Moreover, another study found that mice were protected against allergic inflammation in the lungs via a SCFA-FFA3 mediated enhanced generation of dendritic cells during impaired immune conditions (Trompette et al., 2014). While these findings indicate that both FFA2 and FFA3 possess anti-inflammatory roles via specific roles, there are additional studies that have indicated a pro-inflammatory role. In models of both acute and chronic colitis, DSS-treated FFA2 KO mice demonstrated reduced accumulation of intestinal

polymorphonuclear leukocytes, reduced colonic inflammation and attenuated colonic tissue damage (Sina et al., 2009). In another separate study, however, an increase of inflammation was demonstrated and mortality in a FFA2 KO murine model of colitis. Thus, the role of SCFA receptors as a target for inflammation requires additional studies.

Numerous SCFA-mediated processes in adipocytes have also been investigated to determine a physiological role of SCFA receptors and while some effects are well established, for instance SCFAs-FFA2 mediated suppression of lipolysis in immortalised and primary murine adipocytes (Ge et al., 2008) and, others are the impact on adipogenesis and secretion of orexigenic leptin, are not as understood. Several findings have suggested FFA2 to have a role in adipogenesis, although with opposing effects. FFA2 expression was demonstrated to be upregulated during differentiation of an adipocyte cell line (Hong et al., 2005). However, whether these effects are physiologically relevant is still unclear as differentiation could not be replicated in human primary adipocytes (Dewulf et al., 2013). In *in vivo*, FFA2 has been demonstrated to decrease insulin signalling in white adipose tissue, resulting in protection against diet-induced obesity (Kimura et al., 2013a). However, these effects were specific to the genetic background of the mice as the differences in body weight were only observed in mice of a 129/SvEv but not C57BL/6 background. Additionally, conditions that the mice were kept in also impacted these findings whereby mice that were housed under specific pathogen free conditions had lower concentrations of SCFA in their faecal than mouse housed under standard conditions and were not protected against diet induced obesity (Kimura et al., 2013a). This may be due to the effect of housing conditions on the composition of the intestinal microbiota. FFA3 has also been reported to have a role in regulating adipocyte physiology. In *in vitro*, studies found that FFA3 activation increases leptin secretion, as propionate induced leptin secretion was attenuated by FFA3 small interfering RNA (siRNA) knockdown (Xiong et al., 2004). However, several groups have been unable to detect FFA3 expression in adipose tissue (Hong et al., 2005; Zaibi et al., 2010; Frost et al., 2014).

In the sympathetic nerve ganglia both in mice and human, FFA3 is found to be expressed. Propionate via FFA3 is able to directly activate sympathetic neurons, whilst β-hydroxybutyrate, a ketone body produced during starvation or in diabetes, suppresses

sympathetic activity by antagonising FFA3 (Kimura et al., 2011). This suggest that FFA3 expressed on sympathetic neurons may play in energy expenditure. Additionally, FFA3 was also expressed in the submucosal and myenteric ganglia of the enteric nervous system (Nohr et al., 2013). The significance of FFA3 expressed in these tissues however is not currently known, though FFA3 was found to be localised to neurons of vasoactive intestinal peptide, indicating that SCFAs may be sensed on secretomotor neurons responsible for the regulation of water and electrolyte secretion form enterocytes (Nohr et al., 2013).

Though a substantial amount of evidence has suggested SCFA and its receptors do have roles in a variety of physiological processes, an overview of the published findings make it clear that we are still far from obtaining a full understanding of the exact underlying mechanisms of FFA2 and FFA3 in these processes (Ang and Ding, 2016). The only physiological aspect that studies so far that has not produced contradictory results is the promotion of anorectic gut hormone release, thus whether SCFA receptors are indeed a prime therapeutic target is still unclear.

1.7 Summary and general aims

The novel discovery of SCFAs and their receptors, FFA2 and FFA3, and their role in metabolic regulation, particularly in energy homeostasis has opened the possibility of adapting a physiological approach for anti-obesity treatments. However, the underlying mechanisms of SCFAs and the release of anorectic gut hormones remained poorly understood. An essential system that regulates GPCR signalling capacity to produce specific cellular outcomes is endocytic membrane trafficking. Endocytic membrane trafficking was conventionally considered as a system of plasma membrane signal termination for receptor resensitisation or downregulation, however now has been redefined to a highly complex system that composes of distinct endosomal compartments that regulates signalling in a spatiotemporal manner to produced specific cellular functions. Therefore, this thesis elucidates the trafficking properties of FFA2 and its impact on SCFA-induced signalling and stimulation of anorectic gut hormones release.

Hypothesis:

SCFAs are able to stimulate the release of anorectic gut hormones via FFA2 and/or FFA3 by the regulation of distinctive signalling pathways and trafficking properties.

Therefore, the general aims of this thesis were to:

1. Define the fundamental SCFA-induced signalling pathways.
2. Characterised the modes of endocytic trafficking of FFA2 and its role in FFA2 signalling.
3. Understanding how the above pathways of SCFA can regulate the release of anorectic gut hormones.

Chapter 2:

Materials and Methods

2.1 Materials

2.1.1 Primary antibodies

Antibody	Species	Manufacturer	Catalogue no.	Dilution WB	Dilution IF (FACS/ Confocal)
APPL1	Rabbit	Cell Signalling	3858	1:1000	1:500
β-ARR 1/2	Rabbit	Cell Signalling	4674S	1:1000	N/A
EEA1	Rabbit	Cell Signalling	3288S	N/A	1:500
Flag M1	Mouse	Sigma-Aldrich	F3040	N/A	1:500
GAPDH	Mouse	Millipore	AB2302	1:1000	N/A
Phospho-p38 (Thr183/Tyr185)	Rabbit	Cell Signalling	9211	1:500	N/A
Total-p38 (Thr180/Tyr182)	Rabbit	Cell Signalling	9212	1:500	N/A
GLP-1	Mouse	Abcam	AB23468	1:500	N/A
PYY	Rabbit	Abcam	AB22663	1:1000	N/A

2.1.2 Secondary antibodies

Antibody	Species	Reactivity	Manufacturer	Catalogue no.	Dilution WB	Dilution (FACS/ Confocal)
Alexafluor 488	Goat	Mouse	Thermo Fisher	A11001	N/A	1:1000
Alexafluor 488	Goat	Rabbit	Thermo Fisher	A11008	N/A	1:1000
Alexafluor 555	Goat	Mouse	Thermo Fisher	A21422	N/A	1:1000

Alexafluor 555	Goat	Rabbit	Thermo Fisher	A21428	N/A	1:1000
Alexafluor 647	Goat	Mouse	Thermo Fisher	A21235	N/A	1:1000
Alexafluor 647	Goat	Mouse	Thermo Fisher	A21245	N/A	1:1000
DAPI	N/A	N/A	Sigma-Aldrich	D8417	N/A	1:1000
Horseradish Peroxidase (HRP) conjugated IgG	Goat	Mouse	Santa Cruz	Sc-2005	N/A	1:5000
Horseradish Peroxidase (HRP) conjugated IgG	Mouse	Rabbit	Santa Cruz	Sc-2357	N/A	1:5000

2.1.3 Plasmids

DNA Construct	**Source**
Flag-β2AR	Mark von Zastrow
Flag-LHR	Aylin Hanyaloglu
Flag-FFA2	Natarin Caengprasath
Gαi-Venus	Johnathan Javitch
Gβ	Eric Reiter
Gγ	Eric Reiter
Mcherry-S410A APPL1	Silvia Sposini
Mcherry-S410D APPL1	Silvia Sposini
SEP-LHR	Silvia Sposini
SEP-FFA2	Natarin Caengprasath

2.1.4 Primers and siRNAs

qPCR primers	**5'-3'**
FFA2 (mouse) fwd	CGAGAACTTCACCCAAGAGC
FFA2 (mouse) rev	TGAGGGAACTGAACACCACA
FFA3 (mouse) fwd	CAATACTCTGCATCTGTGAC
FFA3 (mouse) rev	CAGGTAGACGGAAAAGAAA
Cloning primers	
FFA2 (mouse) fwd Afe1	GCTGATGACCCCAGACTGGCACAG
FFA2 (mouse) fwd Xba1	GCTCTAGACTACTCGGTGACAAATTCAGAACTCTG
FFA2 Trunc 296-T	GCAAAGGGGTACAGTGAATTTGTCACCGAG
FFA2 Trunc 323-T	CAATCCTGCCTCCTGAATGCTGGGCAGGG
Prolactin signal sequence	GGTGTCAAATCTACTCTTGTGCCAGGGTGTGGTCTCC
siRNA sequence	**FW 5' – 3'**
Scramble	ATTCTCCGAACGTGTCACG
APPL1 (human)	GACAAGGTCTTTACTAGGTGTATTT
APPL1 (mouse)	Thermo Fisher (MSS231842)
FFA3	Thermo Fisher (MSS248195, MSS248196, MSS248197)

2.1.5 Inhibitors and activators

Inhibitor	**Target**	**Manufacturer**	**Catalogue Number**	**Final concentration**
Cyclohexamide	Protein synthesis	Sigma-Aldrich	C104450	10 μg/ml
Dyngo-4a	Dynamin	Abcam	ABI20689	50 μM
IBMX	Pdes	Sigma-Aldrich	I5879	500 μM
Phenylmethylsulfonyl fluoride	Serine protease	Sigma-Aldrich	P7626	1 mM

Protease inhibitor cocktail EDTA-free tablets	Serine and cysteine proteases	Roche	4693159001	1 tablet per 10 ml
Sodium fluoride (NaF)	Serine/Threonine phosphatase	NEB	P0759S	1 mM
Sodium orthovandate ($NaVO_3$)	Tyrosine phosphatase	Sigma-Aldrich	S6508	1 mM
Ptx	Gαi	Tocris	3097	200 ng/μL
YM254890	G$\alpha_{q/11}$	Wako	257-00631	10 μM

Activators	**Target**	**Manufacturer**	**Catalogue Number**	**Final concentration**
Forskolin	Transmembrane adenylyl cyclase	Cayman	Cay11018	3 μM

2.1.6 Chemical reagents

Reagent	**Manufacturer**
2-Mercaptoethanol	Sigma-Aldrich
Absolute ethanol	VWR
40% Acrylamide/Bis solution	Thermo Fisher
Activated charcoal	Sigma-Aldrich
Ampicillin	Sigma-Aldrich
Agarose Powder	Sigma-Aldrich
Ammonium persulfate (APS)	Sigma-Aldrich
Bovine serum albumin (BSA)	Sigma-Aldrich
Bovine serum albumin fatty acid free	Sigma-Aldrich
Bromophenol blue	Sigma-Aldrich
Chloroform	VWR
Collagenase XI	Sigma-Aldrich

Deoxynucleotiede triphosphate (DNTPs)	Life Technologies
Dminethyl sulphoxyde (DMSO)	Sigma-Aldrich
Dithiothereitol (DTT)	Life Technologies
Ethylenediaminetetraacetic acid (EDTA)	Sigma-Aldrich
Gelatine powder	Sigma-Aldrich
Glycerol	Sigma-Aldrich
HEPES	Gibco
Hydrochloric acid	Sigma-Aldrich
Igepal	Sigma-Aldrich
Isopropanol	VWR
Lysogeny broth or Luria Bertani broth (LB)	MP Biomedicals
Magnesium chloride	Sigma-Aldrich
Methanol	VWR
Monopotassium phosphate	VWR
Paraformaldehyde	Sigma-Aldrich
Phosphate buffered saline (PBS)	Sigma-Aldrich
PBS with Ca^{2+}/Mg^{2+}	Sigma-Aldrich
Poly-D-lysine hydrobromide	Sigma-Aldrich
SDS solution 10% w/v	Bio-Rad
Sodium azide	Sigma-Aldrich
Sodium chloride	Sigma-Aldrich
Sodium acetate	Sigma-Aldrich
Sodium butyrate	Sigma-Aldrich
Sodium propionate	Sigma-Aldrich
Sodium Deoxcycholic acid (monohydrate)	Sigma-Aldrich
Sodium Hydroxide	Sigma-Aldrich
Sodium phosphate dibasic dihydrate	VWR
Tetramethylethylenediamine (TEMED)	Sigma-Aldrich
Tris base	Sigma-Aldrich
Tris HCL	Sigma-Aldrich
Triton X-100	Sigma-Aldrich

Trizol	Life Technologies
Tween 20	Sigma-Aldrich

2.1.7 Kits

Kits	**Manufacturer**
cAMP Dynamic 2	Cisibo
Dnase I, Rnase-free	Thermo Scientific
Fluo-4 Direct Calcium Assay	Thermo Fisher
HiSpeed Plasmid Maxi	Qiagen
IP-One	Cisibo
Proteome Profiler Human Phospho-Kinase Array	R&D Systems
Qiaprep Spin Mini	Qiagen
Qiaquick Gel Extraction	Qiagen
Quick Ligation	NEB
Quikchange II Site-Directed Mutagnesis	Agilent
Superscript™ IV First-Strand Synthesis System	Invitrogen

2.1.8 Cell culture reagents

Reagents	**Manufacturer**
Dulbeccco's modified eagles medium (DMEM) ± phenol red	Sigma-Aldrich
Fetal bovine serum	Sigma-Aldrich
Geneticin (G418)	Thermo Fisher
L-15 Medium (Leibovitz)	Sigma-Aldrich
Lipofectamine 2000	Thermo Fisher
Lipofectamine RNAiMax	Thermo Fisher
Opti-MEM I reduced serum media	Thermo Fisher
Opti-MEM I reduced serum media + HEPES	Thermo Fisher
Penicillin/Streptomycin	Thermo Fisher
Trypsin-EDTA solution	Thermo Fisher

2.1.9 Miscellaneous

Miscellaneous	Manufacturer
0.22 μM syringe filters	Millipore
8 well Nunc Lab-Tek chamber slides	Thermos Scientific
384 low volume well plate	Greiner
DEPC Treated Water	Sigma-Aldrich
DNA loading dye	Bioline
ECL Hyperfilm	GE Healthcare
Fluoromount G with DAPI	Thermo Fisher
Glass bottomed petri dishes (35mm)	Mattek Corporation
Glass coverslips	Menzel-Glazer
Hybond blotting paper	GE Healthcare
Hyperladder DNA marker	Bioline
Luminata Classico HRP substrate	Millipore
Luminata Forte HRP substrate	Millipore
Microamp™ Optical Adhesive Film	Applied Biosystems
Microamp™ Optical 96-Well Reaction Plate	Applied Biosystems
Microscope slides	Appleton Woods
Nitrocellulose blotting membrane	GE Healthcare
Nuclease-Free Water	Ambion
Non-fat dried milk powder	Sigma-Aldrich
Pageruler Plus prestained protein ladder	Thermo Fisher
Plasticware	Corning
Power SYBR® Green PCR Mastermix	Applied Biosystems
Primers	Life Technologies
Rnase Zap	Sigma-Aldrich
SYBR Safe DNA Gel Stain	Invitrogen

2.1.10 Buffers and solutions

Deionized and distilled water was used to prepare all solutions and buffers and were stored at room temperature, unless otherwise stated.

2.1.10.1 General

Phosphate buffered saline (PBS): 140 mM NaCl, 2.5 mM KCl, 1.5 mM KH_2PO_4, pH 7.2, 1.5 mM Na_2HPO_4, pH 7.2

Tris buffered saline (TBS): 130 mM NaCl, 20 mM Tris pH 7.6,

TBS-Tween 20 (TBS-T): 0.2% Tween 20 in TBS (1x)

Tris/Borate/EDTA (TBE): 1 M Tris base, 1 M Boric acid, 0.02 M EDTA

2.1.10.2 Immunofluorescence

FACs buffer: 2% (v/v) FBS in PBS with Ca^{2+}/Mg^{2+}

4% Paraformaldehyde solution: 4% PFA (w/v) in PBS, pH 7.2-7.4 with NaOH. Store at -20°C (long storage) or at +4°C (1 week).

Primary mouse anti-FLAG antibody stripping solution: 0.04 M EDTA in PBS

Cell permeabilization solution: 0.2% Triton-x (w/v) in PBS with Ca^{2+}/Mg^{2+}

Blocking solution and antibody incubation: 2% (v/v) FBS in PBS with Ca^{2+}/Mg^{2+}

2.1.10.3 Western Blotting

Cell lysis buffer: 10mM Tris-HCL (pH 7.5), 0.5 mM EDTA, 150 mM NaCl, 1% (v/v) Triton X-100, 1mM PMSF, 1 mM NaF, 1 mM $NaV0_3$. Stored at 4°C for 1 week.

SDS Tris-Glycine running buffer 10X: 250 mM Tris Base, 1.9 M Glycine pH 8.3, 1% (w/v) SDS

Transfer buffer 10X: 250 mM Tris Base, 1.9 M Glycine pH 8.3

Transfer buffer 1X: Cold distilled water, 10X Transfer buffer, 20% (v/v) Methanol

2X Laemmli buffer: 50 mm Tris-HCl, pH 6.8, 1% (w/v) SDS, 10% (v/v) glycerol, 2% (v/v) β-mercaptoethanol 0.002% (w/v), Bromophenol blue

Stripping buffer: 100 mM β-mercaptoethanol, 2% (v/v) SDS

Blocking buffer and antibody incubation solution: 5% (w/v) non-fat milk in TBS-Tween

2.1.10.4 SDS Polyacrylamide Gels

Separating gel: 380 mM Tris HCL (pH 8.8), 0.1% (v/v) SDS, 1% (w/v) APS, 12% Acrylamide Bis solution, TEMED added at 1:2000

Stacking gel: 80 mM Tris HCL (pH 6.8), 0.1% (w/v) SDS, 1% (w/v) APS, 5% Acrylamide Bis solution, TEMED added at 1:1000

2.1.10.5 Bacterial media

LB Broth: 1% (w/v) Bacto Tryptone, 0.5% (w/v) Yeast extract, 0.5% (w/v) NaCl. Made up in sterile water and autoclaved.

LB Agar: LB Broth + 1.5% (w/v) Agar

NZY+ Broth: 5g NaCl, 10 mM MgCl, 10g NZ amine, 0.5% (w/v) Bacto yeast extract

2.1.10.6 Radioimmunoassay

Phosphate buffer: 1L boiled distilled water and allowed to cool, 48 g $Na_2HPO_4.2H_2O$, 4.14g $KHPO_4$, 18.61g EDTA, 2.5g NaN_3. Stored at +4°C up to a month.

Phosphate buffer with gelatin

The buffer is produced as above, except that 12.5 g gelatin is added. Stored at +4°C up to a month.

Dextran-coated charcoal buffer: 2.4 g Charcoal, 0.24 g Dextran, dissolved in 100 ml phosphate buffer with gelatin and stirred for 20 minutes.

Secretion buffer: 40 mL HBBSS, 1% (v/v) HEPES, 0.1% (w/v) BSA fatty acid free, pH to 7.4 with NaOH.

Cell lysis buffer: 10mL of DW, 0.25 g $C_{24}H_{39}NaO_4.H_2O$ (sodium deoxycholate monohydrate), 0.88g NaCl, 0.5mL Igepal, 80 mM Tris HCL, pH 8, 1 tablet of complete EDTA-free protease cocktail inhibitor. Store at 4°C and use within 1 week.

2.2 Molecular Biology methods

2.2.1 Preparation of chemically competent cells

Propagation of all plasmids in this work was carried out using the *Escherichia coli* (E. coli) DH5α strain. Bacteria, stored at -80°C, was defrosted on ice and streaked onto freshly prepared LB agar plates using sterile technique and incubated at 37°C overnight. Using sterile technique, a single colony was picked and inoculated into 5 mL of LB broth at 37°C on a rocking platform shaker overnight. The following day, 200 μL of the bacteria culture was added and to 200 mL of LB broth and incubated at 37°C on a platform shaker. Aliquots were taken at regular intervals and the optical density (OD) was measured. Once an OD of 0.2-0.4 at 600 nm was reached growth was stalled by incubation of cultures on ice for 10 minutes, before centrifugation at 1118 *g* for 10 minutes at 4°C. The supernatant was removed, and the pellet was resuspended in 30 mL ice-cold sterile 100 mM $CaCl_2$ and 10% glycerol. The cells were then aliquoted and used to immediately or snap-frozen with dry ice and stored at -80°C. This procedure was carried out near a flame to ensure sterility.

2.2.2 Transformation of bacteria by heat shock and purification of plasmid DNA

An aliquot of DH5α cells (50 μL) was thawed on ice and ~1μg of appropriate plasmid DNA was added, mixed gently by tapping and then incubated on ice for 20 minutes. The cells were transferred to a 42°C heat block and heat shocked for 30 seconds and then placed back on

ice for 2 minutes before the addition of 950 μL of LB Broth. The mix was incubated at 37°C for 45 minutes, with shaking to allow cell recovery. The cells were then centrifuged at 2800 *g* in a benchtop microcentrifuge for 5 minutes at room temperature. Using sterile technique, 900 μL of the supernatant was removed and the remaining culture of 100 μL was resuspended and about 50μL of the resuspendended cells are streaked on appropriate-containing (100 μg/mL ampicillin or 50 μg/mL kanamycin) LB agar plates and placed in a 37°C incubator overnight. The next day, a single colony was picked and inoculated in 10 mL (mini-prep) or 200 mL (maxi-prep) of LB broth containing 100 μg/mL ampicillin or 50 μg/mL kanamycin and grown at 37°C on a platform shaker. Cells were then centrifuged at 10000 *g* at 4°C for 15 minutes and the supernatant was removed. Subsequently, the plasmid DNA was purified from this pellet using the QIA Prep Spin Mini (Qiagen) or HiSpeed Plasmid Maxi (Qiagen) kit as described in the manufacturer's manual. The obtained DNA was eluted with DEPC-treated water, concentration and quality was determined using the ND-2000 spectrophotometer (NanoDrop) at A260/A280 and A260/230, respectively. DNA preps would have an optimal A260/A280 ratio of 1.8-2.0 and a A260/230 ratio between 2.00 and 2.20.

2.2.3 Cloning

2.2.3.1 FLAG-tagging FFA2

To N-terminally tag FFA2, the full-length mouse FFA2 was amplified from the mouse FFA2 plasmid with expression vector pCMV6 (Orgiene) using 5'-3' primers containing restriction sequences recognised by the enzymes *XbaI* and *AfeI* (primer sequences in Material and Methods 2.1.4). The PCR reaction was as follows: 5 μL Q5 Reaction Buffer, 1 μL of each forward and reverse primers (at 100 μM), 1 μL of Q5 High Fidelity DNA polymerase, 10 ng of FFA2 template and made up to a total of 50 μL with DEPC-treated water. The reaction mix was then subjected to the following cycling conditions: 95°C for 2 minutes (denaturation), 35 cycles of: 95°C for 20 seconds (denaturation), 67°C for 30 seconds (annealing) and 70°C for 60 seconds (extension); following by a final elongation step of 70°C for 10 minutes.

FFA2 PCR fragment was then subcloned into a pcDNA3.1 vector. The pcDNA 3.1 vector was carrying prolactin signal sequence (primer sequences in Material and Methods 2.1.4) followed

by FLAG-LHR and to replace the LHR sequence with FFA2, the FFA2 insert and LHR were both digested using the restriction enzymes, *XbaI* and *AfeI*. This was carried out by incubating 41 µL of the amplified FFA2 product with 5 µL of CutSmart Buffer and 1 µL of each of the *XbaI* and *AfeI* restriction enzymes to make a final volume of 50 µL. For the FLAG-LHR, the same mix was used with 1 µg of plasmid and made up to 50 µL with DEPC-treated water. The reactions were incubated for 2 hours at 37°C and separated by electrophoresis on a 1% (w/v) agarose gel containing SYBR Safe DNA Gel stain (1:10000). A molecular weight marker, HyperLadder, was loaded alongside the samples to determine size. The insert (approximately 1 kbp) and linearised plasmid containing only the FLAG-tag (approximately 5.4 kpb) were excised and purified with QIAquick Gel Extraction Kit (Qiagen) and the concentration was determined using a ND-2000 spectrophotometer (NanoDrop).

Ligation was then carried out using the Quick Ligation Kit (NEB). 50 - 100 ng of the linearised plasmid was used and combined with the insert at 1:10 ratio. The volume was then adjusted to 10 µL using DEPC-treated water, then 10 µL of the 2 X Quick Ligation Buffer was added, followed by 1 µL of T4 DNA Ligase and vortexed. This reaction was incubated for 10 minutes at room temperature and stopped by placing the reaction on ice before bacterial transformation as described above. Colonies were picked, and the plasmid DNA were isolated using the QIAprep Spin Miniprep Kit (Qiagen). Sequencing was then carried out by Genewiz with T7 (forwards) and BGH (reverse) primers.

2.2.3.2 SEP FFA2

In order to N-terminally tag FFA2 with a superecliptic pHluorin (SEP) tag for TIR-FM imaging, a construct which had already been generated and had a SEP-tag, the SEP-LHR was used (Sposini et al., 2017). The SEP tag from the SEP-LHR and FFA2 from FLAG-FFA2 were digested with restriction enzymes *XbaI* and *AfeI*, which were present in the appropriate regions of the SEP-LHR or FLAG-FFA2. The digestion of SEP-LHR and FLAG-FFA2 with restriction enzymes *XbaI* and *AfeI* and separation by electrophoresis were carried out as described above. The SEP insert (approximately 700 bp) and linearised plasmid containing only FFA2 (approximately 1 kpb) were excised. The products were purified with a QIAquick Gel Extraction Kit (Qiagen) and the concentration was determined using a ND-2000 spectrophotometer (NanoDrop).

Ligation using the Quick Ligation Kit (NEB) and bacterial transformation was carried out as described above. Colonies were picked, and the plasmid DNA were isolated using the QIAprep Spin Miniprep Kit (Qiagen). Sequencing was then carried out by Genewiz with T7 and BGH primers.

2.2.3.3 FLAG-FFA2-296 and 323T mutants

To generate the FLAG-FFA2 with C-tail truncations, FFA2- 296T and 323T, a stop-codon was introduced via site directed mutagenesis. Primers were designed so that the stop-codons would be introduced after the serines on the C-tail (primer sequences in Material and Methods 2.1.4). The primers were designed, and the mutagenesis was carried out according to manufacturer's instructions (QuikChange, Site-Directed Mutagenesis, Stratagene). Briefly a mix was made of the following: 5 µL of 10 X reaction buffer, 10 ng of FLAG-FFA2 plasmid, 125 ng of the forward and reverse FFA2-296 T or FFA2 323T primer and 1 µL of dNTP. DEPC treated water was then added to a final volume of 50 µL and 1 µL of PfuUltra HF DNA polymerase (2.5 U/µL) was added and gently mixed. The following cycling conditions were then used for the reaction: 95°C for 2 minutes, followed by 18 cycles of: 95°C for 30 seconds, 55°C for 60 seconds and finally 68 °C for 5.5 minutes (the latter time calculated according to the plasmid size, 5.5 kb). 1 µL of the restriction enzyme DpnI (10 U/µL) was added and thoroughly mixed by gentle pipetting and incubated at 37°C for 2 hours to digest the non-mutated DNA. Next, 50 µL of XL1-Blue supercompetent cells were thawed on ice and 5 µL of DpnI digest was added and gently mixed. Following this, 50 µL of XL10 Gold cells were thawed on ice and 1 µL of Dpnl digest was added, gently mixed and incubated on ice for 30 minutes. The reaction was then heat pulsed for 45 seconds at 42°C then placed backed on ice for 2 minutes. To the reaction, 500 µL of pre-warmed NZY^+ broth (Material and methods 2.1.10.5) was added and the transformation reaction was incubated at 37°C for 1 hour with shaking and bacteria was transformed as described above. Once bacteria were transformed, colonies were picked, and plasmid DNA was isolated using QIAprep Spin Miniprep Kit. Sequencing was then carried out by Genewiz with T7 and BGH primers.

2.2.4 Quantitative Real-Time PCR (q-RT-PCR)

2.2.4.1 RNA isolation and two step reverse transcription polymerase chain reaction

To isolate cellular RNA from mammalian cell lines, cultures were grown to sub-confluence in 6-well plates. Cells were washed with PBS and then 1 mL of TRIzol® Reagent per well was added and transferred to a RNase free tubes. Chloroform (200 μL per mL of TRIzol) was added to each sample and mixed vigorously for 30 seconds before centrifugation at 12,000 *g* for 15 minutes at 4°C. The upper aqueous phase containing RNA was transferred to a new tube, mixed with isopropanol (500 μL per mL of TRIzol) and incubated for 10 minutes at room temperature. Precipitated RNA was centrifuged at 12,000 *g* for 15 minutes at 4°C and the supernatant was discarded. The RNA pellet was wash with 70% ethanol (1 mL per mL of TRIzol) and centrifuged again at 12,000 g for 15 minutes at 4°C. This washing step was repeated twice more. The pellets were allowed to air dry to ensure the removal of any residual ethanol before dissolving in 20 μL of DEPC-treated water. All surfaces, Gilson pipettes and plastic tube racks were decontaminated with RNAseZap throughout RNA isolation. RNA purity and concentration were assessed using a ND-2000 spectrophotometer.

To ensure no DNA contamination, the RNA was treated with a DNase I treatment kit (Life Technologies) as per manufacturer's instructions. Briefly, to each RNA sample (1 μg/μL) 1 μL of 10X DNase I Reaction Buffer, 1 μL of DNase I, and DEPC treated water (to 10 μL) was added and incubated for 15 minutes at room temperature. DNase I was inactivated by the addition of 1 μL of 25mM EDTA, mixed gently, and heated at 65°C for 10 minutes.

Complimentary DNA (cDNA) was then synthesized from the DNase treated mRNA by the SuperScript IV Reverse Transcriptase kit (Life Technologies). To a nuclease-free microcentrifuge tube, 500 ng mRNA, 1 μL of dNTP mix (10 mM), 1 uL of Random primers (50 ng/uL) and DEPC treated water (to 12 μL) was added. Tubes were heated to 65°C for 5 minutes to denature the secondary RNA structure and then cooled on ice. The reaction was completed by adding 4 μL of 5X first-strand buffer, 2 μL of 0.1M DTT (Invitrogen), 1 μL of RnaseOUT and 1 μL of 200U/μL Superscript IV before placed in a thermocycler with set

temperature as follows: 25°C for 10 minutes, 37°C for 120 minutes and 85°C for 5 minutes. cDNA was used for q-RT-PCR or stored at -20°C.

2.2.4.2 q-RT-PCR Primer optimization

The primer sequences used for the identification of FFA2 had previously been generated by Hudson et al., 2013 and the FFA3 primer sequences were purchased as pre-designed from Sigma-Aldrich UK. Prior to use of these primers in all samples, the concentrations to be used were optimized by varying the primer concentrations between 100 nM to 600 nM and also using different amounts of diluted cDNA – 1:5, 1:10, 1:15, and 1:20. The optimal primer concentration and cDNA amount was chosen according to the one that produced the maximum fluorescent signal and the smallest Ct value.

2.2.4.3 q-RT-PCR analysis

Gene expression was quantified using isolated mRNA and cDNA was used as described above. Relative quantitation of the target template by q-RT-PCR was determined using gene specific primers. q-RT-PCR was carried out in 96-well plates using a total volume of 20 μL per reaction containing of 5 μL of diluted cDNA, 500 nM forward and reverse primers, 10 μL of 1X SYBR-Green PCR Mastermix and nuclease-free water. Each reaction was carried out in triplicates on the same plate and negative control reactions were performed by substituting the cDNA template with nuclease-free water. Reactions were performed using the ABI StepONE sequence systems with the following cycling conditions: 95°C for 15 minutes (denaturation), 40 cycles of 94°C for 15 sec (denaturation) and 60°C for 30 sec (annealing), and finally 72°C for 30 sec (extension). Melting curves were inspected to confirm single product amplification.

To analyse the results, the Comparative C_T method (or $2^{-\Delta\Delta CT}$ method) was used to obtain the relative level of gene transcript (Livak and Schmittgen, 2001). The C_T is the threshold cycle, that decreases linearly with the increasing amount of PCR target. This represents the number of cycles required in the reaction to reach a designated level of fluorescence during the exponential phase of the target amplification. For each gene target, expression C_T values are normalised according to the values of the housekeeping genes (for example, β-actin). The

relative expression of the target genes in the different samples were calculated with the following formula:

$$\Delta CT = C_T \text{ (target gene)} - C_T \text{ (housekeeping gene)}$$

where C_T (target gene) indicates the value of the threshold cycle for the gene of interest and C_T (housekeeping gene) indicates the value of the threshold cycle for the housekeeping gene used for normalisation. The relative expression (RE) was then calculated as follows:

$$RE = 2^{-\Delta\Delta CT} \text{ [where } \Delta\Delta CT = \Delta C_T \text{ (sample)} - \Delta C_T \text{ (control)]}$$

where ΔC_T (sample) (for example, STC-1 cells) indicates the difference between C_T values of the target gene and the house keeping gene calculated for the test sample, ΔC_T (control) indicates the difference between the C_T values of the target gene and the C_T values of the housekeeping genes obtained from the control samples (for example, colonic tissue).

2.3 Intestinal Organoids

2.3.1 Intestinal crypts

All animal procedures undertaken were approved by the UK Home Office Animals (Scientific Procedures) Act 1986 (Project License Number: 00/6474). The protocol for intestinal crypts isolation was adapted from Reimann et al., 2008 and Psichas et al., 2015. Adult male C57BL6 mice (8 – 12 weeks of age) were culled by cervical dislocation and colon (distal to the caecum) was removed by Dr. Noemi Gonzalez Abuin, cleaned and placed into ice-cold L-15 (Leibowitz) medium. Briefly, colons were cut into small pieces and thoroughly cleaned with cold L-15 medium and digested with 0.4mg/mL collagenase XI in high glucose DMEM at 37°C. Resulting crypt suspensions were then centrifuged at 150 *g* for 5 minutes and the pellets were re-suspended with DMEM (supplemented with 10% FBS, 1% Glutamine and 100 µg/ml Primocin). The digestion process was repeated 4 times and the combined crypt suspensions were filtered through a nylon mesh (pore size 300µm) and plated on 24-well, 2% Matrigel-coated plates. The plates were incubated overnight at 37°C in a 5% CO_2 humidified atmosphere.

2.3.2 Intestinal colonic and ileum organoid culture

All animal procedures undertaken were approved by the UK Home Office Animals (Scientific Procedures) Act 1986 (Project License Number: 70/8068). The method outlined below for intestinal organoid culture has been adapted from the method originally presented by Sato et al., 2009 and culturing was carried out by Dr. Noemi Gonzalez Abuin. Briefly, adult male C57BL6 mice (8 weeks of age or older) were culled by cervical dislocation and the ileum (distal 8 cm of intestine from the ileocecal junction) or colon (distal to the caecum), were removed and flushed with cold DPBS. Pieces of the ileum or colon (2-4mm) were excised, further washed with PBS containing 10% FBS and incubated in ice-cold 12.5 mM EDTA PBS on a rotator at 4°C for 30 min (ileum) or 60min (colon). The supernatant was discarded once the intestinal pieces settled and crypts were released in DPBS by mechanical disruption. Next, ice cold PBS containing Ca^{2+} and Mg^{+} was added to neutralise the EDTA. The crypt fragments were filtered through a 70 µM cell strainer and centrifuged at 150 *g* for 5 minutes. The pellets containing crypts were washed twice in basal culture medium (Table 1).

Isolated crypts were then embedded in Matrigel diluted 1:1 in complete growth medium (Table 1) at a density of 500crypts/well. 25 µL/well of the crypt suspension was plated in 48-well plates and placed at 37°C for 60 minutes for the polymerisation of Matrigel to occur (Figure 2.1). Finally, 300 µL of complete growth medium was added to each well and crypts cultured at 37°C in a 5%CO_2 humidified atmosphere. Medium was renewed every 2 -3 days. After 3 days of culturing, CHIR99021 was removed from the complete medium to promote differentiation. Then after 3 days, the 3D intestinal organoids are either ready to use for experiments or passage for maintenance (Figure 2.1). For passaging, organoids are passaged mechanically using Gentle dissociation Reagent (StemCell) as per manufacturer's instruction and transferred to fresh Matrigel.

Organoid culture complete medium

Component	Supplier
Advanced DMEM F12	Invitrogen
GlutaMax	Invitrogen
B27 supplement	Invitrogen
N-2 supplement	Invitrogen
n-Acetylcystein (1.25 mM)	Sigma-Aldrich
50% Wnt conditional media	In-house
10% R-spondin 1	In-house
mNoggin (100 ng/mL)	Peprotech
CHIR99021 (3 µM)	Sigma-Aldrich
mEGF (50 ng/mL)	Peprotech

Table 1.1. Components of complete medium for intestinal organoid culture

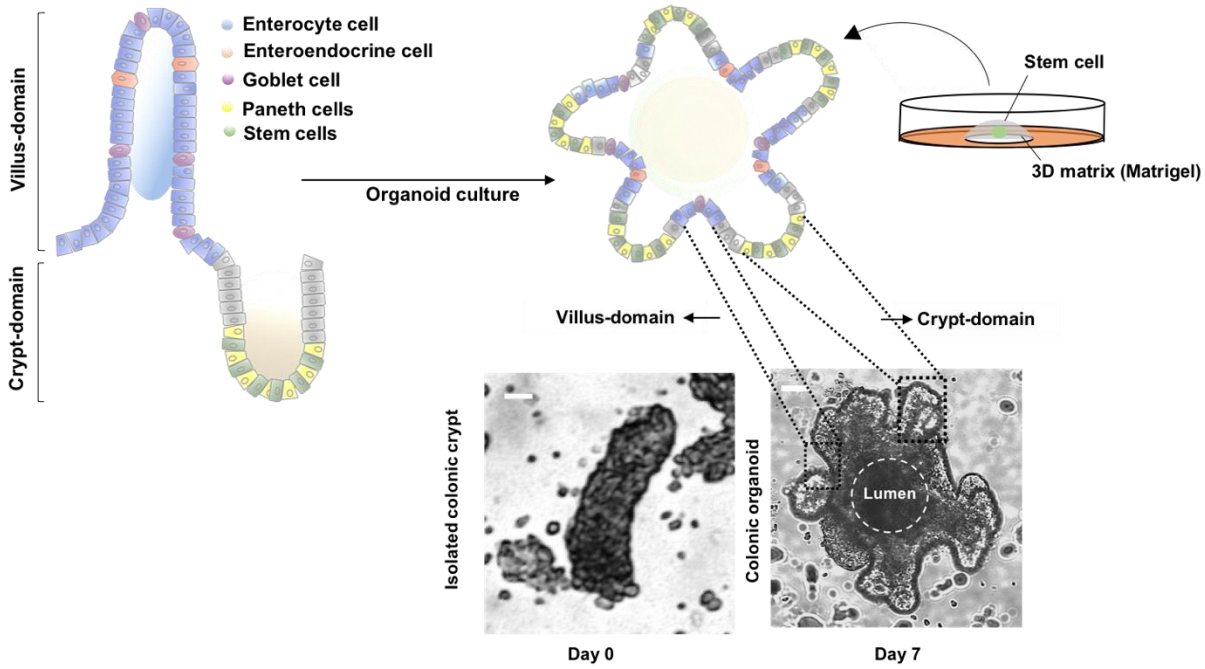


Figure 2.1 Intestinal organoids culture. Schematic of representation of intestinal organoid culture. Intestinal epithelium consists of villus and crypt compartment. The villus comprises of different cells (enterocyte, enteroendocrine and goblet cells), while crypt consist of stem cells and Paneth cells (Left).

Single intestinal stem cell in a 3D-matrix grows into an expanding organoid which comprise all cell types present in intestine (Left). Brightfield images of crypts following isolation from intestine and after 7 days of culture enteroids form budding crypt like structures around a central lumen reminiscent of gut structure (bottom), scale bar is 50 μm.

2.4 Cell culture

Wild-type (WT) HEK 293, STC-1 cells, β-Arr 1/2 KO cells (collaborations with Asuka Inoue) were grown in DMEM supplemented with 10% (v/v) FBS and 1% (v/v) penicillin and streptomycin. HEK 293 cells expressing FLAG-FFA2 or SEP-FFA2 were grown in the same medium but with the addition of 500 μg/mL G418. All cell lines were cultured at 37°C in a 95% O_2/5% CO_2 humidified incubator.

WT, FLAG- or SEP-FFA2 HEK 293, STC-1 and β-Arr 1/2 KO cells in either flask or dishes were passaged when 70-90% confluence was reached. Following removal of culture medium, cells were washed gently with appropriate volume of PBS to remove residual FBS. Then 30 μL/cm^2 of 0.05% trypsin/EDTA in PBS was added to detach cells. After complete detachment, trypsin activity was terminated by adding DMEM and seeded out for either continued culture or for experimental use. STC-1 cells were passaged the same as WT and FLAG- or SEP-FFA2 HEK 293 cells but following trypsin termination with DMEM, cells were transferred into a 50 mL Falcon tube and centrifuged for 5 minutes at 1118 *g*. Supernatant was removed, and cell pellet was resuspended with appropriate volume of DMEM for continued culture. If cells were being passaged for experiments, cells were counted under a light microscope using a haemocytometer and stained with Trypan blue (0.4%) to determine cell viability. 10 μL of cell suspension was loaded and the number of cells within four 1 mm^2 areas were counted. This number was divided by 4 and multiplied by 10,000 to get an average number of cells per mL. The cells were resuspended in DMEM to give the required cell density and were plated out as appropriate. Experiments were routinely carried in 6-, 12-, 24-,48- or 96-well plates.

2.4.1 Transfections of plasmids DNA or siRNA

2.4.1.1 Transient transfections of plasmid DNA using Lipofectamine 2000

STC-1 or HEK 293 cells plated into 6-well plates at approximately 80% confluent were transfected 24 hours post-plating in DMEM supplemented with 10% (v/v) FBS. For each well of transfection, plasmid DNA (typically 0.5 – 3 μg) was combined with 250 μL of Opti-MEM and 5 μL of Lipofectamine 2000 was combined with 250 μL of Opti-MEM in two separate tubes and incubated for 5 minutes at room temperature. These were then mixed and incubated further for 20 minutes at room temperature to allow the complexes to form. The 500 μL mix was then added in drop-wise manner to the cells and incubated at 37°C with 5% CO_2. After approximately 16 hours, the medium was changed back to general culture medium and were split in the appropriate format. Transfected cells were treated for experiment or harvested for RNA extraction 72 hours post transfection. Transfections were also carried out in 12-well plates, 6 or 10 cm dishes which the amounts were adjusted according to surface area.

2.4.1.2 siRNA transfection by Lipofectamine RNAiMAX

STC-1 or HEK 293 cells plated into 6-well plates at approximately 60% confluent were transfected 24 hours post-plating in DMEM supplemented with 10% (v/v) FBS. For each well to be transfected, siRNA at a final concentration of 10 or 200 nM was combined with 250 μL Opti-MEM. Separately, 7 μL of RNAiMAX was combine with 250 μL Opti-MEM. Both mixtures were incubated at room temperature for 5 minutes and then mixed together and incubated further for 20 minutes at room temperature. The mix was then added to the cells in a drop-wise manner to each well and were incubated at 37°C with 5% CO_2. After approximately 16 hours, the medium was changed back to general culture medium and were split in the appropriate format. Transfected cells were treated for experiment or harvested for RNA extraction 96 hours post transfection. Transfections were also carried out in 12-well plates, 6 or 10 cm dishes which the amounts were adjusted according to surface area.

2.4.2 Generation of FLAG-FFA2 and SEP-FFA2 stable HEK 293

HEK 293 cells plated into 10 cm dish at approximately 80% confluency were transfected 24 hours post-plating in DMEM supplemented with 10% (v/v) FBS. For each dish to be transfected, 15 μg of plasmid DNA was combined with 1250 μL Opti-MEM and 25 μL of Lipofectamine 2000 was combined with 1250 μL of Opti-MEM in two separate tubes and incubated for 5 minutes at room temperature. The two mixtures were then mixed and incubated further for 20 minutes at room temperature to allow the complexes to form. The 2500 μL mix was then added in drop-wise manner to the cells and incubated at 37°C with 5% CO_2. Two days post transfection, the medium was changed to general culture medium supplemented with 500 μg/mL G418 and then was replenished every 2 days. The addition of G418 to the medium induced cell death to the cells that did not incorporate the plasmid containing G418 resistance gene. Once cell death was complete, resistant colonies formed and were picked from the plate and individual clones were transferred to a well of 48-well plate. Once confluent, each clone was expanded to a well of 24-,12-, then 6-well plate. Confluent cells were transferred from the 6-well plate to T25cm^2 flask. Each clone was tested via flow cytometry for the expression of FLAG-FFA2 or SEP-FFA2. Both monoclonal or polyclonal cell lines were identified and only clones with high amount FLAG-FFA2 cell surface expression or high amount of GFP fluorescence for SEP-FFA2 were retained. The retained clonal cell lines were then imaged by confocal microscopy prior to expansion and froze for storage at liquid nitrogen.

2.5 Western Blot Analysis

2.5.1 Protein extraction

Cells were treated as appropriate and lysed with lysis buffer (Material & Methods 2.1.10.3). Cells were rinsed twice with ice cold PBS on ice and then lysed with 100 μL (per 6 well plate) or 200 μL (per 6 cm dishes). Dishes were scraped to ensure maximum protein retrieval, transferred intro pre-chilled 1.5 mL Eppendorf tubes and centrifuged at 15,000 *g* for 10 minutes at 4°C. Supernatants were isolated and stored at -20°C or analysed for protein concentration.

2.5.2 Protein concentration

Total protein concentration of cell lysates was determined by Coomassie (Bradford) Protein Assay Kit, a colorimetric protein assay based on the Braford method. The Bradford method is a dye-binding assay in which a Coomassie Brilliant Blue dye binds to the arginine and hydrophobic amino acid residues of the protein, leading to a colour change in response to the protein concentration. In a 96-well plate, 1 µL of cell lysates and 200 µL of Bradford reagent were mixed together, and absorbance was measured at 595 nm. A calibration curve was established each time with BSA diluted in lysis buffer and the concentrations of cell lysates were generated by interpolation of the standard curve. All cell lysates were then diluted to equal concentration with appropriate lysis buffer before protein separation.

2.5.3 SDS polyacrylamide gel electrophoresis

SDS-PAGE was carryout using the Mini-PROTEAN® Electrophoresis cell (Biorad). Proteins were resolved using a 12% separating gel, with a 5% stacking gel (Material and methods 2.1.10.4) and a pre-stained molecular weight marker. Gels were run using 1X running buffer at 100V for 20 minutes followed by 140V for 1-2 hours, depending on the size of protein of interest and degree of separation.

2.5.4 Protein transfer to nitrocellulose membranes

After protein separation, proteins were transferred to a nitrocellulose membrane using a wet transfer system. The stacking gel and the sides of separating gel were removed beyond the sample wells with a razor blade and the gel was equilibrated with wet transfer buffer. The gel was then placed against a nitrocellulose membrane between blotting papers and sponge pads to form a sandwich and then placed perpendicular into the transfer chamber. Transfer was achieved by applying a constant voltage (100V) at 4°C for 1-2 hours to drive the negatively charged proteins from the gel onto the nitrocellulose membrane.

After transfer, proteins were visualised with Ponceau S staining which was subsequently removed with Tris-Buffered Saline with 0.5% Tween20 (TBS-T). Membranes were then

blocked with either 5% (w/v) skimmed milk or BSA in TBS-T for 1 hour at room temperature with constant agitation. The membrane was then washed briefly with TBS-T and then placed in primary antibody at appropriate dilution (Material and Methods 2.1.1) and incubated overnight at 4°C with agitation. Membranes were washed 3 times with TBS-T, each time for 10 minutes, they were incubated in the appropriate HRP-conjugated secondary diluted in blocking buffer for 1 hour at room temperature. The membrane was then washed once more for 3 times, 10 minutes each in TBS-T and subjected to chemiluminescent substrates for detection. Luminata Forte or Classico Western HRP substrate were spread onto the membranes and were then exposed to autoradiography film or imaged with the ImageQuant Las 4000 chemi-imager (GE Healthcare).

2.5.5 Stripping membranes

To visualise a protein that is of the same or similar molecular weight on the same membrane, primary and secondary antibodies were stripped off the membrane using Western blot stripping buffer (Materials and methods 2.1.10.4). To strip the membrane, the membrane was incubated in the buffer that was heated to 60°C with fresh β-mercaptoethanol added and incubated for 45 minutes with agitation at room temperature. The membrane was then wash extensively (typically 5 washes, 15 minutes each) to remove any remaining stripping buffer and was re-blocked with the appropriate blocking buffer, and subsequently probed with primary antibody as described above.

2.6 Cell signalling assays

2.6.1 Ligand preparation

SCFA were prepared fresh for each experiment at 100 mM in PBS, whilst 10 mM stocks were made of 4-CMTB, Cmp1, AZ1729, and AR42026 in DMSO and stored at -20°C until required. On the day of the experiment, SCFA and synthetic ligands underwent serial dilution, typically 10x the required final assay concentration in PBS supplemented with 0.01% fatty acid free BSA to aid in solubilisation.

2.6.2 Calcium mobilisation

Calcium mobilization was measured using the Fluo-4AM Direct Calcium Assay Kit (Invitrogen). Fluo-4 is a calcium sensor that undergoes increased fluorescence in the presence of calcium ions. Its excitation and emission spectra are 494 nm and 506 nm respectively. Cells were plated in a 35 mm glass-bottomed dishes (MatTek) to 60% confluency and loaded with 1 mL of equal amounts of serum free, phenol red free DMEM and calcium dye Fluo-4-AM Direct supplemented with 0.1% BSA fatty acid free for 30 minutes at 37°C and then at room temperature for a further 30 minutes. When inhibitors were used, these were added at the appropriate time before imaging and within the 1-hour dye incubation. Cells were imaged using a Lecia SP5 confocal microscope using a 20X dry objective and a 488nm excitation laser. Movies were recorded at 1 fps for 1 minute before ligand addition and further 10-20 minutes after ligand addition to allow for calcium levels to lower to basal. All experiments conditions were conducted in duplicate and repeated at least 3 times. The fluorescence intensity of each cell was quantified using the ImageJ plugin Time Series Analyser. The maximal intensity was obtained from subtracting the average background intensity (recorded before ligand addition) for each cell and averaged across 20 cells per condition.

2.6.3 cAMP accumulation

For measurement of cAMP accumulation, cells were plated in 96-or 48-well plates and grown to 80% confluency. Cells were pre-treated in serum free DMEM supplemented with 0.1% BSA fatty acid free containing 0.5mM IBMX for 5 minutes prior to ligand addition (5 minutes) in the presence or absence of 3 µM forskolin. If inhibitors were used, these were administered to cells prior to IBMX pretreatment at the appropriate time. Cells were then washed with ice-cold PBS, lysed with Cisbio cAMP lysis buffer before being incubated at room temperature for 10 minutes on a shaking platform. Plates were then scraped, and lysates were transferred to 1.5 mL tubes and centrifuged at 15000 *g* for 10 minutes. The supernatants were transferred into a fresh tube. Levels of cAMP accumulation were measured using the Cisbio Homogenous Time Resolved Fluorescence (HTRF) cAMP Dynamic 2 kit, a competitive TR-FRET-based immunoassay between native cAMP produced by cells and the labelled cAMP. Detection of cAMP accumulation involves an cAMP-specific antibody labelled with terbium cryptate

(donor fluorophore) and cAMP labelled with d2 (acceptor fluorophore). Accumulated cAMP in the cell will lead to a decrease in FRET ratio (Norskov-Lauritsen et al., 2014). In a 384 white bottom well plate, 10 μL of each sample, 5 μL of cAMP dye d2 and 5 μL of anti-cAMP cryptate conjugate was added and incubated in the dark for 1 hour at room temperature. The plate was then read with PHERAstar FSX plate reader (BMG Labtech) equipped with HTRF 337 optic module, with excitation at 340 nm and measurements of emission at 615 nm and 665 nm. FRET ratios were obtained, and cAMP levels were interpolated from a cAMP standard curve and normalised to protein concentration which was determined as described previously. All experiments were conducted in triplicate and repeated at least 3 times.

2.6.4 IP1 accumulation

To measure the accumulation of IP1, cells were plated in 96-or 48-well plates and grown to 80% confluency. Cells were incubated with ligands diluted in serum free DMEM supplemented with 50 mM lithium chloride and 0.1% BSA fatty acid free for 2 hours at 37°C. If inhibitors were used, these were administered to cells prior to ligand stimulation at the appropriate time. Cells were then washed with ice-cold PBS, lysed with Cisbio IP1 lysis buffer before being incubated at room temperature for 10 minutes on a shaking platform. Samples were lysed, scraped and centrifuged as described for the cAMP accumulation assay. Levels of IP1 accumulation were measured using the Cisbio HTRF IP-One kit, this kit is based on the same technology as the cAMP Dynamic 2 kit, a competition between d2 labelled IP1 (acceptor) and IP1 produced by the cell for the binding sites of cryptate-labelled IP1 (donor) antibody. Accumulated IP1 in the cell will lead to a decrease in FRET ratio (Norskov-Lauritsen et al., 2014). In a 384 white bottom well plate, 14 μL of each sample, 3 μL of IP1 dye d2 and 3 μL of anti-IP1 cryptate conjugate was added and incubated in the dark for 1 hour at room temperature. The plate was read with PHERAstar FSX plate reader (BMG Labtech) equipped with HTRF 337 optic module, with excitation at 340 nm and measurements of emission at 615 nm and 665 nm. IP1 levels were interpolated from an IP1 standard curve and normalised to protein concentration which was determined as described previously. All experiments were conducted in triplicate and repeated at least 3 times.

2.6.5 MAPK

To assess the levels of p38 phosphorylation following ligand stimulation, STC-1 cells and SEP-FFA2 HEK 293 cells were plated into a 6-well plate, grown to 90% confluency and serum starved with serum free DMEM supplemented with 0.1% BSA fatty acid free for 2 hours before the experiment. After serum starvation, medium was replaced with fresh serum free DMEM supplemented with 0.1% BSA fatty acid free and if inhibitors were used, these were administered to the cells at the appropriate time before stimulation with ligand at different time points (5, 10, 15, 30 and 60 minutes). Cells were then placed on ice, washed twice with ice-cold PBS and lysed with 100 μL lysis buffer (Material and methods 2.1.10.3). Protein extraction, SDS-gel loading for Western blot and protein transfer to nitrocellulose membrane were the same as described above (Material and methods 2.1.10.3). Once proteins were transferred to the nitrocellulose membrane and blocked in 5% BSA in TBS-T the membrane was incubated in primary phospho-p38 antibody overnight at 4°C. The next day, the membrane was incubated with HRP-anti rabbit secondary antibody for 1 hour, imaged, stripped, blocked and incubated overnight with total-p38 antibody. The next day, the membrane was incubated with HRP-anti rabbit secondary antibody for 1 hour and imaged. The intensity of the bands was quantified using ImageJ and phospho-p38 over total-p38 ratio was calculated.

2.7 Measurement of GLP-1 and PYY secretion using a radioimmunoassay

2.7.1 GLP-1 and PYY secretion

For the measurement of PYY and GLP-1 secretion, STC-1 cells were plated into 24-well plates and grown to 90% confluency. Cells were incubated with ligands diluted in secretion buffer (Material & Methods 2.1.10.6) for 2 hours at 37°C. If inhibitors were used, these were administered to cells at the appropriate time prior to ligand stimulation. The supernatant was collected, and the cells were lysed with GLP-1 lysis buffer (Material & Methods 2.1.10.6). Samples were stored at -20°C or analysed for GLP-1 secretion via radioimmunoassay (RIA). All experiments were conducted in triplicate and repeated at least 3 times.

2.7.2 Radioimmunoassay (RIA)

GLP-1 and PYY release was measured by radioimmunoassay. The principle of the radioimmunoassay (RIA) technique is based on the competition between unlabelled peptide (from the sample) and a known amount of radiolabelled peptide for binding to a fixed concentration of antibody. The concentration of radiolabelled peptide and antibody remain constant. Thus, increasing the concentration of unlabelled peptide will decrease the binding sites available for binding of the radiolabelled peptide. Therefore, the amount of radiolabelled peptide bound to the antibody is inversely proportional to the amount of unlabelled peptide in the sample being assayed. Unknown peptide concentration values were interpolated from standard curve prepared using known concentrations of unlabelled peptide (standard)

2.7.2.1 RIA controls

To assess non-specific binding (NSB), tubes that do not contain antibody were included at the beginning of the assay. Tubes containing either half or twice the volume radio-labelled peptide were included to assess the quality. Tubes with no sample (zero tubes) were placed throughout the assay to monitor assay baseline drift. Quality control (QCs) samples containing plasma spiked with low, medium or high known concentrations of peptide were also added to the beginning and end of each assay. Freeze-dried QCs were reconstituted in DW on the day of the assay.

2.7.2.2 GLP-1 RIA

GLP-1 secretion was measured using an established in-house RIA assay (Kreymann et al., 1987).The antibody shows 100% cross reactivity of all amidated forms of GLP-1 but does not bind with glycine extended forms of GLP-1 (GLP-1 $_{1\text{-}37}$ and GLP-1 $_{7\text{-}37}$) or any other pancreatic or gastrointestinal peptides. GLP-1 peptide was radiolabelled using Iodine I25 (^{125}I) by Professor Kevin Murphy using the iodogen method (Wood et al., 1981) and purified by high pressure liquid chromatography. The assay was performed in a total volume of 350µl. 100µl supernatant or 20 µL lysate samples were added to phosphate buffer (Material & Methods 2.1.10.6) to achieve a total volume of 250 µL. The standard curve was constructed by adding

1, 2, 3, 5, 10, 15, 20, 30, 50 and 100 µL of GLP-1 at a concentration of 0.125pmol/mL were added in tubes of duplicates. 50µl ^{125}I-GLP-1 (10 counts/second) and 50 µL GLP-1 antibody was added to each tube and the assay was incubated for four days at 4°C. Following incubation, 250 µL of dextran coated charcoal buffer (Material & Methods 2.1.10.6) was added to each tube to separate the free from antibody-bound labelled peptide and centrifuged at 150 *g* at 4°C for 1 hour. Radioactivity of the pellet containing free peptide and supernatant containing bound peptide was measured using the NE1600 γ scintillation counter (Thermo Electron Corporation), (intra-assay variation 7%; inter-assay variation 12%).

2.7.2.2 PYY RIA

PYY secretion was measured using a specific and sensitive RIA assay (Adrian et al., 1985). The antiserum (Y21) was produced in rabbits against synthetic porcine PYY coupled to BSA glutaraldehyde. The Y21 antibody cross-reacts fully with biologically active forms of PYY: full length PYY_{1-36} and the truncated fragment PYY_{3-36}. The antibody does not cross-react with other gastrointestinal peptides. ^{125}I-PYY was prepared by Professor Kevin Murphy using the iodogen method (Wood et al., 1981) and purified by high pressure liquid chromatography. The assay was performed in a total volume of 350µl. 100µl supernatant or 20 µL lysate samples were added to phosphate buffer (Material & Methods 2.1.10.6) to achieve a total volume of 250 µL. The standard curve was constructed by adding 1, 2, 3, 5, 10, 15, 20, 30, 50 and 100 µL of synthetic PYY at a concentration of 0.5pmol/mL were added in tubes of duplicates. 50µl ^{125}I-PYY (10 counts/second) and 50 µL PYY antibody was added to each tube and the assay was incubated for 3 days at 4°C before separation of the free from antibody-bound label by immunoprecipitation using sheep anti-rabbit antibody. Free and bound was measured using the NE1600 γ scintillation counter as above, (intra-assay variation 4.2%; inter-assay variation 10.4%).

2.8 Phosphokinase array

A phospho-kinase array (Proteome Profiler Phospho-Kinase Array Kit, R&D Systems) was used to detect simultaneously the relative phosphorylation levels of 46 proteins following ligand stimulation. STC-1 cells were plated into a 6-well plate, grown to 90% confluency and serum

starved with serum free DMEM supplemented with 0.1% BSA fatty acid free for 2 hours before the experiment. After serum starvation, medium was replaced with fresh serum free DMEM supplemented with 0.1% BSA fatty acid free and if inhibitors were used, these were administered to the cells at the appropriate time before stimulation with ligand at different time points. The cells were then washed twice with ice-cold PBS on ice. Lysis Buffer 6 (provided with the array kit) was added to each well and the cells were then left on a rocking platform shaker on ice for 30 minutes before being scraped. The lysates were transferred to pre-chilled 1.5 mL eppendorfs, centrifuged at 15,000 *g* at 4°C for 10 minutes and the supernatant was transferred to new tubes. Total protein was quantified as described previously and 200 µg of lysate was used per array part. The remainder of the procedure was carried out according to the manufacturer's instructions. Membranes were then scanned, and densitometry of spots was carried out using the ImageJ software. Normalisation was made to the reference spots as recommended by the kit.

2.9 Microscopy

2.9.1 Fixed sample preparation

Cells were plated onto glass-coverslips in 24-well plates or in 35-mm glass bottomed dishes and grown to 60-70% confluency. On the day of the experiment, medium was replaced with DMEM without serum and cells were incubated with FLAG M1-antibody (1:500) for 35 minutes at 37°C and for the last 5- or 20-minutes ligands were added. If inhibitors, were used, these were administered to cells at the appropriate time prior to this. Cells were washed twice with ice-cold PBS+Ca^{2+}, $\pm$ washed with stripping buffer to remove surface bound FLAG M1-antobdy and fixed with 4% PFA for 20 minutes at room temperature. Cells were permeabilised for 15 minutes and then blocked with blocking buffer for 1 hour at room temperature. After this, cells were incubated with primary antibody (e.g. APPL1 antibody) diluted in blocking buffer (Material and methods 2.1.2) for 1 hour at room temperature. Following this, cells were incubated with AlexaFluor-conjugated secondary antibodies (1:1000 in blocking buffer) for 1 hour at room temperature in the dark. Cells were then washed with PBS/Ca^{2+} and either imaged immediately after (35-mm glass bottom dishes) for TIR-FM experiments or coverslips

were mounted on glass slides using Fluoromount-G and sealed using clear nail vanish. Coverslips were kept at 4°C.

2.9.2 Confocal microscopy

To visualise receptor in live cells, an antibody feeding assay was carried out where cells were fed live with FLAG M1-antibody (1:500) for 20 minutes at 37°C and AlexaFlour 488 or 555 conjugated secondary antibody (1:1000) for 20 minutes at 37°C in phenol red-free DMEM containing 0.1% BSA fatty acid free prior to ligand treatment. Both live and fixed cells were imaged using TCS-SP5 microscope (Leica) with a 63x oil-immersion objective and 1.4 numerical aperture (NA). The gain and offset controller were adjusted at the outset to ensure signals were not too saturated and then kept constant throughout all experiments. Images were acquired using Leica LAS AF image acquisition software.

2.9.2.1 Quantification of co-localisation

To quantify levels of co-localisation, captured images were analysed using ImageJ or LAS AF Lite (Leica) and multi-channel images were split into corresponding channel. All receptor endosomes were first counted and circled per cell. Receptor endosomes that colocalised with either APPL1, EEA1 or $G\alpha_i$ were quantified. Colocalisation was displayed as percentage of receptor endosomes positive for either APPL1, EEA1 or $G\alpha_i$. A minimum of 10 cells were counted per condition per experiment and repeated at least 3 times.

2.9.3 Total Internal Reflection-Fluorescence Microscopy (TIR-FM)

Cells were imaged using the Elyra PS.1 AxioObsever Z1 motorized inverted microscope with a sCMOS or EMCCD camera and an alpha Plan-Aprochromat 100x/1.46 Oil DIC M27 Elyra objective (Zeiss), with solid-state lasers of 488 nm, 561 nm and/642 nm as light sources. Approximately 15 minutes prior to imaging, culture media was replaced with Opti-MEM reduced serum media supplemented with HEPES. Imaging was then carried out using a Zeiss Elyra PS.1 microscope controlled at 37°C with 5% CO_2. Cells were first visualised under wide-field fluorescence and then brought into focus using TIRF oil immersion objective. Illumination

was then switched to TIRF. The TIRF angle was then changed as appropriate so that single vesicle recycling events could be visualised. Time-lapse movies of whole cells were taken for 60 seconds, at 10 frames per second (fps) using Zen lite acquisition software.

2.9.3.1 Quantitation single vesicle recycling events from TIRF movies

Single vesicle recycling events were identified and counted on a whole cell basis, for the entire duration of the movie (60 seconds). To perform this analysis, czi images were exported and analysed as TIFF stacks using ImageJ plugin Time Series Analyser. Events were defined as an abrupt increase in fluorescence intensity at the cell surface, which then diffused. The number of recycling events was counted and normalized by cell area.

2.10 Flow cytometry

To assess receptor surface expression, cells were plated in 12-well plates and grown to 80% confluency. Cells were incubated with FLAG M1-antibody (1:500) for 20 minutes at 37°C in serum free DMEM. Cells were washed twice with ice-cold PBS/Ca^{2+} and harvested in 500 µL FACS buffer (Material & Methods 2.1.10.2) Cells were transferred to round bottom polypropylene FACS tubes, centrifuged at 1118 *g* at 4°C, the supernatant was removed and resuspended in FACS buffer containing AlexaFluor 488 conjugated anti-mouse secondary-antibody. The cells were then incubated on ice in the dark for 1 hour. After this, cells were centrifuged again as before, washed 2 more times and cells were then resuspended in a final volume of 300 µL. These cells were then analysed on a FACS Calibur Flow cytometer. Cells that were not exposed to any antibodies or secondary antibody alone were used for controls, the latter allowing normalisation to basal cell fluorescence intensity.

2.11 Statistical analysis

Data represent mean ± SE. Statistical significance was determined using Student's *t* test, One-way ANOVA followed by Dunnett post-test, or Two-way ANOVA followed by Bonferroni post-test, using GraphPad Prism. Differences were considered significant at $p<0.05$

Chapter 3:

Investigating FFA2 signalling profiles in enteroendocrine cells and colonic organoids

3.1 Introduction

Enhancing the secretion of anorectic and antidiabetic gut hormones; GLP-1 and PYY from intestinal enteroendocrine L cells has become a therapeutic target for many current drug development programs, as evidence is accumulating that enhanced secretion of GLP-1 and PYY exerts beneficial therapeutic effects for the regulation of diabetes and obesity (Chambers et al., 2015). Several advances have been made in identifying compounds and metabolites that enhance GLP-1 and PYY secretion from intestinal L cells. Among the best characterised triggers of GLP-1 and PYY secretion are SCFAs. SCFAs, derived from bacterial fermentation of non-digestible carbohydrates, are ligands for GPCRs FFA2 and FFA3. Both receptors have been reported to have many therapeutic benefits, however FFA2 has become of particular interest as several lines of evidence indicates that FFA2 is directly involved in SCFA-regulated stimulation of GLP-1 and PYY (Kaji et al., 2011; Tolhurst et al., 2012; Psichas et al., 2015; Chambers et al., 2015).

FFA2 and FFA3 are co-expressed in intestinal enteroendocrine L cells and are both activated by the same SCFAs, acetate (C2), propionate (C3) and butyrate (C4) (Brown et al., 2003; Tolhurst et al., 2012). The receptors also differ in their intracellular signalling capabilities, with FFA2 able to couple to $G\alpha_{q/11}$ and $G\alpha_{i/o}$ and FFA3 coupling to $G\alpha_{i/o}$ only (Brown et al., 2003). The receptors also differ in regulation of anorectic gut hormone from intestinal enteroendocrine L cells. Acetate and propionate at a concentration of 1 mM induced secretion of GLP-1 from colonic cultures, which was not observed in colonic cultures from FFA2 KO mice (Tolhurst et al., 2012). This was further confirmed *in vivo* by propionate infusion stimulating increase of GLP-1 and PPY in plasma, which was also FFA2-dependent (Psichas et al., 2015).

Although there is a large body of evidence suggesting that FFA2 is essential in the release of GLP-1 and PYY by SCFAs, underlying mechanisms of release still remain poorly understood. Efforts in trying to elucidate these mechanisms have mainly been conducted in mouse models and in transformed cell lines. Until recently, however, Sato et al.,2009 developed a novel model that enable the growth of intestinal organoids from intestinal crypts. These organoids

are 3D spherical structures that represent “miniguts” with a lumen and a polarized epithelium containing all characteristic cell populations of the intestinal epithelium. This culture model provides a powerful system to investigate cellular effects of the intestinal epithelium on a molecular level.

Thus, in this chapter, the aim is to identify the G-protein signalling pathways each SCFA activate in the enteroendocrine cell line, STC-1, mouse colonic crypts and 3D mouse colonic organoids.

3.2 Results

3.2.1 Expression of FFA2 mRNA in enteroendocrine L cells

FFA2 has been reported to be highly expressed in enteroendocrine L cells of the colon and also in colonic epithelial and endothelial cells (Tolhurst et al., 2012; Li et al., 2018; Kaji et al., 2014). FFA3 is also expressed in enteroendocrine L cells but enriched more in the ileum. To profile the signalling pathways of FFA2, it was first verified that STC-1 cells and mouse colonic crypts and organoids expressed FFA2 and FFA3 mRNA. As controls, tissue from mouse colonic and ileum were used as they are known to express high levels of FFA2 and FFA3. In all samples, FFA2 and FFA3 were expressed, however in STC-1 cells FFA2 and FFA3 expression levels were lower (Figure 3.1).

To further validate the mouse intestinal organoids, mouse colonic- crypts and organoids and mouse ileum organoids were fixed and immunostained with GLP-1 and PYY antibodies and imaged via confocal. In colonic- crypts and organoids and in ileum organoids, subpopulations of cells were positive for GLP-1 and PYY (Figure 3.2). In colonic crypts, GLP-1 was more dominant than PYY, whereas in colonic organoids PYY was more dominant than GLP-1. In ileum organoids, GLP-1 was more dominantly expressed than PYY. Furthermore, a subpopulation of the colocalised GLP-1 and PYY cells were flask shaped, indicative of an enteroendocrine cell.

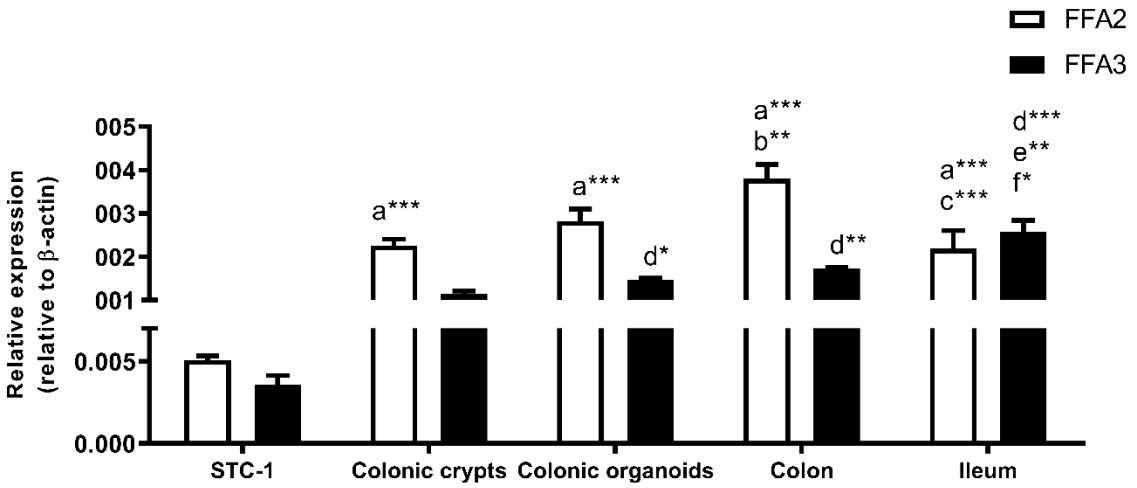


Figure 3.1 FFA2/3 expression in STC-1 cells, colonic crypts and organoids. STC-1 cells grown to confluency, 16-hour old colonic crypts and mature colonic organoids were harvested, and q-PCR was carried out to assess the levels of FFA2 and FFA3 mRNA. Expression levels were normalised to the levels of housekeeping gene β-actin. Data are shown as mean ± SEM, n=3. Two-way ANOVA: Letters: differences among expression between each model: a-c, FFA2; d-f, FFA3; a,d: STC-1 cells; b,e:colonic crypts; c,f: colonic organoids; *p<0.05; ***p<0.0001.

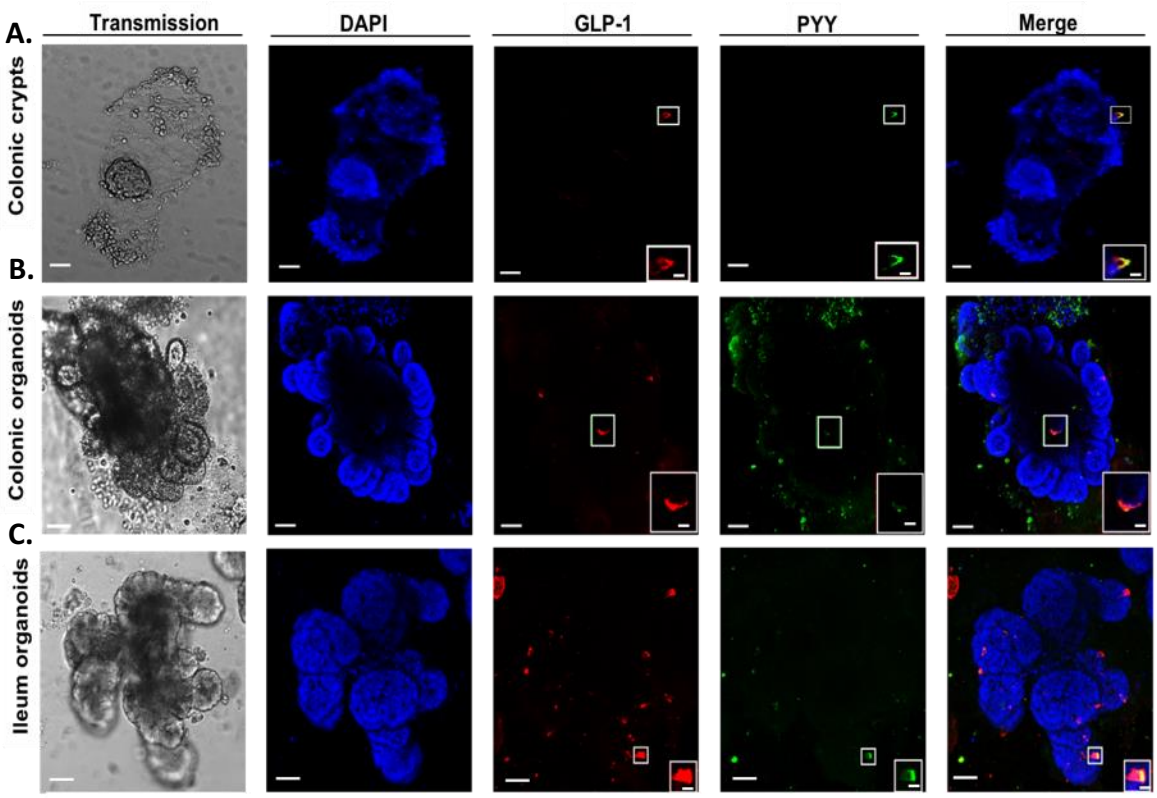


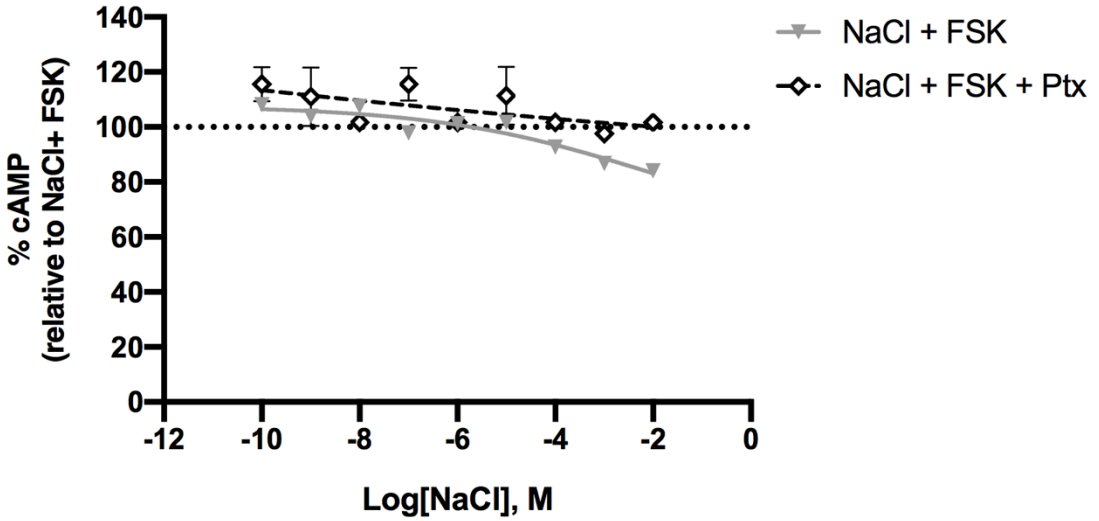
Figure 3.2 Localisation of GLP-1 and PYY in mouse colonic-crypts and intestinal organoids. (A) Colonic crypts and (B & C) differentiated- colonic (B) or ileum organoids (C) were co-stained with GLP-1 (red) and PYY (green). Co-localisation of GLP-1 PYY immunofluorescence in a L cells is shown (merge, yellow). Nuclei were visualised with DAPI (blue). (B & C) is maximum projection. Scale bar for colonic

crypts is 80 µm for large image and inset is 30 µm, for organoids large image is 100 µm and inset is 30 µm.

3.2.2 SCFAs activates Gα_i signalling in enteroendocrine cells

SCFA signalling through FFA2 results in the inhibition of cAMP production and the induction of intracellular calcium mobilisation via dual coupling to G$\alpha_{i/o}$ and G$\alpha_{q/11}$ G proteins, respectively. Although FFA2 coupling to both G$\alpha_{i/o}$ and G$\alpha_{q/11}$ is well established and functional assay measuring, for instance Gα_i-dependent GTPγS binding incorporation and G$\alpha_{q/11}$-dependent Ca^{2+} release are routinely employed, these studies were primarily carried out in HEK 293 or CHO cells overexpressing FFA2 (Le Poul et al., 2003), thus, it was important to first profile SCFA second messenger responses in an enteroendocrine cell system. To this end, SCFAs ability to activate Gα_i and inhibit cAMP induced by forskolin in STC-1 cells was first assessed. STC-1 cells were treated with various concentrations of SCFAs in the presence of forskolin, an artificial elevator of cAMP by the activation of adenylate cyclase (Tang and Hurley, 1998). Levels of cAMP were measured and SCFAs responses were normalised to levels of forskolin and NaCl treated cells (Figure 3.3A, dotted line) as the SCFAs used were all in salt forms. Treatment of cells with NaCl had no significant effect on forskolin-induced cAMP levels (Figure 3.3 A). SCFAs were able to inhibit forskolin induced cAMP in a dose dependent manner with varying potencies (Figure 3.3B and Table 3.1). Acetate and propionate elicited nearly the same potencies in inhibiting forskolin-induced cAMP with pEC_{50} of 4.8 ± 0.41 and 5.1 ± 0.23, respectively, whereas butyrate had the lowest potency with a pEC_{50} of 4.1 ± 0.15 (Table 3.1). To confirm dependence of Gα_i signalling, pertussis toxin (Ptx), an inhibitor of the Gα_i subunit via catalysing its irreversible ADP-ribosylation was utilised (Katada and Ui, 1982). Ptx pre-treatment inhibited the response at all doses, demonstrating SCFA has the ability to decrease levels of forskolin stimulated cAMP in STC-1 via Gα_i.

A.



B.

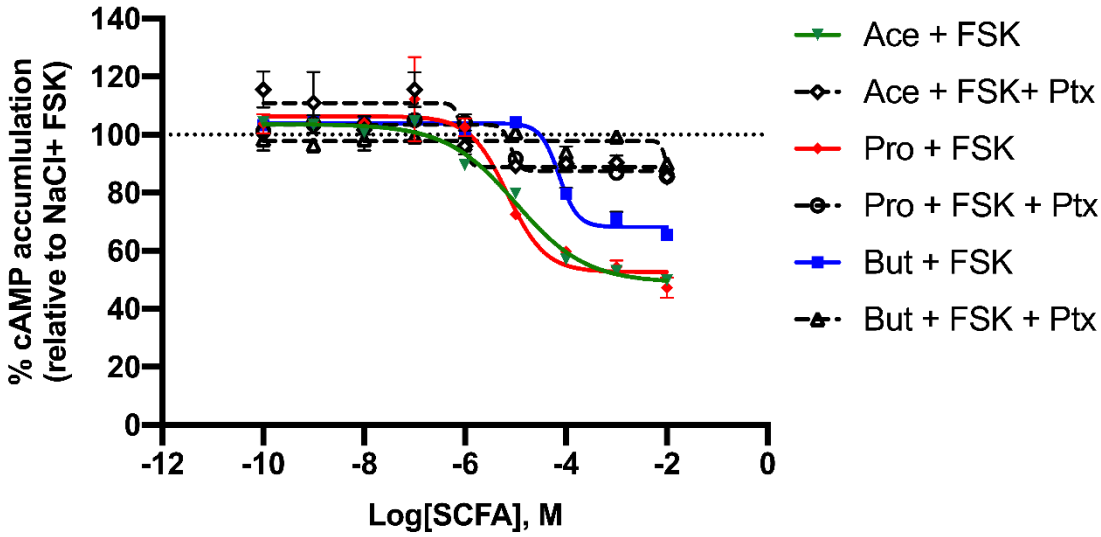


Figure 3.3 SCFA inhibits forskolin induced cAMP in a Gαi/o manner. Dose-response curves for SCFA induced inhibition of forskolin mediated cAMP in STC-1 cells. (A & B) STC-1 cells were treated with or without pertussis toxin (Ptx, 200 ng/ml, 20 hours) and subsequently treated with IBMX (5 minutes, 0.5 mM) and then treated with forskolin (FSK, 3 µM) or a combination of FSK (3 µM) and NaCl (A) or SCFAs (B) at the indicated doses (5 minutes). The maximal forskolin-induced cAMP accumulation in the absences of SCFA was defined as 100% and data are expressed as percentage change of NaCl+FSK. Data represent mean ± SEM, n=3.

SCFA	pEC_{50}
Acetate	4.9 ± 0.19
Propionate	5.1 ± 0.16
Butyrate	4.1 ± 0.15

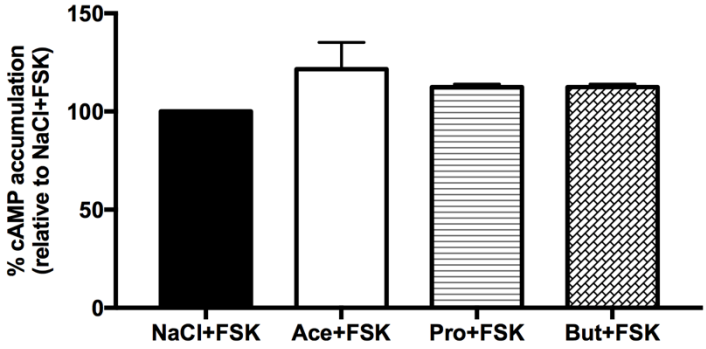
Table 3.1. pEC50 values SCFA mediated inhibition of forskolin induced cAMP. STC-1 cells treated as per Figure 3.3B. Data shown are the pEC_{50} values for each SCFA mediated inhibition of forskolin induced cAMP and are the mean $\pm$ SEM of at least 3 minimum independent experiments.

3.2.3 SCFA inhibits forskolin stimulated cAMP in HEK 293 transiently expressing FLAG FFA2

The above results show that SCFAs in STC-1 enteroendocrine cells are able to inhibit forskolin induced cAMP with maximal responses equivalent to ~1 mM, thus this concentration was used in subsequent experiments. As STC-1 cells also express FFA3, the SCFAs responses in HEK 293 cells expressing a N-terminally FLAG tagged FFA2 (referred hereafter as FLAG-FFA2) were assessed to compare the observed effects of SCFA inhibition of forskolin induced cAMP in STC-1 cells.

STC-1 cells and HEK 293 cells expressing FLAG-FFA2 were treated with SCFAs at 1 mM in the presence of forskolin. Levels of cAMP for each ligand were then calculated and normalised to levels of NaCl+FSK (Figure 3.4). In STC-1 cells, SCFAs at 1 mM decreased forskolin induced cAMP levels with acetate and propionate exhibiting greater efficacy, compared to butyrate, as seen previously (Figure 3.4 B). In HEK 293 cells transiently expressing FLAG-FFA2, SCFAs were also able to decrease levels of forskolin induced cAMP but at levels slightly different to STC-1 cells. Acetate exhibited a nearly similar decrease of 51.5 ± 1.22 % as in the STC-1 cells. Propionate exhibited a slightly greater decrease at 51.7 ± 2.02 %. Butyrate however, exhibited a significantly greater inhibition of forskolin induced cAMP of 57.1 ± 2.50 % than in STC-1 cells. SCFA mediated inhibition of forskolin induced cAMP was not seen in un-transfected HEK 293 cells (Figure 3.4 A). This indicates that SCFA mediated inhibition of forskolin induced cAMP in STC-1 cells may not be mediated solely through FFA2 and that SCFAs may also be activating FFA3.

A.



B.

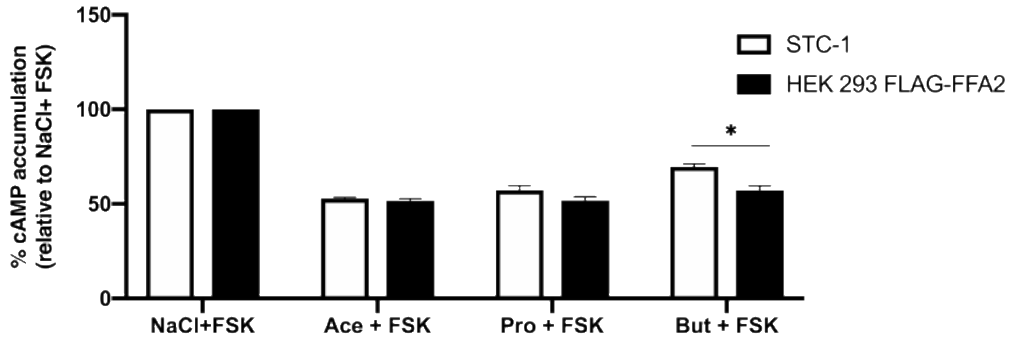


Figure 3.4 SCFAs inhibits forskolin induced cAMP via FFA2. (A) Intracellular levels of cAMP measured in un-transfected HEK 293 cells. Cells were treated with IBMX (5 minutes, 0.5 mM) and then treated with forskolin (FSK, 3 µM) or a combination of FSK (3µM) and NaCl or SCFAs (1 mM) for 5 minutes. (B) Intracellular levels of cAMP measured in STC-1 cells or HEK 293 cells expressing FLAG-FFA2. Cells were treated as in (A). Data are expressed as percentage change of NaCl+FSK and NaCl+FSK is expressed as 100%. Data represent mean ± SEM, n=3; t-test: * $p<0.05$ vs STC-1.

3.2.4 SCFAs activate Gα_i signalling in mouse colonic crypts and organoids

The ability of SCFAs to also inhibit forskolin induced cAMP in a Gα_i dependent manner in mouse colonic-crypts and organoids and in ileum organoids were next determined. Colonic-crypts and organoids and ileum organoids were treated with treated with 1 mM SCFA in the presence of forskolin. Levels of cAMP for each ligand were then calculated and normalised to levels of NaCl+FSK (Figure 3.5 A, B, D, E; dotted line). For the colonic crypts and organoids, stimulation with each SCFAs decreased forskolin induced cAMP in a similar manner to what was observed in STC-1 cells and this decrease was significantly impaired with Ptx (Figure 3.5 A&B). I next asked if this G$\alpha_{i/o}$ signalling was specific to FFA2. To determine this, colonic crypts and organoids were isolated from wild type (WT) or FFA2 knockout (FFA2$^{-/-}$) adult male mice. FFA2 mRNA expression levels in FFA2$^{-/-}$ were verified via qPCR (Figure 3.4 C). In WT colonic-crypts and organoids, SCFA induced inhibition was similar as previously seen. However, in

FFA2$^{-/-}$ colonic- crypts and organoids, SCFA mediated inhibition of forskolin induced cAMP was significantly impaired (Figure 3.5 C & D). This demonstrates that SCFAs activate Gα_i-signalling in the colon via FFA2. In ileum organoids, stimulation with each SCFAs also mediated a significant inhibition of forskolin induced cAMP, however, acetate exhibited a lower decrease of 66.31 $\pm$ 4.06 % than what was observed in the colonic crypts or organoids (Figure 3.5 E). This suggest that SCFAs may exhibit different efficacies in Gα_i-signalling in the ileum and in the colon.

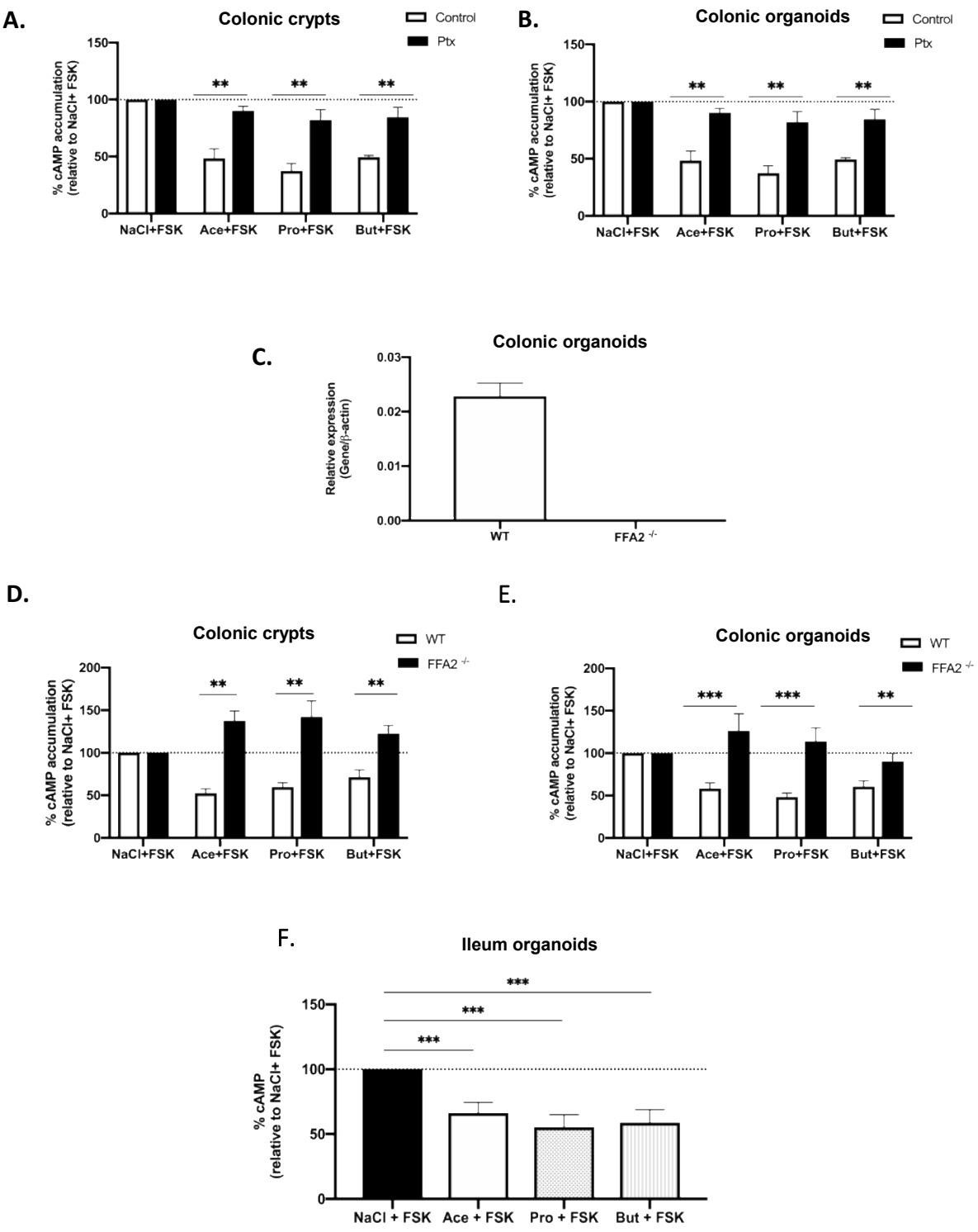


Figure 3.5 SCFAs inhibit forskolin induced cAMP in a Gα_i manner via FFA2 in mouse colonic- crypts and organoids. (A & B) Intracellular levels of cAMP measured in 16-hour-old colonic crypts (A) and mature colonic organoids (B) were treated with or without pertussis toxin (Ptx, 200 ng/ml, 20 hours) and subsequently treated with IBMX (5 minutes, 0.5 mM) and then with forskolin (FSK, 3 µM) or a combination of FSK (3 µM) and NaCl/SCFAs (1 mM) for 5 minutes. Data are expressed as percentage change of NaCl+FSK. Data represent mean ± SEM, n=3 independent experiments, t-test: ** $p<0.01$ vs control. (C) Verification of absence of FFA2 in mature FFA2$^{-/-}$ mouse colonic organoids analyzed via RT-qPCR. (D & E) Intracellular levels of cAMP measured in WT or FFA2$^{-/-}$ 16-hour-old mouse colonic crypts (D) and mature colonic organoids (E) treated with IBMX (5 minutes, 0.5 mM) and then with forskolin

(FSK, 3 μM) or a combination of FSK (3 μM) and NaCl or SCFAs (1 mM) for 5 minutes. Data are expressed as percentage change of NaCl+FSK. Data represent mean ± SEM, n=3 independent experiments, t-test: ** p<0.01; ***p<0.001 vs WT. (F) Intracellular levels of cAMP measured in mature mouse ileum organoids treated with IBMX (5 minutes, 0.5mM) and then with forskolin (FSK, 3 μM) or a combination of FSK (3 μM) and NaCl or SCFAs (1mM) for 5 minutes). Data are expressed as percentage change of NaCl+FSK. Data represent mean ± SEM, n=3 independent experiments, t-test: *** p<0.001 vs NaCl+FSK.

3.2.5 SCFAs are unable to mediate $G\alpha_{q/11}$ signalling in enteroendocrine cells

FFA2 is also coupled to $G\alpha_{q/11}$ and multiple reports have shown that SCFAs at 1 mM induces intracellular calcium mobilisation in many cell types (Tolhurst et al., 2012; Priyadarshini et al., 2015). To verify this, I determined the ability of SCFAs to induce intracellular calcium mobilisation in STC-1 cells. STC-1 cells were incubated with a fluorescence calcium indicator dye prior to ligand stimulation. SCFAs both at 1 mM and 10 mM were unable to induce increase in intracellular calcium levels (Figure 3.6 B & C). Whereas, stimulation with a specific FFA2 synthetic allosteric ligand, 4-CTMB led to a rapid and transient rise in intracellular calcium, and stimulation with a FFA2 synthetic orthosteric ligand, Compound 1 (Cmp1) (Bolognini et al., 2016b), led to a rapid and sustained rise in intracellular calcium mobilisation (Figure 3.5 B&C). A similar profile was also seen in measuring accumulation of intracellular levels of inositol mono-phosphate (IP1), a downstream metabolite of inositol 1,4,5-triphosphate (IP3) (Figure 3.6 D), indicating that the lack of SCFA-mediated intracellular calcium and IP1 responses are not due to a lack of functional FFA2 in these cells.

To investigate if FFA2 activates $G\alpha_i$ or $G\alpha_{q/11}$ to induce intracellular calcium mobilisation, STC-1 cells were treated with 4-CMTB or Cmp1 following a pre-treatment with either Ptx or YM-254890 (YM), a specific $G\alpha_{q/11}$ inhibitor. Pre-treatment of Ptx, did not attenuate 4-CMTB or Cmp1 induced intracellular calcium mobilisation or accumulation of IP1 (Figure 3.6 E&F). Pre-treatment with YM, however, significantly attenuated 4-CMTB- and Cmp1- induced increases in IP1 levels, indicating that both 4-CMTB and Cmp1 activates $G\alpha_{q/11}$ signalling in STC-1 cells (Figure 3.6G).

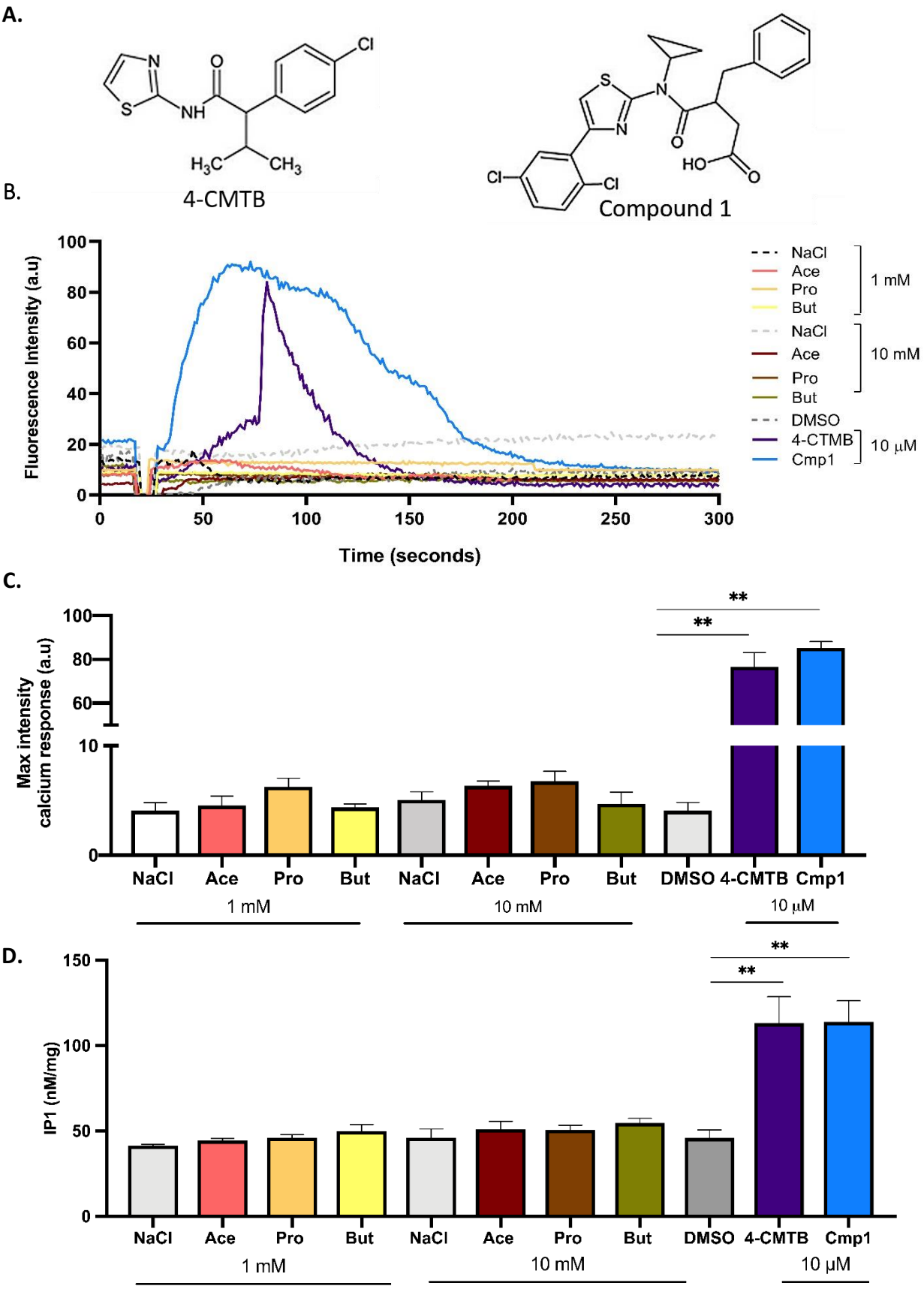


Figure 3.5 continued the following page

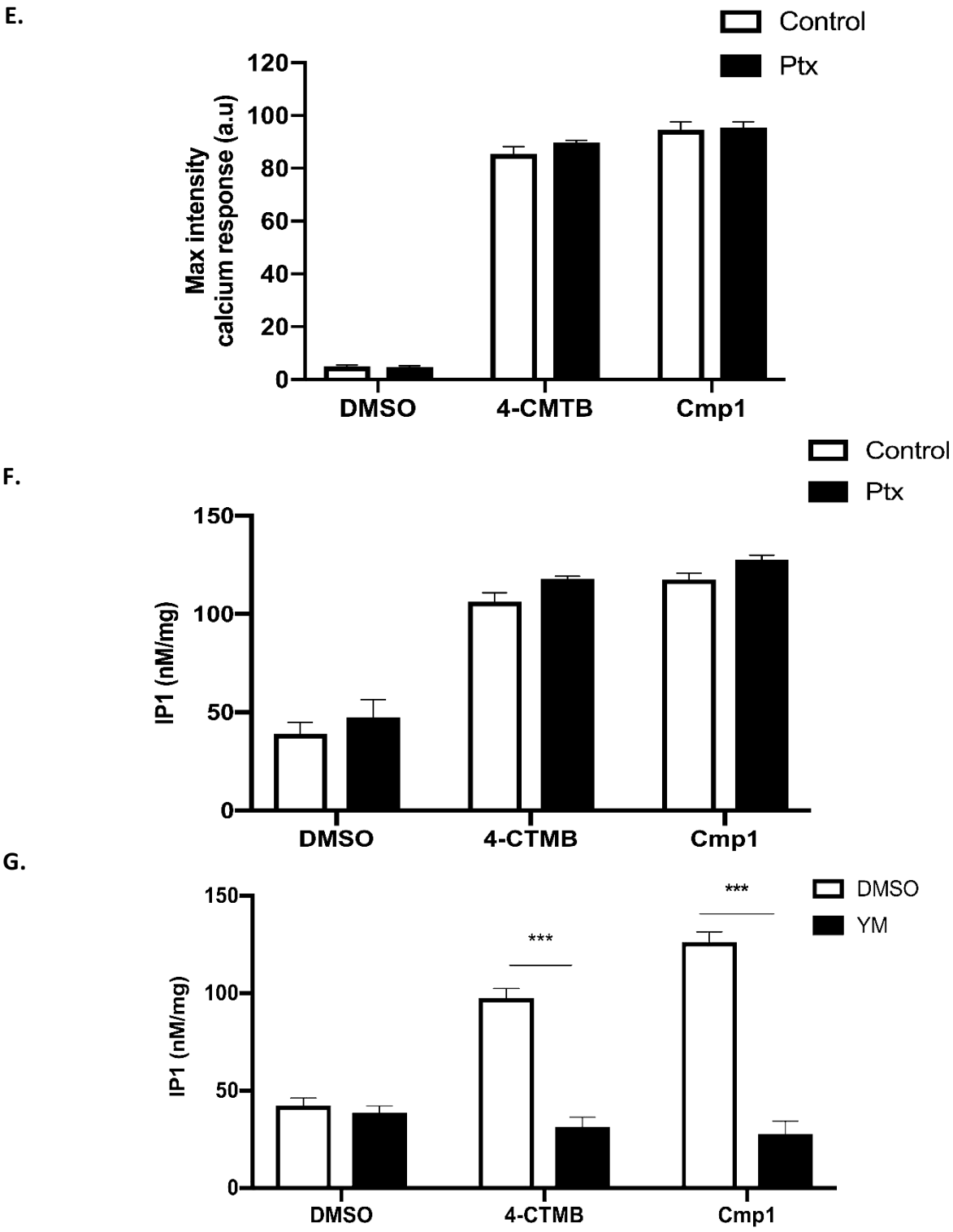


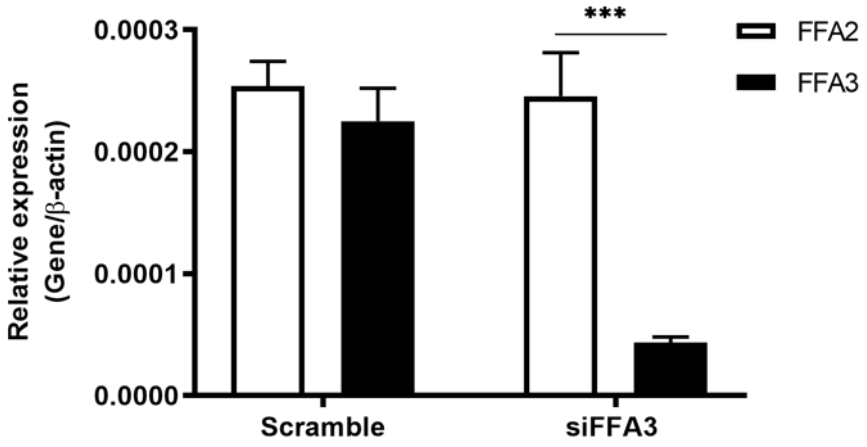
Figure 3.5 SCFAs are unable to induce intracellular calcium mobilisation. (A) Chemical structures of 4-CMTB and compound 1 (Cmp 1), adapted from (Bolognini et al., 2016a). (B & C) Intracellular calcium mobilisation measured in STC-1 cells, incubated with fluorescence calcium indicator Fluo4-AM for 1 hour and imaged live via confocal microscopy for 1 minute before the addition of either NaCl, SCFA (1 and 10 mM), DMSO, 4-CMTB or Cmp1 (10 µM). (B) Single-cell representative fluorescence intensity plots following SCFAs and 4-CMTB/Cmp1 stimulation, expressed in arbitrary units (AU). (C) Average maximal fluorescence intensities from cells in (A). Data represent mean ± SEM of at least 20 cells in

duplicate per 3 independent experiments, t-test ** p<0.01 vs DMSO. (D) Intracellular accumulation of IP1 measured in STC-1 cells treated with either NaCl, SCFA (1 and 10 mM), DMSO, 4-CMTB or Cmp1 (10 μM) for 2 hours. Data represent mean ± SEM; n=3 interdependent experiments. (E) Intracellular calcium mobilisation measured in STC-1 cells, incubated with fluorescence calcium indicator Fluo4-AM for 1 hour following pre-treatment with Ptx (200 ng/mL, 20 hours) and imaged live via confocal microscopy for 1 minute before the addition of either DMSO, 4-CMTB (10 μM) or Cmp1 (10 μM). Data represent mean ± SEM of at least 20 cells in duplicate per 3 independent experiments. (F) Intracellular accumulation of IP1 measured in STC-1 cells pre-treated Ptx (200mg/mL, 20 hours) prior to treatment with either DMSO, 4-CMTB (10 μM) or Cmp1 (10 μM) for 2 hours. Data represent mean ± SEM; n=3 interdependent experiments. (G) Intracellular accumulation of IP1 measured in STC-1 cells pre-treated with DMSO (vehicle) or YM (10 μM) for 10 minutes prior to treatment with either DMSO, 4-CMTB (10 μM) or Cmp1 (10 μM) for 2 hours. Data represent mean ± SEM; n=3 interdependent experiments, t-test *** p<0.001 DMSO vs YM.

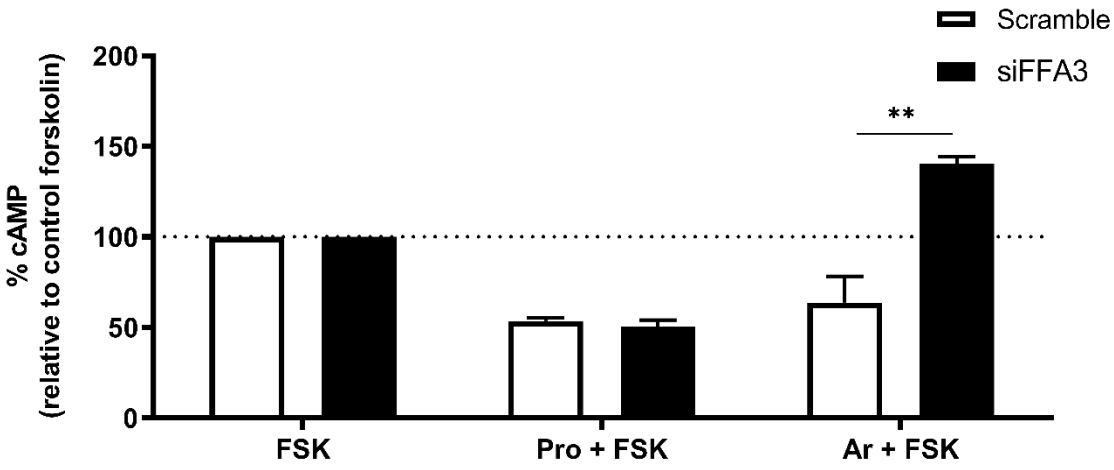
3.2.6 SCFAs are unable to mediate $G\alpha_{q/11}$ despite absence of FFA3

As SCFAs were unable to induce intracellular calcium mobilisation in STC-1 cells, it was speculated that SCFAs may be preferentially activating FFA3 and therefore unable to induce $G\alpha_{q/11}$ signalling. To examine this, cellular levels of FFA3 were knocked down via siRNA in STC-1 cells and $G\alpha_{q/11}$ mediated signalling was measured via intracellular calcium mobilisation and IP1 levels. Efficiency of FFA3 knockdown was verified via qPCR and functionally by measuring inhibition of intracellular forskolin-induced cAMP with a FFA3 synthetic agonist, AR 42062 (AR). Knockdown of FFA3 in the STC-1 cells significantly decreased FFA3 mRNA expression levels compared to siRNA-scramble transfected cells (Figure 3.6 A). To further confirm FFA3 knockdown at a functional level, intracellular cAMP was measured in these cells (siFFA3). In cells transfected with control siRNA, AR and propionate decreased forskolin induced cAMP (Figure 3.6A). In cells transfected with siFFA3, propionate-induced inhibition of forskolin induced cAMP was not attenuated, however, AR-mediated inhibition of forskolin induced cAMP was significantly impaired, compared to scrambled control cells, confirming successful functional knockdown of FFA3 (Figure 3.6 B). However, upon measuring induced intracellular calcium mobilisation and IP1 accumulation, propionate at 1 mM remained unable to induce any $G\alpha_{q/11}$ signalling both in control cells and in siFFA3 cells. Direct activation by Cmp1 elicited a robust increase in intracellular calcium mobilisation and accumulation of intracellular IP1 both in control cells and in siFFA3 cells (Figure 3.6 C&D). This indicates that the inability of SCFAs to activate $G\alpha_{q/11}$ in STC-1 cells is not due to the expression of FFA3 in these cells.

A.



B.



C.

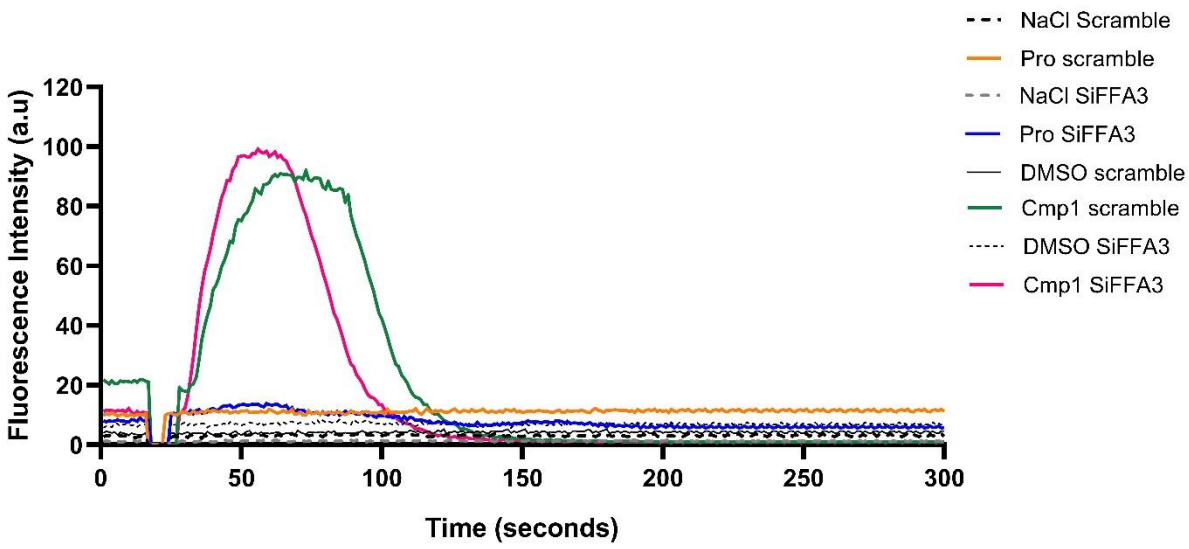


Figure 3.6 continued the following page

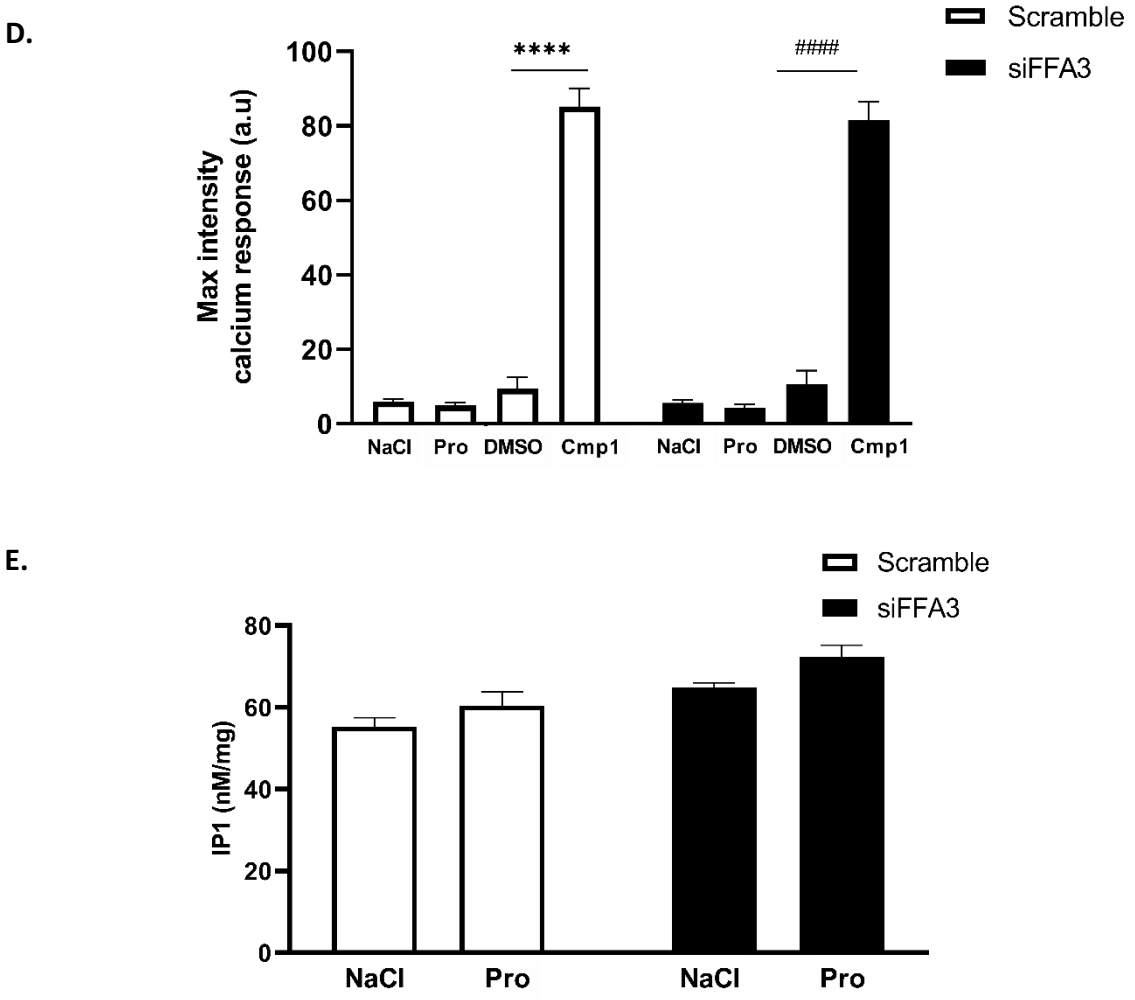
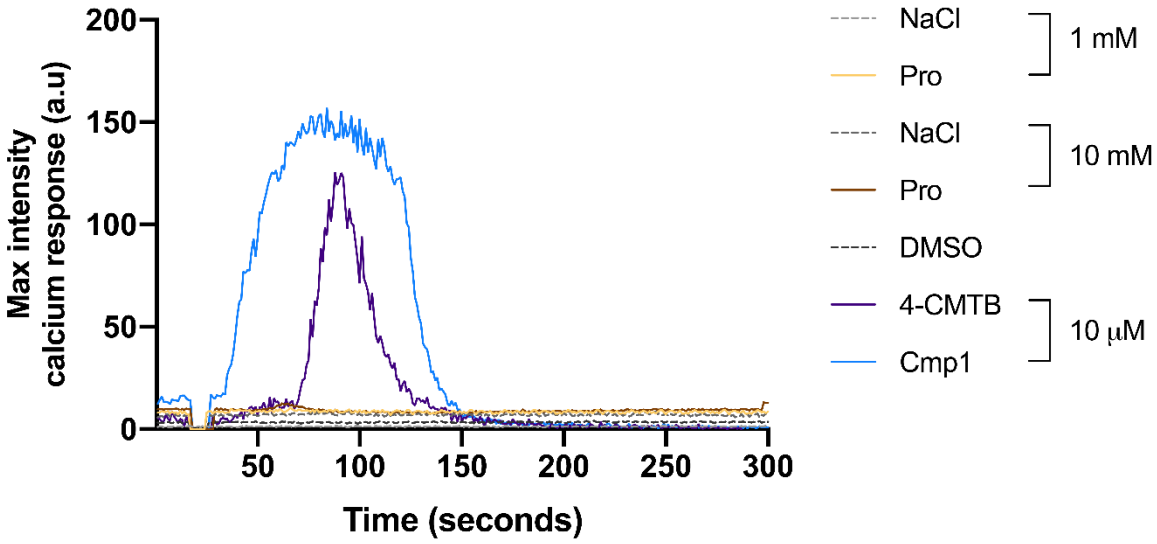


Figure 3.6 SCFAs are unable to elicit Gαq/11 signalling in STC-1 cells that are depleted of FFA3. STC-1 cells were transfected with either scramble or FFA3 siRNA (siFFA3) for 72 hours. After 72 hours, cells were plated for RNA extraction and measurement of intracellular cAMP, calcium mobilisation and accumulation of IP1. (A) Efficiency of FFA3 knockdown was analysed via qPCR. (B) Measurement of intracellular cAMP in scramble or siFFA3 STC-1 cells. Cells were treated with IBMX (5 minutes, 0.5mM) and then with forskolin (FSK, 3µM) or a combination of FSK (3µM) and propionate (Pro, 1 mM) or FSK (3µM) and DMSO/Ar (10 µM) for 5 minutes. Data are expressed as percentage change of FSK. Data represent mean ± SEM, n=3 independent experiments, t-test: ** $p<0.01$ scramble vs siFFA3. (C) Intracellular calcium mobilization measured in scramble and siFFA3 STC-1 cells, incubated with fluorescence calcium indicator Fluo4-AM for 1 hour and imaged live via confocal microscopy for 1 minute before the addition of either NaCl, Pro (1 mM), DMSO or Cmp1 (10 µM). (C) Single-cell representative fluorescence intensity plots following Pro and Cmp1 stimulation, expressed in arbitrary units (AU). (D) Average maximal fluorescence intensities from cells in (C). Data represent mean ± SEM of at least 20 cells in duplicate per 3 independent experiments, t-test ** $p<0.01$ vs DMSO. (E) Intracellular accumulation of IP1 measured in scramble or siFFA3 STC-1 cells treated with NaCl or Pro (1 mM) for 2 hours. Data represent mean ± SEM; n=3 independent experiments.

3.2.7 SCFAs are unable to mediate $G\alpha_{q/11}$ signalling in colonic crypts and organoids

Despite observing SCFAs are unable to mediate $G\alpha_{q/11}$ signalling in STC-1 cells, propionate at 1 mM has been previously reported to be able to induce intracellular calcium mobilisation in mouse colonic crypt cultures (Tolhurst et al., 2012). To confirm this, I examined the ability of propionate to induce intracellular calcium mobilisation in colonic crypts and organoids. After propionate stimulation in colonic crypts both at 1 and 10 mM no calcium response was observed. However, stimulation with 4-CMTB or Cmp1 led to a significant rapid and transient response (Figure 3.7 A & B). Stimulation of colonic organoids with 1 mM propionate, also did not induce a calcium response. To confirm the organoids could produce a calcium response, organoids were subsequently challenged with GW 9508, a ligand for the $G\alpha_{q/11}$-coupled FFA1. There was a robust increase in intracellular calcium in a subpopulation of cells within the organoids (white arrows, Figure 3.7C, Figure 3.7 D&E). Together, this suggest that SCFAs does not show any potential coupling to $G\alpha_{q/11}$ in both STC-1 cells and mouse colonic-crypts and organoids.

A.



B.

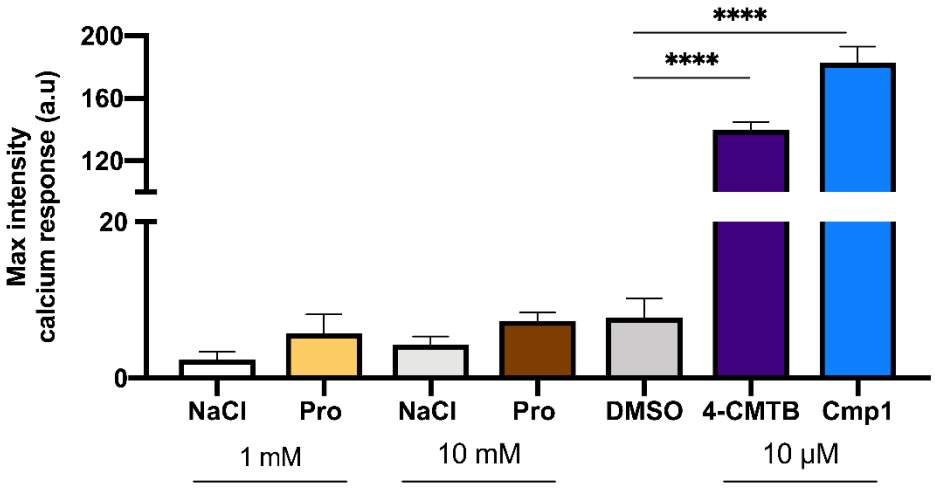
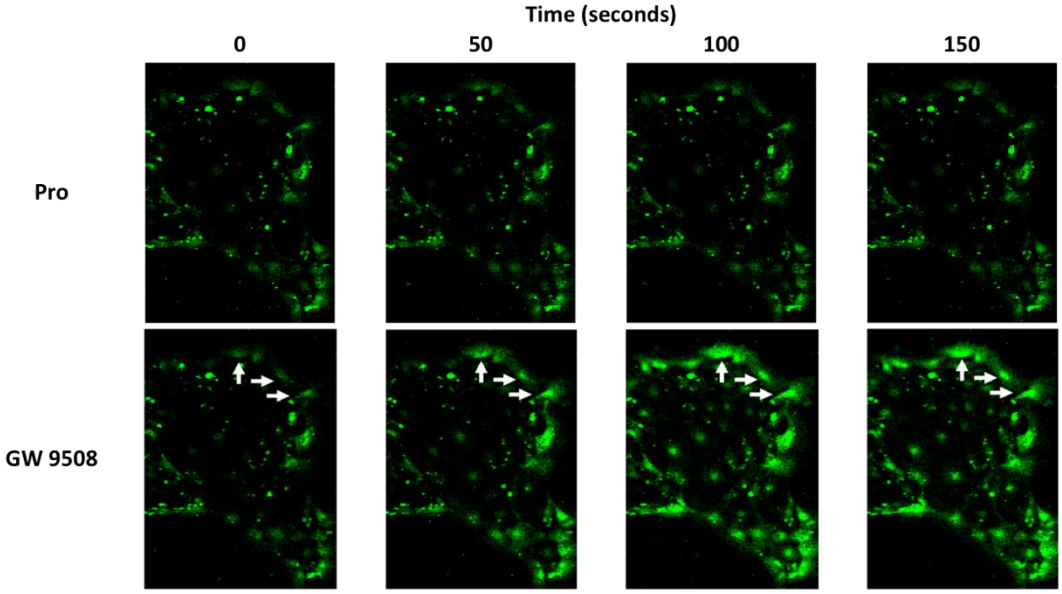


Figure 3.7 continued the following page

C.



D.

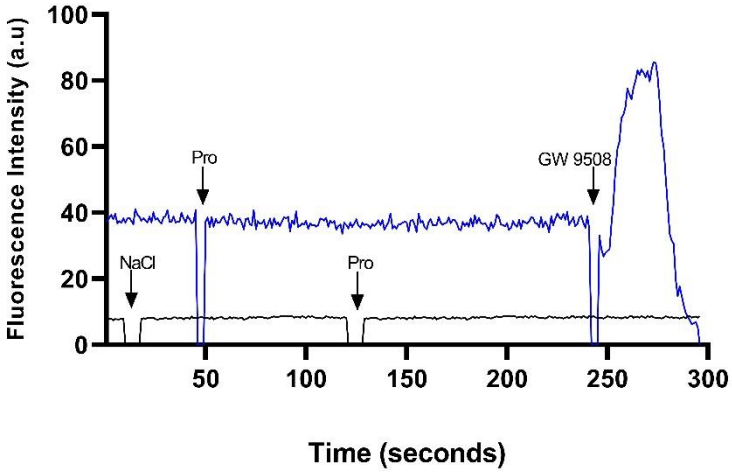


Figure 3.7 continued the following page

E.

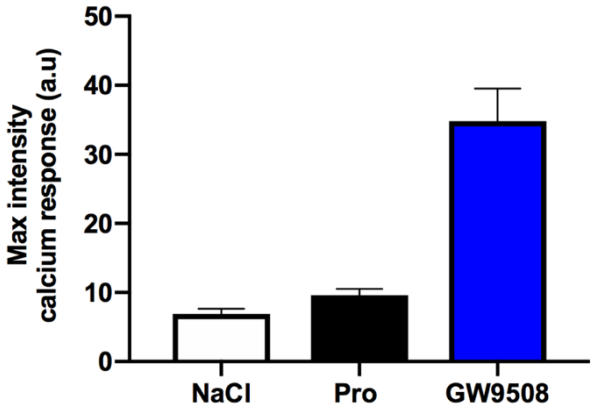


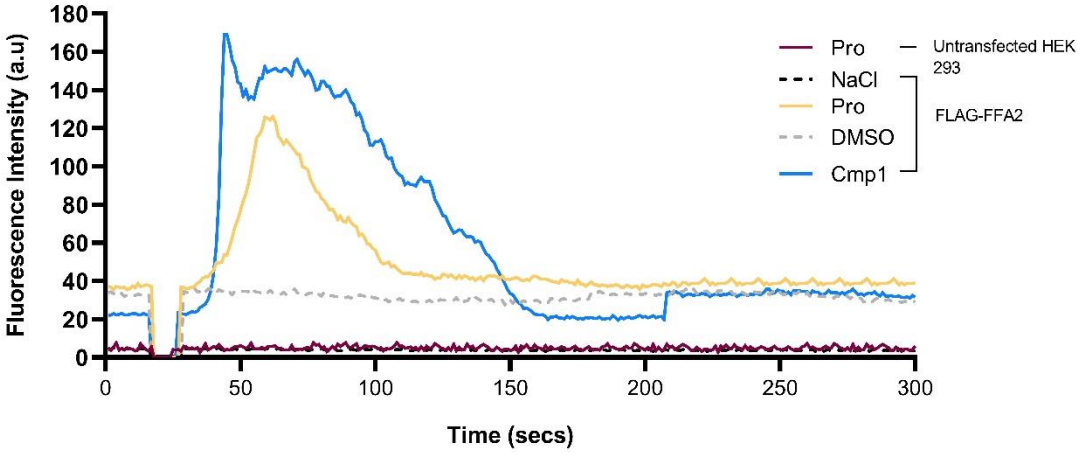
Figure 3.7 SCFAs are unable to induce intracellular calcium in the colon. (A & B) Intracellular calcium mobilisation measured in colonic crypts, crypts were incubated with fluorescence calcium indicator, Fluo4-AM for 1 hour and imaged live via confocal microscopy for 1 minute before NaCl or propionate (1 and 10 mM) or DMSO or 4-CMTB/Cmp1 (10 µM) addition. (A) Single-crypt cell representative fluorescence intensity plots following NaCl/SCFAs and 4-CMTB/Cmp1 stimulation, expressed in arbitrary units (AU). (B) Average maximal fluorescence intensities from cells in (A). Data represent mean ± SEM of at least 20 cells in duplicate per 3 independent experiments, t-test **** $p<0.0001$ vs DMSO. (C-E) Intracellular calcium mobilization measured in colonic organoids, organoids were incubated with fluorescence calcium indicator Fluo4-AM for 1 hour and imaged live via confocal microscopy for 1 minute before Pro (1 mM) or GW 9508 (10 µM) addition. (C & D) Representative time-lapse confocal images (C) and fluorescence intensity plots (D) of organoids following stimulation with propionate (Pro, 1 mM) and GW 9508 (10 µM) addition (arrows). (E) Average maximal fluorescence intensities from cells in (C & D). Data represent mean ± SEM of at least 20 cells in duplicate per 3 independent experiments for propionate and 2 for GW9508.

3.2.7 SCFAs are able to activate $G\alpha_{q/11}$ signalling in HEK 293 cells expressing FFA2

The above results demonstrate that SCFAs do not activate $G\alpha_{q/11}$ signalling via FFA2 in enteroendocrine cells or in colonic crypts and organoids. It was then asked if asked if the inability of SCFAs to activate $G\alpha_{q/11}$ signalling via FFA2 was cellular context-specific. I assessed SCFA-mediated signalling in HEK 293 cells transiently expressing FLAG-FFA2. Treatment of these cells with Cmp1 led to rapid and sustained response, as seen in the STC-1 cells and in mouse colonic crypts (Figure 3.5A & Figure 3.7A). Surprisingly, stimulation with propionate, induced a rapid and transient calcium response that was not observed in un-transfected HEK 293 control cells (Figure 3.8 A). To analyse if this response was $G\alpha_{q/11}$ or $G\alpha_{i}$ mediated, cells were stimulated with propionate or Cmp1 following pre-treatment with Ptx or YM. Pre-treatment of both Ptx and YM, led to a significant decrease of propionate and Cmp1 induced

calcium response. However, decreases of induced calcium response varied from a partial inhibition with Ptx to a complete inhibition in YM. This suggest that intracellular calcium mobilisation of FFA2 induced by propionate and cmp1 may be mediated both via $G\alpha_{i/o}$ and $G\alpha_{q/11}$.

A.



B.

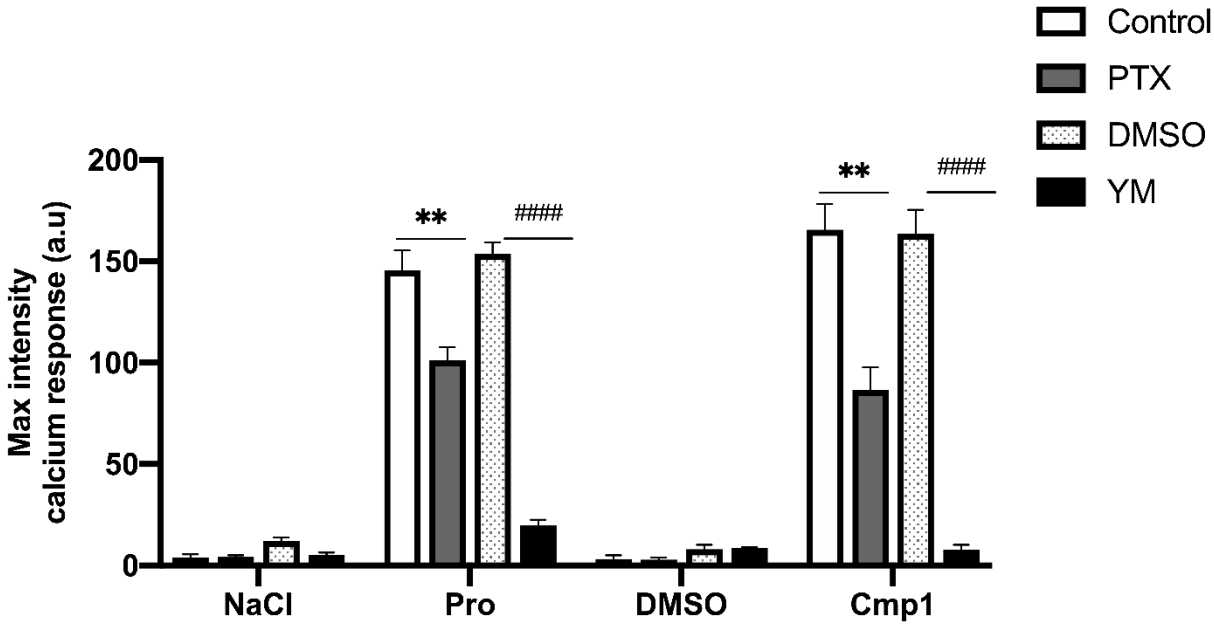


Figure 3.8 FFA2 induced intracellular calcium mobilisation occurs may be partially regulated by and $G\alpha_{q/11}$. (A) Single-cell representative fluorescence intensity plots of intracellular calcium mobilisation measured in HEK 293 cells transiently expressing FLAG-FFA2 cells, incubated with fluorescence calcium indicator Fluo4-AM for 1 hour and imaged live via confocal microscopy for 1 minute before the addition of either NaCl (1 mM), propionate (Pro, 1 mM), DMSO or Cmp1 (10 µM). (B) Intracellular calcium mobilisation measured in HEK 293 cells transiently expressing FLAG-FFA2, pre-treated with Ptx (200 ng/mL, 20 hours), then incubated with fluorescence calcium indicator Fluo4-AM for 1 hour and imaged live via confocal microscopy for 1 minute before the addition of either NaCl, propionate

(Pro, 1 mM), DMSO, 4CMTB (10 μM) or Cmp1 (10 μM). Data represent mean ± SEM of at least 20 cells in duplicate per 3 independent experiments, t-test: **p<0.01 vs control for Ptx; ### p<0.01 vs DMSO for YM.

3.3 Discussion

Characteristics of SCFA signalling via FFA2 have been robustly demonstrated primarily in HEK 293 or CHO cells, however the signalling pathways exerted by SCFAs in enteroendocrine cells have been not been fully characterised. Therefore, it was necessary to first elucidate the SCFA signalling profiles in an enteroendocrine cell model. Using an enteroendocrine cell line, STC-1 cells, colonic crypts and organoids, I demonstrated signalling characteristics that are both similar and distinct to those reported for FFA2 in other cell models.

To elucidate FFA2 signalling profiles, expression levels of FFA2 and FFA3 in these enteroendocrine cell models were confirmed. In addition, the colonic crypts and organoids and ileum organoids were also characterised based on L cells where GLP-1 and PYY cells were found to be colocalised, which is typical of enteroendocrine L cells (Nilsson et al., 1991). Previously, efforts to characterise and delineate FFA2 and FFA3 relied on SCFA binding potencies to each receptor, of which, acetate and butyrate are equipotent and non-selective for both FFA2 and FFA3, whereas propionate is more potent and selective for mouse FFA3 over FFA2 and for human FFA2 the rank order of potency is reported as acetate and propionate equipotent followed by butyrate, whereas for human FFA3 propionate and butyrate is equipotent and followed by acetate (Hudson et al., 2012a). However, these potencies were obtained from HEK 293 cells overexpressing FFA2 or FFA3 and may not be reflective of physiological signalling responses, thus characterising SCFA signalling profiles in the colon was essential. In the colonic crypts and organoids and in ileum organoids, propionate exhibited the highest inhibition of forskolin induced cAMP in all models. In addition, the SCFAs mediated inhibition of forskolin induced cAMP in colonic crypts and organoids was FFA2 dependent. As the STC-1 cells and colonic crypts and organoids both express FFA2 and FFA3, single receptor analysis was difficult. To analyse FFA2-specific signalling, HEK 293 cells expressing FLAG-FFA2 was employed. In HEK 293 cells transiently expressing FLAG-FFA2, the observed inhibitions of forskolin induced cAMP were also similar to the reported potency of SCFAs to mouse FFA2 (Hudson et al., 2012a). This was evident as

butyrate at 1 mM exhibited similar inhibition of forskolin induced cAMP to that of acetate and propionate. Butyrate's inhibition of forskolin induced cAMP was also significantly higher than that observed in the STC-1 cells. Though these differences in inhibition of forskolin induced cAMP may be reflective of FFA2 and FFA3 expression level in each model, this demonstrates the complexity in differentiating the closely related FFA2 and FFA3 and that discrimination simply based on rank order of potency of SCFAs to each receptor is insufficient. Thus, a further understanding beyond G-protein activation such as receptor trafficking or signalling pathway activation downstream of ligand binding is required to fully understand receptor function.

SCFAs at the concentration of 1 mM has been demonstrated to be able to induce a calcium response via FFA2 in many cellular systems including mouse primary colonic L cells (Tolhurst et al., 2012), however, the data presented here demonstrates that SCFAs in the colon does not induce intracellular calcium mobilisation at 1 or 10 mM whereas, synthetic FFA2-allosteric agonist, 4-CMTB and orthosteric agonist, Cmp1 were able to induce a intracellular calcium mobilization via $G\alpha_{q/11}$. Although it may be argued that the inability of the SCFAs to induce intracellular calcium mobilisation may be due to the usage of BSA in aiding solubility of the SCFAs and the co-addition of SCFAs and BSA to the assay media can cause a complex of albumin and SCFAs, thereby decreasing the amount of unbound SCFAs accessible for SCFAs mediated signalling. However, as SCFAs were able to inhibit forskolin induced cAMP and induce intracellular calcium mobilisation and increase intracellular accumulation of IP1 in HEK 293 cells expressing FFA2 FLAG in the presence of the BSA in the assay media, this indicates that the inability of SCFAs to induce intracellular calcium mobilisation, opposed to the synthetic compounds, is not due to the difference in affinity/ligand association rate or variations in solubility characteristics. Additionally, intracellular calcium mobilisation assays were conducted in calcium containing or calcium free conditions (data not shown), indicating it was not a lack of extracellular calcium that could explain differences in this study and that of Tolhurst et al., (2012). Furthermore, in the Tolhurst et al., (2012) study, the identification of an L cell was achieved by labelling L cells with the yellow fluorescent protein, Venus, which allows for the L cells to be readily visible and thus enabling calcium imaging at a single-cell level opposed to calcium imaging in a model where multiple cells are present as in the colonic crypts and organoids used in these experiments. Moreover, by fluorescently labelling the L cells, FFA2 function may have been altered in such a way that G-protein coupling may have

increased, though the FFA2 function characterisation was carried out by calcium imaging, the ability of inhibition of cAMP was not determined (Tolhurst et al., 2012).

The inability of SCFAs to activate $G\alpha_{q/11}$ in the enteroendocrine cells and in the colon may also be due to SCFAs in enteroendocrine cells may preferentially activate $G\alpha_{i}$. This $G\alpha_{i/o}$ preferential coupling was also observed for FFA2 in gastric ghrelin cells, whereby propionate via $G\alpha_{i}$ suppressed ghrelin secretion and not via $G\alpha_{q/11}$ (Engelstoft et al., 2013). This preferential $G\alpha_{i}$ coupling was not due to ghrelin cells lacking $G\alpha_{q/11}$ as these subunits are highly expressed in ghrelin cells (Engelstoft et al., 2013). However, the $G\alpha_{i/o}$ subunits, $G\alpha_{OA}$, $G\alpha_{OB}$ and $G\alpha_{Z}$ (a Ptx in-sensitive $G\alpha_{i/o}$) were found to be highly expressed and enriched in ghrelin cells (Engelstoft et al., 2013). Furthermore, bias for $G\alpha_{I}$ is not only observed for SCFAs, bias for $G\alpha_{i/o}$ was also reported for 4-CMTB which in mouse islets inhibits glucose-stimulated insulin secretion (GSIS) via $G\alpha_{i}$ and is unable to induce an intracellular calcium mobilisation, opposed to acetate which potentiates GSIS through $G\alpha_{q/11}$-induced calcium mobilisation (Priyadarshini et al., 2015). This demonstrates that not only does SCFA potentially display biased agonism signalling, but SCFA-FFA2 signalling is also biased by the cellular background system.

Further, SCFAs remained unable to active $G\alpha_{q/11}$ signalling in STC-1 cells depleted of FFA3. Though it has been reported for the human FFA2, FFA2-$G\alpha_{q/11}$ mediated signalling is enhanced when heterodimerisation complex is formed with FFA3 (Ang et al., 2018). FFA2-FFA3 heterodimerisation have yet to be reported for mouse FFA2 and FFA3. Alternatively, FFA2 may be interacting with other GPCRs in the intestinal tract which may attenuate SCFAs ability to induce intracellular calcium mobilisation. Traditionally, GPCRs were viewed to act as single subunits, or monomers, but mounting evident over the last two decades has shown that GPCRs can routinely form homo- or heterodimers and/or high order oligomers with other GPCRs to modulate signalling and trafficking. A variety of GPCRs have been identified in the intestinal tract for instance, free fatty acid receptor 1 and 4, the calcium sensing receptor (CaSR), the bile acid TGR5 membrane receptor, GPR119 and the umami receptors (T1R1-3), (Reimann et al., 2012). In addition to FFA2 and FFA3, other GPCRs have also been identified in enteroendocrine L cells, such as the cholecystokinin 1 receptor (CCK1R), gastric inhibitory

polypeptide receptor (GIPR), the galanin receptor 1 (GALR1) and the muscarinic receptor 2 (M2). The latter of which is a $G\alpha_{i/o}$ coupled receptor that is reported to regulate the release of GLP-1 in enteroendocrine L cells (Anini and Brubaker, 2003). Alternatively, FFA2 heterodimerization interactions could also be occurring in a manner that may cause to propionate to activate FFA2 distinctively to the FFA2 synthetic ligands, 4-CMTB and Cmp1 which are able to activate $G\alpha_{q/11}$ signalling. 4-CMTB and Cmp1 may be activating FFA2 in 'cis' manner to activate $G\alpha_{q/11}$ signalling, while propionate activation occurs in 'trans' manner where a complex with another GPCR or a homeric complex is form, thus allowing propionate to only activate $G\alpha_{i/o}$ signalling. This 'cis' and 'trans' activation has been demonstrated for the luteinizing hormone receptor (LHR). When LHR mutants, one mutated in function and the other in binding, are co expressed, reconstituted only the human chorionic gonadotropin-mediated but not LH-mediated $G\alpha_{q/11}$ signalling, suggesting the that the organisation with the reconstituted hetero-oligomers limits the LH activation, due the specific geometry within the complex (Jonas et al., 2015).

In HEK 293 cells transiently expressing FLAG-FFA2, propionate was able to activate $G\alpha_{i/o}$ and $G\alpha_{q/11}$ signalling. Interestingly, not only was the induced calcium mobilisation of both propionate and Cmp1 inhibited by YM but also was partially inhibited by Ptx, suggesting that $G\alpha_{i/o}$ in part may also regulate $G\alpha_{q/11}$ activation by FFA2. Inhibition of propionate FFA2-induced calcium mobilisation by Ptx has also been previously reported by Nilsson et al., (2003) as a 70% reduction in calcium mobilisation upon Ptx treatment in CHO cells overexpressing FFA2 was observed. Though, this cross-talk in G-protein activation was not observed for the Cmp1 induced increases in IP1 in the STC-1 cells, where IP1 level was only attenuated by YM and not by Ptx. However, this may be solely due to a difference of G protein coupling, regulation of coupling and difference of receptor levels in STC-1 cells and FLAG-FFA2 HEK 293 cells which may have an impact on the signalling profiles. This difference in receptor G protein signalling profiles was also seen for the GPR142 receptor, where when expressed in HEK 293 cells activates both $G\alpha_{q/11}$ and $G\alpha_{i/o}$, however in primary pancreatic islets only requires $G\alpha_{q/11}$ signalling for stimulation of insulin secretion (Wang et al., 2016). Differential multiplicity coupling of G proteins in one cell type to another cell type may arise from differences in the expression levels of participating G proteins (Nasman et al., 2001). This is particularly true in

a recombinant GPCR expression system, where the relative stoichiometry of receptor to G proteins may vary from that in native cells (Kenakin, 1997). In fact, it has been reported for multiple GPCRs that increases in receptor density can lead to cellular responses not found under conditions of lower receptor expression (Kenakin, 1997). Nonetheless, whether the intracellular calcium mobilization of FFA2 integrates both $G\alpha_{q/11}$ and $G\alpha_{i/o}$, further mechanistic exploration is required to better elucidate this signalling mechanism of FFA2.

In summary, the data presented here provides novel insights into the nature of endogenous SCFAs signalling in enteroendocrine L cells in terms of preference to $G\alpha_i$ coupling. This observation may form the basis of future work, if SCFAs display bias agonism and that such biased agonism may be important for downstream functions of FFA2.

Chapter 4:

FFA2 internalisation is critical for FFA2 mediated signalling

4.1 Introduction

GPCRs have a key role of translating extracellular signals into intracellular effectors with diverse biological functions. The mechanism by which GPCRs carry out this key role was conventionally viewed as a simple cyclical model, whereby receptor activation and termination occurs only at the plasma membrane. This simplified model, is merely insufficient to explain the growing complexity of GPCR signalling, which includes not only mechanisms that modulate GPCR responsiveness such as receptor desensitisation, internalisation and resensitisation (or degradation) but also the vast array of binding proteins that can modulate receptors localisation and cellular signalling events. Emerging reports have now shown that GPCRs can be active in multiple active states, induce non-canonical signalling, and most recently endosomal signalling, all of which occur through the tightly regulated process of intracellular membrane trafficking. Thus, in this chapter I seek to address whether FFA2 signalling is regulated by trafficking.

Many GPCRs are localised primarily on the plasma membrane at steady state and upon ligand activation receptors redistribute from the plasma membrane and into intracellular compartments, undergoing ligand induced internalisation. Ligand-induced internalisation is a well characterised process that was classically viewed as a step to contribute to receptor desensitisation, however, now has evolved as a major mechanism involved in many physiological responses. Briefly, upon ligand activation, the GPCR undergoes a conformation change that results in activation of its cognate G-protein and receptor phosphorylation then occurs by G-protein receptor kinase (GRKs) which promotes recruitment of β-arrestins, uncoupling of the receptor from the G protein and undergoes internalisation (Zhang et al., 2017). Internalisation can occur mainly by two processes: clathrin-dependent endocytosis or clathrin-independent endocytosis. Clathrin-dependent endocytosis (CDE) is generally mediated by β-arrestins by forming a multicomponent complex with the endocytic adaptor protein AP2 and clathrin subsequently forming clathrin coated pits. Following formation of the pits, the GTPase dynamin facilitates fission to all the formation of an endosomes, which is then subject sorting in the endocytic matrix (Delom and Fessart, 2011). Clathrin-

independent endocytosis (CIE) in general utilises an alternative mechanism but is known to use core components of CDE such as dynamin (Mayor et al., 2014).

Receptor internalisation, both constitutive and ligand induced, is a complex process and, as described above, involves multiple steps and a plethora of scaffold and adaptor proteins that can regulate receptor responsiveness and the post endocytic fate. Another process that can regulate receptor internalisation is receptor phosphorylation which can occur at the C-terminal tail and on intracellular loops of the receptor (Ferguson et al., 1996). GPCRs can undergo ligand- and site-specific phosphorylation and this is known to dictate their interaction with β-arrestins and therefore mediates receptor internalisation and also initiate a second wave of signalling via interaction with various signalling molecules such as MAPK. However, there is also evidence that stable GPCR-β-arrestins can be formed without the requirement of phosphorylation sites in the C-terminal tail. For example, mutant receptors of the NK1 receptor and the leukotriene B4 receptor lack phosphorylation sites yet still interact and form stable complexes with β-arrestins (Richardson et al., 2003; Jala et al., 2005). Another mode by which internalisation may be modulated by is the interaction with proteins and motifs that which interact with the C-terminal tail of the receptor such as Tyr-and dileucine (Leu)-based motifs that can be recognised by adaptor protein (AP) complexes associated with the cytosolic face of endocytic membranes, palmitoylation where the addition of palmitic acid (a 16C saturated fatty acid) to C-terminal can impact not receptor signalling but also internalisation.

In addition, accumulating evidence has suggested that internalisation is a requisite for specific signalling events that of which are distinct from the plasma membrane (Chapter 1, 1.7). For example, parathyroid hormone receptor (PTHR) internalization is required for a sustained or persistent $G\alpha_s$ signalling (Ferrandon et al., 2009). Findings from this and other studies show that spatial and temporal regulations of intracellular trafficking are essential for specific cellular events.

FFA2 has become of interest as a potential therapeutic target but surprisingly little is known about the trafficking profile of FFA2. Accordingly, in this chapter I characterise the trafficking

profile of FFA2 and determine that receptor internalisation is important for FFA2 mediated signalling.

4.2 Results

4.2.1 FFA2 is localised at the plasma membrane and at intracellular compartments

To assess the trafficking profile of FFA2, FFA2 was N-terminally tagged with a FLAG tag epitope to exploit the calcium dependent binding properties of the anti-FLAG antibody (referred to hereafter as FLAG-FFA2). HEK 293 cells stably expressing FLAG-FFA2 were then generated.

To visualise the localisation of FFA2, HEK 293 cells first were transiently transfected with FLAG-FFA2 and labelled live with anti-FLAG M1 antibody prior to treatment with NaCl, SCFA, Cmp1, AZ1729 (AZ), a $G\alpha_i$ biased-FFA2 synthetic allosteric ligand or left untreated. In untreated cells or cells treated with NaCl, FFA2 was localised not only at the plasma membrane but also at intracellular sites (Figure 4.1 A, inset), indicating that FFA2 displays constitutive internalisation. In cells treated with SCFAs, Cmp1, or AZ FFA2 appeared to be further internalized. This suggest that FFA2 undergoes both constitutive and ligand induced internalisation (Figure 4.1 A). In contrast to the localisation of the prototypical GPCR, the β2AR, for which the endocytic trafficking is well characterised was determined (Seachrist et al., 2000). In untreated cells, constitutive internalisation of the β2AR was not evident in untreated cells where the receptor was predominantly localised to the plasma membrane and in isoproterenol treated cells there was a robust internalisation was. A similar profile was observed in STC-1 transiently transfected with FLAG-FFA2 or β2AR (Figure 4.1A). This indicates that FFA2 localisation is not specific to HEK 293 cells and is trafficked similarly in STC-1 cells, which express endogenous FFA2.

The SCFA induced internalisation of FFA2 was quantified via flow cytometry. HEK 293 cells transiently expressing FLAG-FFA2 were first labelled live with anti-FLAG M1 antibody. Cells were treated with or without NaCl or SCFA and then labelled with immunofluorescent secondary antibodies. FFA2 internalisation was quantified as the loss of cell-surface

receptors. There was a decrease of FFA2 at the surface following exposure to NaCl and a further significant loss of FFA2 at the surface further with SCFAs, Cmp1 and AZ, confirming FFA2 exhibits constitutive and ligand-induced internalisation in response to all three SCFAs and FFA2 synthetic ligands (Figure 4.1 B).

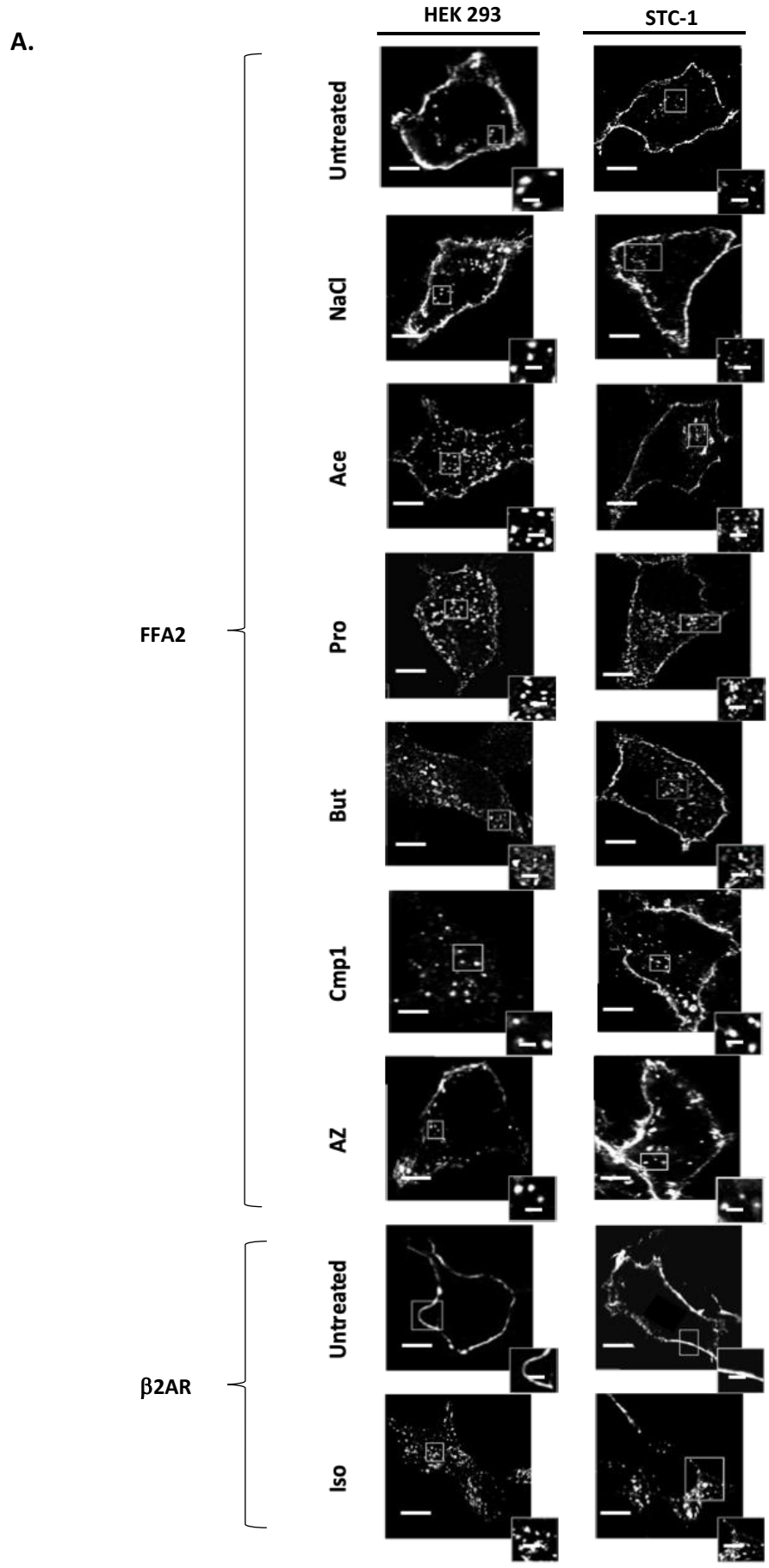


Figure 4.1 continued the following page

B.

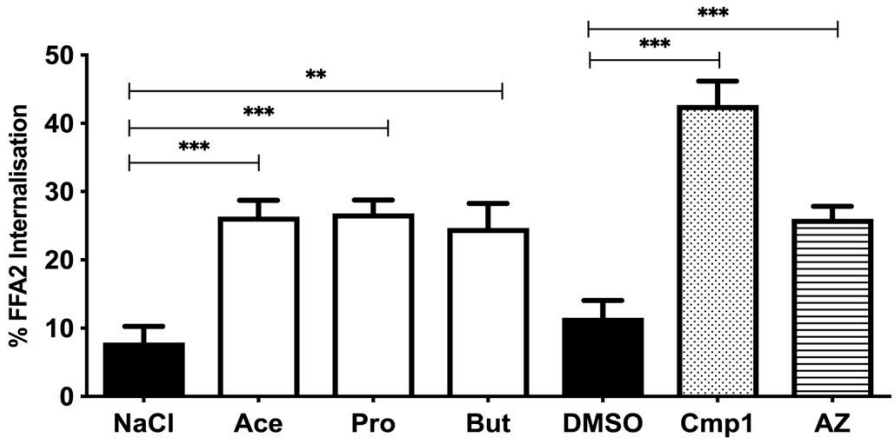


Figure 4.1 Surface and intracellular localisation of FFA2. (A) HEK 293 cells or STC-1 cells transiently expressing FLAG-FFA2 or β2AR stimulated with either NaCl (1mM), SCFAs (1 mM), compound 1 (Cmp1, 10 μM) or AZ1729 (AZ, 10 μM) for FFA2 or isoproterenol (Iso, 10 μM) for β2AR for 20 min following live labelling of anti-FLAG M1 antibody. Cells were then fixed, permeabilized and then labelled with immunofluorescent secondary antibodies. Shown are representative confocal microscopy images, n=10 imaged cells per condition, collected across 3 independent experiments. Scale bar is 10 μm and inset is 5 μm. (B) HEK 293 cells transiently expressing FLAG-FFA2 were labelled with anti-FLAG M1 antibody. Cells were then left untreated or treated with NaCl (1 mM), SCFAs (1mM), DMSO, Cmp1 (10 μM) or AZ (10 μM). The amount of FFA2 internalization was determined by loss of cell-surface receptors as quantified by flow cytometry and data was normalised to cells that had not been exposed to anti-FLAG M1 and immunofluorescent secondary antibodies. Data represent mean ± SEM, n=4 independent experiments; t-test: ** p<0.01; ***p<0.001 vs NaCl or DMSO.

4.2.2 FFA2 ligand induced internalisation is β-arrestin dependent

β-arrestins (β-ARR) are key regulatory proteins for the internalisation of GPCRs. As I've shown that FFA2 displays both constitutive and agonist induced internalisation, it was determined if whether β-ARR was involved in FFA2 internalisation and if there were differences in constitutive and ligand induced FFA2 internalisation in their β-ARR dependence. To investigate the direct involvement of β-ARR in FFA2 internalisation, FLAG-FFA2 were transiently expressed in HEK 293 cells where β-ARR 1/2 have been knocked out via Crispr/Cas 9 (Asuka Inoue). Validation of a complete loss of the β-ARR 1/2 proteins in KO cells versus WT cells was performed via western blot (Figure 4.3A).

Involvement of β-ARR in the internalisation of FFA2 were first determined by visualizing the internalisation of FFA2 expressed in β-ARR KO cells in comparison to FFA2 in wild type HEK 293 cells. In untreated cells or cells treated with NaCl, FFA2 was present at the plasma

membrane and in intracellular vesicles in both WT and β-ARR KO cells. For cells treated with SCFA, compared to WT cells, FFA2 internalisation in β-ARR KO cells appeared to be impaired as FFA2 remained largely at the plasma membrane and the redistribution of FFA2 into intracellular vesicles was not as evident as in WT cells (Figure 4.3B). This was also evident for the β2AR, a classical GPCR that requires β-ARR for its ligand induced internalisation (Figure 4.3 B).

To further investigate whether ligand-induced but not constitutive internalisation of FFA2 is β-ARR dependent, flow cytometry was performed to quantify FFA2 internalisation in β-ARR KO cells. Similar to what was observed from the visualisation of the internalisation of FFA2 in β-ARR KO cell, in cells treated with NaCl there was no significant difference in FFA2 internalisation in WT and β-ARR KO cells. In cells treated with SCFA, FFA2 internalisation was significantly impaired in β-ARR KO cells compared to WT cells (Figure 4.3 C). Similarly, the ligand induced internalisation for the β2AR was also significantly impaired in β-ARR KO cells compared to WT cells (Figure 4.3C). This indicates that ligand-induced internalisation of FFA2 requires β-ARR whereas constitutive internalisation of FFA2 does not and may require a distinct endocytic machinery.

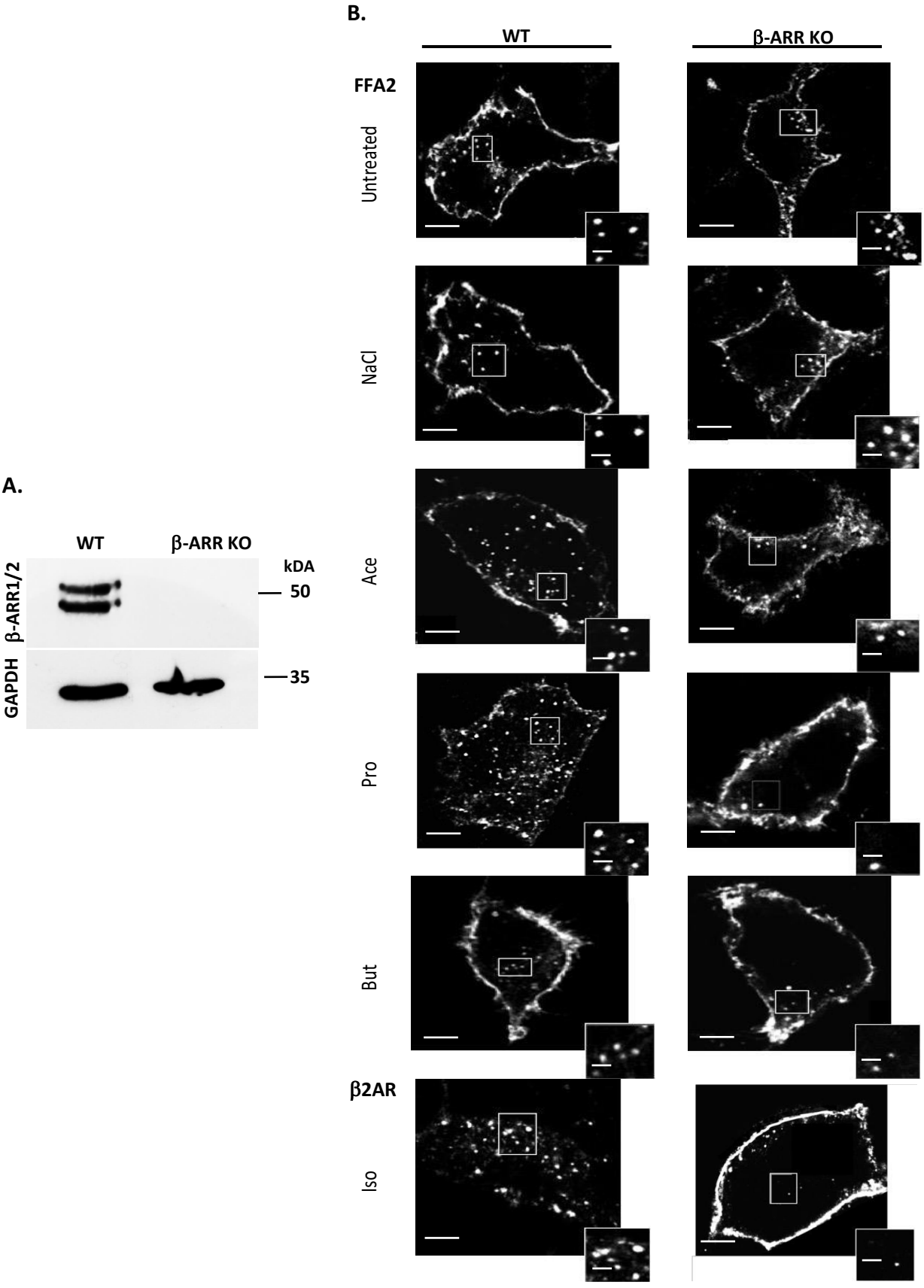


Figure 4.2 continued the following page

C.

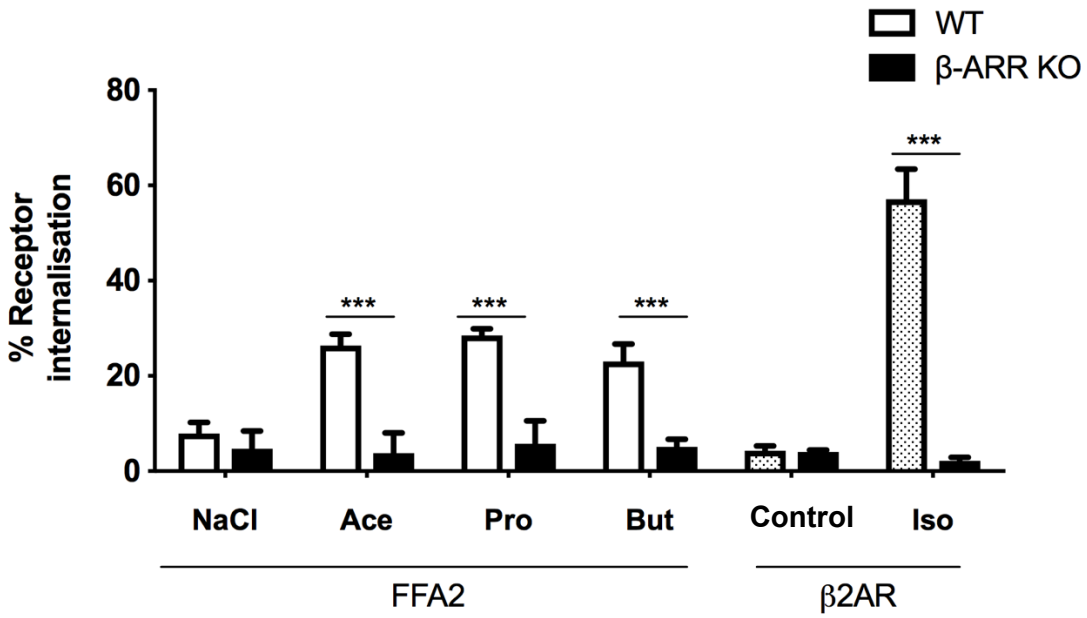


Figure 4.2 FFA2 ligand induced internalisation is β-arrestin dependent. (A) Western blot confirmation of absence of β-ARR expression in WT and in β-ARR KO. (B) HEK 293 cells or STC-1 cells transiently expressing FLAG-FFA2 or β2AR were labelled live with anti-FLAG M1 antibody. Cells were then left untreated or treated with NaCl/SCFA (1mM) for FFA2 or Isoproterenol (Iso, 10 µM) for 20 min. Cells were fixed, permeabilized and then labelled with immunofluorescent secondary antibodies. Shown are representative confocal microscopy. n=10 cells per condition, collected across 3 independent experiments. Scale bar is 10 µm and inset is 5 µm. (C) HEK 293 cells transiently expressing FLAG-FFA2 or β2AR were labelled with anti-FLAG M1 antibody. Cells were then left untreated or treated with NaCl/SCFA (1mM, 20min). The amount of FFA2 internalization was determined by loss of cell-surface receptors as quantified by flow cytometry and data was normalised to untreated cells. Data represent mean ± SEM, n=4 independent experiments; t-test: ** p<0.005; ***p<0.0005 vs β-ARR KO.

4.2.3 Constitutive and ligand-induced internalisation of FFA2 is dynamin-dependent

In addition to β-ARR, the GTPase dynamin is another key regulator in the internalisation of GPCRs and mediates internalisation via CME and non-CME pathways. To determine if constitutive FFA2 internalisation is dynamin mediated, a pharmalogical approach using a chemical inhibitor, Dyngo-4a, a potent selective inhibitor of dynamin GTPase activity (McCluskey et al., 2013) was employed. The exposure time of HEK 293 cells expressing FLAG-FFA2 to Dyngo-4a at 50 µM required to block FFA2 internalisation was first examined. In HEK 293 cells expressing FLAG-FFA2, cells were pre-treated with Dyngo-4A at 0, 15, 30 and 45 minutes and cell surface receptors were labelled prior to treatment propionate or left untreated for 20 minutes. After a 45-minute pre-treatment of Dyngo-4a, FFA2 internalisation

was completely inhibited in both untreated cells and cells treated with propionate (Figure 4.3 A), thus a 45-minute pre-treatment of Dyngo-4a was used for all subsequent experiments.

In cells pre-treated with Dyngo-4a, a strong inhibition of constitutive FFA2 internalisation was observed (Figure 4.4 B). In the same experiments, SCFA-induced internalisation was also inhibited by Dyngo-4a (Figure 4.4 B). FFA2 localisation in Dyngo-4a treated cells remain largely at the plasma membrane in all conditions, in contrast to vehicle treated cells where FFA2 containing endosomes were easily visible. A similar profile was also seen in STC-1 cells transiently expressing FLAG-FFA2 where both constitutive and ligand induced internalisation was inhibited by Dyngo-4a (Figure 4.4 C). These results demonstrate that FFA2 constitutive and ligand-induced internalisation occur in a dynamin-dependent manner.

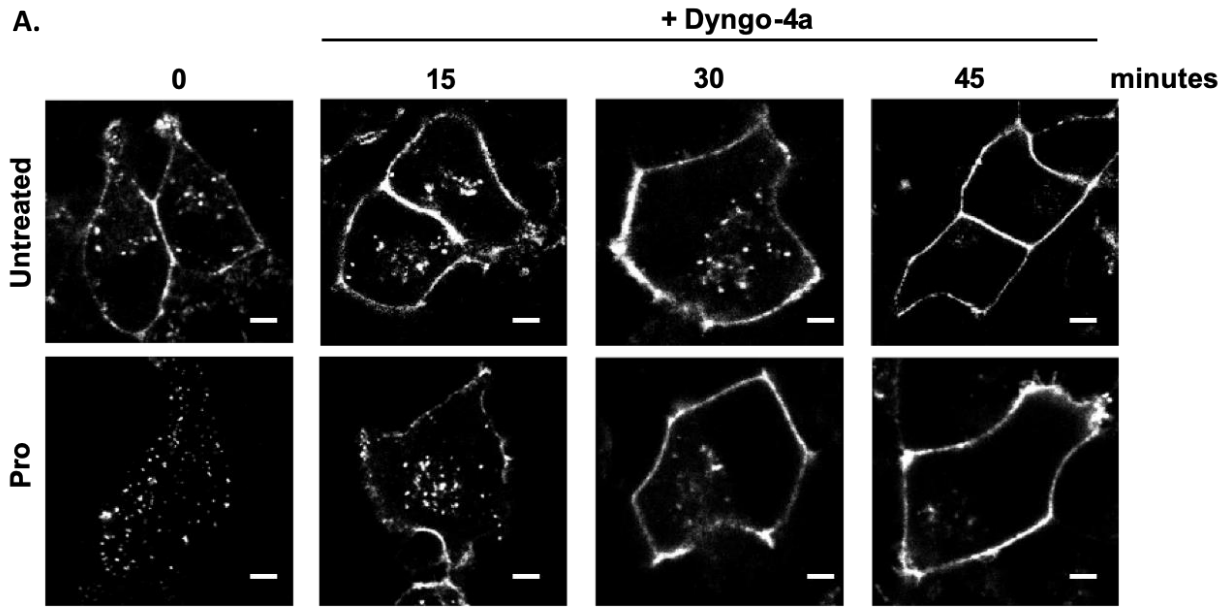


Figure 4.3 continued the following page

B.

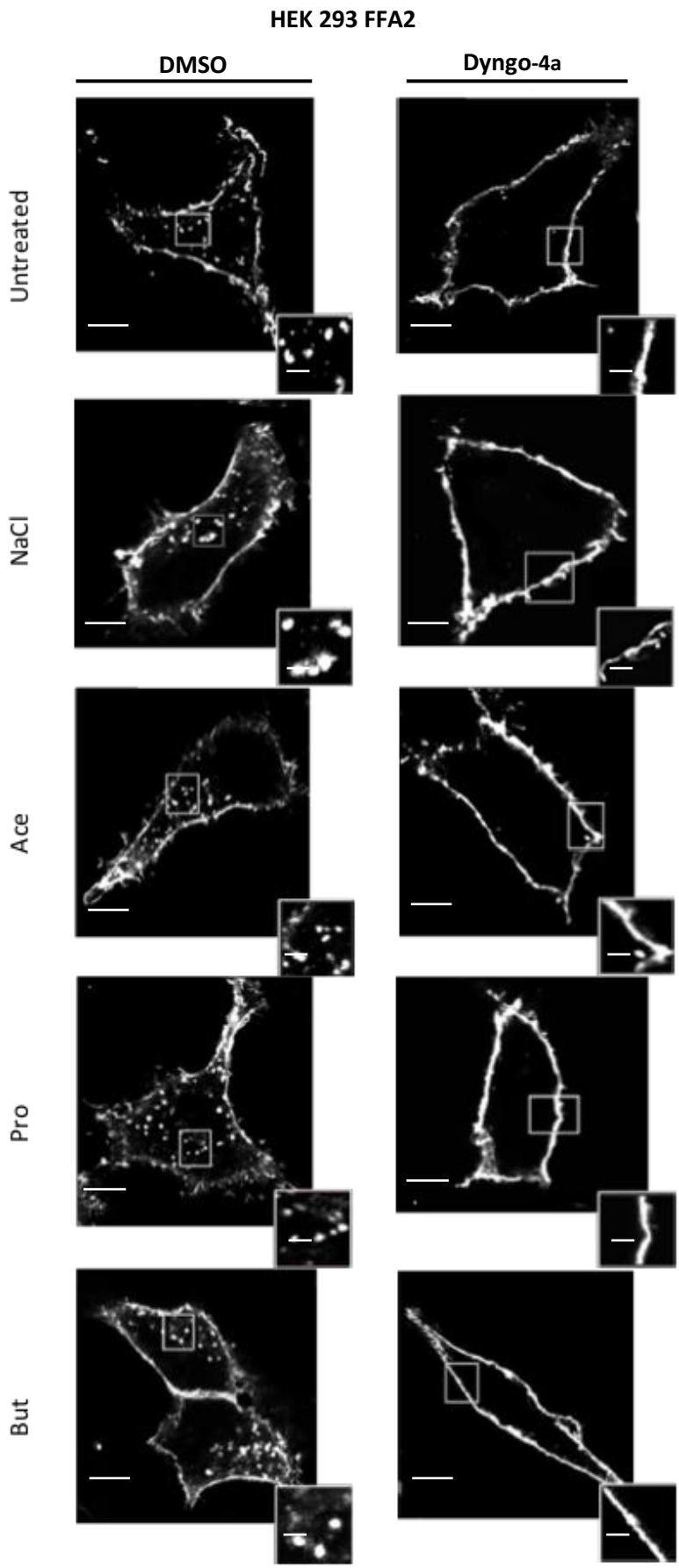


Figure 4.3 continued the following page

C.

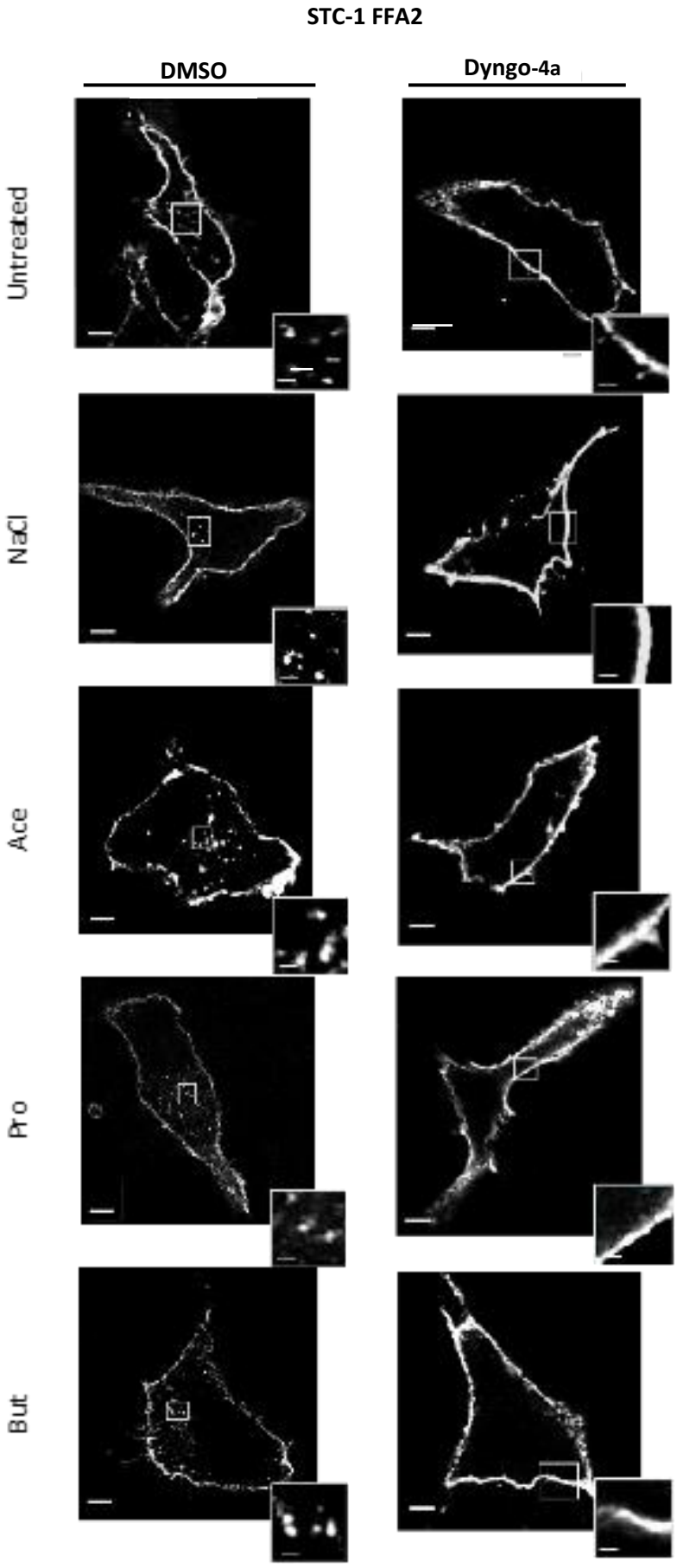


Figure 4.3 A-C legend overleaf

Figure 4.3 Dynamin inhibition blocks constitutive and ligand induced internalisation of FFA2. (A) Representative confocal images of time required for Dyngo-4a, a dynamin inhibitor, to inhibit FFA2 internalisation. HEK 293 cells expressing FLAG-FFA2 were ± pre-treated with Dyngo-4a (50 μM) for 0, 15, 30 or 45 minutes, fed live with anti-FLAG M1 antibody, then with immunofluorescent secondary antibodies and stimulated with propionate (Pro, 1 mM) or left untreated for 20 minutes. HEK 293 (B) and STC-1 cells (C) transiently expressing FLAG-FFA2 were pre-treated with DMSO (vehicle) or Dyngo-4a (50 μM), for 45 minutes prior to cell surface labelling using anti-FLAG M1 antibody. Cells were then left untreated or treated with NaCl/SCFA (1 mM) for FFA2 for 20 min. Cells were fixed, permeabilized and then labelled with immunofluorescent secondary antibodies. Shown are representative confocal microscopy. n=10 cells per condition, collected across 3 independent experiments. Scale bar is 10 μm and inset is 5 μm.

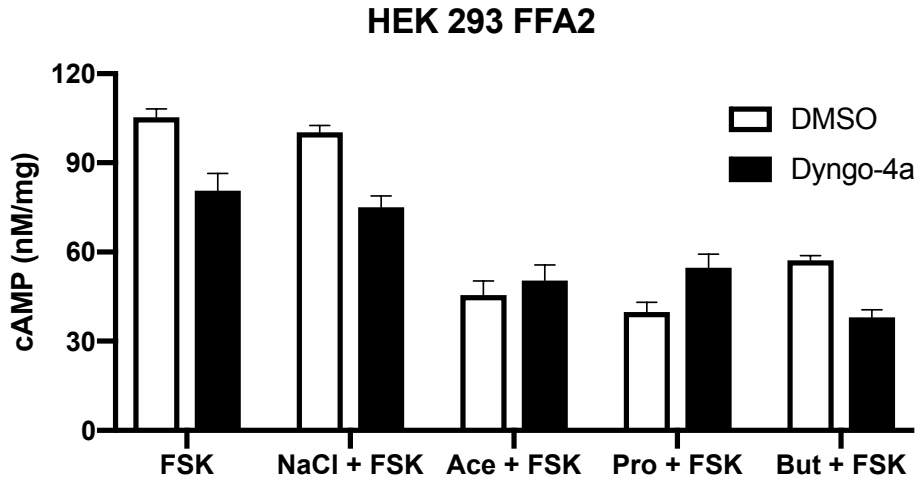
4.2.4 Differential requirement of FFA2 internalisation for FFA2 mediated signalling

For many GPCRs, receptor internalisation is an important regulator for its signalling. Having established that FFA2 ligand-induced internalisation is dependent on β-ARR and dynamin, the role of internalisation in FFA2 was next investigated. To address this question, SCFA's ability to inhibit forskolin stimulated cAMP when FFA2 constitutive and ligand-induced internalisation was blocked via Dyngo-4a was first examined. Cells transiently expressing FLAG-FFA2 were pre-treated with DMSO or Dyngo-4a for 45 minutes and then stimulated with forskolin or co-stimulated with forskolin and NaCl or SCFA. In cells treated with DMSO, I observed a ~50% reduction of forskolin stimulated cAMP by SCFA, as previously seen (Figure 3.4 B). In cells which had been pre-treated with Dyngo-4a, the levels of forskolin stimulated cAMP were reduced (Figure 4.4 A). For the purpose of comparing ligand-mediated changes in forskolin-induced responses, these values were normalised to NaCl+forskolin stimulated cAMP in the presence of DMSO or Dyngo-4A separately. From this comparison, in the presence of Dyngo-4a, SCFA induced inhibition of forskolin stimulated cAMP was significantly impaired (Figure 4.5 A). In STC-1 cells, cells that had been pre-treated with Dyngo-4a, the levels of forskolin stimulated cAMP were reduced as previously seen for the HEK 293 cells expressing FLAG-FFA2 (Figure 4.4 B). Thus, ligand-mediated changes in forskolin-induced responses were normalised to NaCl+forskolin stimulated cAMP in the presence of DMSO or Dyngo-4A separately. Propionate-mediated inhibition of forskolin induced cAMP was significantly impaired in cells pre-treated with Dyngo-4A. Strikingly, a converse significant effect was observed for butyrate as levels of forskolin induced cAMP were further reduced compared to cells pre-treated with DMSO (Figure 4.5 B). To further confirm the requirement of internalisation, the ability of SCFA to inhibit forskolin stimulated cAMP was also examined

in β-ARR KO cells transiently expressing FLAG-FFA2. I found that in β-ARR KO cells, the ability of SCFAs to inhibit forskolin stimulated cAMP was significantly impaired compared to WT cells (Figure 4.6 A). Similar to what was observed when FFA2 internalisation was blocked with Dyngo-4a. This suggest that the FFA2 mediated inhibition of forskolin stimulated cAMP is largely dependent on FFA2 internalisation via a β-ARR and dynamin-dependent pathway.

In chapter 3, I observed that in HEK 293 cells, FFA2 is coupled to both $G\alpha_{i/o}$ and $G\alpha_{q/11}$ thus, I next then examined if FFA2 internalisation was also a requirement for FFA2 $G\alpha_{q/11}$ signalling. Intracellular calcium mobilisation was measured in cells transiently expressing FLAG-FFA2 where receptor internalisation was inhibited by Dyngo-4a. In cells pre-treated with Dyngo-4a, acetate and propionate induced intracellular calcium mobilisation was not attenuated and were at similar levels as cells treated with DMSO. This was also observed in β-ARR KO cells transiently expressing FLAG-FFA2 which SCFAs was able to induce intracellular calcium mobilisation in a similar manner to WT (Figure 4.5 B). A similar profile was also observed in measuring the accumulation of IP1 both in cells that FFA2 internalisation was blocked with Dyngo-4a and in β-ARR KO cells transiently expressing FLAG-FFA2 (Figure 4.5 C). This data demonstrates that FFA2 mediated $G\alpha_{q/11}$ signalling does not require receptor internalisation.

A.



B.

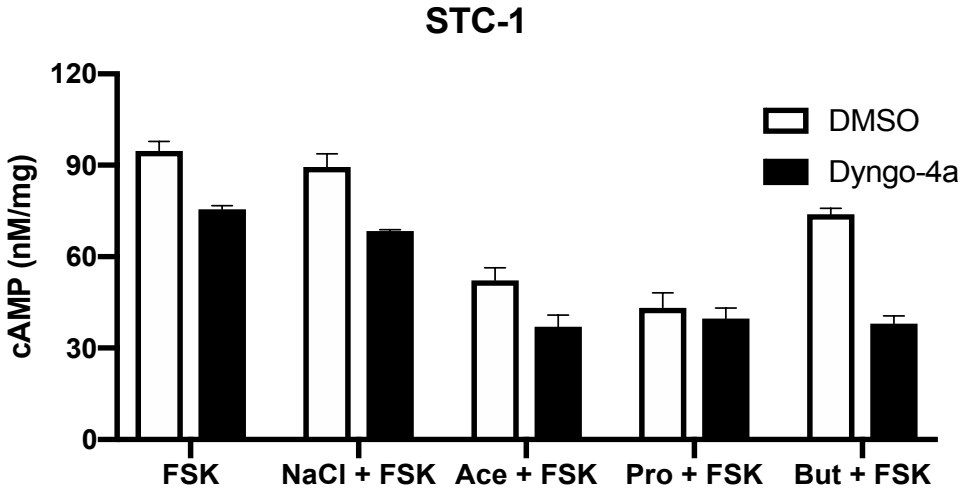
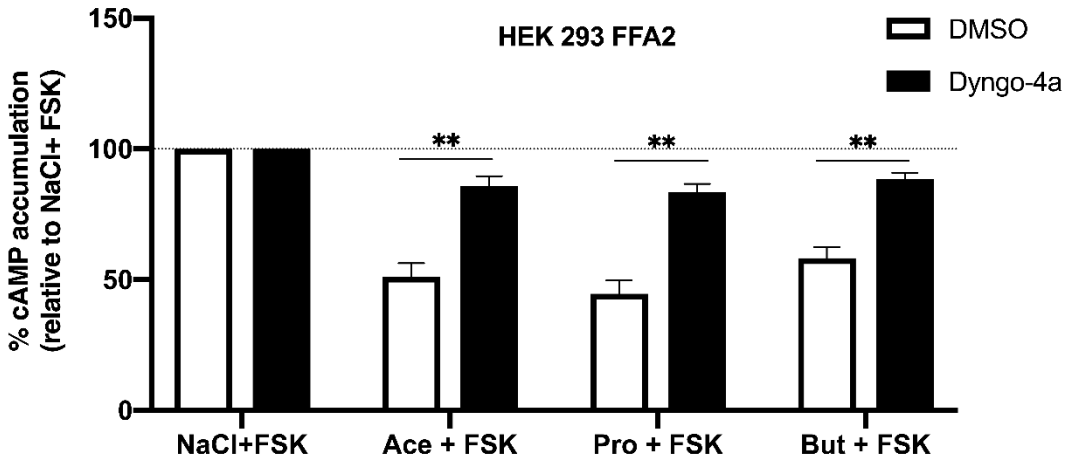
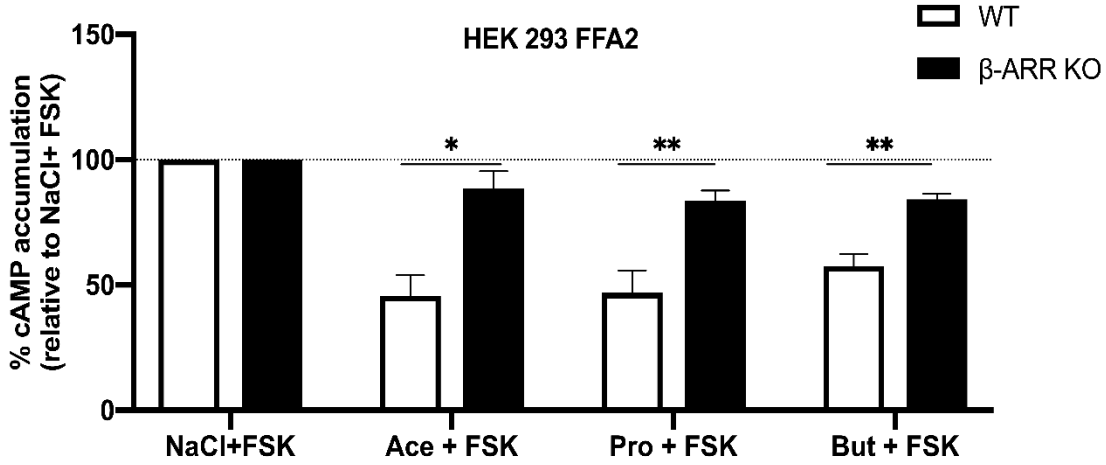


Figure 4.4 Intracellular levels of cAMP pre-treated either with DMSO or Dyngo-4a. HEK 293 cells transiently expressing FLAG-FFA2 (A) or STC-1 cells (B) pre-treated with DMSO or Dyngo-4a (50 µM) for 45 minutes prior to incubation with IBMX (0.5 mM, 5 minutes) and then treated with forskolin (3 FSK µM) or a combination of forskolin with either NaCl (1 mM) or SCFA (1 mM) for 5 minutes.

A.



B.



C.

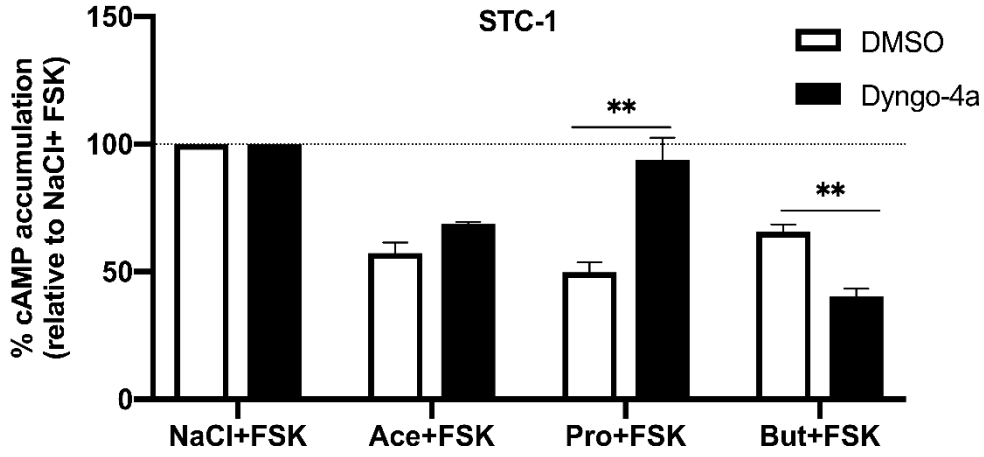
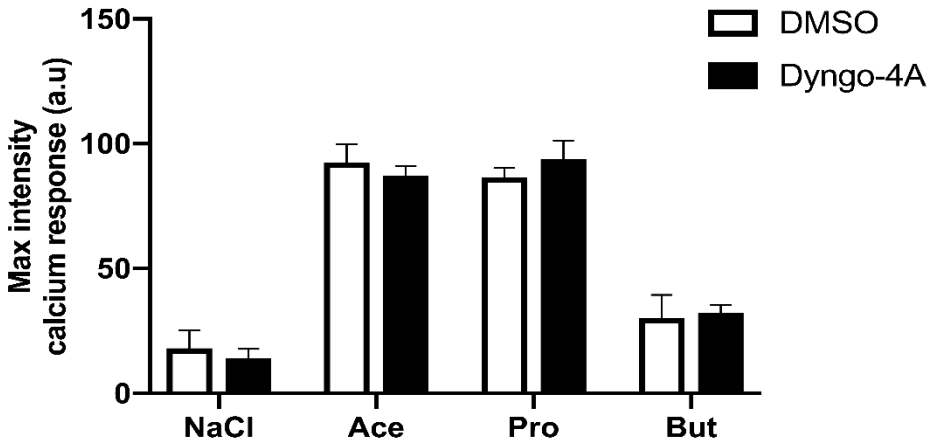
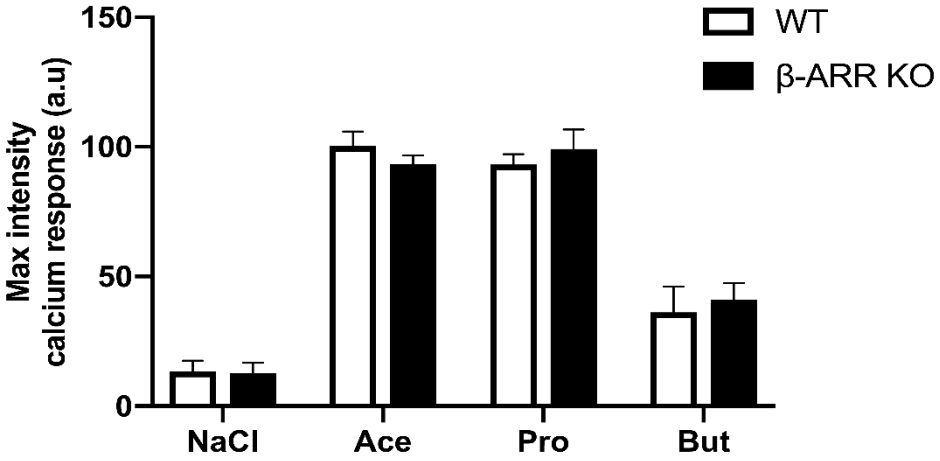


Figure 4.5 continued the following page

D.



E.



F.

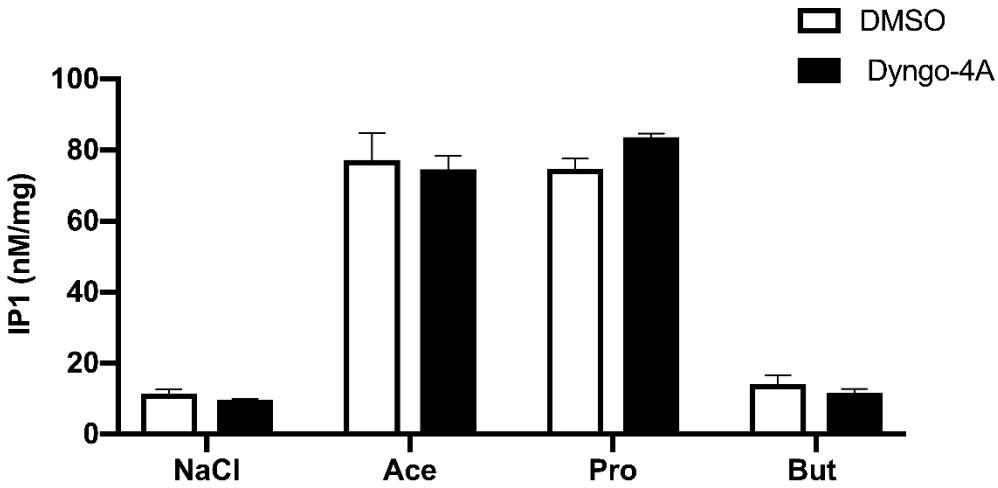


Figure 4.5 continued the following page

G.

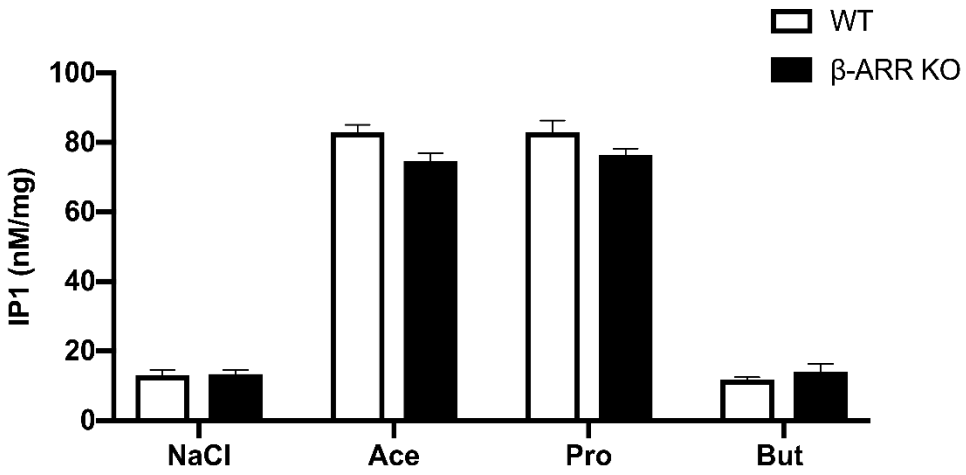


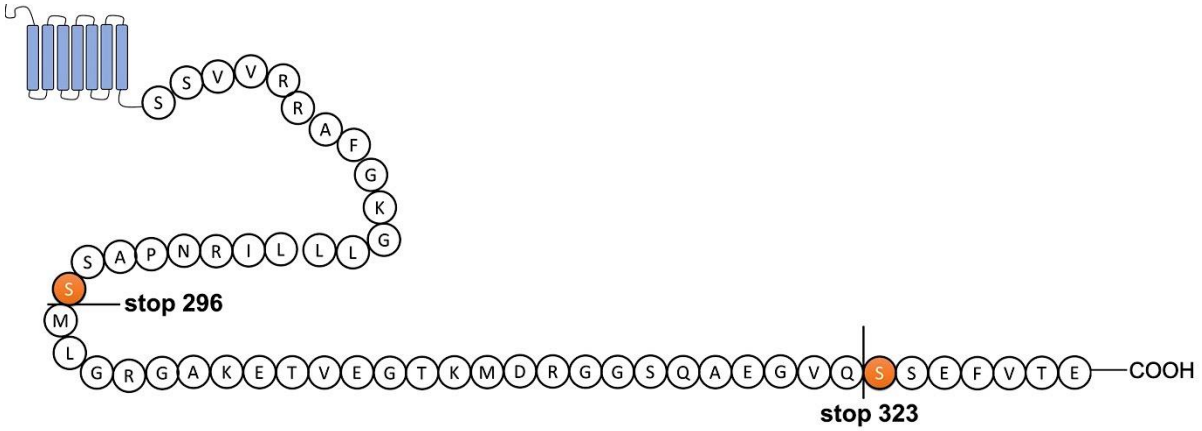
Figure 4.5 FFA2 internalisation is required for Gα_i mediated cAMP but not G$\alpha_{q/11}$. Intracellular levels of cAMP measured in HEK 293 cells transiently expressing FLAG-FFA2 (A) or in STC-1 cells (B) pre-treated with DMSO (vehicle) or Dyngo-4a (50μM), a dynamin inhibitor, for 45 minutes prior to incubation with IBMX (5 minutes, 0.5mM) and then treated with forskolin (FSK, 3μM) or a combination of FSK (3μM) and NaCl or SCFAs (1 mM) for 5 minutes. Data are expressed as percentage change of NaCl+FSK to either DMSO or Dyngo-4a. Data represent mean ± SEM, n=3 independent experiments; t-test ** $p<0.01$ DMSO vs Dyngo-4a. (C) Intracellular levels of cAMP measured HEK 293 (WT) or β-ARR KO cells transiently expressing FLAG-FFA2 were treated with IBMX (5 minutes, 0.5mM) prior to treatment with forskolin (FSK, 3μM) or a combination of FSK (3μM) and NaCl or SCFAs (1mM) for 5 minutes. Data are expressed as percentage change of NaCl+FSK to either WT or β-ARR KO. All data represent mean ± SEM, n=3 independent experiments; t-test ** $p<0.01$ WT vs β-ARR KO. (D) Intracellular calcium mobilization measured in HEK 293 cells transiently expressing FLAG-FFA2, pre-treated with either DMSO (vehicle) or Dyngo-4a (50 μM) for 45 minutes, then incubated with fluorescent calcium indicator Fluo4-AM for 1 hour, and imaged live via confocal microscopy for 1 minute before NaCl or SCFA (1 mM) addition. Data represent mean ± SEM of at least 20 cells in duplicate per 3 independent experiments. (E) Intracellular calcium mobilization measured in HEK 293 cells (WT) or β-ARR KO cells transiently expressing FLAG-FFA2, incubated with fluorescent calcium indicator Fluo4-AM for 1 hour and imaged live via confocal microscopy for 1 minute before NaCl/SCFA (1 mM) addition. Data represent mean ± SEM of at least 20 cells in duplicate per 3 independent experiments. (F) IP1 accumulation measured in HEK 293 cells transiently expressing FLAG-FFA2 were pre-treated with DMSO (vehicle) or Dyngo-4a (50 μM) for 45 minutes prior to treatment with NaCl (1 mM) or SCFA (1mM) for 2 hours; n=3 independent experiments. (G) IP1 accumulation measured in HEK 293 cells or β-ARR KO cells transiently expressing FLAG-FFA2 treated with NaCl or SCFA (1mM) for 2 hours; Data represent mean ± SEM; n=3 independent experiments.

4.2.5 The C-terminal tail of FFA2 is essential for optimal cell surface expression

The C-terminal tail of GPCRs contain motifs that serve to bind to sorting proteins that can influence cell surface expression, signalling pathways and internalisation. In light of this, it was investigated if any C tail sequences modulate the constitutive internalisation of FFA2. To investigate this, I first compared the full length FFA2 and a truncated form of the FFA2 that

lacks the last 7 residues of the C-terminal tail where Serine-323 was mutated to a stop codon termed FFA2-323T (schematic shown in Figure 4.6 A). HEK 293 cells were transfected with these constructs, labelled with anti-FLAG M1 antibody and imaged live via confocal microscopy. As previously seen, in cells expressing the full-length FFA2, receptor was localised to both the plasma membrane and in intracellular vesicles. In cells expressing FFA2-323T, FFA2 was localised exclusively in intracellular vesicles and none at the plasma membrane, suggesting enhanced constitutive internalisation (Figure 4.6 B). I then asked if upstream regions of the C-tail could be involved in internalisation by truncating a larger region of the C-tail. Serine-296 was mutated with a stop codon, termed FFA2-296T (schematic shown in Figure 4.6 A). This truncated receptor was then transfected in HEK 293 cells and compared with the full-length receptor. Compared to full length FFA2, in cells expressing FFA2-296T, cell surface expression of FFA2 was noticeably reduced (Figure 4.6 B). This shows that C-terminal tail of FFA2 may be important for the delivery of FFA2 to the cell surface.

A.



B.

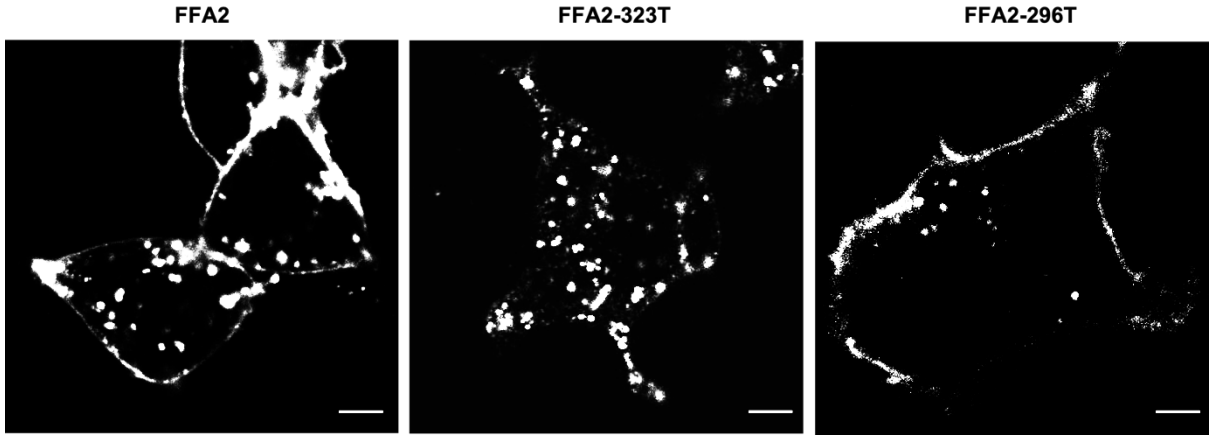


Figure 4.6 The C-terminus of FFA2 is important for its cell surface expression. (A) A schematic of the FFA2 C-terminal tail sequence. Black lines indicate the residues mutated to stop-codons to generate the truncated receptors FFA2-323T and FFA2-296T. (B) Representative confocal images of HEK 293 transfected with either full length FFA2 or the two truncated forms as indicated (all N-terminally FLAG-tagged). Surface receptor was then labelled with an anti-FLAG M1 antibody before labelling with secondary immunofluorescent antibodies and imaged live using confocal microscopy. n=5 cells per condition, collected across 2 independent experiments. Scale bar is 10 µm.

4.2.6 FFA2 is sorted to the recycling pathway

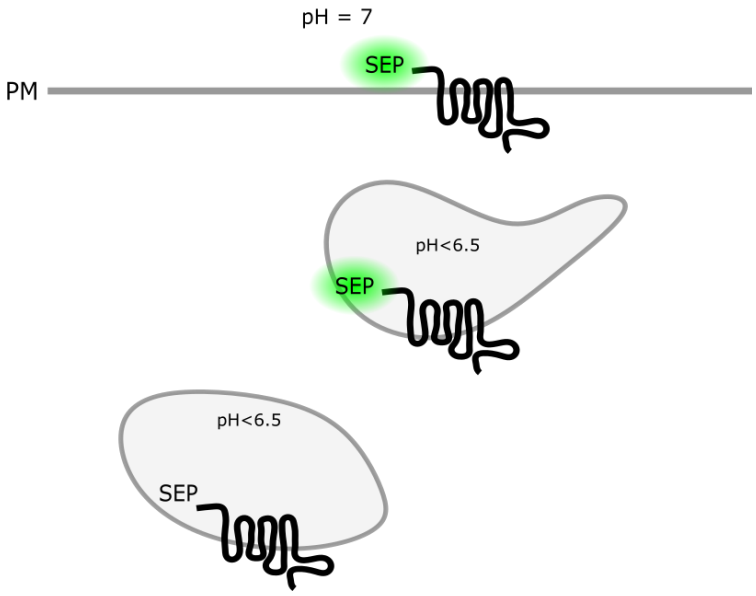
Post internalisation, GPCRs are either sorted for degradation or recycled back to the plasma membrane. For FFA2, the post-endocytic sorting fate is not known. To examine this, recycling of FFA2 in HEK 293 cells was investigated by live-cell total internal reflection fluorescence microscopy (TIR-FM), a microscopy technique that allows the detection of single vesicle events occurring at the plasma membrane, such as receptor recycling. TIR-FM uses light

reflected at a refractive interface that creates an evanescent wave which diminishes exponentially with distance from the interface. A shallow field of illumination (~100 nm) is generated by this evanescent field and fluorescent molecules located at or close to the plasma membrane are illuminated, allowing for the direct visualisation of rapid GPCR recycling events occurring at the plasma membrane (Yudowski et al., 2007). To achieve this, a pH sensitive variant of GFP, known as superecliptic Phluorin (SEP) is expressed as a fusion tag to a receptor. SEP is nonfluorescent at pH values below 6, however brightly fluoresces at a neutral pH (pH > 6) (Miesenbock et al., 1998), thus, enables the detection of receptors upon insertion into the plasma membrane, but not when confined to the acidic lumen of endosomes with an enhanced resolution and increased signal to noise ratio that is achieved by TIR-FM (Figure 4.7 A).

To investigate the recycling of FFA2, I N-terminally tagged FFA2 with SEP (referred hereafter as SEP-FFA2). The correct localisation of SEP-FFA2 at the plasma membrane of HEK 293 cells was confirmed via confocal microscopy, epifluorescence and TIRF-M (Figure 4.7 B). HEK 293 cell stably expressing SEP-FFA2 were then generated.

The SEP-FFA2 clones were assessed for their cell surface expression via flow cytometry and confocal and for their ability to inhibit forskolin induced cAMP in response to SCFAs at comparable level to FLAG-FFA2. The addition of SEP to N terminal of FFA2 did not alter receptor function and was able to exert SCFA mediated inhibition of forskolin induced cAMP at a comparable level to the SCFA mediated inhibition of forskolin induced cAMP in HEK 293 cells stably expressing FLAG-FFA2 (Figure 4.8).

A.



B.

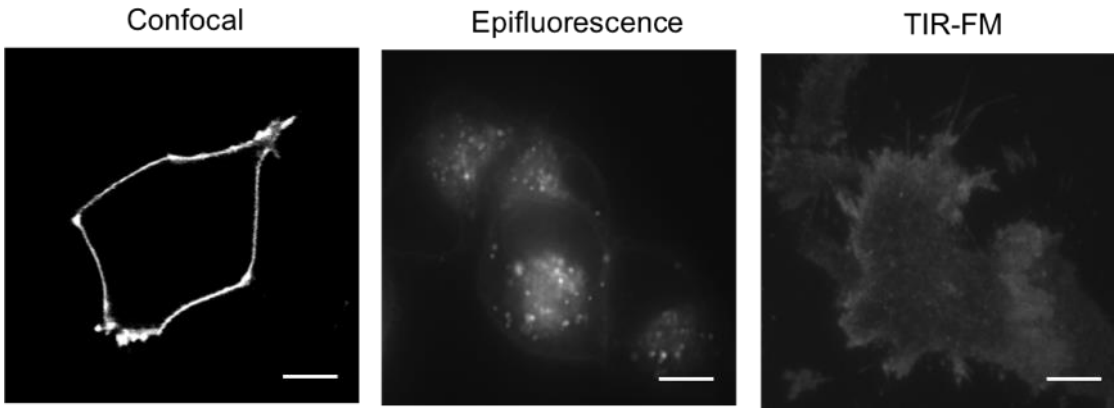


Figure 4.7 Visualisation of SEP-FFA2 (A) Schematic illustrating how recycled SEP-FFA2 is detected using TIR-FM in a pH-dependent manner. (B) HEK 293 cell expressing SEP-FFA2 were imaged by confocal, epifluorescence or TIRF-microscopy; scale bar = 7 µm.

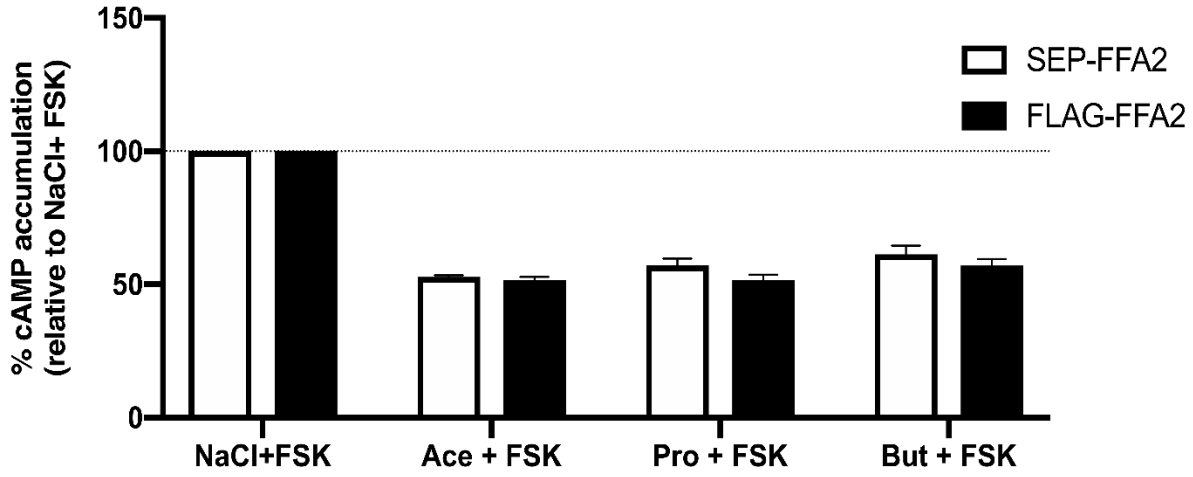


Figure 4.8 SEP-FFA2 induces SCFA-mediated inhibition of forskolin induced cAMP in a similar manner as FLAG-FFA2. (A) Intracellular levels of cAMP were measured in HEK 293 cells stably expressing FLAG-FFA2 or SEP-FFA2. Cells were treated with IBMX (0.5 mM, 5 minutes) and then with forskolin (FSK, 3 μM) and NaCl or SCFA (1 mM) for 5 minutes as indicated. Data are expressed as percentage change of NaCl+FSK and is expressed as 100%. Data represent mean ± SEM, n=3.

To investigate if FFA2 is sorted to the recycling pathway in real-time, SEP-FFA2 cells were imaged live before and after stimulation with either NaCl or propionate at 1 mM with 10-15 cells imaged at 5-minute intervals over a time period of 30 minutes. As individual recycling events are known to occur with fast kinetics (within fractions of a second) and to minimize photobleaching or cell toxicity from a prolonged laser exposure, movies were acquired for 1 minute with frames recorded every 0.1 second, for a total of 600 frames per movie. From this, rapid and transient burst or 'puffs' of SEP-FFA2 fluorescence over the background at the plasma membrane were observed, indicating a reinsertion of the receptor into the plasma membrane (Yudowski et al., 2007) and can be seen more clearly in the sequence time series panel with a bright spot that suddenly appears and diffuses overtime as receptor vesicles fuse with the plasma membrane within seconds (Figure 4.9 B). These recycling events per cell were then counted and normalized to cell area. Recycling events for both cells stimulated with NaCl or propionate remained constant over a time period of 30 minutes (Figure 4.9 C). In cells stimulated with NaCl, the number of recycling events were 0.01 ± 0.01 events/min/cell. This increased upon propionate addition to 0.04 ± 0.001 events/min/cell, suggesting FFA2 undergoes ligand-induced trafficking to the rapid recycling pathway (Figure 4.9 D).

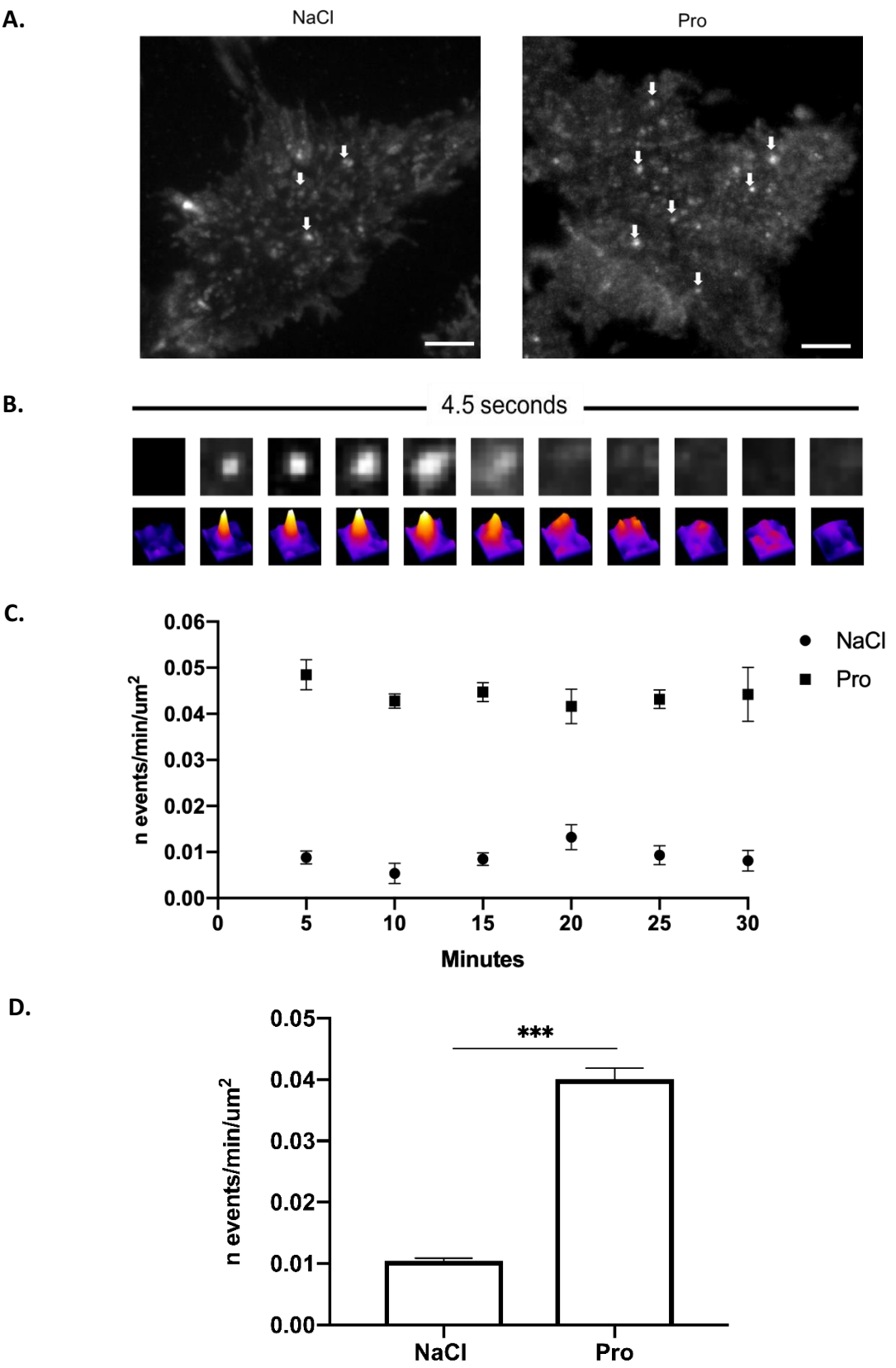


Figure 4.9 FFA2 undergoes ligand-induced trafficking to the recycling pathway. (A) Representative maximum intensity projection images of TIR-FM movies of a HEK 293 cell stably expressing SEP-FFA2 stimulated with NaCl (1 mM) or propionate (Pro, 1 mM). Arrow denotes recycling event. Scare bar= 7 µm. (B) Series of TIR-FM images of a single SEP-FFA2 recycling event following propionate stimulation

with surface plot of fluorescence. (C) Number of recycling events over time following stimulation of NaCl (1 mM) or propionate (Pro, 1 mM) measured by TIR-FM in HEK 293 cells stably expressing SEP-FFA2; n ≥ 3 cells per time point; collected across 3 independent experiments. (D) Number of recycling events measured by TIR-FM in HEK 293 cells stably expressing SEP-FFA2 following stimulation of NaCl (1 mM) or propionate (Pro, 1 mM); n=15 cells per condition; collected across at 3 least 3 independent experiments; *** p<0.001 vs NaCl.

To ensure that the plasma membrane insertion events observed by TIR-FM are indeed recycled receptors and not newly synthesized ones, SEP-FFA2 cells were pre-treated with a protein synthesis inhibitor, cycloheximide. Pre-treatment with cycloheximide had no effect on the number of recycling puffs both in cells treated with NaCl and propionate (Figure 4.9), suggesting plasma insertion events are recycling events.

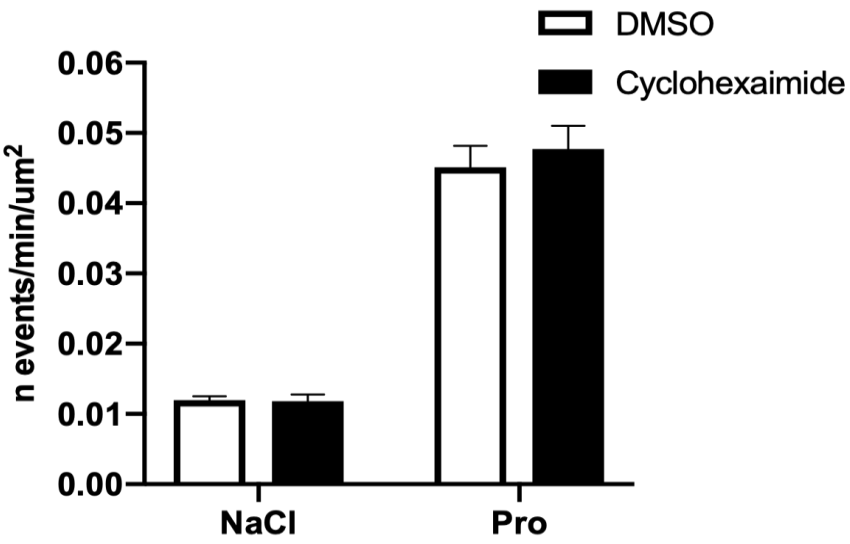


Figure 4.10 FFA2 delivered to the plasma member are not newly synthesized receptors but are recycled ones. Number of recycling events measured by TIR-FM in HEK 293 cells stably expressing SEP-FFA2, pre-treated with DMSO (vehicle) or cycloheximide (10 µg/mL, 90 minutes) prior to NaCl (1 mM) or propionate (1 mM) stimulation; n=10 cells per condition.

4.2.7 Distinct modes of SEP-FFA2 recycling

For other GPCRs, distinct modes of recycling events as measured by TIR-FM have been observed – some events can be on the plasma membrane for a very short period of time (transient) and others can persist for longer before their later diffusion (persistent) (Yu et al.,

2010; Yudowski et al., 2007; Jullie et al., 2014). Distinct modes of recycling are observed for FFA2 (Figure 4.11). Majority (85.4 $\pm$ 2.1%) of SEP-FFA2 puffs appeared abruptly at the plasma membrane before their rapid diffusion to level of surround fluorescence intensity. These events were categorised as 'transient' as these puffs remained visible for approximately 2 seconds. Another event, (7.2 $\pm$ 2.1%) were puffs that persisted on the plasma membrane for a prolonged period of time before their diffusion were defined as 'sustained' events as they remained visible for >2 seconds. The third group of events are 'pre-tail' events; these events had a small but significant increase in fluorescence lasting between 3-10 seconds that preceded to a transient burst of fluorescence. These types of events were 7.1 $\pm$ 1.6% of total events. This is consistent with evidence from others that GPCR recycling can occur via distinct modes, though implications for recycling to occur in such manners are not yet known.

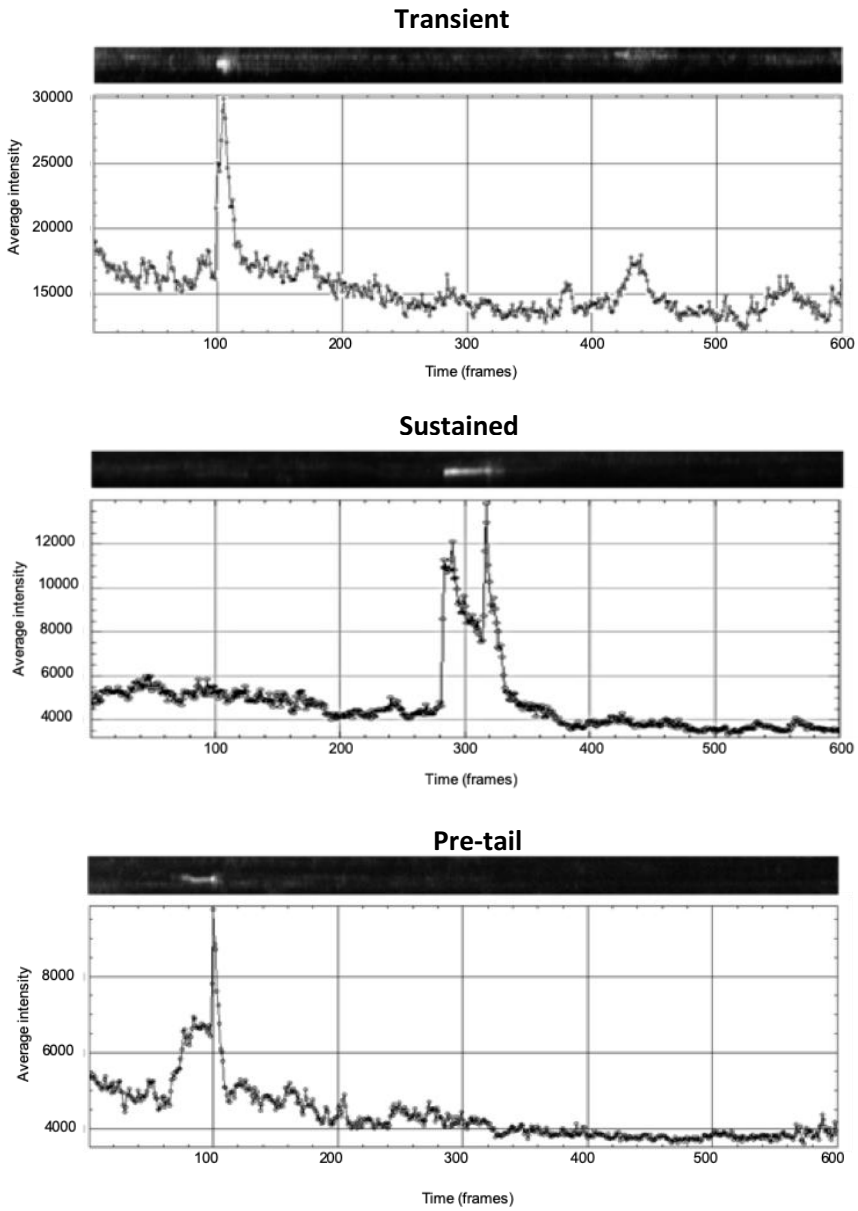


Figure 4.11 Characterisation of SEP-FFA2 recycling modes. Representative intensity plots and kymogprahs which demonstrate three distinct kinetic properties of SEP-FFA2 recycling: transient, sustained and pre-tail events (top) and corresponding fluorescent intensity plots (bottom).

4.3 Discussion

The cellular trafficking of GPCRs is an important process that regulates not only the amount of receptor present at the plasma membrane but also dynamically controls receptor signalling. In this chapter, I have examined FFA2 cellular localisation, ligand-mediated internalisation, mechanisms of constitutive and ligand-induced internalisation and the importance of FFA2 localisation in receptor mediated signalling.

In HEK 293 cells expressing FLAG-FFA2 and in STC-1 cells, FFA2 undergoes constitutive internalisation, this was receptor-specific as constitutive internalisation of the β2AR was not observed. To my knowledge, this is the first report to demonstrate that FFA2 undergoes constitutive internalisation. The physiological role for constitutive trafficking is unclear but some studies suggest it may be import for appropriate receptor redistribution, such as for the cannabinoid-receptor-subtype 1 (CB1) where constitutive internalisation is necessary for targeting the receptor to axonal membranes (McDonald et al., 2007). For the Melanocortin 4 receptor (MC4R), constitutive internalisation is required to target functional receptors to bind to α-melanocyte stimulating hormone in neuronal and hypothalamic cells. The underlying constitutive internalisation could be a result of basal activity of the receptor. For FFA2, basal activity for cAMP and intracellular calcium mobilisation was not observed. However, this possibility is difficult to assess, as there is currently no inverse agonist available for mouse FFA2.

Recruitment of β-ARR to ligand-activated receptors to drive in internalisation from the plasma membrane is a hallmark feature of many GPCRs and here it is demonstrated that β-ARR is also important for FFA2 ligand-induced internalisation. The role for β-ARR in the internalisation of FFA2 has been demonstrated by former studies (Lee et al., 2013; Hudson et al., 2012a; Hudson et al., 2013; Grundmann et al., 2018). Work from Lee et al., 2013, Hudson et al., 2012, Hudson et al., 2013 and Grundmann et al., 2018 demonstrated that ligand-induced FFA2 internalisation was dependent on the recruitment of β-ARR-2. In Lee et al., 2013, however, β-ARR-2 interaction was based upon an internalisation by a FFA2 synthetic compound, phenylacetyl aminothiazole, in contrast to the other studies and my study that used determined β-ARR recruitment via propionate. Interestingly, Grundmann et al., 2018, observed that FFA2 constitutive internalisation was not dependent on β-ARR 2, which in line with my observations that FFA2 constitutive internalisation and ligand-induced internalisation employ a distinct endocytic and or internalisation machineries. However, constitutive internalisation of FFA2 was visualised via a YFP tagged to the C-terminal of the receptor, fluorescently tagging receptors at their C-terminal leads to the visualisation of not

only internalised receptors but also that are newly synthesised (Böhme and Beck-Sickinger, 2009).

The role of β-ARR in FFA2 internalisation was studied using HEK 293 cells with CRISPR/Cas 9 genome edited to stably knockout both β-ARR 1/2 which limited the ability to investigate if there was any selectivity of β-ARRs for ligand-induced internalisation. Previous works (Lee et al., 2013; Hudson et al., 2012a; Hudson et al., 2013; Grundmann et al., 2018) demonstrated that FFA2 internalisation is dependent on β-ARR 2, however β-ARR 1 was assessed. This and other works (Oakley et al., 2000) show that GPCRs have differential affinities for β-ARR, however this original classification may be more complex. For example, ligand-induced internalisation of PAR-2 was originally found to require both β-ARR 1/2, however, it was later found that β-ARR 1 mediates the early phases of receptor internalisation while the β-ARR 2 is important for the late phase (Kumar et al., 2007). In addition, Kumar et al., 2007 and other works have found that there are distinct roles of β-ARR isoforms in signalling in addition to internalisation (Srivastava et al., 2015). Thus, it would be noteworthy to investigate if there is also distinct temporal and functional roles for β-ARR in FFA2 signalling and internalisation.

Dynamin dependent internalisation is the primary pathway of internalisation for GPCRs and other membrane cargo. My results demonstrate that FFA2 constitutive and ligand induced-internalisation is dynamin dependent. Dynamin is involved in many endocytosis pathways such as caveolae-mediated endocytosis that is clathrin-independent (CIE) (Chini and Parenti, 2004) and the fast endophilin-mediated endocytosis (FEME) (Boucrot et al., 2015). GPCRs that undergo both constitutive and ligand-induced internalisation have been reported to utilise distinct dynamin-dependent mechanisms, suggesting perhaps that constitutive and ligand induced internalisation mechanisms may be distinct. For instance, the M3 acetylcholine muscarinic receptor and the glutamate receptor 5a undergo constitutive internalisation via the CIE pathway, and then in the presence of ligand, switches to the CDE pathway (Scarselli and Donaldson, 2009). It would therefore be interesting to further investigate if such a switch is also involved in FFA2 internalisation.

As mentioned above, I have demonstrated that although both constitutive and ligand induced internalisation of FFA2 is dependent on dynamin, constitutive internalisation of FFA2 is β-ARR independent. Such a regulatory phenomenon is however is not unique to FFA2, as similar differences in the mechanism of constitutive versus ligand induced internalisation have been demonstrated for other GPCRs such as the metabotropic glutamate receptor 1 (Dale et al., 2001), Y1 neurotpeptide Y receptor (Holliday et al., 2005), CBR1 (Gyombolai et al., 2013), melanocortin-4 receptor (MC4R) (McDaniel et al., 2012) and FFA1 receptor (Qian et al., 2014).

Mechanistically, prevention of internalisation increases receptors available at the plasma membrane, thereby increasing the availability of receptor to bind to ligand and ultimately increasing receptor desensitisation. Thus, blocking internalisation both through the inhibition of dynamin and in cells that lacked β-ARR may decrease the ability of FFA2 mediated inhibition of forskolin-stimulated cAMP due to enhanced desensitisation or that internalisation is required for this particular FFA2 signalling pathway. This challenges the conventional view that signalling occurs only at plasma membrane and further highlights the recent findings that GPCRs are able to continue or reactivate G protein signalling from endosomes (Eichel and von Zastrow, 2018). From these GPCRs, endosomal signalling occurred in a sustained manner by receptor activation from the exposure to ligands for tens of minutes up to hours, for the FFA2 however, I show that signalling from intracellular compartments can also occur acutely, within 5 minutes of receptor activation. This acute signalling from endosomes have been observed for both the LHR and the D1 dopamine receptor which receptor internalisation was a requisite for acute cAMP responses (Sposini et al., 2017; Kotowski et al., 2011). In contrast to FFA2 mediated inhibition of forskolin-stimulated cAMP requiring receptor internalisation, FFA2 mediated $G\alpha_{q/11}$ signalling did not. Responses of SCFA's ability to induce intracellular calcium mobilisation when FFA2 internalisation was inhibited were similar to those of control cells. This demonstrates a striking spatial discrimination in FFA2 receptor mediated signalling, to which FFA2 mediated- inhibition of forskolin-stimulated cAMP and $G\alpha_{q/11}$ signalling are individually controlled leading to a compartment-specific cellular response. This feature of spatial restriction in signalling has been shown for the $S1P_1$ receptor, when activated by synthetic ligand, FTY20, induced robust internalisation that elicited persistent endosomal $G\alpha_{i/o}$ signalling but was unable to mediate

intracellular calcium mobilisation. However, when activated by the endogenous ligand, S1P, receptors remained largely at the plasma membrane and was able to induce intracellular calcium mobilisation (Mullershausen et al., 2009). Though such signalling could arise from biased agonism, this highlights the importance of receptor localisation induced signalling. More recently, location bias in G protein signalling was also reported for the CaSR. The CaSR signals via $G\alpha_{q/11}$ and $G\alpha_{i/o}$ from the plasma membrane but induces a sustained endosomal signalling only through $G\alpha_{q/11}$ to maintain normal calcium homeostasis and synthesis of parathyroid hormone (Gorvin et al., 2018)

My preliminary observations also demonstrate that the FFA2 C-terminal tail may be important for the delivery of FFA2 to the cell surface. Truncations of the receptor at 7 residues resulted in receptors to be localised predominantly in intracellular vesicles and truncation of the receptor by more than 34 residues resulted in a marked reduced surface expression, suggesting that the residues of this region of the FFA2 C-terminal tail are a likely key determinant for the localisation or the stability of the receptor at the cell surface. The C-terminal tail is known to be essential in mediating optimal surface expression of many GPCRs, including the human FFA2. Mutations of membrane-proximal basic residues of the C-terminal, namely arginine, reduced cell surface expression of the human FFA2 receptor (Okamoto et al., 2013). Serial truncation of the C-C chemokine receptor type 5 and the melanin-concentrating hormone receptor 1 resulted in progressive loss of its cell surface expression (Venkatesan et al., 2001; Tetsuka et al., 2004). In addition to regulating receptor cell surface expression, motifs of the C terminal are also sites of binding proteins such as PDZ domain-containing proteins which are known to be essential for receptor organisation into specific endosomes and post endocytic sorting and recycling. For instance, the LHR internalisation to VEEs requires interactions with the PDZ domain containing protein Gai-interacting protein C terminus (GIPC) (Jean-Alphonse et al., 2014). Thus, it may be pertinent to investigate further the functional roles of the FFA2 mutations and to identify FFA2-interacting proteins to better understand the regulation of FFA2 signalling and trafficking.

Further, by TIR-FM I demonstrate that FFA2 is trafficked to the recycling pathway, this to my knowledge is the first report to demonstrate this. Using this method, the constitutive internalisation of FFA2 visualised in the confocal images of the HEK 293 cells expressing FLAG-

FFA2 was corroborated where I also observe constitutive recycling. The number of events increased following exposure to propionate. In addition, the quantitation of recycling events also revealed the existence of distinct recycling modes, based upon the duration of the vesicle docked at the plasma membrane and the diffusion. As a large number of the recycling events were transient in cells that were unstimulated (NaCl) or stimulated, may indicate that FFA2 requires rapid re-exposure to the extracellular environment for resensitisation. The 'sustained' or the 'kiss-and-wait' mode of plasma membrane insertion is characterised by lingering structures on the plasma membrane before lateral diffusion. This mode of exocytosis has also been observed for the β2AR in primary neuronal cultures (Yu et al., 2010; Yudowski et al., 2006) and the GluR1-containg AMPA in primary hippocampal slice cultures (Makino and Malinow, 2009), however the physiological role of these recycling pathways has yet to be determined. The pre-tail events may represent vesicles that require an endosomal intermediate for exocytosis, for example by distinct Rab or other cargo release proteins as has been shown for mu-opioid receptors (MOR) (Roman-Vendrell et al., 2012). Alternatively, the different modes of receptor recycling may be import for targeting of receptors to microdomains at the plasma membrane required for signalling such as lipid rafts of A-kinase anchoring proteins (AKAPS) (Yudowski et al., 2006).

Though the inhibition of dynamin with Dyngo-4a and the use of β-ARR KO cells has allowed the understanding of the mechanisms of FFA2 internalisation and its impact on signalling, caution should be taken when using such tools. While determining the effects of SCFA induced inhibition of forskolin stimulated cAMP with in the presence of Dyngo-4A, I observed Dyngo-4a decreased levels of forskolin stimulated cAMP compared to DMSO. This could be due to off-targets exerted by Dyngo-4a, however I did not observe any of the similar effects from measuring intracellular calcium mobilisation or accumulation of IP1, indicating that Dyngo-4A did not globally impact signalling and this effect may be specific to the mechanisms of forskolin or the activation of certain adenylyl cyclases that may require endocytosis for activation. This effect was also seen for another study where forskolin-induced cAMP was reduced with Dynasore, another dynamin inhibitor and with PitStop, a clathrin inhibitor (Hardwick et al., 2017). However, other studies reported that Dyngo-4A had little or no effect on basal cAMP or forskolin stimulated cAMP (Tsvetanova and von Zastrow, 2014; Inda et al.,

2016). Mechanisms of forskolin activation of adenylyl cyclase signalling and whether it involves clathrin or dynamin remains to be determined.

In regards to the usage of β-ARR KO cells, a recent seminal work has emerged to demonstrate that caution must be taken when interpreting results from the CRISPR/Cas9-mediated β-ARR KO cells (Luttrell et al., 2018). By using small interfering RNA (siRNA) – or CRISPR/Cas9 – mediated β-ARR knockdown to compare β-ARR and G-protein mediated activation of ERK, it was found that while siRNA mediated β-ARR knockdown attenuated ERK activation, CRISPR/Cas9 – mediated β-ARR knockdown had distinct effects depending on the cell lines and receptors used (Luttrell et al., 2018). Luttrell and colleagues proposed that the notable differences between the cell lines is likely due to that the elimination of β-ARR had led to a cellular rewiring of signalling networks that enabled the cells to survive and thereby relying on G-protein-mediated cellular processes (Luttrell et al., 2018). However, my results demonstrate a loss in G-protein signalling, thus this concern may not apply. To further investigate the dependence of β-ARR in FFA2 internalisation and signalling, effects from siRNA mediated knockdown of β-ARR should be looked along side effects of CRISPR/Cas9 mediated – β-ARR knockdown and rescue experiments that re-introduced β-ARR should be done to support the observed effects seen from β-ARR elimination.

Overall, this chapter has unveiled that FFA2 displays constitutive and ligand-induced FFA2 internalisation and distinct mechanisms may be involved. In addition, these findings indicate that FFA2 trafficking is important for signal activation and raise the intriguing possibility that like other GPCRS, FFA2 also elicits important signalling responses from endosomes.

Chapter 5:

Involvement of the VEE in FFA2 trafficking and signalling

5.1 Introduction

In the previous results chapter, I have demonstrated that in STC-1 cells all SCFAs are able to inhibit forskolin stimulated cAMP via $G\alpha_i$, however it was only propionate that required receptor internalisation to mediate its effect. This suggests a specific spatial requirement is needed for propionate-mediated signalling. Therefore, the potential underlying mechanisms involved in the endocytic trafficking of propionate were next addressed. Understanding the mechanisms of endocytic trafficking that are exerted by propionate would give us further insight into how propionate is able to mediates its function in colon.

Endocytic trafficking of GPCRs is a critical component in defining cellular responses, by controlling both the spatial and temporal parameters of cellular signalling. It is not only involved in the regulation of localisation and downstream signalling but also the duration and extent of specific patterns of heterotrimeric G-protein signalling from the plasma membrane. The main mechanisms governing this is the divergent multistep post-endocytic sorting patterns that GPCRs undergoes; which receptors can either be resensitised by recycling or undergo degradation to lysosomes (detailed in Chapter 1, 1.5.2). During this spatial relocation, receptors can undergo interactions with many compartmentalised specific signalling molecules and cargo proteins that make up this complex endosomal network. Thus, membrane trafficking and signalling is a tightly regulated process that regulates diverse fundamental cellular programs and dysregulation can contribute to perturbed GPCR signalling and adverse physiological effects. The post-endocytic sorting events are not only essential for determining the fate of the internalised receptor but also that they are now appreciated as platforms to allow many GPCRs to continue, or-reactivate, signalling following receptor internalisation, redefining the traditional view that GPCR internalisation is simply a mechanism for signal termination.

The role of endocytic trafficking of GPCRs has been challenged by recent evidence that GPCRs can signal not only from the plasma membrane, but also from the endosome. A larger number of GPCRs have demonstrated the ability to elicit signalling from endosomal compartments

after receptor internalisation (Okazaki et al., 2008; Calebiro et al., 2009; Ferrandon et al., 2009; Werthmann et al., 2012). For example, the thyroid-stimulating hormone receptor (TSHR) requires PKA dependent internalisation to the trans-Golgi network (TGN) to elicit sustained cAMP signalling (Godbole et al., 2017) and the activation of the cAMP response element binding protein (CREB) requires internalisation to the early endosomes (EE) to also produce sustained cAMP signalling for calcium homeostasis (Ferrandon et al., 2009), highlighting that endocytic trafficking is essential to mediate correct signalling cellular outcomes from specific endosome compartments.

The emerging paradigm that receptor endocytic trafficking is important for specific signalling cellular outcomes suggest that another key role of endocytic trafficking is the regulation of receptors to specific endosome compartments for proper receptor function. For example, a seminal study that demonstrates that specific post-endocytic compartmentalisation is essential for receptor function is the LHR, that internalises to the very early endosome (VEE) instead of the classic EE which the prototypical β2AR that internalises to (Jean-Alphonse et al., 2014). The VEE is a distinct compartment that is smaller in diameter and upstream from the classic EE. It does not contain the known EE marker early endosome antigen 1 (EEA1) but instead is positive for the adaptor protein phosphotyrosine interaction, pleckstrin homology domain and leucine zipper containing 1 (APPL1) (Zoncu et al., 2009; Jean-Alphonse et al., 2014). Internalisation of the LHR to this compartment is not only important for receptor recycling but also for the G-protein signalling and the spatiotemporal regulation of MAPK signalling, indicating that the VEE is essential for the functionality of this receptor (Jean-Alphonse et al., 2014; Sposini et al., 2017).

The data from this study made it highly pertinent to investigate if FFA2 undergoes specific post-endocytic sorting and the impact it has on downstream signalling of FFA2. In this chapter, I aim to characterise the mechanisms of membrane trafficking of that exerted by propionate by determining which compartment does FFA2 internalises to. Additionally, if specific localisation of the internalised FFA2 has an impact on FFA2 signalling profile and/or have any impacts to downstream propionate action.

5.2 Results

5.2.1 FFA2 internalises into small, VEE-like endosomes

In Chapter 4, I demonstrated that FFA2 is sorted to the recycling pathway, however the specific compartment that FFA2 internalises to is not known. A simple preliminary indicator of an endosomal compartment is the physical size of endosomal compartments, endosomal compartments such as the EE has a diameter of approximately 1200 – 1400 nm which is the endosomal compartment that β2AR is classically known to internalise to (Jean-Alphonse et al., 2014). Therefore, to study the endosomal targeting of FFA2, the size of FFA2 endosomes in HEK 293 and STC-1 cells transiently expressing FLAG-FFA2 were first determined and compared to β2AR. In HEK 293 and STC-1 cells transiently expressing FLAG-FFA2 or FLAG-β2AR, cell surface receptor were labelled live prior to stimulation with propionate or isoproterenol (β2AR agonist) for 20 minutes or left untreated (Figure 5.1). Endosome size measurements in experimenters revealed that FFA2 is localised to endosomes of ~350-400 nm in diameter both in HEK 293 and STC-1 cells. In contrast to the β2AR that localised to endosomes of approximately ~900-1000 nm in diameter. This suggest that FFA2 locates to a distinct sub-compartment.

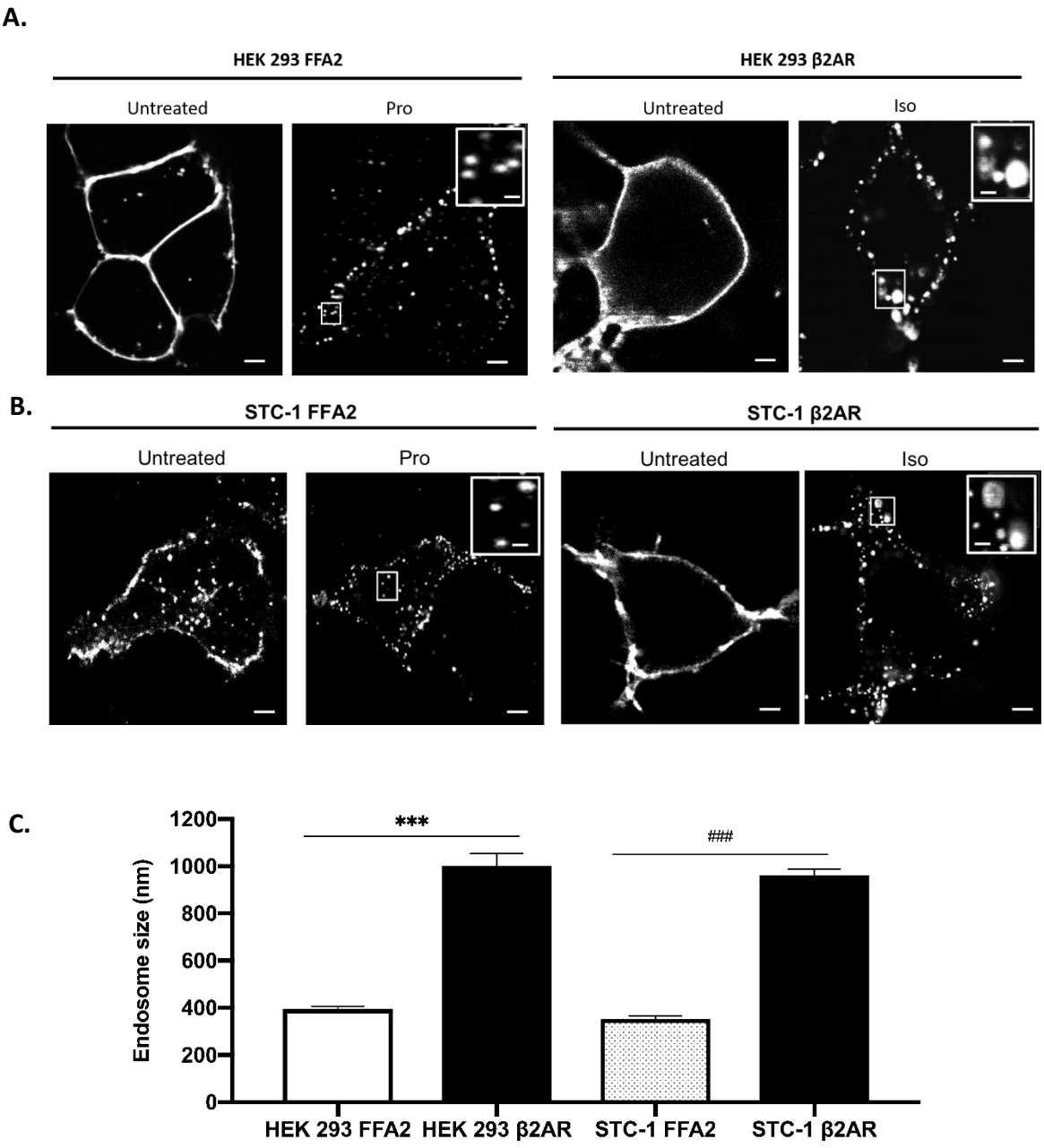


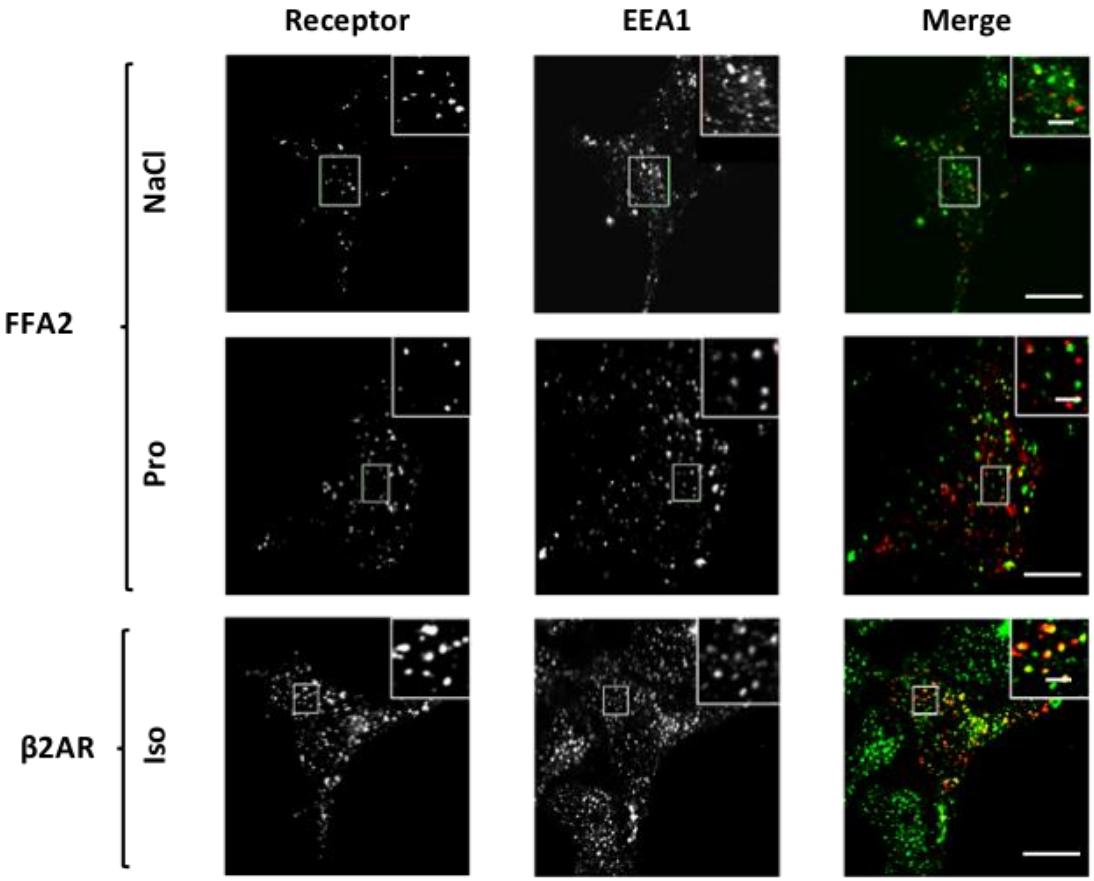
Figure 5.1 FFA2 and β2AR are sorted to distinct endosomes. Representative confocal images of HEK 293 cells (A) or STC-1 cells (B) transiently expressing FLAG-FFA2 or β2AR were labelled with anti-FLAG antibody and imaged live with confocal microscopy before and after the addition propionate (Pro, 1 mM) for FFA2 and isoproterenol (Iso,10 μM) for β2AR for 20 minutes. Scale bars: 10 μm (large image), 3 μm (inset). (C) Bar graph showing endosome diameter which was quantified from images in each condition (20-30 endosomes per cell, n=10 cells per condition). Endosome diameter was measured using ImageJ. Data are presented as mean ± SEM; t test: *** p<0.001 HEK 293 FFA2 vs HEK 293 β2AR, ### p<0.001 STC-1-FFA2 vs STC-1-β2AR.

5.2.2 FFA2 co-localises with endosomes positive for APPL1

The observation that FFA2 internalises to small endosomes then led me to investigate the identity of these small FFA2 endosomes. To investigate this, either FFA2- or β2AR containing endosomes were co-visualised with a classic marker of the EE, early endosomes autoantigen 1 (EEA1). HEK 293 cells transiently expressing FLAG-FFA2 or β2AR were labelled with anti-FLAG M1 antibody prior to stimulation with NaCl or propionate and isoproterenol for 20 minutes or left untreated. Anti-FLAG antibody was stripped with EDTA to strip away surface staining to specifically visualise internalised receptors. The percentage of receptors positive for EEA1 was then quantified. In cells treated with NaCl 13.7 ± 0.79% FFA2 endosomes co-localised to EEA1 and increased to 36 ± 0.27% following propionate treatment. In contrast, the β2AR extensively co-localised with 72.0 ± 1.47% following isoproterenol treatment.

As FFA2 colocalises poorly with EEA1, this may suggest that FFA2 co-localises to the VEE compartment instead. APPL1 has been demonstrated to be recruited to the VEE compartment (Zoncu et al., 2009; Jean-Alphonse et al., 2014). Therefore, it was asked whether FFA2 traffics to APPL1-positive endosomes. To do this I compared FFA2 co-localisation of APPL1 levels to that of LHR, a receptor known to traffic to VEEs whereby APPL1 localises to a subpopulation (Sposini et al., 2017). Representative images of FFA2 and LHR co-localisation with APPL1 are shown in Figure 5.3 A. In cells treated with NaCl, 19.63 ± 0.93% of FFA2 endosomes co-localised with APPL1 and increased to 32.8 ± 0.35% following propionate treatment. This co-localisation was similar to that of LHR whereby 35.167 ± 1.92% colocalised with APPL1 following LH treatment. The ability of FFA2 to traffic to APPL1 endosomes was also analysed in STC-1 cells transiently expressing FLAG-FFA2. In cells treated with NaCl, 18.37 ± 1.55% of FFA2 endosomes co-localised with APPL1 and increased to 31.23 ± 1.18% following propionate treatment. Thus, as both HEK 293 cells and cells endogenously expressing FFA2 internalises to small endosomes and co-localises poorly with EEA1, this indicates that FFA2 traffics to the VEE.

A.



B.

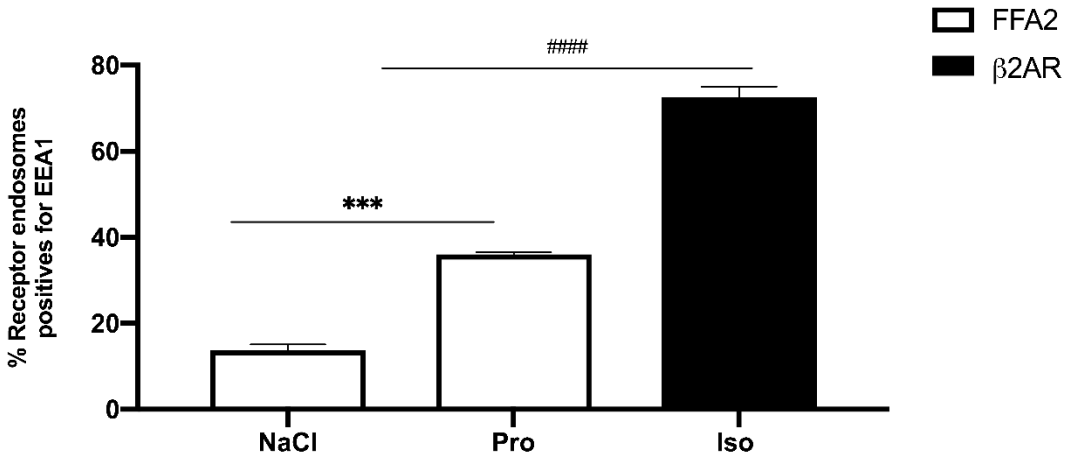
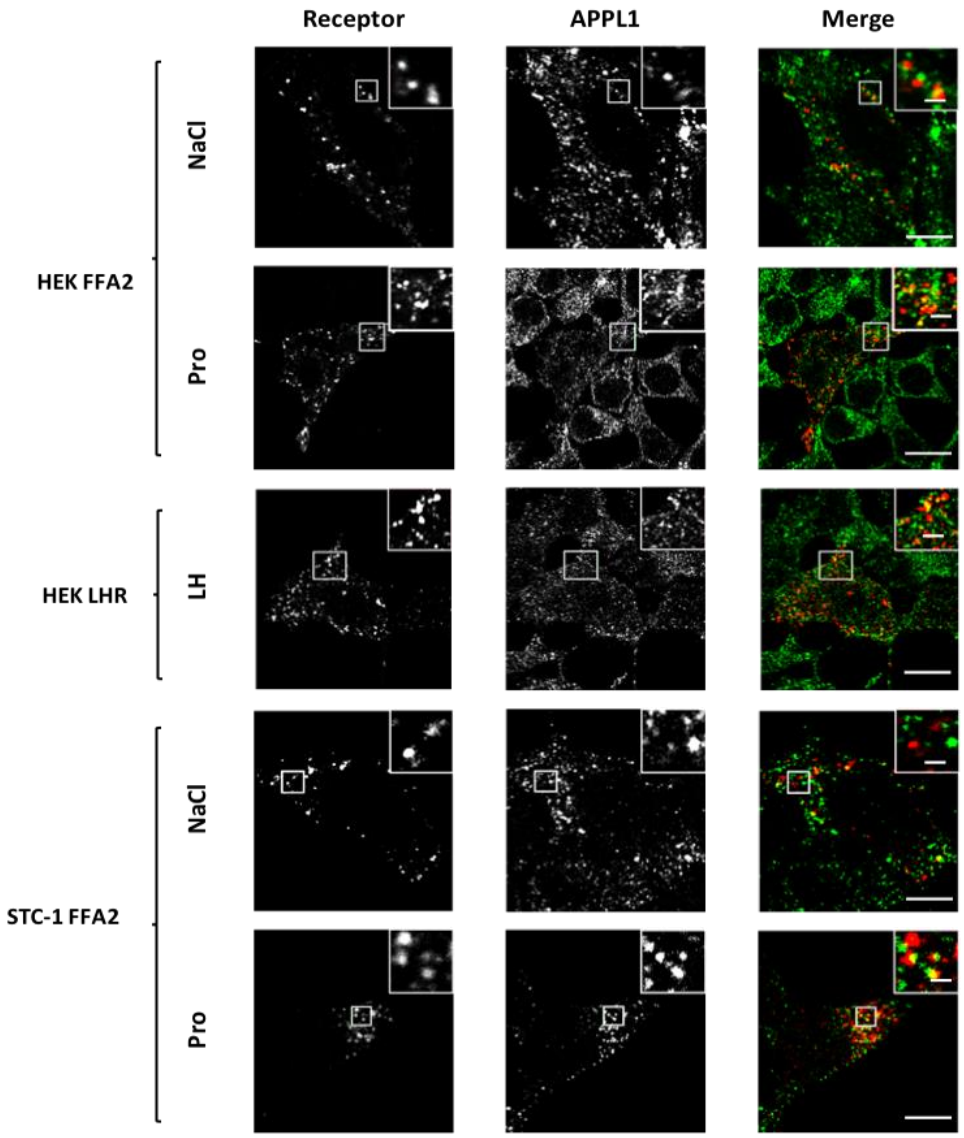


Figure 5.2 FFA2 co-localises poorly with EEA1. HEK 293 cells transiently expressing FLAG-FFA2 or β2AR were labelled with anti-FLAG M1 antibody for 15 minutes and cells were left unstimulated or stimulated with NaCl (1 mM) or propionate (Pro, 1 mM) for FFA2 or isoproterenol (Iso, 10 µM) for β2AR for 20 minutes. Cells were then washed and surface was stripped with EDTA before fixation, permeabilization and staining with antibodies EEA1. Immunofluorescent secondary antibodies were then used to stain FFA2 (red) and EEA1 (green). Representative confocal images are shown in (A). Scale bars: 10 µm, 3 µm (insets). Bar graph showing the percentage of FFA2 and β2AR endosomes co-

localised with EEA1 (%) which was quantified from images in each condition (200 endosomes per condition, 10 cells quantified/condition). Data are presented as mean ± SEM, n= 3 independent experiments; *** p<0.001 vs NaCl for FFA2 ### p<0.001 FFA2 vs β2AR.

A.



B.

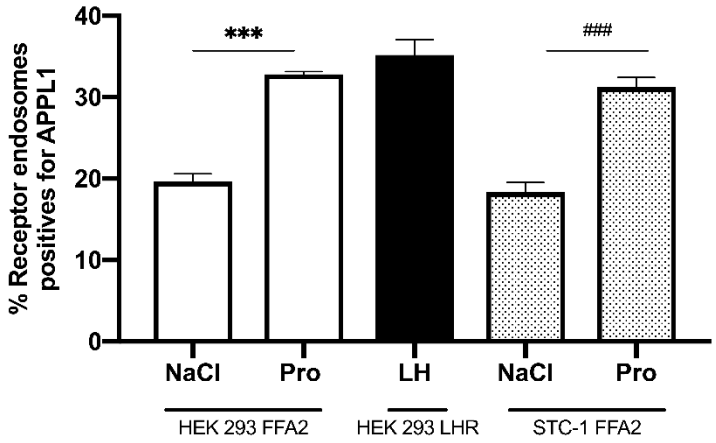


Figure 5.3 FFA2 co-localises with APPL1. HEK 293 cells transiently expressing FLAG-FFA2 or LHR and STC-1 transiently expressing FLAG-FFA2 were labelled with anti-FLAG M1 antibody for 15 minutes and cells were left unstimulated or stimulated with NaCl (1 mM) or propionate (Pro, 1 mM) for FFA2 or LH (10 nM) for LHR for 20 minutes. Cells were then washed and surface was stripped with EDTA before

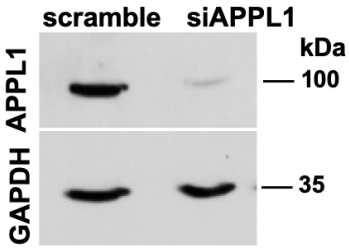
fixation, permeabilization and staining with anti-APPL1. Immunofluorescent secondary antibodies were then used to stain FFA2 (red) and APPL1 (green). Representative confocal images are shown (A). Scale bars: 10 µm (large images), 5 µm (insets). (B) Bar graph showing the percentage of FFA2 or LHR endosomes co-localised to APPL1 (%) which was quantified from images in each condition (200 endosomes per condition, 10 cells quantified/condition). Data are presented as mean ± SEM, n= 3 independent experiments ***, ### p<0.001 vs NaCl.

5.2.3 APPL1 is essential for FFA2 recycling via the VEE

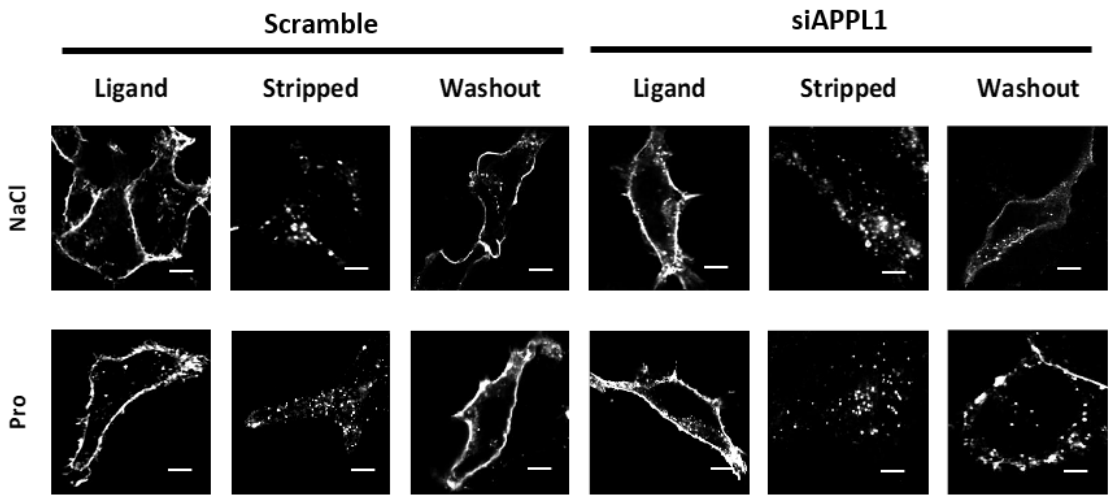
APPL1 is known to be required for recycling of receptors targeted specifically to the VEE (Sposini et al., 2017). To directly address if APPL1 is essential for post-endocytic sorting of FFA2, cellular levels of APPL1 were depleted via siRNA in HEK 293 cells stably expressing FLAG-FFA2. Levels of APPL1 knockdown efficiency was verified by western blot and cells transfected for siRNA-APPL1 were robustly depleted of APPL1 compared to siRNA-scramble transfected cells (Figure 5.4 A). FFA2 internalisation and recycling via confocal microscopy was then assessed. To examine FFA2 internalisation and recycling, cell surface receptor was labelled with anti-FLAG M1 antibody prior to stimulation with either NaCl or propionate. Anti-FLAG antibody was then 'stripped' with EDTA to remove surface bound antibody and further incubated in ligand-free media for 1 hour to allow internalised receptor to recycle. In cells depleted of APPL1, there was no effect in cells treated with NaCl as there was a complete return of the receptor back to the plasma membrane. In cells treated with propionate however, there was a marked inhibition of ligand-induced recycling of FFA2 back to the plasma membrane after ligand removal (Figure 5.4 B).

I next assessed the role of APPL1 in rapid FFA2 recycling via live cell TIR-FM of SEP-FFA2 (described in Chapter 4). Depletion of APPL1 did not affect the number of recycling puffs observed in in cells treated with NaCl, however there was significant reduction of propionate-induced rapid recycling (Figure 5.4 C), consistent with FFA2 recycling was examined by confocal microscopy. Together this suggest that the VEE is essential for ligand-induced FFA2 recycling and not constitutive FFA2 recycling.

A.



B.



C.

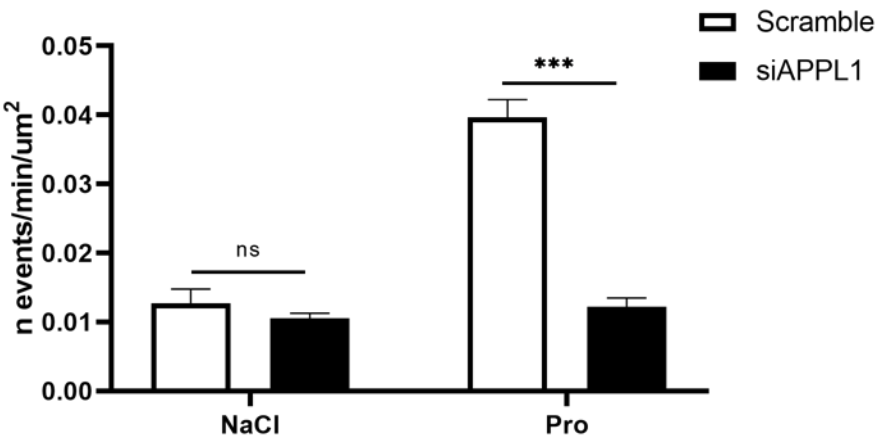


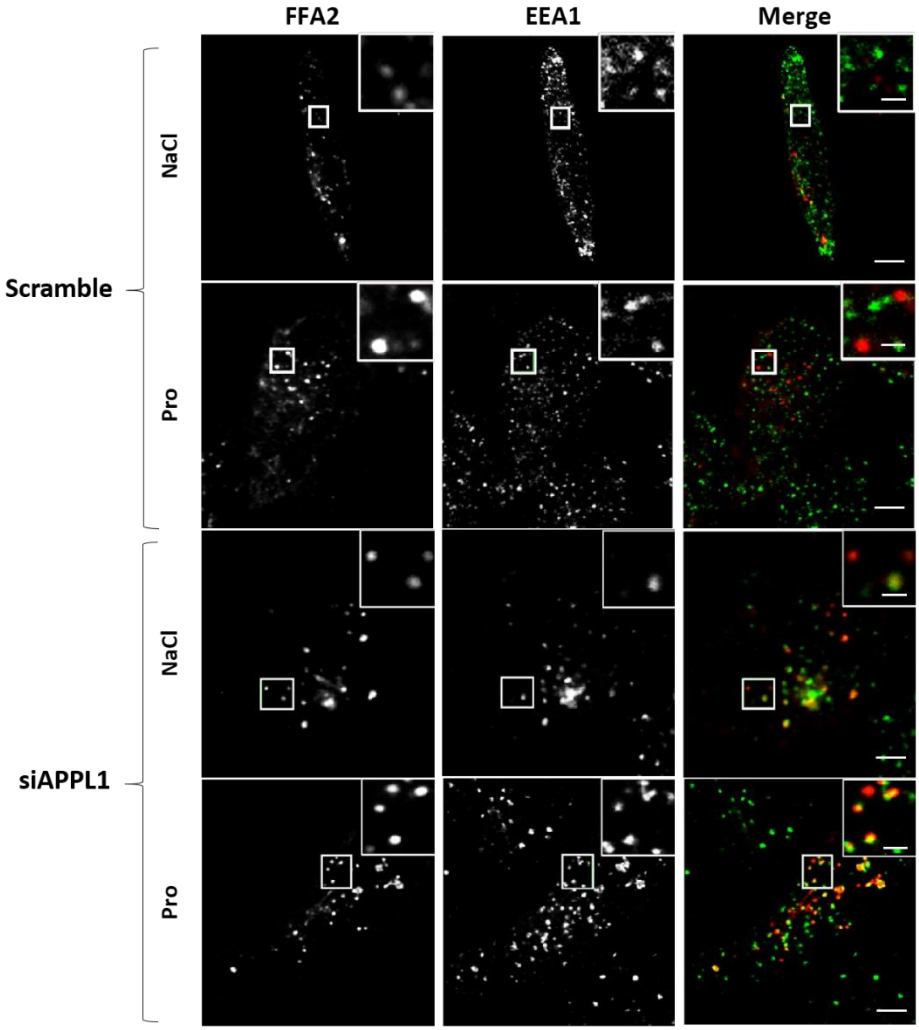
Figure 5.4. APPL1 is required for FFA2 recycling from the VEE. (A) Representative western blot of total cellular levels of APPL1 from lysates collected from HEK 293 cells following siRNA scramble (scramble) or siRNA-APPL1 (siAPPL1). GAPDH was used a loading control. (B) Propionate-induced internalisation and recycling following APPL1 siRNA-mediated knockdown was analysed by confocal microscopy. HEK 293 cells expressing FLAG-FFA2 was labelled with anti-FLAG antibody and cells were stimulated with propionate (Pro, 1 mM, 20 minutes). Surface bound anti-FLAG M1 antibody was removed by PBS/EDTA wash and cells were incubated with ligand-free medium for 1 hour to allow receptor recycling. Scale bar = 10 µm inset is 5 µm. (C) HEK 293 cells expressing SEP-FFA2 transfected with

either siRNA scramble (scramble) or siRNA-APPL1 (siAPPL1) were stimulated with NaCl (1 mM) or propionate (Pro, 1 mM) and recycling was viewed in real-time via TIR-FM from 5 minutes following ligand addition. n=10 cells per condition, collected across at least 3 independent experiments; Data are presented as mean ± SEM; t-test: *** p<0.001 vs NaCl.

5.2.4 APPL1 knockdown may re-route FFA2 to the EE

The inhibition of FFA2 recycling by depletion of APPL1 levels may be due to re-routing the receptor from the VEE to the EE. To assess if the depletion of APPL1 alters endosomal targeting of FFA2, cellular levels of APPL1 were depleted via siRNA in HEK 293 stable expressing FFA2 and EEA1 colocalisation levels in cells stimulated with propionate were assessed. In cells transfected with scramble siRNA, 35.67 ± 1.76% of FFA2 positive endosomes co-localised with EEA1, consistent with previous observations. In cells transfected with siRNA-APPL1, this level of EEA1 co-localisation increased significantly to 79.33 ± 1.20%. This not only demonstrates that targeting of FFA2 to the VEE is important its recycling but that APPL1 has an unprecedented role in directly sorting FFA2 to the VEE.

A.



B.

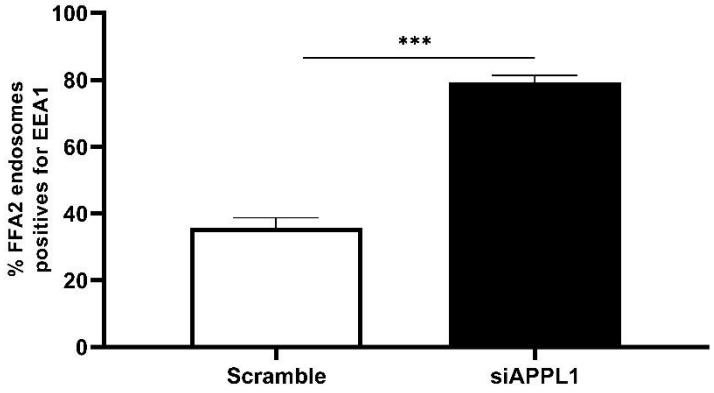


Figure 5.5 APPL1 depletion re-routes FFA2 to EEs. HEK 293 stably expressing FLAG-FFA2 were transfected either with scramble siRNA (scramble) or APPL1 siRNA (siAPPL1). Cells were fed live with anti-FLAG M1 antibody, stimulated with Pro (1 mM) for 20 minutes, stripped to removed surface bound antibody, fixed, permeabilised and subject to primary antibody staining for EEA1. Cells were then labelled with immunofluorescently tagged secondary antibodies for the receptor (red) and EEA1 (green). Representative confocal images are shown in (A). Scale bar = 10 µm inset is 5 µm. Confocal

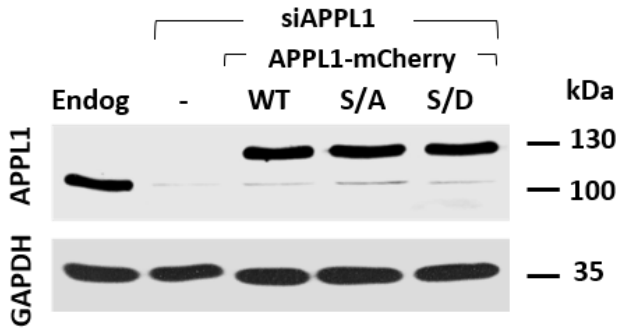
images were quantified to assess the % FFA2 endosomes positive for EEA1 (B). Data are presented as mean ± SEM; n=3, t test: *** p<0.001 vs scramble.

5.2.5 FFA2 recycling is not driven by the PKA phosphorylation of APPL1 on S410

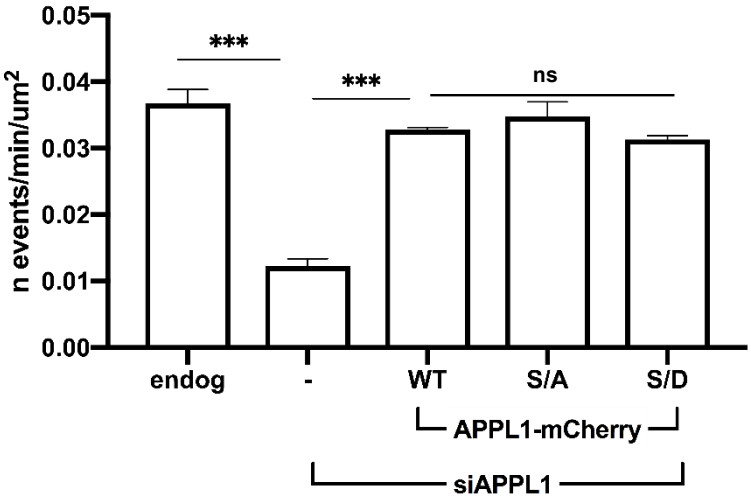
I next assessed the molecular mechanisms of APPL1-dependent FFA2 recycling. For the LHR, a VEE targeted receptor where that recycling is dependent on APPL1, PKA-dependent phosphorylation of APPL1 on Serine 410 (S410) is required for its recycling. I therefore examined whether FFA2 recycling, like the LHR, will also require phosphorylation of PKA on S410. To determine this, I utilised a previously characterised wild-type (WT), phospho-deficient mutant (S410A) and a phospho-mimetic mutant (S410D) of mCherry-APPL1 (Sposini et al., 2017) to assess if VEE-directed recycling of FFA2 could be restored in APPL1 depleted cells by TIR-FM. Western blot analysis demonstrated that the three mCherry constructs following siRNA-mediated depletion of endogenous APPL1 were expressed at similar levels (Figure 5.6 A). In cells depleted of APPL1, FFA2 recycling was restored by expression of WT. In cells expressing both the phospho-deficient mutant S/A and phospho-mimetic mutant S/D, FFA2 recycling was also restored, suggesting FFA2 recycling is not dependent on the phosphorylation of S410 (Figure 5.6 B).

As FFA2 recycling was not dependent on the phosphorylation specifically at S410, I then determined if FFA2 recycling requires PKA activation by using a PKA inhibitor (KT5720). Cells were pre-treated with KT5720 prior to stimulation with propionate and live TIR-FM imaging. KT5720 did not attenuate FFA2 recycling, in contrast to LHR recycling which was potently inhibited (Figure 5.6 C). Together this confirms that APPL1-dependent FFA2 recycling does not require PKA activation on S410 and may be regulated by an alternative mechanism.

A.



B.



C.

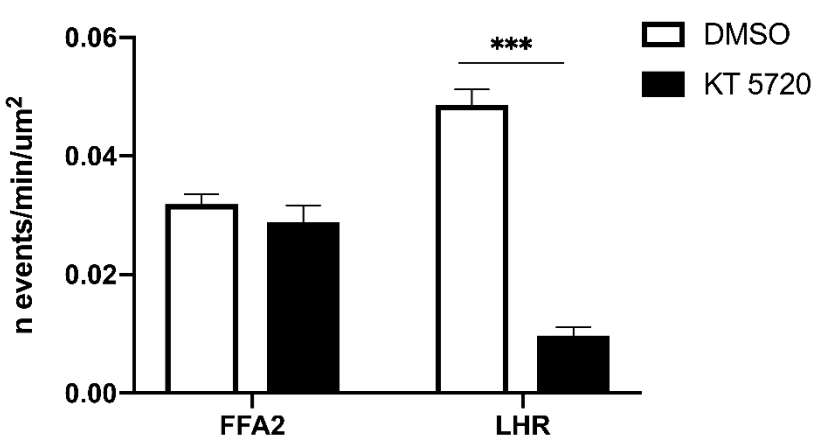


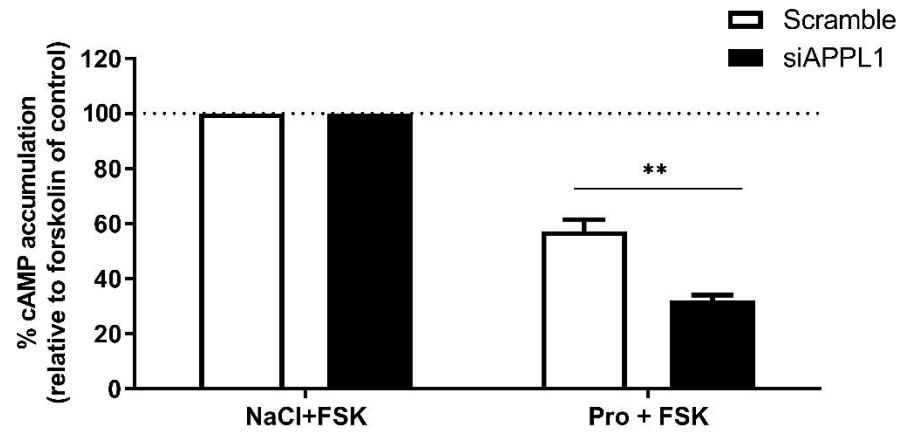
Figure 5.6 FFA2-APPL1 recycling is not regulated by PKA phosphorylation of S410. (A) Representative western blot analysis total cellular levels of APPL1 from lysates collected from HEK 293 cells stably expressing SEP-FFA2 and transiently transfected with mock (endog), siAPPL1 (-), siAPPL1 + mCherry-WT (WT) or -S410A (S/A) or -S410D (S/D) APPL1. GAPDH was used as loading control. (B) FFA2 recycling measured by TIR-FM in HEK 293 cells stably expressing SEP-FFA2 and transfected as in (A). n ≥10 cells per condition were imaged across at least 3 independent experiments; One-way ANOVA: ns, nonsignificant; *** p<0.001. (C) FFA2 and LHR recycling measured in real time by TIR-FM in HEK 293 cells stably expressing SEP-FFA2 or LHR in the presence of Pro (FFA2) and LH (LHR) and pre-treated for 15 minutes with DMSO (vehicle) or PKA inhibitor KT 5720 (10 µM). n=16 cells per condition; data are presented as mean ± SEM; t-test: ***p<0.001 vs DMSO.

5.2.6 APPL1 negatively regulates cAMP signalling of VEE-targeted FFA2

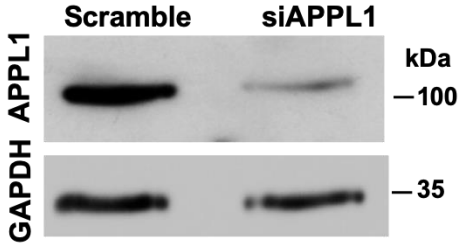
The above data suggest that APPL1 is important for correct post-endocytic sorting of FFA2. The second role of APPL1 in the VEE is to negatively regulate G-protein signalling from this compartment (Sposini et al., 2017). As I have demonstrated that SCFA induced $G\alpha_i$ signalling requires receptor internalisation (Chapter 4), I next examined the potential downstream role of this compartment in FFA2 signalling when APPL1 is knocked down. Propionate induced inhibition of forskolin stimulated cAMP was measured in HEK 293 cells stably expressing FLAG-FFA2 transfected with either scramble or APPL1 siRNA. There was no effect of APPL1 knockdown in levels of NaCl + FSK stimulated cAMP; however, there was an unexpected 2-fold increase in propionate mediated inhibition of forskolin stimulated cAMP (Figure 5.7A).

The ability of APPL1 to negatively regulate $G\alpha_i$ signalling was also determined in STC-1 cells depleted of APPL1. APPL1 depletion in STC-1 cells was confirmed by Western blot (Figure 5.7 B). Similar to what was observed in HEK 293 cells stably expressing FLAG-FFA2, though to a lesser extent, there was an increase in propionate mediated inhibition of forskolin-induced cAMP in APPL1 depleted cells (Figure 5.7 C). This suggests that APPL1 has a role in not only negatively regulating $G\alpha_s$ coupled receptors but also the $G\alpha_i$-coupled FFA2.

A.



B.



C.

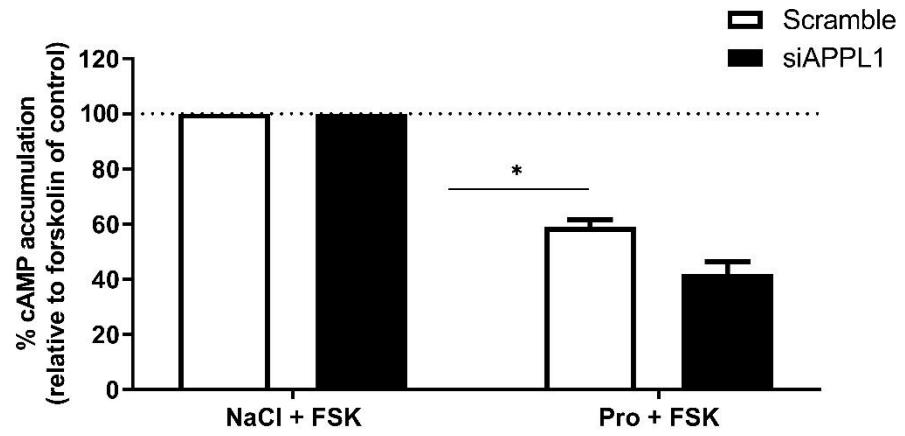


Figure 5.7. APPL1 negatively regulates propionate induced inhibition of forskolin induced cAMP. (A) Intracellular cAMP levels measured in HEK 293 cells expressing FLAG-FFA2 transfected either with siRNA scramble (scramble) or APPL1 siRNA (siAPPL1). Cells were treated with IBMX (0.5mM, 5 minutes) and then with forskolin (FSK, 3 µM) or a combination of NaCl or Pro (1 mM) for 5 minutes. Data are expressed as percentage change of NaCl+FSK and NaCl+FSK expressed is expressed as 100%. Data represent mean ± SEM, n =3; t test: ** $p < 0.01$ vs scramble. (B) Representative western blot of total cellular levels of APPL1 from lysates collected from STC-1 cells following siRNA scramble (scramble) or siRNA-APPL1 (siAPPL1). GAPDH was used a loading control. (C) Intracellular levels measured inSTC-1 cells transfected either with siRNA scramble (scramble) or APPL1 siRNA (siAPPL1). Cells were treated as in (A). Data are expressed as percentage change of NaCl+FSK and NaCl+FSK expressed is expressed as 100%. Data represent mean ± SEM, n =3; t test: * $p < 0.05$ vs scramble.

5.2.7 FFA2 co-localises with $G\alpha_i$ in the VEEs

I then asked are there G-proteins within FFA2 endosomes, if so what kind of endosomes are there as the VEE is known to be a heterogenous compartment thus, I sought to determine if FFA2 colocalises with $G\alpha_i$ in APPL1 positive endosomes. To examine this, I imaged FLAG-FFA2 cells expressing $G\alpha_i$-Venus and assessed levels of APPL1 co-localisation by TIR-FM. TIR-FM was employed as VEE are prevalent in the peripheral regions of cells (Sposini et al., 2017).

In HEK 293 cells expressing FLAG-FFA2 and $G\alpha_i$-Venus, cells were treated with NaCl or propionate for 5 minutes and APPL1 colocalisation levels were assessed. A 5-minute time point was chosen as at this time point, I observed an activation of $G\alpha_i$ signalling. TIR-FM analysis revealed that FFA2 signalling endosomes, marked by $G\alpha_i$-Venus were heterogeneous and characterised by FFA2- $G\alpha_i$ endosomes with and without APPL1 and FFA2-APPL1 endosomes where no $G\alpha_i$ was present (Figure 5.8 A). Analysis of FFA2- $G\alpha_i$ endosomes after NaCl stimulation revealed that ~13% of FFA2- $G\alpha_i$ endosomes contained APPL1 and increased to ~31% of following propionate stimulation. Together this demonstrates that APPL1 is also a marker for a subpopulation of FFA2- $G\alpha_i$ signalling endosomes highly active in the duration of their signalling activity.

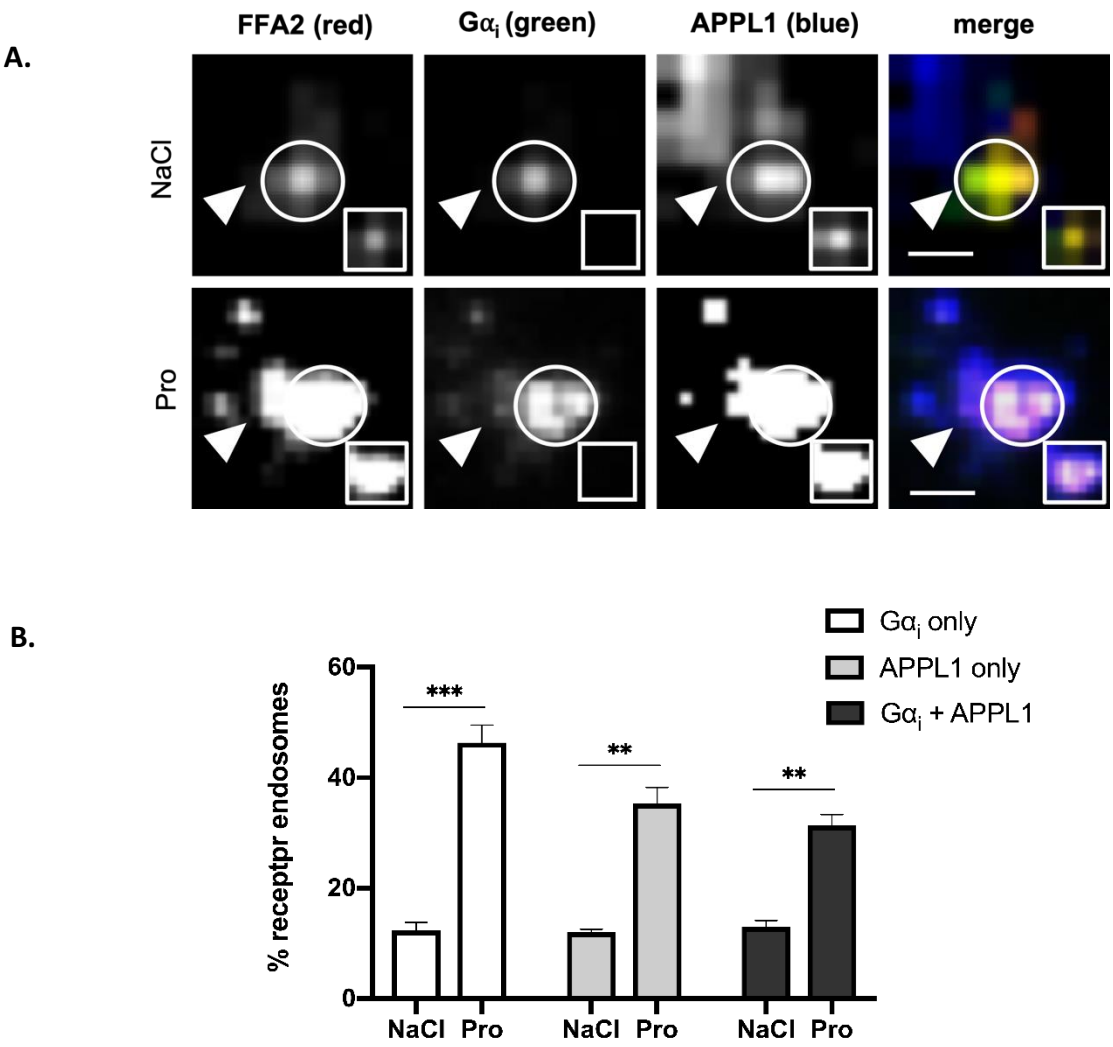


Figure 5.8 FFA2 activates Gαi from the VEEs. (A) Representative TIR-FM images of HEK 293 cells stably expressing FLAG-FFA2, and co-expressing $G\alpha_i$-Venus, after stimulation with NaCl or propionate. Cells were fed lived with anti-FLAG M1 antibody, stimulated with NaCl (1 mM) or propionate (Pro, 1 mM) for 5 minutes, stripped to remove surface bound antibody, fixed, permeabilised and stained with anti-APPL1 antibody followed by immunofluorescent antibodies. Arrow indicate FFA2 endosomes for $G\alpha_i$ only, circles indicate FFA2 endosomes positive for FFA2 and APPL1 and square indicates FFA2 endosomes positive for APPL1 only. Scale bar= 1 µm. (B) Quantification of FFA2-$G\alpha_i$ endosomes positive for either $G\alpha_i$, APPL1 or $G\alpha_i$ and APPL1; n=12 cells per condition from A were quantified across 3 independent experiments.

5.3 Discussion

In summary, this chapter provides evidence that the VEE is involved in the trafficking and signalling of FFA2. I demonstrate that the VEE is important for correct post-endocytic sorting, to the recycling pathway and that they negatively regulate $G\alpha_i$ signalling. Additionally, preliminary data suggest that APPL1 may have a role in directly sorting FFA2 to the VEE.

The identification of a VEE as a novel compartment important not only for trafficking but also signalling for a subset of GPCRs has further contributed to the view that GPCR internalisation is not only a means of G-protein signal termination but signal activation and that the endosomal network is more complex than previously appreciated (Jean-Alphonse et al., 2014; Sposini et al., 2017). The VEE is a distinct compartment upstream from the classic EE, which is the prototypic cargo sorting station. The VEE is considerable smaller, positive for the adaptor protein APPL1 but negative for the EE marker EEA1. In addition, the VEE demonstrates that the post-endocytic fate of GPCRs are not restricted to either the recycling or degradative pathway from the EE, but includes distinct sorting platforms, which are made possible by receptor trafficking to endosomes other than the EE.

The first observation that FFA2 internalises into the VEE compartment was the small endosome size of FFA2 endosomes. This was supported by our knowledge of the small endosome size that LHR internalises to in live HEK 293 cells (Jean-Alphonse et al., 2014) and also the fact that endosomes enlarge as they mature and fuse together along the endocytic pathway (Huotari and Helenius, 2011). Further supporting this, the β2AR, which is a classical EE-localised GPCR was found in much larger endosomes. In addition to the small endosome size, characterising of these endosomes also demonstrates that a large proportion (>60%) of the FFA2 endosomes are negative of EEA1 and 40% of FFA2 endosomes instead were positive for APPL1, which further suggest that FFA2 is primarily targeted to the VEE. In STC-1 cells that endogenously express FFA2, receptors also internalise to a sub-population that is positive for APPL1. However, due to antibody sensitivity issues in STC-1 cells, EEA1 colocalisation could not be carried out to assess if this was the case in STC-1 cells.

Until recently, GPCR recycling has traditionally been thought to occur exclusively from the EEs, however it is now apparent that a subset of GPCRs recycle from the VEE namely; the LHR, FHSR and β1AR (Sposini et al., 2017) and results from this chapter also demonstrate that FFA2 also recycles from this compartment. I also observed that ligand-induced rapid recycling is dependent on APPL1 and not constitutive recycling. This was rather striking as both constitutive and ligand-induced FFA2 internalises to APPL1 however only ligand-induced

recycling was dependent on APPL1. This may indicate that FFA2 constitutive recycling requires a distinct compartment.

For the LHR, sorting to VEE is sequence dependent and requires interaction of the PDZ ligand $G\alpha_i$ interacting protein C terminus (GIPC) with its C-tail (Jean-Alphonse et al., 2014). Sequence-dependent sorting and interactions with PDZ ligands of receptors is a well-established mechanism for GPCRs, among many are the adrenergic, opioid and cannabinoid GPCRs (Romero et al., 2011). PDZ proteins regulate multiple aspects of GPCR function, including endocytosis, coupling to specific G proteins, assembly of downstream signalling pathways and sequence dependent recycling (Romero et al., 2011; Dunn and Ferguson, 2015). Specific sorting sequences in the C-tail or PDZ ligands of the FFA2 has yet to be reported, however as my preliminary data suggest that depletion of APPL1 re-routes the receptor to a larger portion of EEA1 positive endosomes, may suggest that APPL1 may be essential in directing FFA2 to the VEE, as LHR requires GIPC for correct sorting to the VEE (Sposini et al., 2017). Alternatively, re-routing FFA2 to EEA1 positive endosomes could to due to other reasons. First, depleting APPL1 could cause endosomal accumulation of FFA2 that may overwhelm the sorting machinery and disrupt receptor sorting, thus forcing FFA2 to accumulate in EEs. Secondly, depletion of APPL1 may interfere with the incorporation of FFA2 to the tubulovesicular compartment which is important for sorting cargo that APPL1 resides on (Kalaidzidis et al., 2015), thereby disrupting the correct delivery of FFA2 to the VEE. Thirdly, the knockdown of APPL1 may influence key endosomal sorting proteins that are involved with APPL1 such as the ADP-ribosylating factor 6 (Arf6), a small GTPase is known to be important for the recycling of the intregrin-β-1 receptor (Chen et al., 2014; Diggins and Webb, 2017) and additionally Arf proteins have been reported to interact with the intracellular loops of GPCRs (Kanamarlapudi et al., 2012). Thus, the effects of FFA2 sorting to the EEs could be due to changes in the stability of sorting proteins of the APPL1 endosomal compartment. However, as these observations was based only upon colocalisation levels of EEA1 from fixed cells, live cell imaging to determine endosome size and morphology should be carried out. In addition, the direct sorting of FFA2 to the VEE by APPL1 could also be determined quantitatively by examining the interaction of FFA2 and APPL1 using Bioluminescence Resonance Energy Transfer (BRET), a biophysical technique that allows the study of protein-protein interaction in live intact cells.

For many GPCRs, such as the β2AR, recycling is regulated by PKA phosphorylation (Vistein and Puthenveedu) and for the LHR that recycling is APPL1-dependent is also regulated by PKA phosphorylation (Sposini et al., 2017), thus I attempted to identify if FFA2-APPL1 recycling was regulated by PKA phosphorylation as for the LHR. FFA2-APPL1 dependent recycling was not regulated by PKA phosphorylation. However, given FFA2 is a $G\alpha_i$-coupled receptor, this was not necessarily unanticipated. An alternative mechanism to be explored is if FFA2 receptor recycling can be regulated by protein kinase C (PKC). Though I have demonstrated that FFA2 $G\alpha_{q/11}$ signalling does not require receptor internalisation (Chapter 4), however, as FFA2 propionate-induced calcium signalling may be regulated both by $G\alpha_{q/11}$ and $G\alpha_i$, I propose that $G\alpha_{q/11}$ signalling from the plasma membrane may promote FFA2 endosomal signalling via G-protein crosstalk between the plasma membrane to and endomembrane signalling. This crosstalk has been demonstrated for the PTHR, where the $G\beta\gamma$ release from $G\alpha_I$ coupled to the β2AR can stimulate endosomal adenylyl cyclase to sustain PTHR cAMP signalling (Jean-Alphonse et al., 2017), demonstrating receptor crosstalk between plasma membrane and endomembrane signalling. Receptor recycling regulated by PKC phosphorylation has been demonstrated for mu-opioid receptor (Bowman et al., 2015). In addition, APPL1 at Serine 430 has been identified as site that undergoes phosphorylation of PKC (Liu et al., 2012).

APPL1 is known to negatively regulate LHR, FSHR and β1AR (Sposini et al., 2017) signalling, all of which are $G\alpha_s$-coupled receptors, interestingly from my data, I observe that APPL1 is able to also negatively regulate FFA2-$G\alpha_i$ signalling. To my knowledge, this is the first to report that APPL1 is capable to negatively regulate a $G\alpha_i$-coupled receptor. This observation that APPL1 is also able to negatively regulate a $G\alpha_i$-coupled receptor in addition to $G\alpha_s$-coupled receptors may indicate that APPL1 is able to regulate distinct G-proteins, suggesting distinct microdomains within the VEE may exist. This also may be evident by the co-localisation of $G\alpha_i$ G proteins with APPL1 upon stimulation with propionate. However, more evidence is needed to confirm if $G\alpha_i$ G proteins does indeed exist within the microdomains of the VEE and to clarify this the development of active $G\alpha_i$ nanobodies will be very useful in order to visualise activated $G\alpha_i$. For the exact mechanism of how APPL1 negatively regulates endosomal G protein signalling is currently unknown and at this stage I can only speculate how APPL1

negatively regulates distinct G-protein signalling. APPL1 is a multifunctional adaptor protein that contains multiple domains that allows APPL1 to interact with a vast array of proteins. Among them, the pleckstrin homology (PH) domain is a small modular domain that can bind to many proteins including Gβγ (Lodowski et al., 2003). Binding of a Gβγ complex via agonist induced activation of receptors to the PH domain increases interactions with another PH domain ligand, G-protein-coupled receptor kinases (GRKs), specifically GRK2 (Scheffzek and Welti, 2012). GRK2 is member of GRKs that phosphorylates GPCRs and desensitizes agonist induced receptors. The GRK2 contains a PH domain that can directly bind to the Gβγ complex where it phosphorylates the receptor and thereby inhibiting signalling by Gβγ. Thus, via the PH domain, APPL1 may indirectly negatively regulate G protein signalling.

This chapter provides evidence that highlights the developing appreciation of the significance of the discrete subcellular compartments in GPCR function and signalling. I have provided novel mechanistic insights into FFA2 trafficking and provided evidence that FFA2, a $G\alpha_i$ coupled receptor, internalises to the VEE where its endosomal signalling is regulated the VEE in addition to the reported $G\alpha_s$ coupled receptors. Whether such mechanisms are important for FFA2 downstream signalling, such as release of anorectic gut hormones are yet to be elucidated.

Chapter 6:

Endosomal signalling regulates propionate-mediated gut hormone release in enteroendocrine cells

6.1 Introduction

Endocytic signalling and trafficking are a deeply integrated processes that regulates specific cellular processes. Understanding how trafficking and signalling are integrated has proved to be important in enhancing our understanding how these receptors function *in vivo*. What has become clear is that receptor internalisation is highly essential in signal regulation and delineating mechanisms by which receptors are directed to their correct signalling site is paramount in the field of GPCR biology.

Though it has become clear FFA2 is the essential receptor for GLP-1 and PYY release, many studies have focused on the regulation of secretion but studies of the mechanisms controlling the release have been limited. The current understanding of how FFA2 regulates the release of GLP-1 and PYY is via SCFA's ability to elicit calcium signalling by $G\alpha_{q/11}$ coupling (Bolognini et al., 2016b) and not via FFA2 coupling to $G\alpha_i$ as evident by propionate-induced hormone secretion being unaffected in the presence of Ptx (Tolhurst et al., 2012; Bolognini et al., 2016b). However, as current evidence suggests receptor signalling is not the only the mechanism that defines a cellular response but also the complex processes of endocytic trafficking of a receptor and the integration of these process that controls diverse fundamental cellular programs. For example, it has been reported that internalisation of the GLP-1 receptor (GLP-1R) is requisite for insulin secretion in a rat pancreatic beta-cell line (Kuna et al., 2013)

Despite recent progress in elucidating the mechanism underlying SCFAs-mediated gut hormone release, the intracellular signalling pathways regulating gut hormone release remain understudied. As I have demonstrated a key role of receptor internalisation, I determine whether receptor trafficking is essential for propionate-induced gut hormone release. Further, I reveal additional potential pathways that are involved in propionate-induced gut hormone release.

6.2 Results

6.2.1 Propionate induced GLP-1 release is mediated via $G\alpha_i$ but not $G\alpha_{q/11}$

The signalling pathways underlying propionate-stimulated gut hormone release are poorly understood and understudied. To study the underlying mechanisms of propionate induced gut hormone secretion, the ability of propionate to stimulate the release of GLP-1 and PYY in STC-1 cells was first determined. The release of GLP-1 and PYY were determined via radioimmunoassay (RIA) in STC-1 cells stimulated with forskolin, used as a positive control and propionate at 1 mM. GLP-1 and PYY release was calculated and normalised to basal levels (Figure 6.1 & 6.2, dotted line). In STC-1 cells treated with propionate or forskolin, there was no PYY release detected (Figure 6.1 A). In contrast, forskolin and propionate significantly stimulated an increase in GLP-1 (Figure 6.1 B).

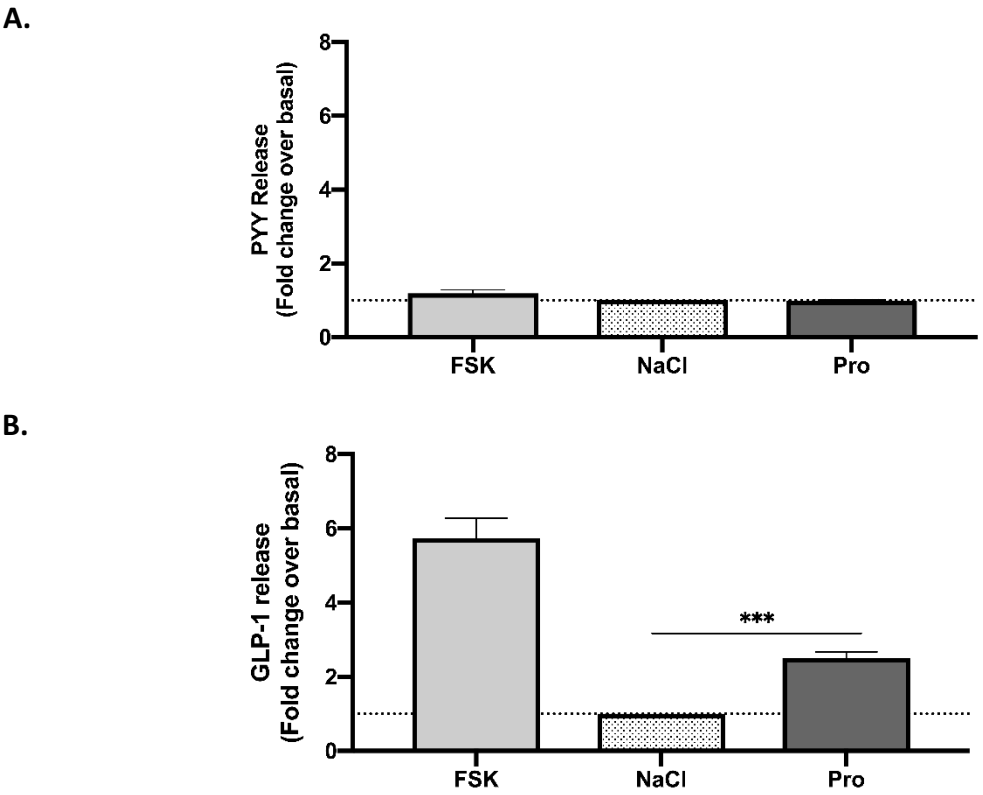
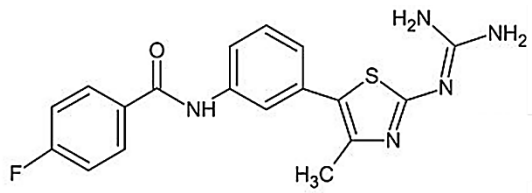


Figure 6.1 Propionate stimulates GLP-1 release from STC-1 cells. STC-1 cells stimulated with forskolin (10 μM) and NaCl (1 mM) or propionate (Pro, 1 mM) for 2 hours. PYY (A) and GLP-1 (B) content of media and cells was determined by RIA. PYY and GLP-1 secretion is expressed as fold change over NaCl secretion Data are expressed as mean ± SEM, n=3; t-test: *** $p<0.001$ vs NaCl.

The role of $G\alpha_i$ and $G\alpha_{q/11}$ signalling in mediating the ability of propionate to stimulate GLP-1 secretion was next assessed. The involvement of $G\alpha_i$ signalling was first examined. STC-1 cells were pre-treated with and without Ptx prior to stimulation with either forskolin (10 μM) or NaCl, propionate (1 mM), Cmp1, or AZ1729 (AZ), a $G\alpha_i$ -FFA2 biased compound used as a positive control for $G\alpha_i$ dependence. In control cells, there was a ~1.5-fold increase in GLP-1 release mediated by propionate compared to NaCl as seen above and Cmp1 induced a ~5-fold increase. The AZ compound also stimulated the GLP-1 release but to a lesser degree than propionate (Figure 6.2 A). In the presence of Ptx, there were no significant effects on forskolin induced release of GLP-1 in the presence of Ptx. However, propionate, Cmp1 and AZ induced GLP-1 release was significantly impaired. (Figure 6.2 A). This suggest that propionate-, Cmp1-, and Az- mediated release of GLP-1 is dependent on $G\alpha_i$ signalling in STC-1 enteroendocrine cells.

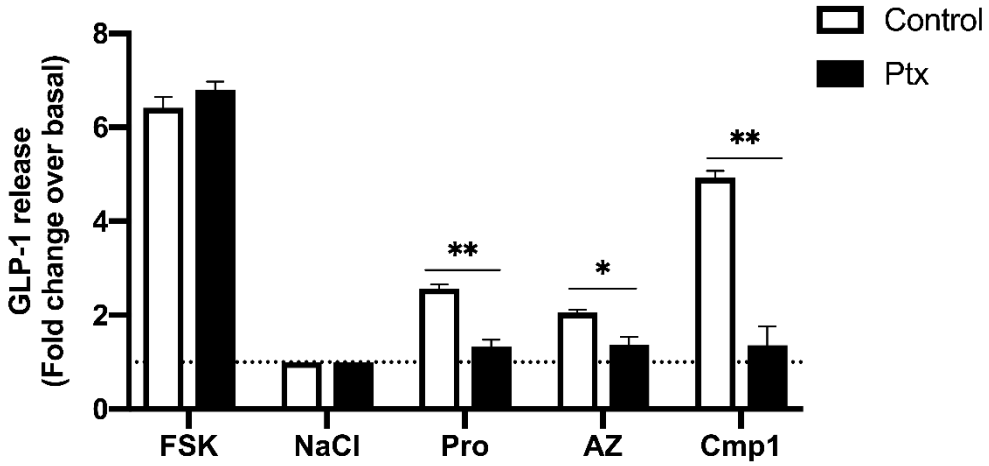
The involvement of $G\alpha_{q/11}$ signalling in mediating the ability of propionate to stimulate GLP-1 secretion was next examined. STC-1 cells were pre-treated with DMSO (vehicle) or YM-254890 (YM) prior to stimulation with either forskolin, NaCl, propionate or Cmp1. In cells pre-treated with YM, there was a slight but nonsignificant decrease of forskolin induced fold change of GLP-1. For propionate stimulated cells however, induced GLP-1 release was not attenuated in the presence of YM and were similar to cells pre-treated with DMSO. The Cmp1 induced GLP-1 release was significantly impaired in the presence of YM. This data demonstrates that $G\alpha_{q/11}$ signalling is not involved propionate mediated release of GLP-1 in STC-1 enteroendocrine cells and interestingly, Cmp1 induced GLP-1 release is mediated by both $G\alpha_i$ and $G\alpha_{q/11}$ signalling.

A.



AZ1729

B.



C.

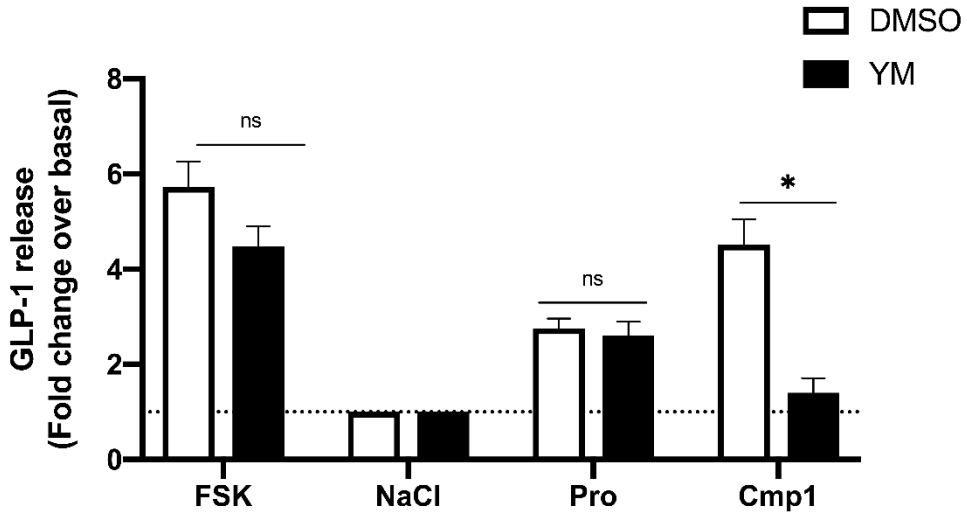


Figure 6.2 Propionate induced GLP-1 is dependent on Gαi and not Gαq/11. Chemical formula of AZ1729 is shown in (A), adapted from (Bolognini et al., 2016a). GLP-1 secretion measured in STC-1 cells pre-treated with pertussis toxin (Ptx, 200 ng/ml, 20 hours) (B) or $G\alpha_{q/11}$ inhibitor, YM-254890 (YM, 10 µM, 10 minutes) (C). (A) STC-1 cells were treated with or without Ptx (200 ng/ml, 20 hours) and subsequently stimulated with either forskolin (FSK, 10 µM), NaCl (1 mM), propionate (1 mM), DMSO, Compound 1 (Cmp1, 10 µM) or AZ1729 (AZ, 10 µM) for 2 hours. (B) STC-1 cells were treated with DMSO (vehicle) or YM (10 µM, 10 minutes) and subsequently stimulated with either forskolin (FSK, 10 µM), NaCl (1 mM), propionate (1 mM), DMSO, Compound 1 (Cmp1, 10 µM) or AZ1729 (Az, 10 µM) for 2 hours. GLP-1 content of media and cells was determined by RIA. Total GLP-1 secretion is expressed as fold change over NaCl secretion. Data are expressed as mean ± SEM, n=3; t-test: * $p<0.05$, ** $p<0.01$ versus control (A) or DMSO (B).

6.2.2 Propionate induced GLP-1 release is dynamin dependent

In Chapter 4, I demonstrated that propionate $G\alpha_i$ signalling requires internalisation in STC-1 cells, I then sought out to determine if propionate induced GLP-1 release was also dependent on receptor internalisation. To examine this STC-1 cells were pre-treated with DMSO (vehicle) or Dyngo-4a (45 minutes) prior to stimulation with either forskolin, NaCl, propionate, AZ or Cmp1. In cells treated with Dyngo-4a, forskolin induced GLP-1 release was significantly reduced compared to DMSO pre-treated cells suggesting Dyngo-4a may be interfering with GLP-1 exocytosis machinery and/or dynamin may be required in the exocytosis machinery of GLP-1 (Figure 6.4 A). To avoid this, Dyngo-4a was co-incubated with forskolin, NaCl, propionate, AZ or Cmp1 for 5 minutes and then removed. The 5-minute timepoint mimics the acute inhibition of receptor internalisation when the dependence of internalisation for the inhibition of forskolin induced cAMP was measured. After Dyngo-4a was removed, forskolin, NaCl, propionate, AZ or Cmp1 was then re-added. In cells treated with Dyngo-4a for 5 minutes, forskolin levels were slightly reduced, in cells treated with propionate and Cmp1 however, there was a marked significant reduction of GLP-1 release compared to DMSO treated cells. Interestingly, a converse significant effect was observed for AZ where its induced GLP-1 release is increased in the presence of Dyngo-4a. This suggests that internalisation is required for both for propionate and Cmp1 to mediate GLP-1 release in enteroendocrine cells whereas restricting the receptor the plasma membrane may be needed for AZ to stimulate the release of GLP-1.

As the inhibition of receptor internalisation increased AZ induced GLP-1 release, it was verified if receptor restricted at the plasma membrane would enhance its ability to inhibit forskolin stimulated cAMP. In STC-1 cells, pre-treated with Dyngo-4A, propionate and Cmp1 mediated inhibition of forskolin stimulated cAMP was significantly impaired. The inhibition of the forskolin induced cAMP for AZ, however, was further enhanced in the presence of Dyngo-4a, similar to what was observed for the GLP-1 induced release. Taken together, this demonstrates differential spatial requirements for propionate and AZ is required for proper signalling.

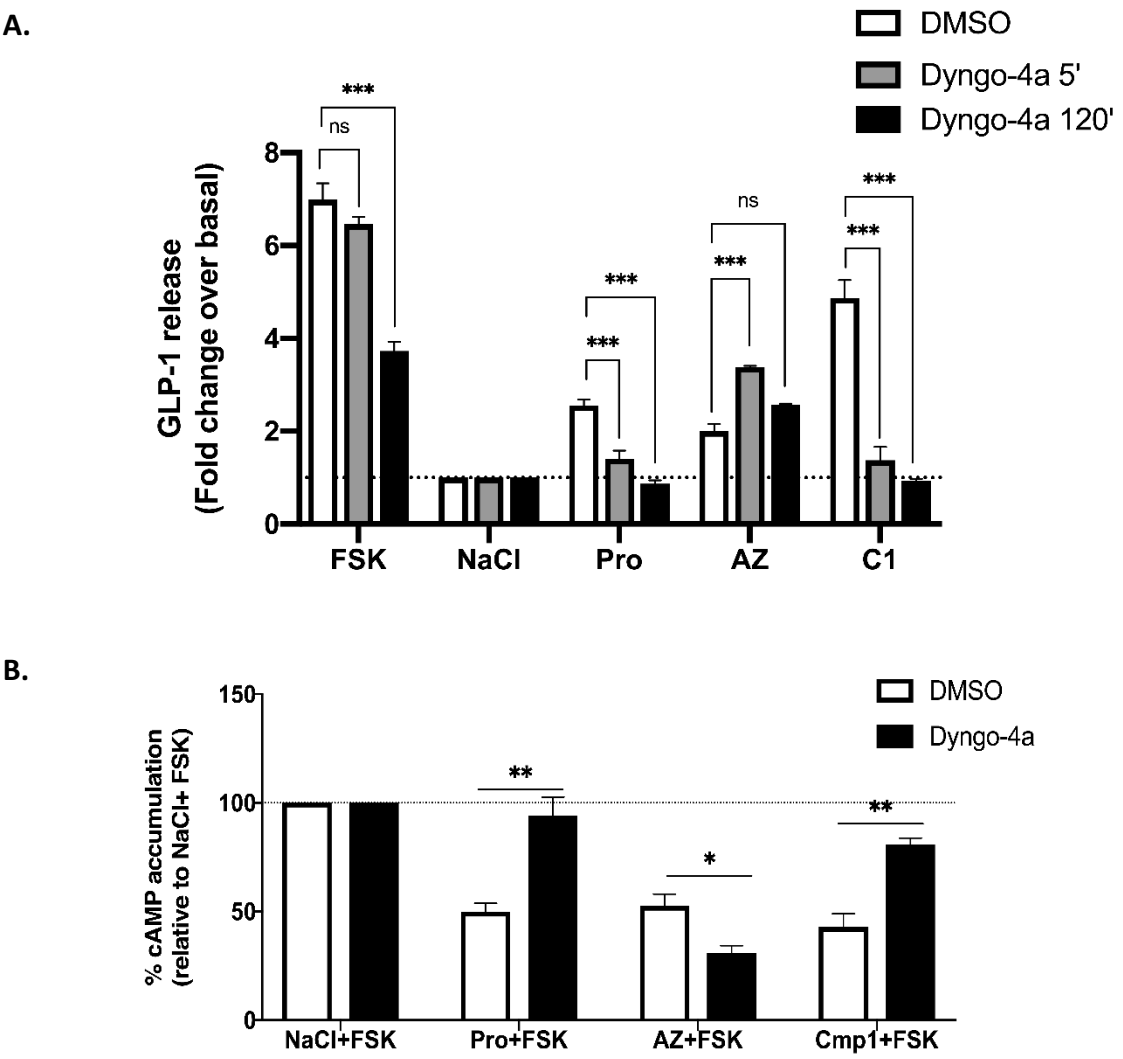


Figure 6.4 Propionate induced GLP-1 requires receptor internalisation. (A) GLP-1 secretion measured in STC-1 cells pre-treated with DMSO (vehicle) or Dyngo-4a (50 µM) for 45 minutes. Dyngo-4a was then co-incubated with either forskolin (10 µM), NaCl (1 mM), propionate (Pro, 1 mM) AZ1729 (AZ, 10 µM) or Cmp1 (10 µM) at two time points. The first for 5 minutes and then removed and the second for 2 hours and kept throughout the stimulation of period. GLP-1 content of media and cells was determined by RIA. Total GLP-1 secretion is expressed as fold change over NaCl secretion. Data are expressed as mean ± SEM, n=3. Two-way ANOVA: *** $p<0.001$. (B) Intracellular cAMP levels measured in STC-1 cells pre-treated with DMSO (vehicle) or Dyngo-4a (50 µM) for 45 minutes. Cells were then treated with IBMX (0.5 mM, 5 minutes) prior to treatment with forskolin (FSK, 3µM) or a combination of either NaCl (1mM), propionate (Pro, 1mM), Az (10 µM) or Cmp1 (10 µM). Data are expressed as percentage of NaCl+FSK and NaCl+FSK is expressed as 100%. Data are expressed as mean ± SEM, n=3; t-test: ** $p<0.01$, * $p<0.05$ vs DMSO.

6.2.3 Does APPL1 regulate propionate-induced GLP-1 secretion?

In Chapter 5 I demonstrated that in STC-1 cells depleted of APPL1, propionate exhibited enhanced $G\alpha_i$ signalling. Together with the above observation that $G\alpha_i$ regulates propionate-mediated GLP-1 release, I asked if whether an enhanced $G\alpha_i$ signalling via APPL1 knockdown can also enhance the propionate-mediated GLP-1 release. To this end, GLP-1 release was measured in STC-1 cells transfected with either scramble or APPL1 siRNA and then treated with forskolin or NaCl or propionate (1 mM). Preliminary data (n=1) suggest that APPL1 depletion had no effect on forskolin or propionate induced GLP-1 secretion. However, further analysis needs to be carried out.

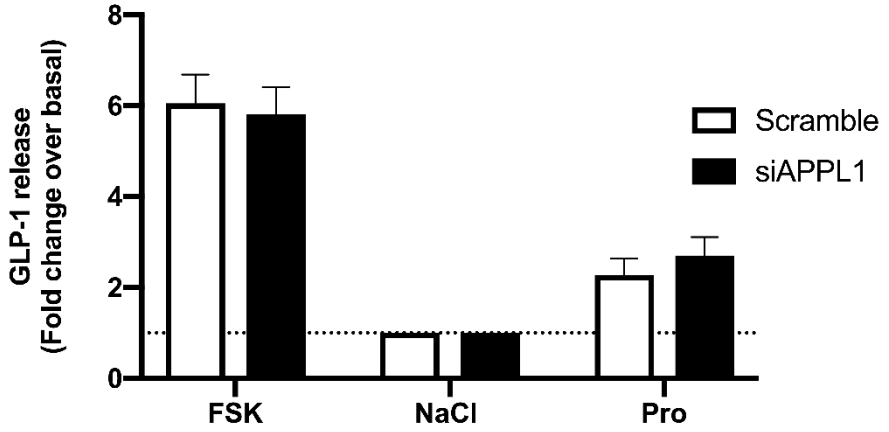


Figure 6.5 Effect of APPL1 depletion on propionate-induced GLP-1. GLP-1 secretion measured in STC-1 cells transfected with either siRNA scramble (scramble) or APPL1 SiRNA (SiAPPL1). Cells were then stimulated with forskolin (10 μM) and NaCl (1 mM) or propionate (Pro, 1 mM) for 2 hours. GLP-1 content of media and cells was determined by RIA. Total GLP-1 secretion is expressed as fold change over NaCl secretion. Data are expressed as mean ± SEM, n=1.

6.2.3 A phospho-kinase array reveals propionate induced p38 activation may require receptor internalisation

The above data demonstrates that propionate mediated GLP-1 release does not occur via $G\alpha_{q/11}$ and as propionate is unable to activate $G\alpha_{q/11}$ signalling both in STC-1 cells and colonic crypts and organoids (Chapter 3) but does require receptor internalisation to inhibit forskolin induced cAMP (Chapter 4). I then asked what other downstream signalling pathways does require propionate induced internalisation. To address this question, a phosphor-kinase array

was carried out in STC-1 cells that were pre-treated with either DMSO (vehicle) or Dyngo-4a (45 minutes) and stimulated at 5 and 30 minutes with NaCl or propionate (1 mM). The 5- and 30-minute time point was chosen to determine G-protein dependent (5 minute) and G-protein independent activation (30 minute). The resulting protein lysates were then used to probe phospho-kinase array membranes that detected 43 different phospho-kinases. Images of the blots are shown (Figure 6.6 A). Densitometry analysis and fold change over NaCl at each time point for each target at the 5- and 30- minutes time points were calculated (Figure 6.6 Bi and ii). A 1.5-fold ratio change was chosen as a cut-off to determine an increase in phosphorylation level (Figure 6.6 Bii, dotted line). In control cells, 16 of the 43 phospho-kinases were phosphorylated after 5 or 30 minutes of propionate stimulation. However, only p38α, EGF-R, MSK1/2 and Hck, were phosphorylated in a time dependent manner. In the presence of Dyngo-4a, the phosphorylation of these kinases was markedly dampened in a time dependent manner. In contrast, there was also a subset of kinases that were further upregulated in the presence of Dyngo-4A compared to DMSO treated cells, suggesting Dyngo-4a didn't not have a globally impact on the regulation of these kinases and that propionate may be required to remain at the plasma membrane to activate these kinases (Figure 6.6 Ci and ii). However, only the kinases that required propionate internalisation were analysed further.

A.

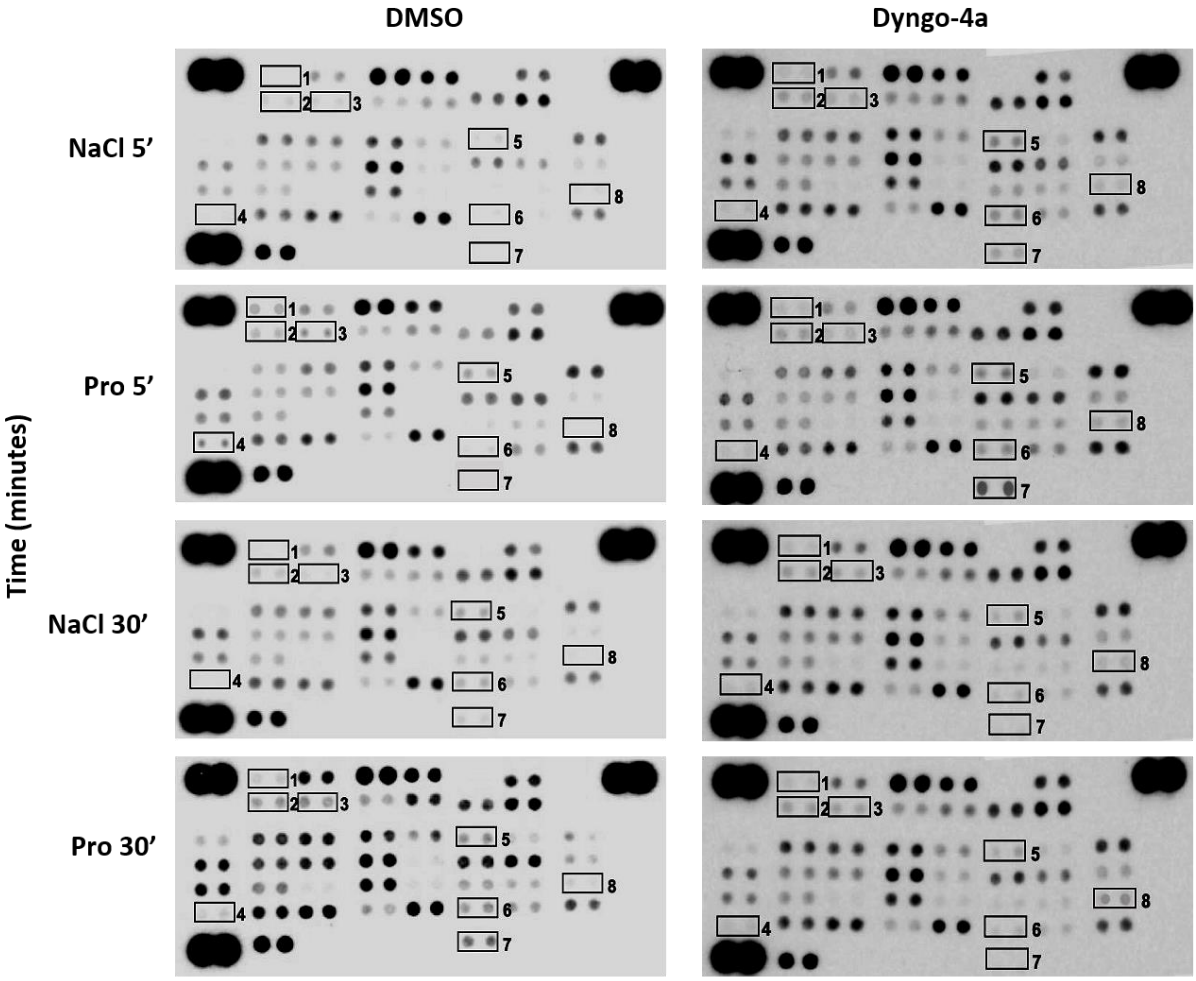


Figure 6.6 continued the following page

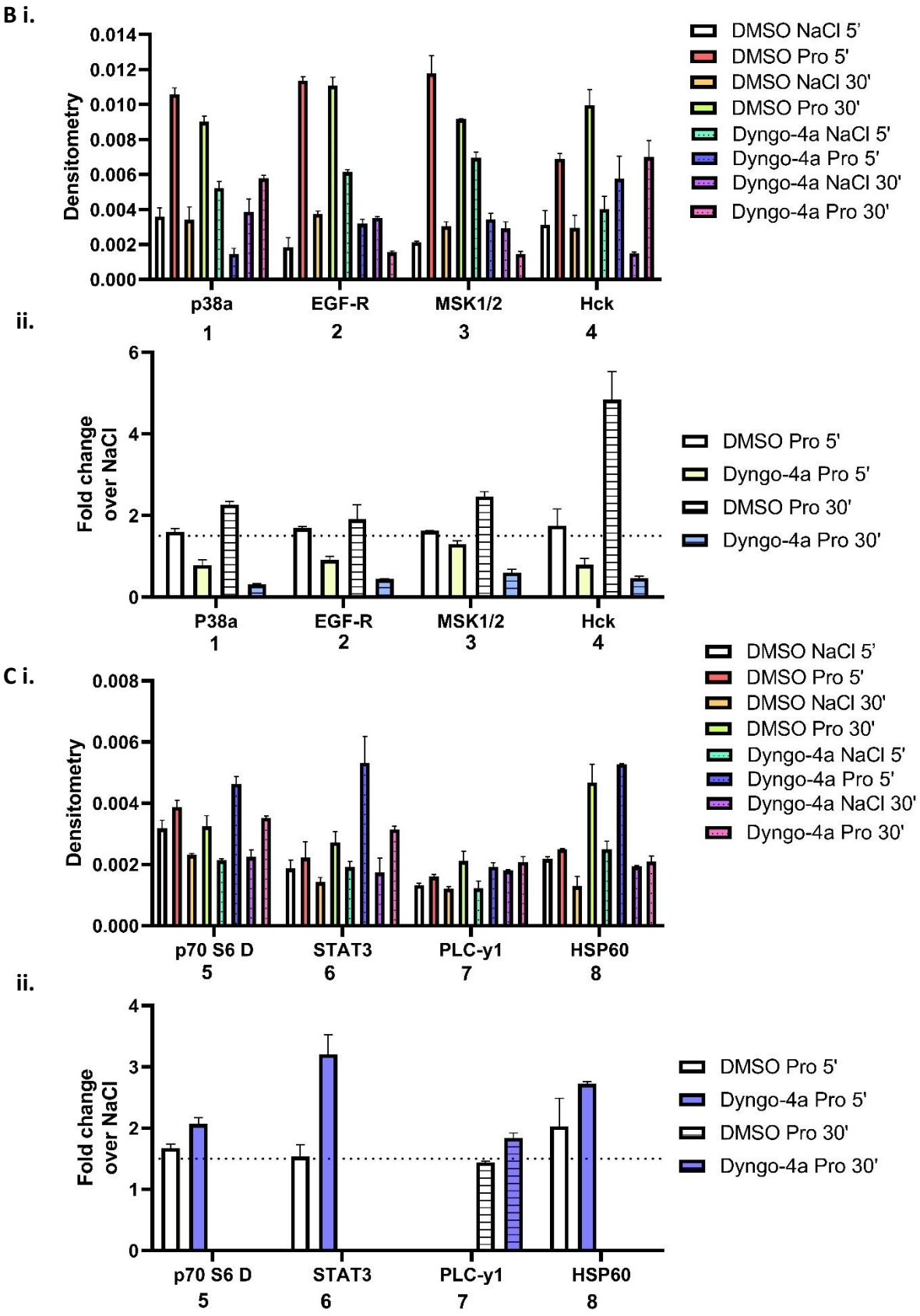


Figure 6.6 legend overleaf

Figure 6.6. Phospho-kinase array data reveals kinases that may require propionate induced internalisation in enteroendocrine cells. STC-1 cells were pre-treated with DMSO (vehicle) or Dyngo-4a (50 μM) for 45 minutes prior to stimulation with NaCl (1 mM) or propionate (Pro, 1 mM) at 5 and 30 minutes and subject to probing for activation of 43 different kinases with a phospho-kinase array kit. (A) Blots showing location of kinase antibodies spotted onto the array. Signals of relevant kinases in response to Dyngo-4a effects are indicated by numbers. (B & C) Bar graphs showing levels of phosphorylation that decreased (B) and increased (C) in the presence of Dyngo-4a. (Bi & Ci) Quantitation of mean spot pixel densities. (Bii & Cii) Fold changes over NaCl in levels of phosphorylation. Results are shown as mean ± SEM of densitometric or fold change values.

To corroborate the findings from the array, the activation of p38 was verified via Western blot. STC-1 cells were pre-treated with DMSO or Dyngo-4a (50 μM) for 45 minutes and then stimulated with NaCl or propionate (1 mM) for 5 and 30 minutes. Lysates were immunoblotted with a phospho-antibody recognising all four p38 isoforms (α, β, δ, γ). In cells pre-treated with DMSO, I observed a robust p38 activation across both time points following propionate stimulation as seen in the phosphokinase array. In cells pre-treated with Dyngo-4a however, levels of p38 induced by NaCl were markedly increased compared to DMSO treated cells. Thus, propionate induced internalisation for the activation of p38 cannot be determined and further experiments to verify increased in p38 basal levels in the presence of Dyngo-4a is required (Figure 6.7).

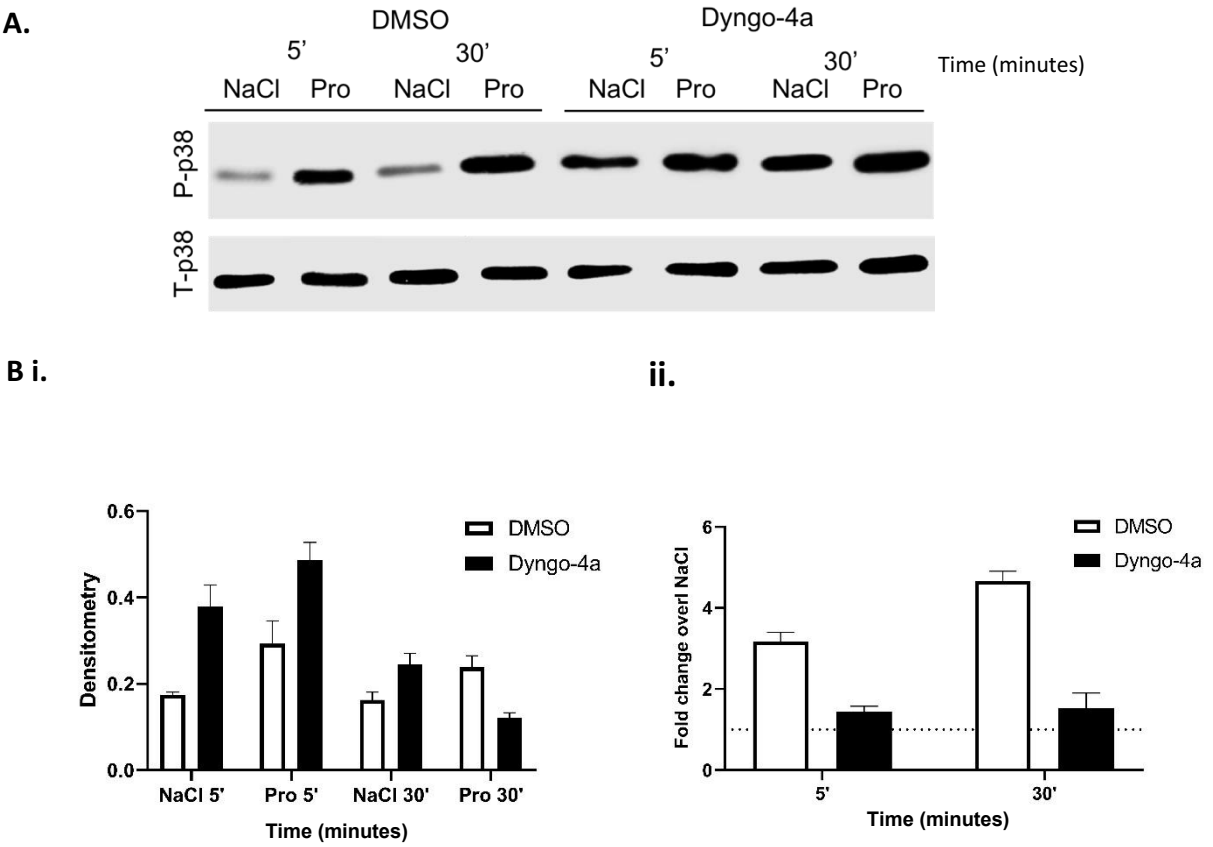


Figure 6.7 p38 activation may require propionate induced internalisation in enteroendocrine cells. (A) Representative Western blot showing phosphorylated p38 (P-p38) and total p38 (t-p38) of lysates from STC-1 cells prepared after pre-treatment with DMSO or Dyngo-4a (50 µM) for 45 minutes prior to addition of NaCl or propionate (Pro, 1 mM) at the indicated time points. Cell lysates were collected for Western blot analysis and probed for P-p38. Membranes were stripped and re-probed with t-p38 which was used as a loading control. (B i) Densitometry analysis of P-p38 normalised to total-p38 of lysates pre-treated with DMSO (white) and Dyngo-4a (black). (B ii) Fold change of densitometry analysis of P-p38 levels normalised to NaCl of DMSO or Dyngo-4a at each time point stimulation with total-p38. Data are expressed as mean ± SEM n=2.

It was next determined if propionate-mediated phosphorylation could be inhibited by the specific p38α/β inhibitor, SB 203580 via Western blot. STC-1 cells were pre-treated with DMSO (vehicle) or SB 203580 (5 µM) for 30 minutes before stimulation with NaCl or propionate (1 mM) at 5 and 30 minutes. Pre-treatment with SB 203580 prevented propionate-induced phosphorylation compared to cells pre-treated with DMSO (Figure 6.8 A and B).

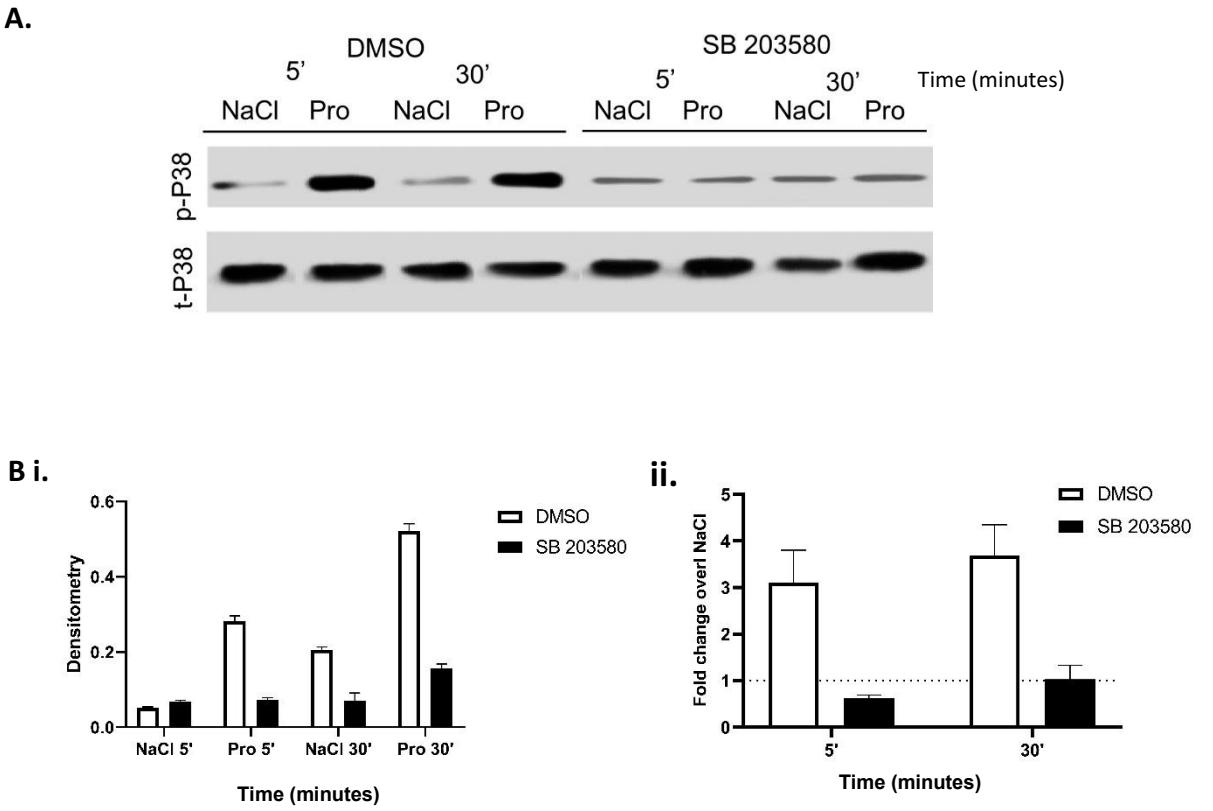


Figure 6.8 Propionate activates p38. (A) Representative Western blot showing phosphorylated p38 (P-p38) and total p38 (t-p38) of lysates from STC-1 cells demonstrating p38 inhibitor, SB 203580 reduces propionate-induced phosphorylation of p38. STC-1 cells were pre-treated with DMSO or SB 203580 (5 µM) for 30 minutes prior to stimulation of NaCl (1 mM) or propionate (Pro, 1 mM) at the indicated time points. Cell lysates were then collected for Western blot analysis and probed for P-p38. Membranes were stripped and re-probed with t-p38 which was used as a loading control. (B i) Densitometry analysis of P-p38 normalised to total-p38 of lysates pre-treated with DMSO (white) and SB 203580 (black). (B ii) Fold change of densitometry analysis of P-p38 levels normalised to NaCl of DMSO or SB 205380 at each time point stimulation with total-p38. Data are expressed as mean ± SEM n=2.

6.2.4 p38 does not regulate FFA2 recycling

In Chapter 5, I observed that APPL1-dependent FFA2 recycling was not mediated by PKA APPL1 phosphorylation, thus, I questioned if p38 could be involved in FFA2 recycling instead. To examine this, HEK 293 cells expressing SEP-FFA2 were pre-treated with DMSO or SB 203580, a prior to stimulation with NaCl or propionate (1 mM) and was imaged live by TIR-FM. Pre-treatment of SB 203580 did not attenuate FFA2 recycling and recycling events were similar to DMSO pre-treated cells (Figure 6.9 A).

As SEP-FFA2 recycling was not affected by SB 203580, I questioned if propionate-mediated phosphorylation could be inhibited by SB 203580 in HEK 293 expressing SEP-FFA2, as seen in STC-1 cells. HEK 293 cells expressing SEP-FFA2 expressing cells were pre-treated with DMSO (vehicle) or SB 203580 (5 µM) for 30 minutes before stimulation with NaCl or propionate (1 mM) at 5 and 30 minutes. Pre-treatment with SB 203580 slightly increased NaCl levels of p38, however SB 203580 prevented propionate-induced phosphorylation compared to cells pre-treated with DMSO (Figure 6.9 B and C).

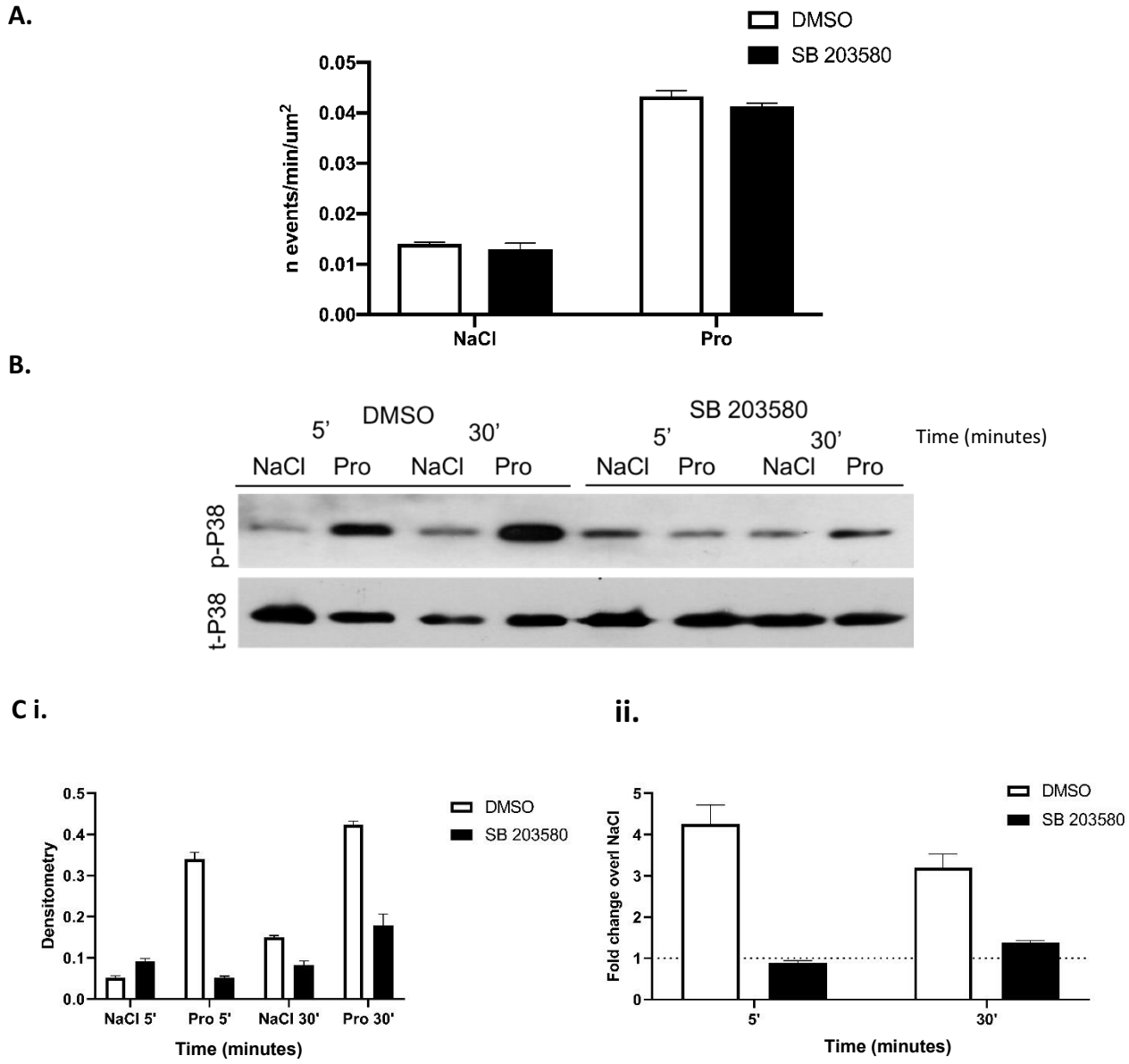


Figure 6.9 FFA2 recycling is not regulated by the phosphorylation of p38. (A) p38 inhibitor, SB 203580 does not attenuate FFA2 recycling. FFA2 recycling measured in real time by TIR-FM in HEK 293 cells

expressing SEP-FFA2 in the presence of propionate (Pro, 1 mM) following pre-treatment for 30 minutes with DMSO (vehicle) or SB 203580 (5 μM). Data are expressed as mean ± SEM, n=16 cells per condition. (B) Representative Western blot showing phosphorylated p38 (P-p38) and total p38 (t-p38) of lysates of HEK 293 cells expressing SEP-FFA2 demonstrating p38 inhibitor, SB 203580 reduces propionate-induced phosphorylation of p38. HEK 293 cells expressing SEP-FFA2 pre-treated with DMSO or SB 203580 (5 μM) for 30 minutes prior to stimulation of NaCl (1 mM) or propionate (Pro, 1 mM) at the indicated time points. Cell lysates were then collected for Western blot analysis and probed for P-p38. Membranes were stripped and re-probed with t-p38 which was used as a loading control. (B i) Densitometry analysis of P-p38 normalised to t-p38 of lysates pre-treated with DMSO (white) and SB 203580 (black). (B ii) Fold change of densitometry analysis of P-p38 levels normalised to NaCl of DMSO or SB 205380 at each time point stimulation with total-p38. Data are expressed as mean ± SEM n=2.

6.2.5 p38 may regulate propionate-induced GLP-1 release

The role of p38 in the regulation of propionate-mediated GLP-1 release was next assessed. In cells pre-treated with SB 203580, there was no significant effect on forskolin induced secretion of GLP-1. In cells stimulated with propionate however, there was a partial but significant reduction in GLP-1 release. Taken together, this demonstrates that P38 may regulate propionate-mediated GLP-1 release in enteroendocrine cells.

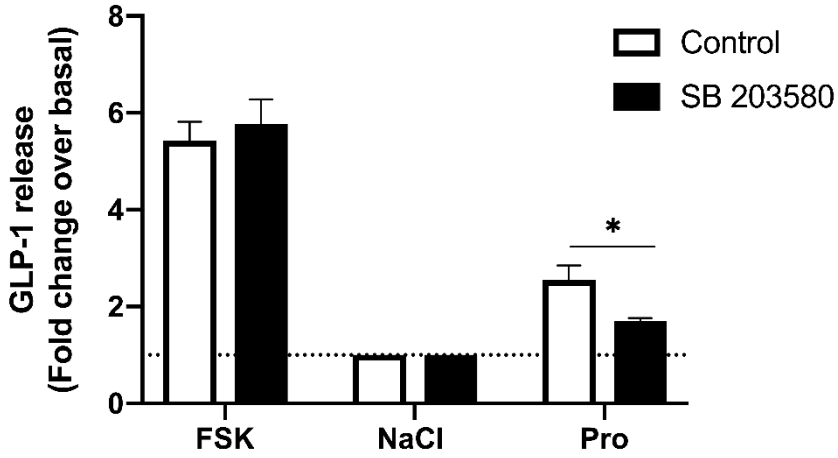


Figure 6.10 Propionate induced GLP-1 is partially regulated by p38 (B) p38 inhibitor, SB 203580 partially reduces propionate-mediated GLP-1 release. STC-1 cells were pre-treated with DMSO or SB 203580 (5 μM) for 30 minutes and added during stimulation with either forskolin (10 μM), NaCl (1 mM) or propionate (Pro, 1 mM) for 2 hours. GLP-1 content of media and cells was determined by RIA Total GLP-1 secretion is expressed a fold change over NaCl secretion. Data are expressed as mean ± SEM, n=3; t-test: * $p<0.05$ vs DMSO.

6.3 Discussion

In this chapter, I have demonstrated three main findings in understanding the mechanisms of propionate regulation of GLP-1 release: (1) propionate-mediated GLP-1 release involves $G\alpha_i$ signalling but not $G\alpha_{q/11}$; (2) receptor internalisation is a requirement of propionate-mediated GLP-1 release and (3) p38 is partially involved in propionate-mediated GLP-1 release.

To unravel the molecular mechanisms regulating propionate induced gut hormone release in enteroendocrine cells, it was first verified that propionate at 1 mM was able to stimulate the release of GLP-1 and PYY. Propionate was able to stimulate GLP-1, however PYY was undetectable in either the lysates or secretion samples. PYY was also undetected in cells treated with forskolin, an artificial elevator of cAMP, which is often used as a positive control for the release of GLP-1 and PYY as both GLP-1 and PYY secretion are enhanced by the activation of the PKA pathway (Drucker et al., 1987; Brubaker et al., 1998). Recent studies have also reported unable to detect PYY in STC-1 cells (Kuhre et al., 2016). Conversely, minor studies have reported measurable PYY storage in and secretion from STC-1 cells (Geraedts et al., 2009; Hand et al., 2013), though, the study conducted by Garaedts et al., 2009 reported that the measured levels were below, or at the lower end of detection of the assay. However, given quality controls samples containing PYY were within the standard curve range, undetectable PYY in the STC-1 cells may indicate more of a variability of PYY expression and secretion, rather than a limitation to the detection of PYY from this assay.

Although mounting evidence has demonstrated that FFA2 to be the main receptor responsible for the release of GLP-1 and PYY, the molecular mechanisms regulating FFA2 in the release of anorectic gut hormones are limited. To begin to understand the molecular mechanisms of FFA2 in the release of GLP-1 in enteroendocrine cells, the role of G-protein signalling was first examined. In STC-1 cells, propionate mediated GLP-1 release was impaired in the presence of Ptx indicating the role of $G\alpha_i$ in propionate-induced release of GLP-1. However, a number of studies did not find propionate-mediated GLP-1 release to be attenuated in the presence of Ptx (Tolhurst et al., 2012; Bolognini et al., 2016a), but the study by Tolhurst et al., 2012 observed that in mice colonic crypt cultures, though not significant, in the presence of Ptx, propionate-induced GLP-1 release was reduced. In addition, also in mice

colonic crypts, though not significant, propionate-induced GLP-1 release was found to be also reduced in the presence of Ptx (Psichas, 2013). Furthermore, the study by Bolognini et al., 2016 and Tolhurst et al., 2012 measured only the active form of GLP-1 secretion via an ELISA method, opposed to an RIA that measures total GLP-1 used in these experiments and in Psichas, 2013. Active or intact GLP-1 rapidly degrades and only accounts of 10-15% of the total GLP-1 secreted and therefore are in low concentrations (Holst, 2007). The measurement of total GLP-1 not only measures the active form of GLP-1 but also GLP-1 metabolites. Thus, measuring total GLP-1 may be a better indication of the overall secretory responses.

Evidence exploring the role of GLP-1 and $G\alpha_i$ seems to be limited and somewhat conflicting. The somatostatin hormone binds to the $G\alpha_i$ coupled-somatostatin receptors 1-5 to inhibit GLP-1 release in L cells via (Chisholm and Greenberg, 2002). In contrast, acetylcholine via the M1 and the $G\alpha_i$ coupled-M2 muscarinic receptor stimulates GLP-1 release in both human and murine L cells (Lim and Brubaker, 2006). However, both studies did not explore the direct involvement of $G\alpha_i$ signalling and the release of GLP-1. In contrast to the data presented in this chapter which shows a clear dependence of $G\alpha_i$ in the release of GLP-1. In addition to $G\alpha_i$ signalling, $G\alpha_i$ may directly be involved in the regulation the exocytosis of hormone secretion via $G\beta\gamma$. It has been well characterised that upon activation presynaptic $G\alpha_{i/o}$ coupled receptor, $G\beta\gamma$ can interact with certain members of the Soluble NSF Attachment Protein Receptor (SNARE) protein complexes that mediate vesicle fusion, for instance, Synataxin1A, which catalyses membrane fusion and exocytosis (Wells et al., 2012). Interestingly, Synatiaxin 1A, has been shown to important for the exocytosis release of GLP-1 in enteroendocrine L cells (Wheeler et al., 2017). Future work to elucidate if the $\beta\gamma$ subunits coupled to $G\alpha_i$ via FFA2 can also interact with such proteins would be pertinent.

The reported main mechanisms of GLP-1 secretion in enteroendocrine L cells are via membrane depolarisation and increased intracellular calcium concentrations exerted by nutrient sensors, however, my data indicates that $G\alpha_{q/11}$ signalling is not involved in propionate-mediated release of GLP-1. Although, it may be argued that propionate is unable to stimulate intracellular calcium mobilisation (Chapter 3) and thus the inhibition of $G\alpha_{q/11}$ signalling will not influence GLP-1 release, propionate's inability to induce an intracellular

calcium response represents an only acute signalling response. Intracellular signalling pathways are discretely activated but may converge to produce sophisticated cellular regulation.

To date, the only study that explores the role $G\alpha_{q/11}$ signalling in propionate-mediated GLP-1 release was conducted by Bolognini et al., 2016a. Propionate-mediated GLP-1 at 1 mM, in the presence of FR900359, another $G\alpha_{q/11}$ inhibitor, was significantly attenuated in colonic crypts (Bolognini et al., 2016a). However, a recent study demonstrated that FR900359 not only inhibits $G\alpha_{q/11}$-mediated signalling but also the $G\beta\gamma$-mediated signalling (Gao and Jacobson, 2016). Thus, FR900359 may not be an accurate indication of the involvement of $G\alpha_{q/11}$ signalling and is tempting to speculate that the reduced propionate-mediated GLP-1 release in the presence of FR900359 may also be partially regulated by $G\beta\gamma$. Interestingly, I find that the Cmp1-mediated GLP-1 responses were inhibited both by Ptx and YM, indicating the involvement of both Ga_i and $G\alpha_{q/11}$, however Cmp1 activates intracellular calcium mobilisation discretely via $G\alpha_{q/11}$ in STC-1 cells (Chapter 3). This further highlight that acute G protein signalling may be distinct from that of downstream signalling.

As propionate induced GLP-1 was not dependent on $G\alpha_{q/11}$ but required $G\alpha_i$ and receptor internalisation, a phosphokinase array was employed to determine what other downstream signalling pathways propionate could activate and required receptor internalisation. The phosphokinase array revealed a subset of kinases that were phosphorylated following propionate stimulation and required receptor internalisation. p38, one of the kinases that activation required propionate-induced internalisation was chosen to be further analysed as a validated p38 antibody as readily available. Propionate activation of p38 was found to partially regulate propionate-mediated GLP-1 release whereby the p38 inhibitor, SB 203580, propionate-mediated GLP-1 release was partially inhibited. The involvement of the p38 signalling pathway in regulating GLP-1 responses was also seen for the induced GLP-1 secretion by meat hydrolysate and essential amino acid and low molecular weight chitosan were inhibited by SB 203580 in the human NCI-H716 enteroendocrine cell line (Reimer, 2006; Liu et al., 2013). Further studies in mouse colonic crypts and organoids could directly assess the role of p38 in propionate-mediated GLP-1 release.

GPCRs recycling can be regulated by the phosphorylation of a variety of proteins, observing the propionate is able to active p38 in the STC-1 cells I sought out to determine if the phosphorylation of p38 regulates FFA2 recycling. FFA2 recycling was not regulated by p38, however preliminary data shows that, in addition to propionate activating p38 in STC-1 cells, propionate also activates p38 in SEP-FFA2 HEK 293 cells. Suggesting a potential role of FFA2 in the p38, however by which means is yet it be defined. Furthermore, my preliminary data demonstrates that propionate activates p38 and that its phosphorylation is dependent on propionate-induced internalisation. p38 signalling is known to be associated with inflammation and can regulate multiple responses such as expression of pro-inflammatory mediators, chemotaxis and leukocyte function. SCFAs via both FFA2 and FFA3 have been previously been shown to activate the p38 pathway in many cellular systems and have a role regulating inflammatory responses, although propionate-induced phosphorylation of p38 has not been directly related to inflammatory outcomes in these experiments. In mouse neutrophils, SCFAs activate p38 to regulate neutrophil migration in Ptx sensitive manner, indicating a role of $G\alpha_i$ (Vinolo et al., 2011). In human monocytes and MCF-7 breast cancer cells, SCFAs activates p38 via $G\alpha_{q/11}$ to attenuate cytokine expressions (Ang and Ding, 2016; Yonezawa et al., 2007). The heterodimerization of the human FFA2 and FFA3 also activates p38 signalling (Ang et al., 2018). Contrastingly, in mouse colon epithelial cells, both FFA2 and FFA3 were implicated in the inhibition of p38 and ERK1/2 phosphorylation to reduce colitis (Kim et al., 2013). Whether propionate in the colon activates p38 to exert pro- or anti-inflammatory actions, remains to be determined.

In addition to p38, the array also highlighted other pathways that required propionate-mediated internalisation such as EGFR, STAT5b and HCK. Due to limited time, these kinases weren't explored. EGFR may be of interest as the phosphorylation of EGFR is required for GLP-1 to prevent neural cell apoptosis in diabetic encephalopathy (Kimura et al., 2013b).

The role of APPL1 in the regulation of propionate-induced GLP-1 release was also explored, however preliminary data suggest that APPL1 may not have a role in propionate-induced GLP-1 release. This could be due to multiple reasons. First, efficiency of cellular depletion of APPL1 in the STC-1 cells was not as robust as what was observed of APPL1 depletion in HEK 293 cells

(Chapter 5), thus the role of APPL1 in propionate-induced GLP-1 release could not be fully assessed. To overcome this, APPL1 knockdown via Crispr/Cas9 system could be used in mice and colonic crypts and organoids could be isolated from these mice subsequently examine propionate-induced GLP-1 release. Secondly, APPL1 may have other roles in FFA2 regulation, such as promoting GLP-1 and PYY production, rather than a direct role in GLP-1 secretion. However, further analysis is warranted.

Receptor internalisation has been shown to be requisite not only for G protein signalling but also for important for downstream cellular functions (Thomsen et al., 2018) and here I have also demonstrated that propionate-induced internalisation is required for GLP-1 release in enteroendocrine cells. To my knowledge, this is the first report to demonstrate that receptor internalisation is required for propionate-mediated GLP-1 release in enteroendocrine cells. Additionally, I have also demonstrated that the AZ compound, in contrast to propionate, requires the receptor to be restricted to the plasma membrane to induced GLP-1 secretion. Initially, the AZ compound was employed to use as a tool to assess the role of $G\alpha_i$ in GLP-1 secretion by FFA2. However, the AZ compound induced GLP-1 secretion, compared to propionate was lower and only partially impaired with Ptx. In Bolognini et al., 2016a, the AZ compound was reported unable to stimulate the release of GLP-1 from colonic crypts. However, as only active form of GLP-1 was measured and the concentration of AZ that was used was at the half maximal dose, in contrast to these studies that used the full maximal dose. Strikingly, I found that in this study inhibition of receptor internalisation enhanced the ability of AZ to induce GLP-1 secretion. Thus, rather than the lack of GLP-1 secretion from its bias coupling to $G\alpha_i$ it was a receptor spatial requirement that regulated this compound's ability to stimulate GLP-1 release. Further, the inhibition of internalisation also enhanced AZ ability to inhibit forskolin induced cAMP, in contrast to propionate and Cmp1 which required receptor internalisation for proper signalling. This further highlights that this compound and propionate may exhibit 'location bias' in mediating GLP-1 secretion by FFA2.

Though, the use of Dyngo-4a identified the importance of receptor internalisation and GLP-1 secretion, caution must be taken when interpreting results from the usage of a pharmacological inhibitor of dynamin. Upon validation of p38 by Western blot in the presence of Dyngo-4a, unexpectedly, NaCl levels were markedly increased and propionate-induced

receptor internalisation as a requirement for p38 activation could not be determined. However, our lab has also previously observed an increased in basal levels of other kinases such as phospho-ERK in the presence of Dyngo-4a in HEK 293 cells (Jean-Alphonse et al., 2014). Increased basal levels of kinases in the presence of Dygno-4a may suggest off-targets effects of this compound, however, others have not reported an increase in basal levels of kinases in the presence of Dyngo-4a (Eichel et al., 2016). Additionally, a 2-hour co-incubation of Dyngo-4a markedly decrease forskolin induced GLP-1 release compared to the DMSO treated cells. There may be several reasons for this. Firstly, as previously mentioned in Chapter 4, the activation of certain adenylyl cyclases may require endocytosis that may be dynamin dependent for its activation. Secondly, dynamin proteins may be involved in the exocytosis machinery of GLP-1 release. Though currently there are no reported specific roles of dynamin involved in the exocytosis machinery of GLP-1 release, however dynamin has been reported to have a role in other hormone's secretion machinery. For example, dynamin 2 is involved in insulin granule exocytosis, whereby, cells expressing dominant-interfering dynamin mutant (Dyn/K44A) and Dynamin 2 siRNA resulted in inhibition of glucose-stimulated insulin secretion (Min et al., 2007). Furthermore, Dynamin 2 is also important for the secretory vesicle's formation from the Golgi apparatus and hormone release from neuroendocrine cells (Yang et al., 2001). However, Dyngo-4a is only reported to inhibit Dynamin 1 (McCluskey et al., 2013). Thirdly, dynamins have also been found in complexes of docking SNAREs, such as SNARE-interacting proteins and syntaxin (Arneson et al., 2008), the latter of which is known to be involved the exocytosis of GLP-1 in enteroendocrine L cells (Wheeler et al., 2017). Nonetheless, my data demonstrates that the acute inhibition of internalisation impaired propionate-mediated release of GLP-1 without effecting forskolin mediated GLP-1 release. Similarly, the acute inhibition of internalisation of the calcium sensing receptor (CaSR) impacts the second sustained wave of serum response element (SRF) gene activation (Gorvin et al., 2018). Mechanisms of forskolin activation of adenyl cyclase signalling and its dependence on dynamin or whether dynamin is also involved in GLP-1 secretion machinery warrants further characterisation.

In summary, the findings from this chapter have provided novel insights into the mechanisms regulating propionate-mediated GLP-1 release in enteroendocrine cells and further highlights

the role of receptor internalisation in control of not only spatiotemporal FFA2 signalling but also its contribution to the release of anorectic gut hormone release.

Chapter 7:

General discussion and future perspectives

The work carried out in this thesis has investigated the molecular mechanisms regulating SCFAs-induced release of anorectic gut hormones in enteroendocrine cells and has revealed novel trafficking properties of FFA2 that involve the novel endosomal compartment, VEE. The main findings of this thesis are: i) SCFAs are unable to induce $G\alpha_{q/11}$-mediated intracellular calcium mobilisation in the colon; ii) receptor internalisation is required for propionate-induced inhibition of forskolin-mediated cAMP and the release of GLP-1 in enteroendocrine cells; iii) FFA2 internalises into a novel endosomal compartment, the VEE, where it is able to elicit $G\alpha_i$ signalling that is negatively regulated by APPL1 and recycle back to the plasma membrane in an APPL1-dependent manner. Together, these findings strongly suggest that propionate's ability to stimulate the release of anorectic gut hormones, over the other SCFAs, requires the integration of membrane trafficking and endosomal signalling, this contributes towards an improved understanding of GPCR regulation and endosomal signalling for therapeutic implications.

SCFAs ability to induce $G\alpha_{q/11}$-mediated intracellular calcium mobilisation has been demonstrated in different cell lines that overexpress FFA2 (Bolognini et al., 2016a), as well as in primary cells that endogenously express FFA2 (Tolhurst et al., 2012), however the data presented here indicates that SCFAs both in an enteroendocrine cell line (STC-1) and in colonic crypts and organoids do not induce $G\alpha_{q/11}$-mediated intracellular calcium mobilisation (Figure 3.6). This was only specific to SCFAs as the FFA2 synthetic orthosteric ligand, Cmp1, and allosteric ligand, 4-CMTB, were able to elicit $G\alpha_{q/11}$-mediated intracellular calcium mobilisation (Figure 3.6 and 3.7). SCFAs inability to induce $G\alpha_{q/11}$-mediated intracellular calcium mobilisation is paradoxical to what is known for the signalling properties of FFA2, particularly for the secretion of GLP-1 and PYY in enteroendocrine L cells. The reported main mechanism for the secretion of GLP-1 and PYY from enteroendocrine L cells is induced by raised intracellular calcium levels. Calcium is released from intracellular stores following membrane depolarisation as a result of increased sodium-dependent cell excitability and calcium influx, thus leading to exocytosis of GLP-1 and PYY containing vesicles (Spreckley and Murphy, 2015). In addition, another second messenger that regulates secretion of GLP-1 and PYY is the increased levels of intracellular cAMP via $G\alpha_s$ (Reimann et al., 2006). In fact, for several hormones, that are secreted from endocrine cells, such as insulin, increased cAMP

levels and calcium plays pivotal roles in hormone exocytosis. Accordingly, nutrient sensing GPCRs, such as CaSR, and non-nutrient sensing receptors, such as bile acid receptor TGR5, that are able to stimulate the release of GLP-1 from enteroendocrine L cells have collectively proposed that the main mechanism responsible in stimulating the release of GLP-1 is via its ability to induce $G\alpha_{q/11}$-signalling or $G\alpha_s$-signalling, respectively (Covington et al., 2006; Bala et al., 2014). Additionally, for FFA1, both $G\alpha_{q/11}$– and $G\alpha_s$–signalling is required for its mediated GLP-1 release (Hauge et al., 2015). However, not every GPCR that regulates secretion of hormones require $G\alpha_{q/11}$–signalling or $G\alpha_s$–signalling to achieve this. For example, the pituitary adenylate cyclase-activated polypeptide receptor and GLP-1R both couple to $G\alpha_{q/11}$ and potentiates insulin secretion from mice pancreatic β-cells but does not require $G\alpha_{q/11}$–signalling to do so as secretion of insulin was not modulated in mice that lacked both $G\alpha_q$ and $G\alpha_{11}$ (Sassmann et al., 2010). For FFA4, the secretion of ghrelin was mediated by $G\alpha_i$ as Ptx impaired its ghrelin secretion (Engelstoft et al., 2013), suggesting hormone secretion is not limited to $G\alpha_{q/11}$– or $G\alpha_s$–signalling. As my data indicates that SCFAs are unable to induce $G\alpha_{q/11}$-mediated intracellular calcium mobilisation and the specific $G\alpha_{q/11}$ inhibitor, YM-254890, did not modulate propionate induced GLP-1 release in STC-1 cells but is inhibited by Ptx (Figure 6.3), suggests that SCFAs regulates the release of GLP-1 via a $G\alpha_i$ specific mechanism and is not dependent on release of intracellular calcium by propionate. Though calcium-independent exocytosis for the release of GLP-1 have not been reported, there has been reports for insulin secretion that typically requires calcium-dependent exocytosis for its secretion can also be secreted via a calcium-independent exocytosis. In pancreatic β-cells, glucose stimulated the release of insulin, without changes in intracellular calcium levels (Wollheim et al., 1987; Sato et al., 1998; Komatsu et al., 1995).

Though FFA2 has been the main receptor implicated for propionate-induced GLP-1 and PYY secretion from enteroendocrine L cells (Tolhurst et al., 2012; Bolognini et al., 2016a; Psichas et al., 2015; Brooks et al., 2017), due to the fact that FFA3 is also expressed in these cells within the GI tract, and in the models used in this thesis (Figure 3.1), the likeliness of propionate signalling via FFA3 in addition to FFA2 in STC-1 cells and in colonic crypts and organoids cannot be excluded. Thus, propionate binding to FFA3 and hindering its ability to induce $G\alpha_{q/11}$-mediated intracellular calcium mobilisation is highly plausible. Though I have

demonstrated that the suppression of FFA3 in the STC-1 cells via RNA interference did not reverse the inability of propionate to activate $G\alpha_{q/11}$ signalling (Figures 3.7), RNA interference of FFA3 may not have completely abolished its protein levels (Figure 3.6). Therefore, any low levels of FFA3 may still hamper propionate-mediated $G\alpha_{q/11}$ signalling. To clarify this, a FFA3 knockout in STC-1 cells via CRISPR/Cas9 and colonic crypts and organoids generated from these FFA3 knockout mice will be useful to decipher if indeed propionate does activate FFA3 as well as FFA2. However, caution must be taken when interpreting results from receptor knockout models, particularly for FFA2 and FFA3. FFA2 and FFA3 not only share a relatively high sequence identify of 43%, but in mouse are also are tandemly located adjacent to each other on chromosome 7 (Bjursell et al., 2011; Bolognini et al., 2016b). Thus, by modifying the transcript for one gene may affect the transcription of the other. In addition, the pharmacology may also be affected through the loss of the other receptor through redundancy and functional compensation. Two groups have indeed reported altered receptor expressions, in FFA3 knockout models, FFA2 is down-regulated (Zaibi et al., 2010), whereas in FFA2 knockout models, FFA3 is upregulated (Bjursell et al., 2011).

Alternatively, FFA2 may be forming a heterocomplex with FFA3, thus altering FFA2 signalling capacity. To examine heterodimerisation, a preliminary approach to use could be BRET experiments to identify whether FFA2 and FFA3 interact in STC-1 cells. To visualise receptor interaction at a single molecule level with high spatiotemporal resolution, optical methods such as single-molecule imaging via TIR-FM can also be carried out (Jonas et al., 2015; Calebiro and Sungkaworn, 2018). If FFA2 and FFA3 does indeed engage in a heteroreceptor complex, its functional significance in enteroendocrine cells should be determined. One approach to assess the importance of receptor heterodimerisation is via transmembrane (TM) interfering peptides to disrupt receptor heteromers specifically without affecting individual receptor function. TM interfering peptides are modelled on transmembrane domains of GPCRs that form the dimer interface and either restrain the formation of the heterocomplex or modulate the conformations within complexes, without effecting homomers of either receptor (Satake et al., 2013). This approach has been employed successfully for several GPCR heteromers such as the adenosine A_{2A} receptor (A_{2A}) and the dopamine D2 receptor (D2) heteromer, whereby the destabilisation of the A_{2A}-D2 heteromer by a disruption peptide impaired significant A_{2A}-D2 functions such as the A_{2A} -mediated inhibition of D2-induced depression of striatal

neuronal firing in striatal neurons (Azdad et al., 2009). Additionally, as there are numerous nutrient and non-nutrient receptors expressed in enteroendocrine cells, receptor crosstalk between FFA2 and other receptors is also possible and should be considered.

The evidence that propionate-induced secretion of GLP-1 was $G\alpha_i$-mediated led to the investigation of possible mechanisms regulating this, especially as all SCFAs could activate this G protein pathway. Therein, the basic trafficking properties of FFA2 was investigated and revealed intriguing trafficking properties that has not been reported for FFA2 before. FFA2 undergoes dynamin dependent, but β-arrestin-independent, constitutive internalisation, but does not enter the recycling pathway. In contrast, ligand-induced internalisation was both dynamin and β-arrestin-dependent (Figure 4.2) and internalised into VEE endosomes where it required APPL1 to recycle back to the plasma membrane (Figure 5.3 and 5.4). However, what remains to be clarified are the mechanisms regulating these distinct internalisation and post-endocytic sorting pathways for constitutive and ligand-induced FFA2 trafficking. To address these, specific molecular interactions and localisation of endogenous proteins could be identified via a proximity-dependent labelling approach combined with quantitative mass spectrometry-based proteomics. Using engineered ascorbic acid peroxidise (APEX) tags that binds with high affinity and in a rapid manner (< 1 minute), biotinylated proteins of interest and quantitative proteomics can uncover intricate details of not only GPCR signalling complexes but also specific localised interactions that are both time- and organelle-specific, while achieving high temporal and spatial resolution (Paek et al., 2017; Lobingier et al., 2017). This approach could be used to understand the mechanisms of FFA2 constitutive internalisation versus ligand induced in addition to the mechanisms regulating FFA2-APPL1 dependent recycling, as no specific recycling sequence/protein partner has been identified for FFA2.

The importance of receptor internalisation was highlighted when the inhibition of internalisation impaired propionate's ability to inhibit forskolin induced cAMP (Figure 4.5) and, more significantly, propionate's ability to stimulate the release of GLP-1 (Figure 6.3), indicating that receptor internalisation is a requirement for propionate to functionally fulfil its properties. Currently in our laboratory we are identifying if internalisation is also required for anorectic gut hormone release in colonic crypts and organoids. If internalisation is indeed

required for propionate-induced anorectic gut hormone this will not only shed light on the mechanistic requirements of propionate to stimulate the release of anorectic gut hormones but may also pave the way for the development of therapeutics specialised to enhance internalisation and thus promote propionate-induced GLP-1 secretion. For example, the utilisation of cholesterol-conjugated antagonist that accumulates in the lumen of endosomal compartments selectively blocked endosomal signalling of the neurokinin 1 receptor and calcitonin-gene related receptor has been reported to be an effective nociceptive treatment in animal models (Jensen et al., 2017; Yarwood et al., 2017). Similarly, a cholesterol-conjugated antagonist of PAR-2 prevented sustained hyperexcitability of nociceptors in the colon and thus has been proposed to be viable target for the treatment of IBS pain (Jimenez-Vargas et al., 2018). Therefore, a similar approach can be applied for propionate, whereby propionate is conjugated to cholesterol which enhances the tethering of propionate to the membranes of endosomal compartments and thus directly activate FFA2 and/or FFA3 to stimulate the release of GLP-1. Currently, for propionate-induced GLP-1 secretion, the exact receptor (FFA2 or FFA3) for which internalisation is required needs to be defined and the FFA3 Crispr/Cas9 KO models will also be beneficial to clarify this.

As internalisation is a critical aspect for propionate-induced signalling it was important to identify the localisation of propionate endosomal signalling. FFA2 internalises into the VEE endosomal compartment with some that are positive for APPL1, and within APPL1 endosomes FFA2-$G\alpha_i$ mediated inhibition of forskolin induced cAMP is negatively regulated (Figure 5.7). APPL1 is known to negatively regulate $G\alpha_s$-coupled receptors, LHR, FSHR and β1AR endosomal signalling (Sposini et al., 2017), thus this is the first report of APPL1 able to also negatively regulate a $G\alpha_i$-coupled receptor endosomal signalling. What is rather intriguing is the ability of APPL1 to regulate G protein signalling of such diverse GPCRs and may suggest that distinct microdomains exists that function to specifically regulate distinct G-protein signalling within this endosomal compartment. Although heterogeneity within endosomes is known (Bowman et al., 2016), distinct microdomains within the VEE have yet to be defined. If such distinct microdomains does indeed exist within APPL1-positive endosomes or the VEEs, it will add new depth to spatial regulation of GPCR endosomal signalling. This will not only allow the differentiation of signalling from the plasma membrane

and endosome but also between different endosomal compartments, for example, EE and VEEs, where different signalling pathways of different GPCRs can be activated, and possibly at different magnitudes. To characterise this, mini-G proteins or nanobody biosensors that recognise the activated form of different G proteins ($G\alpha_i$, $G\alpha_s$, $G\alpha_q$) can be used with super-resolution microscopy techniques such as photoactivated localisation microscopy (PALM) and structured illumination microscopy (SIM) to visualise the spatial organisation and localisation or even co-localisation of each G protein. In addition to endosomal G protein signalling, it will be interesting to see if APPL1 is also able to act as a scaffold for β-arrestin-mediated endosomal signalling or other endosomal signalling pathways such as p38. Another role that can be attributed to the APPL1 endosomes are that they may function as a molecular switch that can regulate both trafficking and signalling. As I demonstrate that APPL1 is important for FFA2 recycling (Figure 5.4) and also negativity regulates FFA2-$G\alpha_i$ mediated signalling, I propose that APPL1 acts as a switch to switch off FFA2 endosomal signalling to allow it to recycle back to the plasma membrane. Such a regulatory mechanism of terminating G protein endosomal signalling has been demonstrated with the retromer complex of the ASRT domains, which terminates sustained cAMP signalling of the internalised PTHRs (Feinstein et al., 2011).

While the applications of these methods will most certainly provide a more in-depth understanding of the molecular mechanisms regulating propionate-induced GLP-1 secretion, fundamental questions regarding FFA2 pharmacology remain to be clarified and how the aforementioned proposed models can contribute to development of propionate as an efficient therapeutic to stimulate the release of GLP-1. An approach that will greatly provide a more comprehensive understanding of the intricate details into the complex pharmacology of FFA2 is a crystal structure. Currently, the only structural information available for FFA2 is from a model based on the recently published crystal structure of FFA1, however as FFA2 shares low sequence identity to FFA1 (30%), the current FFA1-based homology model of FFA2 may not be accurate (Tikhonova, 2017), nonetheless, it has provided important insights of FFA2 pharmacology particularly for how FFA2 synthetic ligands may bind to FFA2 and activates its signalling pathway. 4-CMTB, a FFA2 synthetic allosteric ligand, binds to FFA2 in two modes, briefly through the orthosteric site and then induces a sustained activation through the allosteric site (Tikhonova, 2017). As for Cmp 1, a synthetic ligand that contains a

carboxylate moiety that is essential in the SCFAs to engage with the orthosteric binding site, the exact binding modes have not been fully elucidated, but it has been reported for the human FFA2 to interact with more residues in the transmembrane domains than SCFAs, thus, making Cmp 1 more potent than SCFAs (Hudson et al., 2013). From these models, it therefore may not be surprising that there was marked difference in the ability of synthetic ligands to elicit $G\alpha_{q/11}$-signalling compared to SCFAs in the colon. However, it is unknown if there are distinct FFA2 conformations amongst the individual specific SCFAs, which result in distinct trafficking or signalling properties. These signalling differences are an important factor to consider for the development of ligands for FFA2 and whether or not are there indications where a 'super agonist' might be the desired product over SCFAs or propionate specifically, despite the ability of both propionate and the synthetic ligands to elicit the stimulation of GLP-1. Additionally, any possible side effects of synthetic ligands is another important feature to consider. In fact, partial or biased agonists, agonists that activates the receptor but have only partial efficacy of a biological effect relative to full agonists or activates a specific pathway, are preferable over full agonist. As an example, A_1 adenosine receptor agonists are partial and have fewer side effects than full agonists for the treatment of cardiac arrhythmias (Szentmiklosi et al., 2015). In addition, PAMs may also be more preferential, as they can enhance orthosteric ligands such as propionate, without any intrinsic effect and therefore reduces chances of any adverse side effects.

Another fundamental aspect that a FFA2 crystal structure will help clarify is the dynamics of propionate association and dissociation to and from FFA2. Understanding the kinetics involved in ligand binding to the receptor is an important parameter for the development of therapeutics and one feature that has attracted a lot of attention is ligand residence time. There is a growing body of evidence that suggest an increase in residence time of an agonist bound to the receptor positively correlates with functional extended efficacy (Guo et al., 2012) and that optimising kinetics of agonist to achieve a sustained residence time could result in the improvement of sustained signalling by internalised receptors (Hothersall et al., 2016). However, there is also evidence where a shorter residency time may be preferred particularly for target-based toxicity (Hothersall et al., 2016), for instance, sustained signalling evoked by ergot agonist of the 5-hydroxytryptamine$_{2B}$ receptor leads to adverse effects associated with cardiac valvulopathic (Unett et al., 2013). Interestingly, it has been

demonstrated that the clinical applications of PTHR ligands are based on their residency time, with short-acting agonists having roles in osteoporosis and long-acting agonists are in involved hypoparathyroidism (Rosenblatt, 2009). As it is currently not known whether an increased or decreased duration of propionate residency time to FFA2 will provide any therapeutic benefits and that endosomal signalling is an important feature of propionate's downstream signalling, this makes propionate a viable target for further characterisation of its binding kinetics. The understanding of propionate binding kinetics can offer exciting opportunities to improve and prolong propionate efficacy not only for the regulation of food intake but may also beneficial for chronic weight management.

In overweight adults, acute administration of inulin-propionate ester, a modified form of propionate that selectively increases colonic propionate production, was able to reduce food intake and increase plasma concentrations of GLP-1 and PYY, however, chronic administration of inulin-propionate ester did not modulate levels of food intake or postprandial GLP-1 and PYY, suggesting a likely of downregulation of FFA2 or FFA3 (Chambers et al., 2015). Downregulation of GPCRs occur following continued or intermittent agonist treatment and remains a challenge for most drug discovery programs and hinders the advancement of efficient therapeutics. To overcome this, accumulating evidence has suggested a bias agonism approach (Rankovic et al., 2016) and therefore, I propose two models that targets APPL1 in an opposing manner due to its distinct roles in the VEE, either of which may improve propionate efficiency and minimise loss of receptor activity. First, overexpressing APPL1 in the colon could enhance sensitivity to FFA2 via increasing rates of FFA2 recycling and therefore promote the resensitisation of FFA2 for propionate to continue stimulating the release of GLP-1. Second, suppressing APPL1 in the colon to achieve an enhanced $G\alpha_i$ signalling and thereby increasing propionate-mediated stimulation of GLP-1 release. However, phenotypes of mice models lacking APPL1 in colon should first be characterised, as global suppression of APPL1 is associated with insulin resistance and hyperglycaemia in lean mice (Cheng et al., 2009) and glucose intolerance, impaired glucose-stimulated secretion, insulin resistance in diabetic and obese mice (Wang et al., 2013; Cheng et al., 2012). Although the suppression of APPL1 may decrease FFA2 recycling as proposed from the first model, this model selectively enhances $G\alpha_i$ signalling and in turn could also enhance FFA3 $G\alpha_i$ signalling which together with FFA2 could produce a pronounced secretion of GLP-1 via $G\alpha_i$ signalling.

If either of these approaches could improve chronic propionate treatment, then this may form the basis for a screening platform that could identify small molecules that could 'fine-tune' the regulation of propionate signalling from the VEE. Further, it is highly plausible that the ability of propionate to stimulate the release of GLP-1 from enteroendocrine cells is via both FFA2 and FFA3, and drug targets developed to mimic or enhance the properties of propionate, rather than deciphering the main receptor responsible, may be a more attractive approach.

In conclusion, the work presented in this thesis has uncovered important molecular mechanisms governing the regulation of propionate-induced release of GLP-1 from enteroendocrine cells and has revealed novel FFA2 trafficking properties that involves signalling from the VEE, which may, at least in part, shed light on the mechanistic requirements of propionate to fulfil its properties of stimulating the release of anorectic gut hormones from enteroendocrine cells in the colon (summarised in a proposed model, Figure 7.1). It has also contributed to an improved understanding of GPCR regulation and the therapeutic implications of endocytic trafficking; a system classically thought to terminate plasma membrane signalling and enable receptor resensitisation or downregulation, to a highly regulated complex system that incorporates trafficking and signalling not only between distinct endosomal compartments but also within microdomains of endomembranes to regulate specific cellular functions. The identification of the VEE and its ability to function both as a signalling and trafficking platform for a subset of GPCRs has attracted the interest to identify additional GPCRs that can signal from the VEE, as well other additional endosomal compartments that other GPCRs use. GPCRs represent the most important class of current drug targets, thus specific cellular outcomes achieved from GPCR endosomal signalling and the diversified endosomal compartment could pave ways for exciting new therapeutic opportunities. With the advancement of new technologies and tools, an emerging number of drug development programs have now shifted from a simple agonist/antagonist method in targeting drugs, to a more complex model that specifically targets a specific endosomal pathway for a more prolonged effect as well as reducing its adverse side effects.

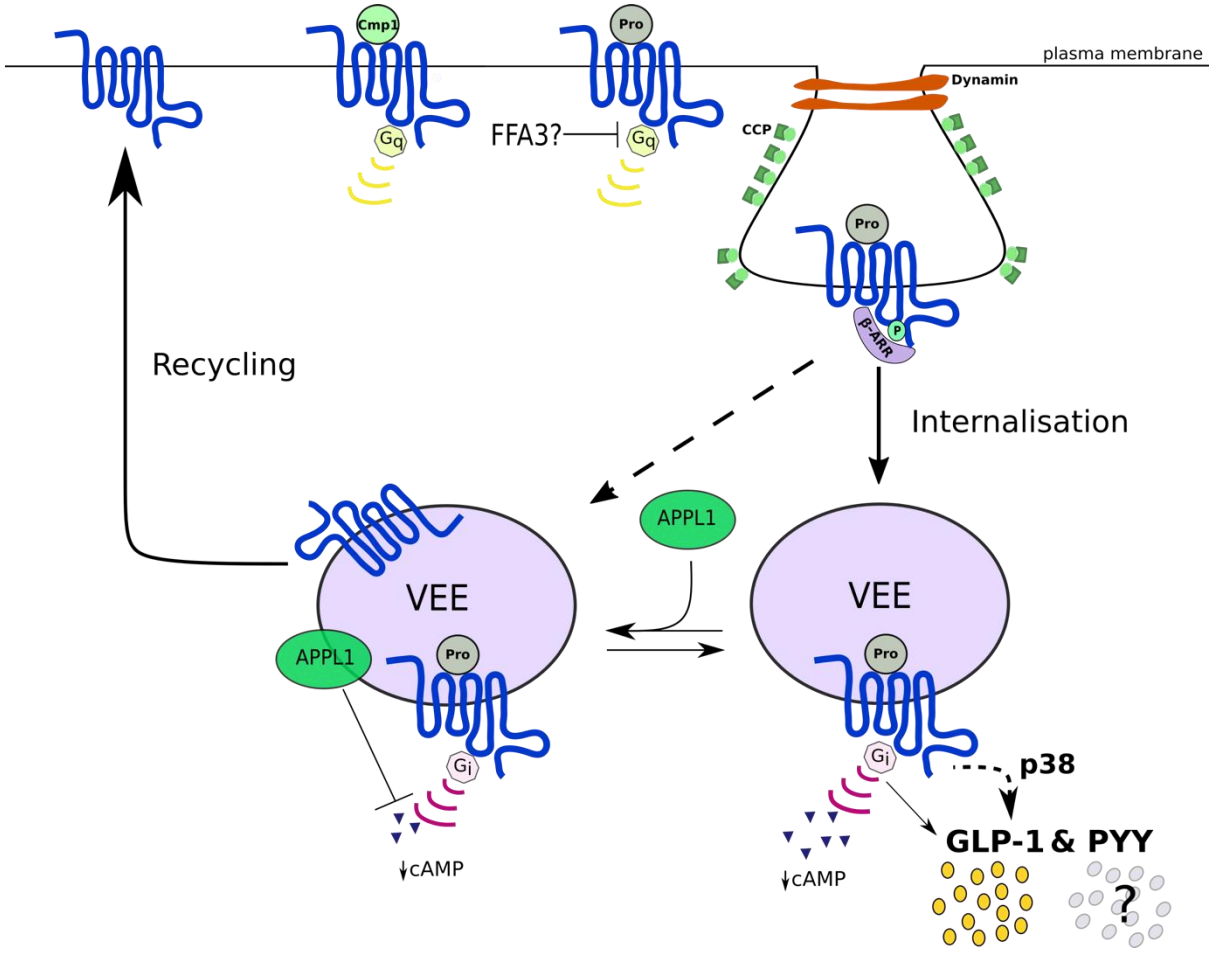


Figure 7.1 Proposed model for APPL1-dependent regulation of FFA2 endosomal signalling and the release of anorectic gut hormones in enteroendocrine cells. FFA2 at the plasma membrane activated by Cmp1 is able to signal via $G\alpha_{q/11}$ to induce intracellular calcium mobilisation but when activated by propionate, its $G\alpha_{q/11}$-induced calcium mobilisation may be hindered by the presence of FFA3 in the colon. Propionate then induces FFA2 internalisation into either an APPL1-negative VEE or APP1-positive VEEs (dotted line). From the VEE, FFA2 activates $G\alpha_i$-induced inhibition of forskolin mediated cAMP, triggering the release of GLP-1 that is partially regulated by p38 activation (dotted line). Within distinct microdomains of APPL1 of the VEE, FFA2 $G\alpha_i$-signalling is terminated via APPL1 negative regulation and FFA2 is recycled back to the plasma membrane.

References

ABBOTT, C. R., MONTEIRO, M., SMALL, C. J., SAJEDI, A., SMITH, K. L., PARKINSON, J. R., GHATEI, M. A. & BLOOM, S. R. 2005. The inhibitory effects of peripheral administration of peptide YY(3-36) and glucagon-like peptide-1 on food intake are attenuated by ablation of the vagal-brainstem-hypothalamic pathway. *Brain Res,* 1044**,** 127-31.

ADRIAN, T. E., FERRI, G. L., BACARESE-HAMILTON, A. J., FUESSL, H. S., POLAK, J. M. & BLOOM, S. R. 1985. Human distribution and release of a putative new gut hormone, peptide YY. *Gastroenterology,* 89**,** 1070-7.

AL TULAIHI, B. & ALHABIB, S. 2017. Uncertainties around incretin-based therapies: A literature review. *Saudi Pharm J,* 25**,** 1-7.

ALEX, S., LANGE, K., AMOLO, T., GRINSTEAD, J. S., HAAKONSSON, A. K., SZALOWSKA, E., KOPPEN, A., MUDDE, K., HAENEN, D., AL-LAHHAM, S., ROELOFSEN, H., HOUTMAN, R., VAN DER BURG, B., MANDRUP, S., BONVIN, A. M., KALKHOVEN, E., MULLER, M., HOOIVELD, G. J. & KERSTEN, S. 2013. Short-chain fatty acids stimulate angiopoietin-like 4 synthesis in human colon adenocarcinoma cells by activating peroxisome proliferator-activated receptor gamma. *Mol Cell Biol,* 33**,** 1303-16.

ALLEN, M. D., NEUMANN, S. & GERSHENGORN, M. C. 2011. Occupancy of both sites on the thyrotropin (TSH) receptor dimer is necessary for phosphoinositide signaling. *Faseb j,* 25**,** 3687-94.

ALONSO, V. & FRIEDMAN, P. A. 2013. Minireview: ubiquitination-regulated G protein-coupled receptor signaling and trafficking. *Mol Endocrinol,* 27**,** 558-72.

ALVAREZ, S. E., HARIKUMAR, K. B., HAIT, N. C., ALLEGOOD, J., STRUB, G. M., KIM, E. Y., MACEYKA, M., JIANG, H., LUO, C., KORDULA, T., MILSTIEN, S. & SPIEGEL, S. 2010. Sphingosine-1-phosphate is a missing cofactor for the E3 ubiquitin ligase TRAF2. *Nature,* 465**,** 1084-8.

AMANO, M., NAKAYAMA, M. & KAIBUCHI, K. 2010. Rho-kinase/ROCK: A key regulator of the cytoskeleton and cell polarity. *Cytoskeleton (Hoboken),* 67**,** 545-54.

ANG, Z. & DING, J. L. 2016. GPR41 and GPR43 in Obesity and Inflammation - Protective or Causative? *Front Immunol,* 7**,** 28.

ANG, Z., XIONG, D., WU, M. & DING, J. L. 2018. FFAR2-FFAR3 receptor heteromerization modulates short-chain fatty acid sensing. *Faseb j,* 32**,** 289-303.

ANGERS, S., SALAHPOUR, A. & BOUVIER, M. 2002. Dimerization: an emerging concept for G protein-coupled receptor ontogeny and function. *Annu Rev Pharmacol Toxicol,* 42**,** 409-35.

ANINI, Y. & BRUBAKER, P. L. 2003. Muscarinic receptors control glucagon-like peptide 1 secretion by human endocrine L cells. *Endocrinology,* 144**,** 3244-50.

ARNESON, L. N., SEGOVIS, C. M., GOMEZ, T. S., SCHOON, R. A., DICK, C. J., LOU, Z., BILLADEAU, D. D. & LEIBSON, P. J. 2008. Dynamin 2 regulates granule exocytosis during NK cell-mediated cytotoxicity. *Journal of Immunology,* 181**,** 6995-7001.

AUDET, N., CHARFI, I., MNIE-FILALI, O., AMRAEI, M., CHABOT-DORE, A. J., MILLECAMPS, M., STONE, L. S. & PINEYRO, G. 2012. Differential association of receptor-Gbetagamma complexes with beta-arrestin2 determines recycling bias and potential for tolerance of delta opioid receptor agonists. *J Neurosci,* 32**,** 4827-40.

AZDAD, K., GALL, D., WOODS, A. S., LEDENT, C., FERRE, S. & SCHIFFMANN, S. N. 2009. Dopamine D2 and adenosine A2A receptors regulate NMDA-mediated excitation in

accumbens neurons through A2A-D2 receptor heteromerization. *Neuropsychopharmacology,* 34**,** 972-86.

AZZI, M., CHAREST, P. G., ANGERS, S., ROUSSEAU, G., KOHOUT, T., BOUVIER, M. & PINEYRO, G. 2003. Beta-arrestin-mediated activation of MAPK by inverse agonists reveals distinct active conformations for G protein-coupled receptors. *Proc Natl Acad Sci U S A,* 100**,** 11406-11.

BACHE, K. G., RAIBORG, C., MEHLUM, A. & STENMARK, H. 2003. STAM and Hrs are subunits of a multivalent ubiquitin-binding complex on early endosomes. *J Biol Chem,* 278**,** 12513-21.

BAGGIO, L. L., HUANG, Q., BROWN, T. J. & DRUCKER, D. J. 2004. Oxyntomodulin and glucagon-like peptide-1 differentially regulate murine food intake and energy expenditure. *Gastroenterology,* 127**,** 546-58.

BAHOUTH, S. W. & NOOH, M. M. 2017. Barcoding of GPCR trafficking and signaling through the various trafficking roadmaps by compartmentalized signaling networks. *Cell Signal,* 36**,** 42-55.

BALA, V., RAJAGOPAL, S., KUMAR, D. P., NALLI, A. D., MAHAVADI, S., SANYAL, A. J., GRIDER, J. R. & MURTHY, K. S. 2014. Release of GLP-1 and PYY in response to the activation of G protein-coupled bile acid receptor TGR5 is mediated by Epac/PLC-epsilon pathway and modulated by endogenous H2S. *Front Physiol,* 5**,** 420.

BARNETT, B. P., HWANG, Y., TAYLOR, M. S., KIRCHNER, H., PFLUGER, P. T., BERNARD, V., LIN, Y. Y., BOWERS, E. M., MUKHERJEE, C., SONG, W. J., LONGO, P. A., LEAHY, D. J., HUSSAIN, M. A., TSCHOP, M. H., BOEKE, J. D. & COLE, P. A. 2010. Glucose and weight control in mice with a designed ghrelin O-acyltransferase inhibitor. *Science,* 330**,** 1689-92.

BARTLETT, S. E., ENQUIST, J., HOPF, F. W., LEE, J. H., GLADHER, F., KHARAZIA, V., WALDHOER, M., MAILLIARD, W. S., ARMSTRONG, R., BONCI, A. & WHISTLER, J. L. 2005. Dopamine responsiveness is regulated by targeted sorting of D2 receptors. *Proc Natl Acad Sci U S A,* 102**,** 11521-6.

BATTERHAM, R. L., COWLEY, M. A., SMALL, C. J., HERZOG, H., COHEN, M. A., DAKIN, C. L., WREN, A. M., BRYNES, A. E., LOW, M. J., GHATEI, M. A., CONE, R. D. & BLOOM, S. R. 2002. Gut hormone PYY(3-36) physiologically inhibits food intake. *Nature,* 418**,** 650-4.

BAUCH, C., KOLIWER, J., BUCK, F., HONCK, H. H. & KREIENKAMP, H. J. 2014. Subcellular sorting of the G-protein coupled mouse somatostatin receptor 5 by a network of PDZ-domain containing proteins. *PLoS One,* 9**,** e88529.

BEGLINGER, C., DEGEN, L., MATZINGER, D., D'AMATO, M. & DREWE, J. 2001. Loxiglumide, a CCK-A receptor antagonist, stimulates calorie intake and hunger feelings in humans. *Am J Physiol Regul Integr Comp Physiol,* 280**,** R1149-54.

BEHNIA, R. & MUNRO, S. 2005. Organelle identity and the signposts for membrane traffic. *Nature,* 438**,** 597-604.

BHATNAGAR, A., WILLINS, D. L., GRAY, J. A., WOODS, J., BENOVIC, J. L. & ROTH, B. L. 2001. The dynamin-dependent, arrestin-independent internalization of 5-hydroxytryptamine 2A (5-HT2A) serotonin receptors reveals differential sorting of arrestins and 5-HT2A receptors during endocytosis. *J Biol Chem,* 276**,** 8269-77.

BI, S. & MORAN, T. H. 2002. Actions of CCK in the controls of food intake and body weight: lessons from the CCK-A receptor deficient OLETF rat. *Neuropeptides,* 36**,** 171-81.

BJURSELL, M., ADMYRE, T., GORANSSON, M., MARLEY, A. E., SMITH, D. M., OSCARSSON, J. & BOHLOOLY, Y. M. 2011. Improved glucose control and reduced body fat mass in free fatty acid receptor 2-deficient mice fed a high-fat diet. *Am J Physiol Endocrinol Metab,* 300**,** E211-20.

BLOEMEN, J. G., OLDE DAMINK, S. W., VENEMA, K., BUURMAN, W. A., JALAN, R. & DEJONG, C. H. 2010. Short chain fatty acids exchange: Is the cirrhotic, dysfunctional liver still able to clear them? *Clin Nutr,* 29**,** 365-9.

BLOEMEN, J. G., VENEMA, K., VAN DE POLL, M. C., OLDE DAMINK, S. W., BUURMAN, W. A. & DEJONG, C. H. 2009. Short chain fatty acids exchange across the gut and liver in humans measured at surgery. *Clin Nutr,* 28**,** 657-61.

BLUNDELL, J., DE GRAAF, C., HULSHOF, T., JEBB, S., LIVINGSTONE, B., LLUCH, A., MELA, D., SALAH, S., SCHURING, E., VAN DER KNAAP, H. & WESTERTERP, M. 2010. Appetite control: methodological aspects of the evaluation of foods. *Obes Rev,* 11**,** 251-70.

BÖHME, I. & BECK-SICKINGER, A. G. 2009. Illuminating the life of GPCRs. *Cell communication and signaling : CCS,* 7**,** 16-16.

BOLOGNINI, D., MOSS, C. E., NILSSON, K., PETERSSON, A. U., DONNELLY, I., SERGEEV, E., KONIG, G. M., KOSTENIS, E., KUROWSKA-STOLARSKA, M., MILLER, A., DEKKER, N., TOBIN, A. B. & MILLIGAN, G. 2016a. A Novel Allosteric Activator of Free Fatty Acid 2 Receptor Displays Unique Gi-functional Bias. *J Biol Chem,* 291**,** 18915-31.

BOLOGNINI, D., TOBIN, A. B., MILLIGAN, G. & MOSS, C. E. 2016b. The Pharmacology and Function of Receptors for Short-Chain Fatty Acids. *Mol Pharmacol,* 89**,** 388-98.

BONIFACINO, J. S. & TRAUB, L. M. 2003. Signals for sorting of transmembrane proteins to endosomes and lysosomes. *Annu Rev Biochem,* 72**,** 395-447.

BORGSTROM, B. 1988. Mode of action of tetrahydrolipstatin: a derivative of the naturally occurring lipase inhibitor lipstatin. *Biochim Biophys Acta,* 962**,** 308-16.

BOUCROT, E., FERREIRA, A. P., ALMEIDA-SOUZA, L., DEBARD, S., VALLIS, Y., HOWARD, G., BERTOT, L., SAUVONNET, N. & MCMAHON, H. T. 2015. Endophilin marks and controls a clathrin-independent endocytic pathway. *Nature,* 517**,** 460-5.

BOUVIER, M., HAUSDORFF, W. P., DE BLASI, A., O'DOWD, B. F., KOBILKA, B. K., CARON, M. G. & LEFKOWITZ, R. J. 1988. Removal of phosphorylation sites from the beta 2-adrenergic receptor delays onset of agonist-promoted desensitization. *Nature,* 333**,** 370-3.

BOWMAN, S. L., SHIWARSKI, D. J. & PUTHENVEEDU, M. A. 2016. Distinct G protein-coupled receptor recycling pathways allow spatial control of downstream G protein signaling. *J Cell Biol,* 214**,** 797-806.

BOWMAN, S. L., SOOHOO, A. L., SHIWARSKI, D. J., SCHULZ, S., PRADHAN, A. A. & PUTHENVEEDU, M. A. 2015. Cell-autonomous regulation of Mu-opioid receptor recycling by substance P. *Cell Rep,* 10**,** 1925-36.

BRAY, G. A. & GREENWAY, F. L. 2007. Pharmacological treatment of the overweight patient. *Pharmacol Rev,* 59**,** 151-84.

BROOKS, L., VIARDOT, A., TSAKMAKI, A., STOLARCZYK, E., HOWARD, J. K., CANI, P. D., EVERARD, A., SLEETH, M. L., PSICHAS, A., ANASTASOVSKAJ, J., BELL, J. D., BELL-ANDERSON, K., MACKAY, C. R., GHATEI, M. A., BLOOM, S. R., FROST, G. & BEWICK, G. A. 2017. Fermentable carbohydrate stimulates FFAR2-dependent colonic PYY cell expansion to increase satiety. *Mol Metab,* 6**,** 48-60.

BROOM, I., WILDING, J., STOTT, P., MYERS, N. & GROUP, U. K. M. S. 2002. Randomised trial of the effect of orlistat on body weight and cardiovascular disease risk profile in obese patients: UK Multimorbidity Study. *Int J Clin Pract,* 56**,** 494-9.

BROUSSARD, J. A., LIN, W.-H., MAJUMDAR, D., ANDERSON, B., EASON, B., BROWN, C. M. & WEBB, D. J. 2012. The endosomal adaptor protein APPL1 impairs the turnover of leading edge adhesions to regulate cell migration. *Mol Biol Cell,* 23**,** 1486-1499.

BROWN, A. J., GOLDSWORTHY, S. M., BARNES, A. A., EILERT, M. M., TCHEANG, L., DANIELS, D., MUIR, A. I., WIGGLESWORTH, M. J., KINGHORN, I., FRASER, N. J., PIKE, N. B., STRUM, J. C., STEPLEWSKI, K. M., MURDOCK, P. R., HOLDER, J. C., MARSHALL, F. H., SZEKERES, P. G., WILSON, S., IGNAR, D. M., FOORD, S. M., WISE, A. & DOWELL, S. J. 2003. The Orphan G protein-coupled receptors GPR41 and GPR43 are activated by propionate and other short chain carboxylic acids. *J Biol Chem,* 278**,** 11312-9.

BRUBAKER, P. L., SCHLOOS, J. & DRUCKER, D. J. 1998. Regulation of glucagon-like peptide-1 synthesis and secretion in the GLUTag enteroendocrine cell line. *Endocrinology,* 139**,** 4108-14.

BUHMANN, H., LE ROUX, C. W. & BUETER, M. 2014. The gut-brain axis in obesity. *Best Pract Res Clin Gastroenterol,* 28**,** 559-71.

BURFORD, N. T., CLARK, M. J., WEHRMAN, T. S., GERRITZ, S. W., BANKS, M., O'CONNELL, J., TRAYNOR, J. R. & ALT, A. 2013. Discovery of positive allosteric modulators and silent allosteric modulators of the mu-opioid receptor. *Proc Natl Acad Sci U S A,* 110**,** 10830-5.

BUROKAS, A., MOLONEY, R. D., DINAN, T. G. & CRYAN, J. F. 2015. Microbiota regulation of the Mammalian gut-brain axis. *Adv Appl Microbiol,* 91**,** 1-62.

BUSE, J. B., ROSENSTOCK, J., SESTI, G., SCHMIDT, W. E., MONTANYA, E., BRETT, J. H., ZYCHMA, M. & BLONDE, L. 2009. Liraglutide once a day versus exenatide twice a day for type 2 diabetes: a 26-week randomised, parallel-group, multinational, open-label trial (LEAD-6). *Lancet,* 374**,** 39-47.

BUTCHER, A. J., PRIHANDOKO, R., KONG, K. C., MCWILLIAMS, P., EDWARDS, J. M., BOTTRILL, A., MISTRY, S. & TOBIN, A. B. 2011. Differential G-protein-coupled receptor phosphorylation provides evidence for a signaling bar code. *J Biol Chem,* 286**,** 11506-18.

CAHILL, T. J., 3RD, THOMSEN, A. R., TARRASCH, J. T., PLOUFFE, B., NGUYEN, A. H., YANG, F., HUANG, L. Y., KAHSAI, A. W., BASSONI, D. L., GAVINO, B. J., LAMERDIN, J. E., TRIEST, S., SHUKLA, A. K., BERGER, B., LITTLE, J. T., ANTAR, A., BLANC, A., QU, C. X., CHEN, X., KAWAKAMI, K., INOUE, A., AOKI, J., STEYAERT, J., SUN, J. P., BOUVIER, M., SKINIOTIS, G. & LEFKOWITZ, R. J. 2017. Distinct conformations of GPCR-beta-arrestin complexes mediate desensitization, signaling, and endocytosis. *Proc Natl Acad Sci U S A,* 114**,** 2562-2567.

CALEBIRO, D. & GODBOLE, A. 2018. Internalization of G-protein-coupled receptors: Implication in receptor function, physiology and diseases. *Best Pract Res Clin Endocrinol Metab,* 32**,** 83-91.

CALEBIRO, D., NIKOLAEV, V. O., GAGLIANI, M. C., DE FILIPPIS, T., DEES, C., TACCHETTI, C., PERSANI, L. & LOHSE, M. J. 2009. Persistent cAMP-signals triggered by internalized G-protein-coupled receptors. *PLoS Biol,* 7**,** e1000172.

CALEBIRO, D. & SUNGKAWORN, T. 2018. Single-Molecule Imaging of GPCR Interactions. *Trends Pharmacol Sci,* 39**,** 109-122.

CAMP, N. D., LEE, K. S., CHERRY, A., WACKER-MHYRE, J. L., KOUNTZ, T. S., PARK, J. M., HARRIS, D. A., ESTRADA, M., STEWART, A., STELLA, N., WOLF-YADLIN, A. & HAGUE, C. 2016. Dynamic mass redistribution reveals diverging importance of PDZ-ligands for G protein-coupled receptor pharmacodynamics. *Pharmacol Res,* 105**,** 13-21.

CAO, T. T., DEACON, H. W., RECZEK, D., BRETSCHER, A. & VON ZASTROW, M. 1999. A kinase-regulated PDZ-domain interaction controls endocytic sorting of the beta2-adrenergic receptor. *Nature,* 401**,** 286-90.

CHAMBERS, E. S., VIARDOT, A., PSICHAS, A., MORRISON, D. J., MURPHY, K. G., ZAC-VARGHESE, S. E., MACDOUGALL, K., PRESTON, T., TEDFORD, C., FINLAYSON, G. S., BLUNDELL, J. E., BELL, J. D., THOMAS, E. L., MT-ISA, S., ASHBY, D., GIBSON, G. R., KOLIDA, S., DHILLO, W. S., BLOOM, S. R., MORLEY, W., CLEGG, S. & FROST, G. 2015. Effects of targeted delivery of propionate to the human colon on appetite regulation, body weight maintenance and adiposity in overweight adults. *Gut,* 64**,** 1744-54.

CHARFI, I., ABDALLAH, K., GENDRON, L. & PINEYRO, G. 2018. Delta opioid receptors recycle to the membrane after sorting to the degradation path. *Cell Mol Life Sci,* 75**,** 2257-2271.

CHELIKANI, P. K., HAVER, A. C. & REIDELBERGER, R. D. 2005. Intravenous infusion of peptide YY(3-36) potently inhibits food intake in rats. *Endocrinology,* 146**,** 879-88.

CHEN, P. W., LUO, R., JIAN, X. & RANDAZZO, P. A. 2014. The Arf6 GTPase-activating proteins ARAP2 and ACAP1 define distinct endosomal compartments that regulate integrin alpha5beta1 traffic. *J Biol Chem,* 289**,** 30237-48.

CHEN, W., REN, X. R., NELSON, C. D., BARAK, L. S., CHEN, J. K., BEACHY, P. A., DE SAUVAGE, F. & LEFKOWITZ, R. J. 2004. Activity-dependent internalization of smoothened mediated by beta-arrestin 2 and GRK2. *Science,* 306**,** 2257-60.

CHENG, K. K., IGLESIAS, M. A., LAM, K. S., WANG, Y., SWEENEY, G., ZHU, W., VANHOUTTE, P. M., KRAEGEN, E. W. & XU, A. 2009. APPL1 potentiates insulin-mediated inhibition of hepatic glucose production and alleviates diabetes via Akt activation in mice. *Cell Metab,* 9**,** 417-27.

CHENG, K. K. Y., LAM, K. S. L., WU, D., WANG, Y., SWEENEY, G., HOO, R. L. C., ZHANG, J. & XU, A. 2012. APPL1 potentiates insulin secretion in pancreatic β cells by enhancing protein kinase Akt-dependent expression of SNARE proteins in mice. *Proceedings of the National Academy of Sciences of the United States of America,* 109**,** 8919-8924.

CHINI, B. & PARENTI, M. 2004. G-protein coupled receptors in lipid rafts and caveolae: how, when and why do they go there? *J Mol Endocrinol,* 32**,** 325-38.

CHINI, B. & PARENTI, M. 2009. G-protein-coupled receptors, cholesterol and palmitoylation: facts about fats. *J Mol Endocrinol,* 42**,** 371-9.

CHISHOLM, C. & GREENBERG, G. R. 2002. Somatostatin-28 regulates GLP-1 secretion via somatostatin receptor subtype 5 in rat intestinal cultures. *Am J Physiol Endocrinol Metab,* 283**,** E311-7.

CHO, D., ZHENG, M., MIN, C., MA, L., KUROSE, H., PARK, J. H. & KIM, K. M. 2010. Agonist-induced endocytosis and receptor phosphorylation mediate resensitization of dopamine D(2) receptors. *Mol Endocrinol,* 24**,** 574-86.

CHO, I., YAMANISHI, S., COX, L., METHE, B. A., ZAVADIL, J., LI, K., GAO, Z., MAHANA, D., RAJU, K., TEITLER, I., LI, H., ALEKSEYENKO, A. V. & BLASER, M. J. 2012. Antibiotics in early life alter the murine colonic microbiome and adiposity. *Nature,* 488**,** 621-6.

CHRISTOFORIDIS, S., MCBRIDE, H. M., BURGOYNE, R. D. & ZERIAL, M. 1999. The Rab5 effector EEA1 is a core component of endosome docking. *Nature,* 397**,** 621-5.

COSTANZI, S., NEUMANN, S. & GERSHENGORN, M. C. 2008. Seven transmembrane-spanning receptors for free fatty acids as therapeutic targets for diabetes mellitus: pharmacological, phylogenetic, and drug discovery aspects. *J Biol Chem,* 283**,** 16269-73.

COTTET, M., FAKLARIS, O., MAUREL, D., SCHOLLER, P., DOUMAZANE, E., TRINQUET, E., PIN, J. P. & DURROUX, T. 2012. BRET and Time-resolved FRET strategy to study GPCR oligomerization: from cell lines toward native tissues. *Front Endocrinol (Lausanne),* 3**,** 92.

COTTRELL, G. S., PADILLA, B., PIKIOS, S., ROOSTERMAN, D., STEINHOFF, M., GEHRINGER, D., GRADY, E. F. & BUNNETT, N. W. 2006. Ubiquitin-dependent down-regulation of the neurokinin-1 receptor. *J Biol Chem,* 281**,** 27773-83.

COVINGTON, D. K., BRISCOE, C. A., BROWN, A. J. & JAYAWICKREME, C. K. 2006. The G-protein-coupled receptor 40 family (GPR40-GPR43) and its role in nutrient sensing. *Biochem Soc Trans,* 34**,** 770-3.

CUMMINGS, D. E. & OVERDUIN, J. 2007. Gastrointestinal regulation of food intake. *J Clin Invest,* 117**,** 13-23.

CUMMINGS, J. H. & MACFARLANE, G. T. 1997. Role of intestinal bacteria in nutrient metabolism. *JPEN J Parenter Enteral Nutr,* 21**,** 357-65.

CUNNINGHAM, M. R., NISAR, S. P., COOKE, A. E., EMERY, E. D. & MUNDELL, S. J. 2013. Differential endosomal sorting of a novel P2Y12 purinoreceptor mutant. *Traffic,* 14**,** 585-98.

DAAKA, Y., LUTTRELL, L. M., AHN, S., DELLA ROCCA, G. J., FERGUSON, S. S., CARON, M. G. & LEFKOWITZ, R. J. 1998. Essential role for G protein-coupled receptor endocytosis in the activation of mitogen-activated protein kinase. *J Biol Chem,* 273**,** 685-8.

DAKIN, C. L., SMALL, C. J., BATTERHAM, R. L., NEARY, N. M., COHEN, M. A., PATTERSON, M., GHATEI, M. A. & BLOOM, S. R. 2004. Peripheral oxyntomodulin reduces food intake and body weight gain in rats. *Endocrinology,* 145**,** 2687-95.

DALE, L. B., BHATTACHARYA, M., SEACHRIST, J. L., ANBORGH, P. H. & FERGUSON, S. S. 2001. Agonist-stimulated and tonic internalization of metabotropic glutamate receptor 1a in human embryonic kidney 293 cells: agonist-stimulated endocytosis is beta-arrestin1 isoform-specific. *Mol Pharmacol,* 60**,** 1243-53.

DALRYMPLE, M. B., PFLEGER, K. D. & EIDNE, K. A. 2008. G protein-coupled receptor dimers: functional consequences, disease states and drug targets. *Pharmacol Ther,* 118**,** 359-71.

DANN, C. E., HSIEH, J. C., RATTNER, A., SHARMA, D., NATHANS, J. & LEAHY, D. J. 2001. Insights into Wnt binding and signalling from the structures of two Frizzled cysteine-rich domains. *Nature,* 412**,** 86-90.

DANSINGER, M. L., GLEASON, J. A., GRIFFITH, J. L., SELKER, H. P. & SCHAEFER, E. J. 2005. Comparison of the Atkins, Ornish, Weight Watchers, and Zone diets for weight loss and heart disease risk reduction: a randomized trial. *JAMA,* 293**,** 43-53.

DARDENO, T. A., CHOU, S. H., MOON, H. S., CHAMBERLAND, J. P., FIORENZA, C. G. & MANTZOROS, C. S. 2010. Leptin in human physiology and therapeutics. *Front Neuroendocrinol,* 31**,** 377-93.

DATE, Y., KOJIMA, M., HOSODA, H., SAWAGUCHI, A., MONDAL, M. S., SUGANUMA, T., MATSUKURA, S., KANGAWA, K. & NAKAZATO, M. 2000. Ghrelin, a novel growth hormone-releasing acylated peptide, is synthesized in a distinct endocrine cell type in the gastrointestinal tracts of rats and humans. *Endocrinology,* 141**,** 4255-61.

DATE, Y., MURAKAMI, N., TOSHINAI, K., MATSUKURA, S., NIIJIMA, A., MATSUO, H., KANGAWA, K. & NAKAZATO, M. 2002. The role of the gastric afferent vagal nerve in ghrelin-induced feeding and growth hormone secretion in rats. *Gastroenterology,* 123**,** 1120-8.

DAVENPORT, A. P., ALEXANDER, S. P., SHARMAN, J. L., PAWSON, A. J., BENSON, H. E., MONAGHAN, A. E., LIEW, W. C., MPAMHANGA, C. P., BONNER, T. I., NEUBIG, R. R., PIN, J. P., SPEDDING, M. & HARMAR, A. J. 2013. International Union of Basic and Clinical Pharmacology. LXXXVIII. G protein-coupled receptor list: recommendations for new pairings with cognate ligands. *Pharmacol Rev,* 65**,** 967-86.

DEACON, C. F. 2004. Circulation and degradation of GIP and GLP-1. *Horm Metab Res,* 36**,** 761-5.

DEFEA, K. A., VAUGHN, Z. D., O'BRYAN, E. M., NISHIJIMA, D., DERY, O. & BUNNETT, N. W. 2000. The proliferative and antiapoptotic effects of substance P are facilitated by formation of a beta -arrestin-dependent scaffolding complex. *Proc Natl Acad Sci U S A,* 97**,** 11086-91.

DELHANTY, P. J., NEGGERS, S. J. & VAN DER LELY, A. J. 2012. Mechanisms in endocrinology: Ghrelin: the differences between acyl- and des-acyl ghrelin. *Eur J Endocrinol,* 167**,** 601-8.

DELOM, F. & FESSART, D. 2011. Role of Phosphorylation in the Control of Clathrin-Mediated Internalization of GPCR. *International journal of cell biology,* 2011**,** 246954-246954.

DEN BESTEN, G., VAN EUNEN, K., GROEN, A. K., VENEMA, K., REIJNGOUD, D. J. & BAKKER, B. M. 2013. The role of short-chain fatty acids in the interplay between diet, gut microbiota, and host energy metabolism. *J Lipid Res,* 54**,** 2325-40.

DEWULF, E. M., GE, Q., BINDELS, L. B., SOHET, F. M., CANI, P. D., BRICHARD, S. M. & DELZENNE, N. M. 2013. Evaluation of the relationship between GPR43 and adiposity in human. *Nutr Metab (Lond),* 10**,** 11.

DHANVANTARI, S., IZZO, A., JANSEN, E. & BRUBAKER, P. L. 2001. Coregulation of glucagon-like peptide-1 synthesis with proglucagon and prohormone convertase 1 gene expression in enteroendocrine GLUTag cells. *Endocrinology,* 142**,** 37-42.

DIGGINS, N. L. & WEBB, D. J. 2017. APPL1 is a multifunctional endosomal signaling adaptor protein. *Biochem Soc Trans,* 45**,** 771-779.

DING, Y., CAO, Y., WANG, B., WANG, L., ZHANG, Y., ZHANG, D., CHEN, X., LI, M. & WANG, C. 2016. APPL1-Mediating Leptin Signaling Contributes to Proliferation and Migration of Cancer Cells. *PLoS One,* 11**,** e0166172.

DONG, C., FILIPEANU, C. M., DUVERNAY, M. T. & WU, G. 2007. Regulation of G protein-coupled receptor export trafficking. *Biochim Biophys Acta,* 1768**,** 853-70.

DORES, M. R., GRIMSEY, N. J., MENDEZ, F. & TREJO, J. 2016. ALIX Regulates the Ubiquitin-Independent Lysosomal Sorting of the P2Y1 Purinergic Receptor via a YPX3L Motif. *PLoS One,* 11**,** e0157587.

DORES, M. R., LIN, H., N, J. G., MENDEZ, F. & TREJO, J. 2015. The alpha-arrestin ARRDC3 mediates ALIX ubiquitination and G protein-coupled receptor lysosomal sorting. *Mol Biol Cell,* 26**,** 4660-73.

DORES, M. R. & TREJO, J. 2015. GPCR sorting at multivesicular endosomes. *Methods Cell Biol,* 130**,** 319-32.

DROR, R. O., ARLOW, D. H., MARAGAKIS, P., MILDORF, T. J., PAN, A. C., XU, H., BORHANI, D. W. & SHAW, D. E. 2011. Activation mechanism of the beta2-adrenergic receptor. *Proc Natl Acad Sci U S A,* 108**,** 18684-9.

DRUCKER, D. J., PHILIPPE, J., MOJSOV, S., CHICK, W. L. & HABENER, J. F. 1987. Glucagon-like peptide I stimulates insulin gene expression and increases cyclic AMP levels in a rat islet cell line. *Proc Natl Acad Sci U S A,* 84**,** 3434-8.

DUNN, H. A. & FERGUSON, S. S. 2015. PDZ Protein Regulation of G Protein-Coupled Receptor Trafficking and Signaling Pathways. *Mol Pharmacol,* 88**,** 624-39.

DYER, J., HOSIE, K. B. & SHIRAZI-BEECHEY, S. P. 1997. Nutrient regulation of human intestinal sugar transporter (SGLT1) expression. *Gut,* 41**,** 56-9.

EDFALK, S., STENEBERG, P. & EDLUND, H. 2008. Gpr40 is expressed in enteroendocrine cells and mediates free fatty acid stimulation of incretin secretion. *Diabetes,* 57**,** 2280-7.

EGEROD, K. L., ENGELSTOFT, M. S., GRUNDDAL, K. V., NOHR, M. K., SECHER, A., SAKATA, I., PEDERSEN, J., WINDELOV, J. A., FUCHTBAUER, E. M., OLSEN, J., SUNDLER, F., CHRISTENSEN, J. P., WIERUP, N., OLSEN, J. V., HOLST, J. J., ZIGMAN, J. M., POULSEN, S. S. & SCHWARTZ, T. W. 2012. A major lineage of enteroendocrine cells coexpress CCK, secretin, GIP, GLP-1, PYY, and neurotensin but not somatostatin. *Endocrinology,* 153**,** 5782-95.

EICHEL, K., JULLIE, D., BARSI-RHYNE, B., LATORRACA, N. R., MASUREEL, M., SIBARITA, J. B., DROR, R. O. & VON ZASTROW, M. 2018. Catalytic activation of beta-arrestin by GPCRs. *Nature,* 557**,** 381-386.

EICHEL, K., JULLIÉ, D. & VON ZASTROW, M. 2016. β-Arrestin drives MAP kinase signalling from clathrin-coated structures after GPCR dissociation. *Nature cell biology,* 18**,** 303-310.

EICHEL, K. & VON ZASTROW, M. 2018. Subcellular Organization of GPCR Signaling. *Trends Pharmacol Sci,* 39**,** 200-208.

ENGELSTOFT, M. S., PARK, W. M., SAKATA, I., KRISTENSEN, L. V., HUSTED, A. S., OSBORNE-LAWRENCE, S., PIPER, P. K., WALKER, A. K., PEDERSEN, M. H., NOHR, M. K., PAN, J., SINZ, C. J., CARRINGTON, P. E., AKIYAMA, T. E., JONES, R. M., TANG, C., AHMED, K., OFFERMANNS, S., EGEROD, K. L., ZIGMAN, J. M. & SCHWARTZ, T. W. 2013. Seven transmembrane G protein-coupled receptor repertoire of gastric ghrelin cells. *Mol Metab,* 2**,** 376-92.

ERDMANN, K. S., MAO, Y., MCCREA, H. J., ZONCU, R., LEE, S., PARADISE, S., MODREGGER, J., BIEMESDERFER, D., TOOMRE, D. & DE CAMILLI, P. 2007. A role of the Lowe syndrome protein OCRL in early steps of the endocytic pathway. *Dev Cell,* 13**,** 377-90.

ERLANSON-ALBERTSSON, C. 2005. How palatable food disrupts appetite regulation. *Basic Clin Pharmacol Toxicol,* 97**,** 61-73.

FAIPOUX, R., TOME, D., GOUGIS, S., DARCEL, N. & FROMENTIN, G. 2008. Proteins activate satiety-related neuronal pathways in the brainstem and hypothalamus of rats. *J Nutr,* 138**,** 1172-8.

FALKEN, Y., HELLSTROM, P. M., HOLST, J. J. & NASLUND, E. 2011. Changes in glucose homeostasis after Roux-en-Y gastric bypass surgery for obesity at day three, two months, and one year after surgery: role of gut peptides. *J Clin Endocrinol Metab,* 96**,** 2227-35.

FAN, T., VARGHESE, G., NGUYEN, T., TSE, R., O'DOWD, B. F. & GEORGE, S. R. 2005. A role for the distal carboxyl tails in generating the novel pharmacology and G protein activation profile of mu and delta opioid receptor hetero-oligomers. *J Biol Chem,* 280**,** 38478-88.

FEINSTEIN, T. N., WEHBI, V. L., ARDURA, J. A., WHEELER, D. S., FERRANDON, S., GARDELLA, T. J. & VILARDAGA, J. P. 2011. Retromer terminates the generation of cAMP by internalized PTH receptors. *Nat Chem Biol,* 7**,** 278-84.

FERGUSON, S. S., DOWNEY, W. E., 3RD, COLAPIETRO, A. M., BARAK, L. S., MENARD, L. & CARON, M. G. 1996. Role of beta-arrestin in mediating agonist-promoted G protein-coupled receptor internalization. *Science,* 271**,** 363-6.

FERRANDON, S., FEINSTEIN, T. N., CASTRO, M., WANG, B., BOULEY, R., POTTS, J. T., GARDELLA, T. J. & VILARDAGA, J. P. 2009. Sustained cyclic AMP production by parathyroid hormone receptor endocytosis. *Nat Chem Biol,* 5**,** 734-42.

FERRE, S., BALER, R., BOUVIER, M., CARON, M. G., DEVI, L. A., DURROUX, T., FUXE, K., GEORGE, S. R., JAVITCH, J. A., LOHSE, M. J., MACKIE, K., MILLIGAN, G., PFLEGER, K. D., PIN, J. P., VOLKOW, N. D., WALDHOER, M., WOODS, A. S. & FRANCO, R. 2009. Building a new conceptual framework for receptor heteromers. *Nat Chem Biol,* 5**,** 131-4.

FIELD, B. C., WREN, A. M., PETERS, V., BAYNES, K. C., MARTIN, N. M., PATTERSON, M., ALSARAF, S., AMBER, V., WYNNE, K., GHATEI, M. A. & BLOOM, S. R. 2010. PYY3-36 and oxyntomodulin can be additive in their effect on food intake in overweight and obese humans. *Diabetes,* 59**,** 1635-9.

FINUCANE, M. M., STEVENS, G. A., COWAN, M. J., DANAEI, G., LIN, J. K., PACIOREK, C. J., SINGH, G. M., GUTIERREZ, H. R., LU, Y., BAHALIM, A. N., FARZADFAR, F., RILEY, L. M. & EZZATI, M. 2011. National, regional, and global trends in body-mass index since 1980: systematic analysis of health examination surveys and epidemiological studies with 960 country-years and 9.1 million participants. *Lancet,* 377**,** 557-67.

FLEISCHER, J., BUMBALO, R., BAUTZE, V., STROTMANN, J. & BREER, H. 2015. Expression of odorant receptor Olfr78 in enteroendocrine cells of the colon. *Cell Tissue Res,* 361**,** 697-710.

FLORES-OTERO, J., AHN, K. H., DELGADO-PERAZA, F., MACKIE, K., KENDALL, D. A. & YUDOWSKI, G. A. 2014. Ligand-specific endocytic dwell times control functional selectivity of the cannabinoid receptor 1. *Nat Commun,* 5**,** 4589.

FLORES-RODRIGUEZ, N., KENWRIGHT, D. A., CHUNG, P.-H., HARRISON, A. W., STEFANI, F., WAIGH, T. A., ALLAN, V. J. & WOODMAN, P. G. 2015. ESCRT-0 marks an APPL1-independent transit route for EGFR between the cell surface and the EEA1-positive early endosome. *J Cell Sci,* 128**,** 755-767.

FOTIADIS, D., QIAN, P., PHILIPPSEN, A., BULLOUGH, P. A., ENGEL, A. & HUNTER, C. N. 2004. Structural analysis of the reaction center light-harvesting complex I photosynthetic core complex of Rhodospirillum rubrum using atomic force microscopy. *J Biol Chem,* 279**,** 2063-8.

FRITSCHY, J. M. & MOHLER, H. 1995. GABAA-receptor heterogeneity in the adult rat brain: differential regional and cellular distribution of seven major subunits. *J Comp Neurol,* 359**,** 154-94.

FROST, G., CAI, Z., RAVEN, M., OTWAY, D. T., MUSHTAQ, R. & JOHNSTON, J. D. 2014. Effect of short chain fatty acids on the expression of free fatty acid receptor 2 (Ffar2), Ffar3 and early-stage adipogenesis. *Nutrition & diabetes,* 4**,** e128-e128.

FULLER, M., LI, X., FISCH, R., BUGHARA, M., WICKSTEED, B., KOVATCHEVA-DATCHARY, P. & LAYDEN, B. T. 2016. FFA2 Contribution to Gestational Glucose Tolerance Is Not Disrupted by Antibiotics. *PLoS One,* 11**,** e0167837.

FULLER, M., PRIYADARSHINI, M., GIBBONS, S. M., ANGUEIRA, A. R., BRODSKY, M., HAYES, M. G., KOVATCHEVA-DATCHARY, P., BÄCKHED, F., GILBERT, J. A., LOWE, W. L., JR. & LAYDEN, B. T. 2015. The short-chain fatty acid receptor, FFA2, contributes to gestational glucose homeostasis. *Am J Physiol Endocrinol Metab,* 309**,** E840-E851.

GAGE, R. M., KIM, K. A., CAO, T. T. & VON ZASTROW, M. 2001. A transplantable sorting signal that is sufficient to mediate rapid recycling of G protein-coupled receptors. *J Biol Chem,* 276**,** 44712-20.

GAGE, R. M., MATVEEVA, E. A., WHITEHEART, S. W. & VON ZASTROW, M. 2005. Type I PDZ ligands are sufficient to promote rapid recycling of G Protein-coupled receptors independent of binding to N-ethylmaleimide-sensitive factor. *J Biol Chem,* 280**,** 3305-13.

GAINETDINOV, R. R., PREMONT, R. T., BOHN, L. M., LEFKOWITZ, R. J. & CARON, M. G. 2004. Desensitization of G protein-coupled receptors and neuronal functions. *Annu Rev Neurosci,* 27**,** 107-44.

GALGANI, J. & RAVUSSIN, E. 2008. Energy metabolism, fuel selection and body weight regulation. *Int J Obes (Lond),* 32 Suppl 7**,** S109-19.

GAN, Z., RAM, S., OBER, R. J. & WARD, E. S. 2013. Using multifocal plane microscopy to reveal novel trafficking processes in the recycling pathway. *J Cell Sci,* 126**,** 1176-1188.

GANT-BRANUM, R. L., BROUSSARD, J. A., MAHSUT, A., WEBB, D. J. & MCLEAN, J. A. 2010. Identification of phosphorylation sites within the signaling adaptor APPL1 by mass spectrometry. *Journal of proteome research,* 9**,** 1541-1548.

GANTZ, I., ERONDU, N., MALLICK, M., MUSSER, B., KRISHNA, R., TANAKA, W. K., SNYDER, K., STEVENS, C., STROH, M. A., ZHU, H., WAGNER, J. A., MACNEIL, D. J., HEYMSFIELD, S. B. & AMATRUDA, J. M. 2007. Efficacy and safety of intranasal peptide YY3-36 for weight reduction in obese adults. *J Clin Endocrinol Metab,* 92**,** 1754-7.

GAO, Z. G. & JACOBSON, K. A. 2016. On the selectivity of the Galphaq inhibitor UBO-QIC: A comparison with the Galphai inhibitor pertussis toxin. *Biochem Pharmacol,* 107**,** 59-66.

GARDINER, J. V., JAYASENA, C. N. & BLOOM, S. R. 2008. Gut hormones: a weight off your mind. *J Neuroendocrinol,* 20**,** 834-41.

GARDNER, L. A., NAREN, A. P. & BAHOUTH, S. W. 2007. Assembly of an SAP97-AKAP79-cAMP-dependent protein kinase scaffold at the type 1 PSD-95/DLG/ZO1 motif of the human beta(1)-adrenergic receptor generates a receptosome involved in receptor recycling and networking. *J Biol Chem,* 282**,** 5085-99.

GARVEY, W. T., RYAN, D. H., LOOK, M., GADDE, K. M., ALLISON, D. B., PETERSON, C. A., SCHWIERS, M., DAY, W. W. & BOWDEN, C. H. 2012. Two-year sustained weight loss and metabolic benefits with controlled-release phentermine/topiramate in obese and overweight adults (SEQUEL): a randomized, placebo-controlled, phase 3 extension study. *Am J Clin Nutr,* 95**,** 297-308.

GE, H., LI, X., WEISZMANN, J., WANG, P., BARIBAULT, H., CHEN, J. L., TIAN, H. & LI, Y. 2008. Activation of G protein-coupled receptor 43 in adipocytes leads to inhibition of lipolysis and suppression of plasma free fatty acids. *Endocrinology,* 149**,** 4519-26.

GERAEDTS, M. C., TROOST, F. J. & SARIS, W. H. 2009. Peptide-YY is released by the intestinal cell line STC-1. *J Food Sci,* 74**,** H79-82.

GIL, K., BUGAJSKI, A. & THOR, P. 2011. Electrical vagus nerve stimulation decreases food consumption and weight gain in rats fed a high-fat diet. *J Physiol Pharmacol,* 62**,** 637-46.

GIRADA, S. B., KUNA, R. S., BELE, S., ZHU, Z., CHAKRAVARTHI, N. R., DIMARCHI, R. D. & MITRA, P. 2017. Galphas regulates Glucagon-Like Peptide 1 Receptor-mediated cyclic AMP generation at Rab5 endosomal compartment. *Mol Metab,* 6**,** 1173-1185.

GODBOLE, A., LYGA, S., LOHSE, M. J. & CALEBIRO, D. 2017. Internalized TSH receptors en route to the TGN induce local Gs-protein signaling and gene transcription. *Nat Commun,* 8**,** 443.

GODDARD, A. D. & WATTS, A. 2012. Regulation of G protein-coupled receptors by palmitoylation and cholesterol. *BMC Biol,* 10**,** 27.

GOMES, I., AYOUB, M. A., FUJITA, W., JAEGER, W. C., PFLEGER, K. D. & DEVI, L. A. 2016. G Protein-Coupled Receptor Heteromers. *Annu Rev Pharmacol Toxicol,* 56**,** 403-25.

GORVIN, C. M., ROGERS, A., HASTOY, B., TARASOV, A. I., FROST, M., SPOSINI, S., INOUE, A., WHYTE, M. P., RORSMAN, P., HANYALOGLU, A. C., BREITWIESER, G. E. & THAKKER, R. V. 2018. AP2? Mutations Impair Calcium-Sensing Receptor Trafficking and Signaling, and Show an Endosomal Pathway to Spatially Direct G-Protein Selectivity. *Cell Rep,* 22**,** 1054-1066.

GRAFF, E. C., FANG, H., WANDERS, D. & JUDD, R. L. 2016. Anti-inflammatory effects of the hydroxycarboxylic acid receptor 2. *Metabolism,* 65**,** 102-13.

GRIMSEY, N. J., AGUILAR, B., SMITH, T. H., LE, P., SOOHOO, A. L., PUTHENVEEDU, M. A., NIZET, V. & TREJO, J. 2015. Ubiquitin plays an atypical role in GPCR-induced p38 MAP kinase activation on endosomes. *J Cell Biol,* 210**,** 1117-31.

GRIMSEY, N. J., NARALA, R., RADA, C. C., MEHTA, S., STEPHENS, B. S., KUFAREVA, I., LAPEK, J., GONZALEZ, D. J., HANDEL, T. M., ZHANG, J. & TREJO, J. 2018. A Tyrosine Switch on NEDD4-2 E3 Ligase Transmits GPCR Inflammatory Signaling. *Cell Rep,* 24**,** 3312-3323.e5.

GRUNDMANN, M., MERTEN, N., MALFACINI, D., INOUE, A., PREIS, P., SIMON, K., RUTTIGER, N., ZIEGLER, N., BENKEL, T., SCHMITT, N. K., ISHIDA, S., MULLER, I., REHER, R., KAWAKAMI, K., INOUE, A., RICK, U., KUHL, T., IMHOF, D., AOKI, J., KONIG, G. M., HOFFMANN, C., GOMEZA, J., WESS, J. & KOSTENIS, E. 2018. Lack of beta-arrestin signaling in the absence of active G proteins. *Nat Commun,* 9**,** 341.

GUO, D., MULDER-KRIEGER, T., AP, I. J. & HEITMAN, L. H. 2012. Functional efficacy of adenosine A(2)A receptor agonists is positively correlated to their receptor residence time. *Br J Pharmacol,* 166**,** 1846-59.

GUPTA, N., MARTIN, P. M., PRASAD, P. D. & GANAPATHY, V. 2006. SLC5A8 (SMCT1)-mediated transport of butyrate forms the basis for the tumor suppressive function of the transporter. *Life Sci,* 78**,** 2419-25.

GUREVICH, V. V. & GUREVICH, E. V. 2008. GPCR monomers and oligomers: it takes all kinds. *Trends Neurosci,* 31**,** 74-81.

GUREVICH, V. V. & GUREVICH, E. V. 2018a. Arrestins and G proteins in cellular signaling: The coin has two sides. *Sci Signal,* 11.

GUREVICH, V. V. & GUREVICH, E. V. 2018b. Arrestin-mediated signaling: Is there a controversy? *World J Biol Chem,* 9**,** 25-35.

GYOMBOLAI, P., BOROS, E., HUNYADY, L. & TURU, G. 2013. Differential beta-arrestin2 requirements for constitutive and agonist-induced internalization of the CB1 cannabinoid receptor. *Mol Cell Endocrinol,* 372**,** 116-27.

HABIB, A. M., RICHARDS, P., CAIRNS, L. S., ROGERS, G. J., BANNON, C. A., PARKER, H. E., MORLEY, T. C., YEO, G. S., REIMANN, F. & GRIBBLE, F. M. 2012. Overlap of endocrine

hormone expression in the mouse intestine revealed by transcriptional profiling and flow cytometry. *Endocrinology,* 153**,** 3054-65.

HALL, R. A., OSTEDGAARD, L. S., PREMONT, R. T., BLITZER, J. T., RAHMAN, N., WELSH, M. J. & LEFKOWITZ, R. J. 1998. A C-terminal motif found in the beta2-adrenergic receptor, P2Y1 receptor and cystic fibrosis transmembrane conductance regulator determines binding to the Na+/H+ exchanger regulatory factor family of PDZ proteins. *Proc Natl Acad Sci U S A,* 95**,** 8496-501.

HAND, K. V., BRUEN, C. M., O'HALLORAN, F., PANWAR, H., CALDERWOOD, D., GIBLIN, L. & GREEN, B. D. 2013. Examining acute and chronic effects of short- and long-chain fatty acids on peptide YY (PYY) gene expression, cellular storage and secretion in STC-1 cells. *Eur J Nutr,* 52**,** 1303-13.

HANSEN, K. B., ROSENKILDE, M. M., KNOP, F. K., WELLNER, N., DIEP, T. A., REHFELD, J. F., ANDERSEN, U. B., HOLST, J. J. & HANSEN, H. S. 2011. 2-Oleoyl glycerol is a GPR119 agonist and signals GLP-1 release in humans. *J Clin Endocrinol Metab,* 96**,** E1409-17.

HANYALOGLU, A. C., MCCULLAGH, E. & VON ZASTROW, M. 2005. Essential role of Hrs in a recycling mechanism mediating functional resensitization of cell signaling. *Embo j,* 24**,** 2265-83.

HANYALOGLU, A. C. & VON ZASTROW, M. 2008. Regulation of GPCRs by endocytic membrane trafficking and its potential implications. *Annu Rev Pharmacol Toxicol,* 48**,** 537-68.

HARDWICK, J. C., CLASON, T. A., TOMPKINS, J. D., GIRARD, B. M., BARAN, C. N., MERRIAM, L. A., MAY, V. & PARSONS, R. L. 2017. Recruitment of endosomal signaling mediates the forskolin modulation of guinea pig cardiac neuron excitability. *Am J Physiol Cell Physiol,* 313**,** C219-c227.

HASDEMIR, B., MURPHY, J. E., COTTRELL, G. S. & BUNNETT, N. W. 2009. Endosomal deubiquitinating enzymes control ubiquitination and down-regulation of protease-activated receptor 2. *J Biol Chem,* 284**,** 28453-66.

HAUGE, M., VESTMAR, M. A., HUSTED, A. S., EKBERG, J. P., WRIGHT, M. J., DI SALVO, J., WEINGLASS, A. B., ENGELSTOFT, M. S., MADSEN, A. N., LUCKMANN, M., MILLER, M. W., TRUJILLO, M. E., FRIMURER, T. M., HOLST, B., HOWARD, A. D. & SCHWARTZ, T. W. 2015. GPR40 (FFAR1) - Combined Gs and Gq signaling in vitro is associated with robust incretin secretagogue action ex vivo and in vivo. *Mol Metab,* 4**,** 3-14.

HAUSER, A. S., ATTWOOD, M. M., RASK-ANDERSEN, M., SCHIOTH, H. B. & GLORIAM, D. E. 2017. Trends in GPCR drug discovery: new agents, targets and indications. *Nat Rev Drug Discov,* 16**,** 829-842.

HE, C., WEI, Y., SUN, K., LI, B., DONG, X., ZOU, Z., LIU, Y., KINCH, L. N., KHAN, S., SINHA, S., XAVIER, R. J., GRISHIN, N. V., XIAO, G., ESKELINEN, E. L., SCHERER, P. E., WHISTLER, J. L. & LEVINE, B. 2013. Beclin 2 functions in autophagy, degradation of G protein-coupled receptors, and metabolism. *Cell,* 154**,** 1085-1099.

HENRY, A. G., HISLOP, J. N., GROVE, J., THORN, K., MARSH, M. & VON ZASTROW, M. 2012. Regulation of endocytic clathrin dynamics by cargo ubiquitination. *Dev Cell,* 23**,** 519-32.

HENRY, A. G., WHITE, I. J., MARSH, M., VON ZASTROW, M. & HISLOP, J. N. 2011. The role of ubiquitination in lysosomal trafficking of delta-opioid receptors. *Traffic,* 12**,** 170-84.

HERRMANN, C., GOKE, R., RICHTER, G., FEHMANN, H. C., ARNOLD, R. & GOKE, B. 1995. Glucagon-like peptide-1 and glucose-dependent insulin-releasing polypeptide plasma levels in response to nutrients. *Digestion,* 56**,** 117-26.

HINNEBUSCH, B. F., MENG, S., WU, J. T., ARCHER, S. Y. & HODIN, R. A. 2002. The effects of short-chain fatty acids on human colon cancer cell phenotype are associated with histone hyperacetylation. *J Nutr,* 132**,** 1012-7.

HIRASAWA, A., TSUMAYA, K., AWAJI, T., KATSUMA, S., ADACHI, T., YAMADA, M., SUGIMOTO, Y., MIYAZAKI, S. & TSUJIMOTO, G. 2005. Free fatty acids regulate gut incretin glucagon-like peptide-1 secretion through GPR120. *Nat Med,* 11**,** 90-4.

HISLOP, J. N. & VON ZASTROW, M. 2011. Role of ubiquitination in endocytic trafficking of G-protein-coupled receptors. *Traffic,* 12**,** 137-48.

HOLLIDAY, N. D., LAM, C. W., TOUGH, I. R. & COX, H. M. 2005. Role of the C terminus in neuropeptide Y Y1 receptor desensitization and internalization. *Mol Pharmacol,* 67**,** 655-64.

HOLST, J. J. 2007. The physiology of glucagon-like peptide 1. *Physiol Rev,* 87**,** 1409-39.

HONG, Y. H., NISHIMURA, Y., HISHIKAWA, D., TSUZUKI, H., MIYAHARA, H., GOTOH, C., CHOI, K. C., FENG, D. D., CHEN, C., LEE, H. G., KATOH, K., ROH, S. G. & SASAKI, S. 2005. Acetate and propionate short chain fatty acids stimulate adipogenesis via GPCR43. *Endocrinology,* 146**,** 5092-9.

HOPE, D. C. D., TAN, T. M. M. & BLOOM, S. R. 2018. No Guts, No Loss: Toward the Ideal Treatment for Obesity in the Twenty-First Century. *Front Endocrinol (Lausanne),* 9**,** 442.

HOPKINS, M., FINLAYSON, G., DUARTE, C., WHYBROW, S., RITZ, P., HORGAN, G. W., BLUNDELL, J. E. & STUBBS, R. J. 2016. Modelling the associations between fat-free mass, resting metabolic rate and energy intake in the context of total energy balance. *Int J Obes (Lond),* 40**,** 312-8.

HOTHERSALL, J. D., BROWN, A. J., DALE, I. & RAWLINS, P. 2016. Can residence time offer a useful strategy to target agonist drugs for sustained GPCR responses? *Drug Discov Today,* 21**,** 90-96.

HUDSON, B. D., CHRISTIANSEN, E., TIKHONOVA, I. G., GRUNDMANN, M., KOSTENIS, E., ADAMS, D. R., ULVEN, T. & MILLIGAN, G. 2012a. Chemically engineering ligand selectivity at the free fatty acid receptor 2 based on pharmacological variation between species orthologs. *Faseb j,* 26**,** 4951-4965.

HUDSON, B. D., DUE-HANSEN, M. E., CHRISTIANSEN, E., HANSEN, A. M., MACKENZIE, A. E., MURDOCH, H., PANDEY, S. K., WARD, R. J., MARQUEZ, R., TIKHONOVA, I. G., ULVEN, T. & MILLIGAN, G. 2013. Defining the molecular basis for the first potent and selective orthosteric agonists of the FFA2 free fatty acid receptor. *J Biol Chem,* 288**,** 17296-312.

HUDSON, B. D., SMITH, N. J. & MILLIGAN, G. 2011. Experimental challenges to targeting poorly characterized GPCRs: uncovering the therapeutic potential for free fatty acid receptors. *Adv Pharmacol,* 62**,** 175-218.

HUOTARI, J. & HELENIUS, A. 2011. Endosome maturation. *Embo j,* 30**,** 3481-500.

HUTTENRAUCH, F., POLLOK-KOPP, B. & OPPERMANN, M. 2005. G protein-coupled receptor kinases promote phosphorylation and beta-arrestin-mediated internalization of CCR5 homo- and hetero-oligomers. *J Biol Chem,* 280**,** 37503-15.

INDA, C., DOS SANTOS CLARO, P. A., BONFIGLIO, J. J., SENIN, S. A., MACCARRONE, G., TURCK, C. W. & SILBERSTEIN, S. 2016. Different cAMP sources are critically involved in G protein-coupled receptor CRHR1 signaling. *J Cell Biol,* 214**,** 181-95.

IRANNEJAD, R., PESSINO, V., MIKA, D., HUANG, B., WEDEGAERTNER, P. B., CONTI, M. & VON ZASTROW, M. 2017. Functional selectivity of GPCR-directed drug action through location bias. *Nat Chem Biol,* 13**,** 799-806.

IRANNEJAD, R., TOMSHINE, J. C., TOMSHINE, J. R., CHEVALIER, M., MAHONEY, J. P., STEYAERT, J., RASMUSSEN, S. G., SUNAHARA, R. K., EL-SAMAD, H., HUANG, B. & VON ZASTROW, M. 2013. Conformational biosensors reveal GPCR signalling from endosomes. *Nature,* 495**,** 534-8.

JACOB, C., COTTRELL, G. S., GEHRINGER, D., SCHMIDLIN, F., GRADY, E. F. & BUNNETT, N. W. 2005. c-Cbl mediates ubiquitination, degradation, and down-regulation of human protease-activated receptor 2. *J Biol Chem,* 280**,** 16076-87.

JALA, V. R., SHAO, W. H. & HARIBABU, B. 2005. Phosphorylation-independent beta-arrestin translocation and internalization of leukotriene B4 receptors. *J Biol Chem,* 280**,** 4880-7.

JEAN-ALPHONSE, F., BOWERSOX, S., CHEN, S., BEARD, G., PUTHENVEEDU, M. A. & HANYALOGLU, A. C. 2014. Spatially restricted G protein-coupled receptor activity via divergent endocytic compartments. *J Biol Chem,* 289**,** 3960-77.

JEAN-ALPHONSE, F. & HANYALOGLU, A. C. 2011. Regulation of GPCR signal networks via membrane trafficking. *Mol Cell Endocrinol,* 331**,** 205-14.

JEAN-ALPHONSE, F. G., WEHBI, V. L., CHEN, J., NODA, M., TABOAS, J. M., XIAO, K. & VILARDAGA, J. P. 2017. beta2-adrenergic receptor control of endosomal PTH receptor signaling via Gbetagamma. *Nat Chem Biol,* 13**,** 259-261.

JENSEN, D. D., LIEU, T., HALLS, M. L., VELDHUIS, N. A., IMLACH, W. L., MAI, Q. N., POOLE, D. P., QUACH, T., AURELIO, L., CONNER, J., HERENBRINK, C. K., BARLOW, N., SIMPSON, J. S., SCANLON, M. J., GRAHAM, B., MCCLUSKEY, A., ROBINSON, P. J., ESCRIOU, V., NASSINI, R., MATERAZZI, S., GEPPETTI, P., HICKS, G. A., CHRISTIE, M. J., PORTER, C. J. H., CANALS, M. & BUNNETT, N. W. 2017. Neurokinin 1 receptor signaling in endosomes mediates sustained nociception and is a viable therapeutic target for prolonged pain relief. *Sci Transl Med,* 9.

JIANG, X., ZHOU, Y., WU, K. K., CHEN, Z., XU, A. & CHENG, K. K. 2017. APPL1 prevents pancreatic beta cell death and inflammation by dampening NFkappaB activation in a mouse model of type 1 diabetes. *Diabetologia,* 60**,** 464-474.

JIMENEZ-VARGAS, N. N., PATTISON, L. A., ZHAO, P., LIEU, T., LATORRE, R., JENSEN, D. D., CASTRO, J., AURELIO, L., LE, G. T., FLYNN, B., HERENBRINK, C. K., YEATMAN, H. R., EDGINGTON-MITCHELL, L., PORTER, C. J. H., HALLS, M. L., CANALS, M., VELDHUIS, N. A., POOLE, D. P., MCLEAN, P., HICKS, G. A., SCHEFF, N., CHEN, E., BHATTACHARYA, A., SCHMIDT, B. L., BRIERLEY, S. M., VANNER, S. J. & BUNNETT, N. W. 2018. Protease-activated receptor-2 in endosomes signals persistent pain of irritable bowel syndrome. *Proc Natl Acad Sci U S A,* 115**,** E7438-E7447.

JONAS, K. C., FANELLI, F., HUHTANIEMI, I. T. & HANYALOGLU, A. C. 2015. Single molecule analysis of functionally asymmetric G protein-coupled receptor (GPCR) oligomers reveals diverse spatial and structural assemblies. *J Biol Chem,* 290**,** 3875-92.

JONAS, K. C. & HANYALOGLU, A. C. 2017. Impact of G protein-coupled receptor heteromers in endocrine systems. *Mol Cell Endocrinol,* 449**,** 21-27.

JONES, B., BUENAVENTURA, T., KANDA, N., CHABOSSEAU, P., OWEN, B. M., SCOTT, R., GOLDIN, R., ANGKATHUNYAKUL, N., CORREA, I. R., JR., BOSCO, D., JOHNSON, P. R., PIEMONTI, L., MARCHETTI, P., SHAPIRO, A. M. J., COCHRAN, B. J., HANYALOGLU, A.

C., INOUE, A., TAN, T., RUTTER, G. A., TOMAS, A. & BLOOM, S. R. 2018. Targeting GLP-1 receptor trafficking to improve agonist efficacy. *Nat Commun,* 9**,** 1602.
JORDAN, B. A. & DEVI, L. A. 1999. G-protein-coupled receptor heterodimerization modulates receptor function. *Nature,* 399**,** 697-700.
JULLIE, D., CHOQUET, D. & PERRAIS, D. 2014. Recycling endosomes undergo rapid closure of a fusion pore on exocytosis in neuronal dendrites. *J Neurosci,* 34**,** 11106-18.
KAIRUPAN, T. S., AMITANI, H., CHENG, K. C., RUNTUWENE, J., ASAKAWA, A. & INUI, A. 2016. Role of gastrointestinal hormones in feeding behavior and obesity treatment. *J Gastroenterol,* 51**,** 93-103.
KAJI, I., KARAKI, S. & KUWAHARA, A. 2014. Short-chain fatty acid receptor and its contribution to glucagon-like peptide-1 release. *Digestion,* 89**,** 31-6.
KAJI, I., KARAKI, S., TANAKA, R. & KUWAHARA, A. 2011. Density distribution of free fatty acid receptor 2 (FFA2)-expressing and GLP-1-producing enteroendocrine L cells in human and rat lower intestine, and increased cell numbers after ingestion of fructo-oligosaccharide. *J Mol Histol,* 42**,** 27-38.
KALAIDZIDIS, I., MIACZYNSKA, M., BREWINSKA-OLCHOWIK, M., HUPALOWSKA, A., FERGUSON, C., PARTON, R. G., KALAIDZIDIS, Y. & ZERIAL, M. 2015. APPL endosomes are not obligatory endocytic intermediates but act as stable cargo-sorting compartments. *Journal of Cell Biology,* 211**,** 123-44.
KANAMARLAPUDI, V., OWENS, S. E., SAHA, K., POPE, R. J. & MUNDELL, S. J. 2012. ARF6-dependent regulation of P2Y receptor traffic and function in human platelets. *PLoS One,* 7**,** e43532-e43532.
KARAKI, S., MITSUI, R., HAYASHI, H., KATO, I., SUGIYA, H., IWANAGA, T., FURNESS, J. B. & KUWAHARA, A. 2006. Short-chain fatty acid receptor, GPR43, is expressed by enteroendocrine cells and mucosal mast cells in rat intestine. *Cell Tissue Res,* 324**,** 353-60.
KATADA, T. & UI, M. 1982. Direct modification of the membrane adenylate cyclase system by islet-activating protein due to ADP-ribosylation of a membrane protein. *Proc Natl Acad Sci U S A,* 79**,** 3129-33.
KATZMANN, D. J., ODORIZZI, G. & EMR, S. D. 2002. Receptor downregulation and multivesicular-body sorting. *Nat Rev Mol Cell Biol,* 3**,** 893-905.
KEARN, C. S., BLAKE-PALMER, K., DANIEL, E., MACKIE, K. & GLASS, M. 2005. Concurrent stimulation of cannabinoid CB1 and dopamine D2 receptors enhances heterodimer formation: a mechanism for receptor cross-talk? *Mol Pharmacol,* 67**,** 1697-704.
KEAVER, L., XU, B., JACCARD, A. & WEBBER, L. 2018. Morbid obesity in the UK: A modelling projection study to 2035. *Scand J Public Health***,** 1403494818794814.
KENAKIN, T. 1997. Differences between natural and recombinant G protein-coupled receptor systems with varying receptor/G protein stoichiometry. *Trends Pharmacol Sci,* 18**,** 456-64.
KENAKIN, T. 2013. New concepts in pharmacological efficacy at 7TM receptors: IUPHAR review 2. *Br J Pharmacol,* 168**,** 554-75.
KENAKIN, T. 2017. A Scale of Agonism and Allosteric Modulation for Assessment of Selectivity, Bias, and Receptor Mutation. *Mol Pharmacol,* 92**,** 414-424.
KENNEDY, J. E. & MARCHESE, A. 2015. Regulation of GPCR Trafficking by Ubiquitin. *Prog Mol Biol Transl Sci,* 132**,** 15-38.

KHAN, S. M., SLENO, R., GORA, S., ZYLBERGOLD, P., LAVERDURE, J. P., LABBE, J. C., MILLER, G. J. & HEBERT, T. E. 2013. The expanding roles of Gbetagamma subunits in G protein-coupled receptor signaling and drug action. *Pharmacol Rev,* 65**,** 545-77.

KIEFFER, D. A., MARTIN, R. J. & ADAMS, S. H. 2016. Impact of Dietary Fibers on Nutrient Management and Detoxification Organs: Gut, Liver, and Kidneys. *Adv Nutr,* 7**,** 1111-1121.

KIM, M. H., KANG, S. G., PARK, J. H., YANAGISAWA, M. & KIM, C. H. 2013. Short-chain fatty acids activate GPR41 and GPR43 on intestinal epithelial cells to promote inflammatory responses in mice. *Gastroenterology,* 145**,** 396-406.e1-10.

KIM, S., SATO, Y., MOHAN, P. S., PETERHOFF, C., PENSALFINI, A., RIGOGLIOSO, A., JIANG, Y. & NIXON, R. A. 2016. Evidence that the rab5 effector APPL1 mediates APP-βCTF-induced dysfunction of endosomes in Down syndrome and Alzheimer's disease. *Molecular psychiatry,* 21**,** 707-716.

KIMURA, I., INOUE, D., MAEDA, T., HARA, T., ICHIMURA, A., MIYAUCHI, S., KOBAYASHI, M., HIRASAWA, A. & TSUJIMOTO, G. 2011. Short-chain fatty acids and ketones directly regulate sympathetic nervous system via G protein-coupled receptor 41 (GPR41). *Proc Natl Acad Sci U S A,* 108**,** 8030-5.

KIMURA, I., OZAWA, K., INOUE, D., IMAMURA, T., KIMURA, K., MAEDA, T., TERASAWA, K., KASHIHARA, D., HIRANO, K., TANI, T., TAKAHASHI, T., MIYAUCHI, S., SHIOI, G., INOUE, H. & TSUJIMOTO, G. 2013a. The gut microbiota suppresses insulin-mediated fat accumulation via the short-chain fatty acid receptor GPR43. *Nat Commun,* 4**,** 1829.

KIMURA, R., OKOUCHI, M., KATO, T., IMAEDA, K., OKAYAMA, N., ASAI, K. & JOH, T. 2013b. Epidermal growth factor receptor transactivation is necessary for glucagon-like peptide-1 to protect PC12 cells from apoptosis. *Neuroendocrinology,* 97**,** 300-8.

KIYONO, M., SATOH, T. & KAZIRO, Y. 1999. G protein beta gamma subunit-dependent Rac-guanine nucleotide exchange activity of Ras-GRF1/CDC25(Mm). *Proc Natl Acad Sci U S A,* 96**,** 4826-31.

KOBILKA, B. K. 2007. G protein coupled receptor structure and activation. *Biochim Biophys Acta,* 1768**,** 794-807.

KOMATSU, M., SCHERMERHORN, T., AIZAWA, T. & SHARP, G. W. 1995. Glucose stimulation of insulin release in the absence of extracellular Ca2+ and in the absence of any increase in intracellular Ca2+ in rat pancreatic islets. *Proc Natl Acad Sci U S A,* 92**,** 10728-32.

KOPELMAN, P. 2007. Health risks associated with overweight and obesity. *Obes Rev,* 8 Suppl 1**,** 13-7.

KORNER, J., INABNET, W., FEBRES, G., CONWELL, I. M., MCMAHON, D. J., SALAS, R., TAVERAS, C., SCHROPE, B. & BESSLER, M. 2009. Prospective study of gut hormone and metabolic changes after adjustable gastric banding and Roux-en-Y gastric bypass. *Int J Obes (Lond),* 33**,** 786-95.

KOSINSKI, J. R., HUBERT, J., CARRINGTON, P. E., CHICCHI, G. G., MU, J., MILLER, C., CAO, J., BIANCHI, E., PESSI, A., SINHAROY, R., MARSH, D. J. & POCAI, A. 2012. The glucagon receptor is involved in mediating the body weight-lowering effects of oxyntomodulin. *Obesity (Silver Spring),* 20**,** 1566-71.

KOTOWSKI, S. J., HOPF, F. W., SEIF, T., BONCI, A. & VON ZASTROW, M. 2011. Endocytosis promotes rapid dopaminergic signaling. *Neuron,* 71**,** 278-90.

KOVAL, A., AHMED, K. & KATANAEV, V. L. 2016. Inhibition of Wnt signalling and breast tumour growth by the multi-purpose drug suramin through suppression of heterotrimeric G proteins and Wnt endocytosis. *Biochem J,* 473**,** 371-81.

KREYMANN, B., WILLIAMS, G., GHATEI, M. A. & BLOOM, S. R. 1987. Glucagon-like peptide-1 7-36: a physiological incretin in man. *Lancet,* 2**,** 1300-4.

KROEGER, K. M., HANYALOGLU, A. C., SEEBER, R. M., MILES, L. E. & EIDNE, K. A. 2001. Constitutive and agonist-dependent homo-oligomerization of the thyrotropin-releasing hormone receptor. Detection in living cells using bioluminescence resonance energy transfer. *J Biol Chem,* 276**,** 12736-43.

KRUDEWIG, R., LANGER, B., VOGLER, O., MARKSCHIES, N., ERL, M., JAKOBS, K. H. & VAN KOPPEN, C. J. 2000. Distinct internalization of M2 muscarinic acetylcholine receptors confers selective and long-lasting desensitization of signaling to phospholipase C. *J Neurochem,* 74**,** 1721-30.

KRUPNICK, J. G. & BENOVIC, J. L. 1998. The role of receptor kinases and arrestins in G protein-coupled receptor regulation. *Annu Rev Pharmacol Toxicol,* 38**,** 289-319.

KUHRE, R. E., WEWER ALBRECHTSEN, N. J., DEACON, C. F., BALK-MOLLER, E., REHFELD, J. F., REIMANN, F., GRIBBLE, F. M. & HOLST, J. J. 2016. Peptide production and secretion in GLUTag, NCI-H716, and STC-1 cells: a comparison to native L-cells. *J Mol Endocrinol,* 56**,** 201-11.

KUMAR, P., LAU, C. S., MATHUR, M., WANG, P. & DEFEA, K. A. 2007. Differential effects of beta-arrestins on the internalization, desensitization and ERK1/2 activation downstream of protease activated receptor-2. *Am J Physiol Cell Physiol,* 293**,** C346-57.

KUMARI, P., SRIVASTAVA, A., GHOSH, E., RANJAN, R., DOGRA, S., YADAV, P. N. & SHUKLA, A. K. 2017. Core engagement with beta-arrestin is dispensable for agonist-induced vasopressin receptor endocytosis and ERK activation. *Mol Biol Cell,* 28**,** 1003-1010.

KUNA, R. S., GIRADA, S. B., ASALLA, S., VALLENTYNE, J., MADDIKA, S., PATTERSON, J. T., SMILEY, D. L., DIMARCHI, R. D. & MITRA, P. 2013. Glucagon-like peptide-1 receptor-mediated endosomal cAMP generation promotes glucose-stimulated insulin secretion in pancreatic beta-cells. *Am J Physiol Endocrinol Metab,* 305**,** E161-70.

LANKELMA, J. M., NIEUWDORP, M., DE VOS, W. M. & WIERSINGA, W. J. 2015. The gut microbiota in internal medicine: implications for health and disease. *Neth J Med,* 73**,** 61-8.

LAUFFER, B. E., MELERO, C., TEMKIN, P., LEI, C., HONG, W., KORTEMME, T. & VON ZASTROW, M. 2010. SNX27 mediates PDZ-directed sorting from endosomes to the plasma membrane. *J Cell Biol,* 190**,** 565-74.

LE POUL, E., LOISON, C., STRUYF, S., SPRINGAEL, J. Y., LANNOY, V., DECOBECQ, M. E., BREZILLON, S., DUPRIEZ, V., VASSART, G., VAN DAMME, J., PARMENTIER, M. & DETHEUX, M. 2003. Functional characterization of human receptors for short chain fatty acids and their role in polymorphonuclear cell activation. *J Biol Chem,* 278**,** 25481-9.

LE ROUX, C. W., PATTERSON, M., VINCENT, R. P., HUNT, C., GHATEI, M. A. & BLOOM, S. R. 2005. Postprandial plasma ghrelin is suppressed proportional to meal calorie content in normal-weight but not obese subjects. *J Clin Endocrinol Metab,* 90**,** 1068-71.

LEE, J. R., HAHN, H. S., KIM, Y. H., NGUYEN, H. H., YANG, J. M., KANG, J. S. & HAHN, M. J. 2011. Adaptor protein containing PH domain, PTB domain and leucine zipper (APPL1)

regulates the protein level of EGFR by modulating its trafficking. *Biochem Biophys Res Commun,* 415**,** 206-11.

LEE, S. P., SO, C. H., RASHID, A. J., VARGHESE, G., CHENG, R., LANCA, A. J., O'DOWD, B. F. & GEORGE, S. R. 2004. Dopamine D1 and D2 receptor Co-activation generates a novel phospholipase C-mediated calcium signal. *J Biol Chem,* 279**,** 35671-8.

LEE, S. U., IN, H. J., KWON, M. S., PARK, B. O., JO, M., KIM, M. O., CHO, S., LEE, S., LEE, H. J., KWAK, Y. S. & KIM, S. 2013. beta-Arrestin 2 mediates G protein-coupled receptor 43 signals to nuclear factor-kappaB. *Biol Pharm Bull,* 36**,** 1754-9.

LEE, T., SCHWANDNER, R., SWAMINATH, G., WEISZMANN, J., CARDOZO, M., GREENBERG, J., JAECKEL, P., GE, H., WANG, Y., JIAO, X., LIU, J., KAYSER, F., TIAN, H. & LI, Y. 2008. Identification and functional characterization of allosteric agonists for the G protein-coupled receptor FFA2. *Mol Pharmacol,* 74**,** 1599-609.

LEFKOWITZ, R. J. & SHENOY, S. K. 2005. Transduction of receptor signals by beta-arrestins. *Science,* 308**,** 512-7.

LEVIN, F., EDHOLM, T., SCHMIDT, P. T., GRYBACK, P., JACOBSSON, H., DEGERBLAD, M., HOYBYE, C., HOLST, J. J., REHFELD, J. F., HELLSTROM, P. M. & NASLUND, E. 2006. Ghrelin stimulates gastric emptying and hunger in normal-weight humans. *J Clin Endocrinol Metab,* 91**,** 3296-302.

LI, H., LI, H. F., FELDER, R. A., PERIASAMY, A. & JOSE, P. A. 2008. Rab4 and Rab11 coordinately regulate the recycling of angiotensin II type I receptor as demonstrated by fluorescence resonance energy transfer microscopy. *J Biomed Opt,* 13**,** 031206.

LI, J., JIA, H., CAI, X., ZHONG, H., FENG, Q., SUNAGAWA, S., ARUMUGAM, M., KULTIMA, J. R., PRIFTI, E., NIELSEN, T., JUNCKER, A. S., MANICHANH, C., CHEN, B., ZHANG, W., LEVENEZ, F., WANG, J., XU, X., XIAO, L., LIANG, S., ZHANG, D., ZHANG, Z., CHEN, W., ZHAO, H., AL-AAMA, J. Y., EDRIS, S., YANG, H., WANG, J., HANSEN, T., NIELSEN, H. B., BRUNAK, S., KRISTIANSEN, K., GUARNER, F., PEDERSEN, O., DORE, J., EHRLICH, S. D., BORK, P. & WANG, J. 2014. An integrated catalog of reference genes in the human gut microbiome. *Nat Biotechnol,* 32**,** 834-41.

LI, J., MAO, X., DONG, L. Q., LIU, F. & TONG, L. 2007. Crystal structures of the BAR-PH and PTB domains of human APPL1. *Structure,* 15**,** 525-33.

LI, M., VAN ESCH, B., WAGENAAR, G. T. M., GARSSEN, J., FOLKERTS, G. & HENRICKS, P. A. J. 2018. Pro- and anti-inflammatory effects of short chain fatty acids on immune and endothelial cells. *Eur J Pharmacol,* 831**,** 52-59.

LI, X., LETOURNEAU, D., HOLLERAN, B., LEDUC, R., LAVIGNE, P. & LAVOIE, C. 2017. Galphas protein binds ubiquitin to regulate epidermal growth factor receptor endosomal sorting. *Proc Natl Acad Sci U S A,* 114**,** 13477-13482.

LIM, G. E. & BRUBAKER, P. L. 2006. Glucagon-Like Peptide 1 Secretion by the L-Cell. *Diabetes,* 55**,** S70.

LIN, D. C., QUEVEDO, C., BREWER, N. E., BELL, A., TESTA, J. R., GRIMES, M. L., MILLER, F. D. & KAPLAN, D. R. 2006. APPL1 associates with TrkA and GIPC1 and is required for nerve growth factor-mediated signal transduction. *Mol Cell Biol,* 26**,** 8928-41.

LIU, L. L., LAWRENCE, J. M., DAVIS, C., LIESE, A. D., PETTITT, D. J., PIHOKER, C., DABELEA, D., HAMMAN, R., WAITZFELDER, B. & KAHN, H. S. 2010. Prevalence of overweight and obesity in youth with diabetes in USA: the SEARCH for Diabetes in Youth study. *Pediatr Diabetes,* 11**,** 4-11.

LIU, M., ZHOU, L., WEI, L., VILLARREAL, R., YANG, X., HU, D., RIOJAS, R. A., HOLMES, B. M., LANGLAIS, P. R., LEE, H. & DONG, L. Q. 2012. Phosphorylation of adaptor protein

containing pleckstrin homology domain, phosphotyrosine binding domain, and leucine zipper motif 1 (APPL1) at Ser430 mediates endoplasmic reticulum (ER) stress-induced insulin resistance in hepatocytes. *J Biol Chem,* 287**,** 26087-93.

LIU, S. H., HUANG, Y. W., WU, C. T., CHIU, C. Y. & CHIANG, M. T. 2013. Low molecular weight chitosan accelerates glucagon-like peptide-1 secretion in human intestinal endocrine cells via a p38-dependent pathway. *J Agric Food Chem,* 61**,** 4855-61.

LIU, Z., XIAO, T., PENG, X., LI, G. & HU, F. 2017. APPLs: More than just adiponectin receptor binding proteins. *Cell Signal,* 32**,** 76-84.

LIVAK, K. J. & SCHMITTGEN, T. D. 2001. Analysis of relative gene expression data using real-time quantitative PCR and the 2(-Delta Delta C(T)) Method. *Methods,* 25**,** 402-8.

LOBINGIER, B. T., HUTTENHAIN, R., EICHEL, K., MILLER, K. B., TING, A. Y., VON ZASTROW, M. & KROGAN, N. J. 2017. An Approach to Spatiotemporally Resolve Protein Interaction Networks in Living Cells. *Cell,* 169**,** 350-360.e12.

LODOWSKI, D. T., PITCHER, J. A., CAPEL, W. D., LEFKOWITZ, R. J. & TESMER, J. J. 2003. Keeping G proteins at bay: a complex between G protein-coupled receptor kinase 2 and Gbetagamma. *Science,* 300**,** 1256-62.

LOHSE, M. J., ANDEXINGER, S., PITCHER, J., TRUKAWINSKI, S., CODINA, J., FAURE, J. P., CARON, M. G. & LEFKOWITZ, R. J. 1992. Receptor-specific desensitization with purified proteins. Kinase dependence and receptor specificity of beta-arrestin and arrestin in the beta 2-adrenergic receptor and rhodopsin systems. *J Biol Chem,* 267**,** 8558-64.

LOHSE, M. J., NUBER, S. & HOFFMANN, C. 2012. Fluorescence/bioluminescence resonance energy transfer techniques to study G-protein-coupled receptor activation and signaling. *Pharmacol Rev,* 64**,** 299-336.

LUTTRELL, L. M. & LEFKOWITZ, R. J. 2002. The role of beta-arrestins in the termination and transduction of G-protein-coupled receptor signals. *J Cell Sci,* 115**,** 455-65.

LUTTRELL, L. M., ROUDABUSH, F. L., CHOY, E. W., MILLER, W. E., FIELD, M. E., PIERCE, K. L. & LEFKOWITZ, R. J. 2001. Activation and targeting of extracellular signal-regulated kinases by beta-arrestin scaffolds. *Proc Natl Acad Sci U S A,* 98**,** 2449-54.

LUTTRELL, L. M., WANG, J., PLOUFFE, B., SMITH, J. S., YAMANI, L., KAUR, S., JEAN-CHARLES, P. Y., GAUTHIER, C., LEE, M. H., PANI, B., KIM, J., AHN, S., RAJAGOPAL, S., REITER, E., BOUVIER, M., SHENOY, S. K., LAPORTE, S. A., ROCKMAN, H. A. & LEFKOWITZ, R. J. 2018. Manifold roles of beta-arrestins in GPCR signaling elucidated with siRNA and CRISPR/Cas9. *Sci Signal,* 11.

MACFARLANE, S. & MACFARLANE, G. T. 2003. Regulation of short-chain fatty acid production. *Proc Nutr Soc,* 62**,** 67-72.

MACIA, L., TAN, J., VIEIRA, A. T., LEACH, K., STANLEY, D., LUONG, S., MARUYA, M., IAN MCKENZIE, C., HIJIKATA, A., WONG, C., BINGE, L., THORBURN, A. N., CHEVALIER, N., ANG, C., MARINO, E., ROBERT, R., OFFERMANNS, S., TEIXEIRA, M. M., MOORE, R. J., FLAVELL, R. A., FAGARASAN, S. & MACKAY, C. R. 2015. Metabolite-sensing receptors GPR43 and GPR109A facilitate dietary fibre-induced gut homeostasis through regulation of the inflammasome. *Nat Commun,* 6**,** 6734.

MACLEAN, P. S., WING, R. R., DAVIDSON, T., EPSTEIN, L., GOODPASTER, B., HALL, K. D., LEVIN, B. E., PERRI, M. G., ROLLS, B. J., ROSENBAUM, M., ROTHMAN, A. J. & RYAN, D. 2015. NIH working group report: Innovative research to improve maintenance of weight loss. *Obesity (Silver Spring),* 23**,** 7-15.

MADSBAD, S. 2009. Exenatide and liraglutide: different approaches to develop GLP-1 receptor agonists (incretin mimetics)--preclinical and clinical results. *Best Pract Res Clin Endocrinol Metab,* 23**,** 463-77.

MAHMUD, Z. A., JENKINS, L., ULVEN, T., LABEGUERE, F., GOSMINI, R., DE VOS, S., HUDSON, B. D., TIKHONOVA, I. G. & MILLIGAN, G. 2017. Three classes of ligands each bind to distinct sites on the orphan G protein-coupled receptor GPR84. *Sci Rep,* 7**,** 17953.

MAKINO, H. & MALINOW, R. 2009. AMPA receptor incorporation into synapses during LTP: the role of lateral movement and exocytosis. *Neuron,* 64**,** 381-90.

MALBON, C. C. 2005. G proteins in development. *Nat Rev Mol Cell Biol,* 6**,** 689-701.

MAO, X., KIKANI, C. K., RIOJAS, R. A., LANGLAIS, P., WANG, L., RAMOS, F. J., FANG, Q., CHRIST-ROBERTS, C. Y., HONG, J. Y., KIM, R. Y., LIU, F. & DONG, L. Q. 2006. APPL1 binds to adiponectin receptors and mediates adiponectin signalling and function. *Nat Cell Biol,* 8**,** 516-23.

MARCHESE, A. & BENOVIC, J. L. 2001. Agonist-promoted ubiquitination of the G protein-coupled receptor CXCR4 mediates lysosomal sorting. *J Biol Chem,* 276**,** 45509-12.

MARCHESE, A., PAING, M. M., TEMPLE, B. R. & TREJO, J. 2008. G protein-coupled receptor sorting to endosomes and lysosomes. *Annu Rev Pharmacol Toxicol,* 48**,** 601-29.

MARCHESE, A. & TREJO, J. 2013. Ubiquitin-dependent regulation of G protein-coupled receptor trafficking and signaling. *Cell Signal,* 25**,** 707-16.

MARTINI, L., WALDHOER, M., PUSCH, M., KHARAZIA, V., FONG, J., LEE, J. H., FREISSMUTH, C. & WHISTLER, J. L. 2007. Ligand-induced down-regulation of the cannabinoid 1 receptor is mediated by the G-protein-coupled receptor-associated sorting protein GASP1. *Faseb j,* 21**,** 802-11.

MASLOWSKI, K. M., VIEIRA, A. T., NG, A., KRANICH, J., SIERRO, F., YU, D., SCHILTER, H. C., ROLPH, M. S., MACKAY, F., ARTIS, D., XAVIER, R. J., TEIXEIRA, M. M. & MACKAY, C. R. 2009. Regulation of inflammatory responses by gut microbiota and chemoattractant receptor GPR43. *Nature,* 461**,** 1282-6.

MATSON, C. A., REID, D. F., CANNON, T. A. & RITTER, R. C. 2000. Cholecystokinin and leptin act synergistically to reduce body weight. *Am J Physiol Regul Integr Comp Physiol,* 278**,** R882-90.

MAYOR, S., PARTON, R. G. & DONALDSON, J. G. 2014. Clathrin-independent pathways of endocytosis. *Cold Spring Harbor perspectives in biology,* 6**,** a016758.

MAZUY, C., HELLEBOID, A., STAELS, B. & LEFEBVRE, P. 2015. Nuclear bile acid signaling through the farnesoid X receptor. *Cell Mol Life Sci,* 72**,** 1631-50.

MCCLUSKEY, A., DANIEL, J. A., HADZIC, G., CHAU, N., CLAYTON, E. L., MARIANA, A., WHITING, A., GORGANI, N. N., LLOYD, J., QUAN, A., MOSHKANBARYANS, L., KRISHNAN, S., PERERA, S., CHIRCOP, M., VON KLEIST, L., MCGEACHIE, A. B., HOWES, M. T., PARTON, R. G., CAMPBELL, M., SAKOFF, J. A., WANG, X., SUN, J. Y., ROBERTSON, M. J., DEANE, F. M., NGUYEN, T. H., MEUNIER, F. A., COUSIN, M. A. & ROBINSON, P. J. 2013. Building a better dynasore: the dyngo compounds potently inhibit dynamin and endocytosis. *Traffic,* 14**,** 1272-89.

MCDANIEL, F. K., MOLDEN, B. M., MOHAMMAD, S., BALDINI, G., MCPIKE, L., NARDUCCI, P., GRANELL, S. & BALDINI, G. 2012. Constitutive cholesterol-dependent endocytosis of melanocortin-4 receptor (MC4R) is essential to maintain receptor responsiveness to alpha-melanocyte-stimulating hormone (alpha-MSH). *J Biol Chem,* 287**,** 21873-90.

MCDONALD, N. A., HENSTRIDGE, C. M., CONNOLLY, C. N. & IRVING, A. J. 2007. An essential role for constitutive endocytosis, but not activity, in the axonal targeting of the CB1 cannabinoid receptor. *Mol Pharmacol,* 71**,** 976-84.

MCGARVEY, J. C., XIAO, K., BOWMAN, S. L., MAMONOVA, T., ZHANG, Q., BISELLO, A., SNEDDON, W. B., ARDURA, J. A., JEAN-ALPHONSE, F., VILARDAGA, J. P., PUTHENVEEDU, M. A. & FRIEDMAN, P. A. 2016. Actin-Sorting Nexin 27 (SNX27)-Retromer Complex Mediates Rapid Parathyroid Hormone Receptor Recycling. *J Biol Chem,* 291**,** 10986-1002.

MCGAVIGAN, A. K. & MURPHY, K. G. 2012. Gut hormones: the future of obesity treatment? *Br J Clin Pharmacol,* 74**,** 911-9.

MCNEIL, N. I., CUMMINGS, J. H. & JAMES, W. P. 1979. Rectal absorption of short chain fatty acids in the absence of chloride. *Gut,* 20**,** 400-3.

MCNELIS, J. C., LEE, Y. S., MAYORAL, R., VAN DER KANT, R., JOHNSON, A. M., WOLLAM, J. & OLEFSKY, J. M. 2015. GPR43 Potentiates beta-Cell Function in Obesity. *Diabetes,* 64**,** 3203-17.

MEHTA, A., MARSO, S. P. & NEELAND, I. J. 2017. Liraglutide for weight management: a critical review of the evidence. *Obes Sci Pract,* 3**,** 3-14.

MIACZYNSKA, M., CHRISTOFORIDIS, S., GINER, A., SHEVCHENKO, A., UTTENWEILER-JOSEPH, S., HABERMANN, B., WILM, M., PARTON, R. G. & ZERIAL, M. 2004. APPL proteins link Rab5 to nuclear signal transduction via an endosomal compartment. *Cell,* 116**,** 445-56.

MICHINEAU, S., ALHENC-GELAS, F. & RAJERISON, R. M. 2006. Human bradykinin B2 receptor sialylation and N-glycosylation participate with disulfide bonding in surface receptor dimerization. *Biochemistry,* 45**,** 2699-707.

MIESENBOCK, G., DE ANGELIS, D. A. & ROTHMAN, J. E. 1998. Visualizing secretion and synaptic transmission with pH-sensitive green fluorescent proteins. *Nature,* 394**,** 192-5.

MILLIGAN, G. 2004. G protein-coupled receptors: oligomerisation and association with accessory proteins. *Semin Cell Dev Biol,* 15**,** 261.

MILLIGAN, G. 2007. G protein-coupled receptor dimerisation: molecular basis and relevance to function. *Biochim Biophys Acta,* 1768**,** 825-35.

MILLIGAN, G., BOLOGNINI, D. & SERGEEV, E. 2017. Ligands at the Free Fatty Acid Receptors 2/3 (GPR43/GPR41). *Handb Exp Pharmacol,* 236**,** 17-32.

MIN, L., LEUNG, Y. M., TOMAS, A., WATSON, R. T., GAISANO, H. Y., HALBAN, P. A., PESSIN, J. E. & HOU, J. C. 2007. Dynamin is functionally coupled to insulin granule exocytosis. *J Biol Chem,* 282**,** 33530-6.

MITSUUCHI, Y., JOHNSON, S. W., SONODA, G., TANNO, S., GOLEMIS, E. A. & TESTA, J. R. 1999. Identification of a chromosome 3p14.3-21.1 gene, APPL, encoding an adaptor molecule that interacts with the oncoprotein-serine/threonine kinase AKT2. *Oncogene,* 18**,** 4891-8.

MORAN, T. H., KATZ, L. F., PLATA-SALAMAN, C. R. & SCHWARTZ, G. J. 1998. Disordered food intake and obesity in rats lacking cholecystokinin A receptors. *Am J Physiol,* 274**,** R618-25.

MORAN, T. H. & KINZIG, K. P. 2004. Gastrointestinal satiety signals II. Cholecystokinin. *Am J Physiol Gastrointest Liver Physiol,* 286**,** G183-8.

MULLERSHAUSEN, F., ZECRI, F., CETIN, C., BILLICH, A., GUERINI, D. & SEUWEN, K. 2009. Persistent signaling induced by FTY720-phosphate is mediated by internalized S1P1 receptors. *Nat Chem Biol,* 5**,** 428-34.

MUNDELL, S. J., LUO, J., BENOVIC, J. L., CONLEY, P. B. & POOLE, A. W. 2006. Distinct clathrin-coated pits sort different G protein-coupled receptor cargo. *Traffic,* 7**,** 1420-31.

MURPHY, C. F., DOCHERTY, N. G. & LE ROUX, C. W. 2017. Liraglutide: another reason to target prediabetes? *Oncotarget,* 8**,** 99203-99204.

MURPHY, K. G. & BLOOM, S. R. 2006. Gut hormones and the regulation of energy homeostasis. *Nature,* 444**,** 854-9.

NAGATAKE, T., FUJITA, H., MINATO, N. & HAMAZAKI, Y. 2014. Enteroendocrine cells are specifically marked by cell surface expression of claudin-4 in mouse small intestine. *PLoS One,* 9**,** e90638.

NAKAGAWA, T. & ASAHI, M. 2013. beta1-adrenergic receptor recycles via a membranous organelle, recycling endosome, by binding with sorting nexin27. *J Membr Biol,* 246**,** 571-9.

NAKAGAWA, T., SAKURAI, T., NISHIOKA, T. & TOUHARA, K. 2005. Insect sex-pheromone signals mediated by specific combinations of olfactory receptors. *Science,* 307**,** 1638-42.

NASMAN, J., KUKKONEN, J. P., AMMOUN, S. & AKERMAN, K. E. 2001. Role of G-protein availability in differential signaling by alpha 2-adrenoceptors. *Biochem Pharmacol,* 62**,** 913-22.

NEVES, S. R., RAM, P. T. & IYENGAR, R. 2002. G protein pathways. *Science,* 296**,** 1636-9.

NGUYEN, D. M. & EL-SERAG, H. B. 2010. The epidemiology of obesity. *Gastroenterol Clin North Am,* 39**,** 1-7.

NILSSON, N. E., KOTARSKY, K., OWMAN, C. & OLDE, B. 2003. Identification of a free fatty acid receptor, FFA2R, expressed on leukocytes and activated by short-chain fatty acids. *Biochem Biophys Res Commun,* 303**,** 1047-52.

NILSSON, O., BILCHIK, A. J., GOLDENRING, J. R., BALLANTYNE, G. H., ADRIAN, T. E. & MODLIN, I. M. 1991. Distribution and immunocytochemical colocalization of peptide YY and enteroglucagon in endocrine cells of the rabbit colon. *Endocrinology,* 129**,** 139-48.

NISHIZAWA, N., NIIDA, A., MASUDA, Y., KUMANO, S., YOKOYAMA, K., HIRABAYASHI, H., AMANO, N., OHTAKI, T. & ASAMI, T. 2017. Antiobesity Effect of a Short-Length Peptide YY Analogue after Continuous Administration in Mice. *ACS Med Chem Lett,* 8**,** 628-631.

NOBLES, K. N., XIAO, K., AHN, S., SHUKLA, A. K., LAM, C. M., RAJAGOPAL, S., STRACHAN, R. T., HUANG, T. Y., BRESSLER, E. A., HARA, M. R., SHENOY, S. K., GYGI, S. P. & LEFKOWITZ, R. J. 2011. Distinct phosphorylation sites on the beta(2)-adrenergic receptor establish a barcode that encodes differential functions of beta-arrestin. *Sci Signal,* 4**,** ra51.

NOHR, M. K., PEDERSEN, M. H., GILLE, A., EGEROD, K. L., ENGELSTOFT, M. S., HUSTED, A. S., SICHLAU, R. M., GRUNDDAL, K. V., POULSEN, S. S., HAN, S., JONES, R. M., OFFERMANNS, S. & SCHWARTZ, T. W. 2013. GPR41/FFAR3 and GPR43/FFAR2 as cosensors for short-chain fatty acids in enteroendocrine cells vs FFAR3 in enteric neurons and FFAR2 in enteric leukocytes. *Endocrinology,* 154**,** 3552-64.

NORSKOV-LAURITSEN, L., THOMSEN, A. R. & BRAUNER-OSBORNE, H. 2014. G protein-coupled receptor signaling analysis using homogenous time-resolved Forster resonance energy transfer (HTRF(R)) technology. *Int J Mol Sci,* 15**,** 2554-72.

O'MALLEY, K. L., JONG, Y. J., GONCHAR, Y., BURKHALTER, A. & ROMANO, C. 2003. Activation of metabotropic glutamate receptor mGlu5 on nuclear membranes mediates intranuclear Ca2+ changes in heterologous cell types and neurons. *J Biol Chem,* 278**,** 28210-9.

OAKLEY, R. H., LAPORTE, S. A., HOLT, J. A., CARON, M. G. & BARAK, L. S. 2000. Differential affinities of visual arrestin, beta arrestin1, and beta arrestin2 for G protein-coupled receptors delineate two major classes of receptors. *J Biol Chem,* 275**,** 17201-10.

OFFERMANNS, S., COLLETTI, S. L., LOVENBERG, T. W., SEMPLE, G., WISE, A. & AP, I. J. 2011. International Union of Basic and Clinical Pharmacology. LXXXII: Nomenclature and Classification of Hydroxy-carboxylic Acid Receptors (GPR81, GPR109A, and GPR109B). *Pharmacol Rev,* 63**,** 269-90.

OK, H. G., KIM, S. Y., LEE, S. J., KIM, T. K., HUH, B. K. & KIM, K. H. 2018. Can oliceridine (TRV130), an ideal novel micro receptor G protein pathway selective (micro-GPS) modulator, provide analgesia without opioid-related adverse reactions? *Korean J Pain,* 31**,** 73-79.

OKAMOTO, Y., BERNSTEIN, J. D. & SHIKANO, S. 2013. Role of C-terminal membrane-proximal basic residues in cell surface trafficking of HIV coreceptor GPR15 protein. *J Biol Chem,* 288**,** 9189-99.

OKAZAKI, M., FERRANDON, S., VILARDAGA, J. P., BOUXSEIN, M. L., POTTS, J. T., JR. & GARDELLA, T. J. 2008. Prolonged signaling at the parathyroid hormone receptor by peptide ligands targeted to a specific receptor conformation. *Proc Natl Acad Sci U S A,* 105**,** 16525-30.

ORSKOV, C., RABENHOJ, L., WETTERGREN, A., KOFOD, H. & HOLST, J. J. 1994. Tissue and plasma concentrations of amidated and glycine-extended glucagon-like peptide I in humans. *Diabetes,* 43**,** 535-9.

OVERTON, H. A., FYFE, M. C. & REYNET, C. 2008. GPR119, a novel G protein-coupled receptor target for the treatment of type 2 diabetes and obesity. *Br J Pharmacol,* 153 Suppl 1**,** S76-81.

PAEK, J., KALOCSAY, M., STAUS, D. P., WINGLER, L., PASCOLUTTI, R., PAULO, J. A., GYGI, S. P. & KRUSE, A. C. 2017. Multidimensional Tracking of GPCR Signaling via Peroxidase-Catalyzed Proximity Labeling. *Cell,* 169**,** 338-349.e11.

PANDEY, K. 2009. Functional roles of short sequence motifs in the endocytosis of membrane receptors. *Front Biosience,* 14**,** 5339.

PARK, P. S., LODOWSKI, D. T. & PALCZEWSKI, K. 2008. Activation of G protein-coupled receptors: beyond two-state models and tertiary conformational changes. *Annu Rev Pharmacol Toxicol,* 48**,** 107-41.

PARKINSON, J. R., CHAUDHRI, O. B., KUO, Y. T., FIELD, B. C., HERLIHY, A. H., DHILLO, W. S., GHATEI, M. A., BLOOM, S. R. & BELL, J. D. 2009. Differential patterns of neuronal activation in the brainstem and hypothalamus following peripheral injection of GLP-1, oxyntomodulin and lithium chloride in mice detected by manganese-enhanced magnetic resonance imaging (MEMRI). *Neuroimage,* 44**,** 1022-31.

PERRY, S. J. & LEFKOWITZ, R. J. 2002. Arresting developments in heptahelical receptor signaling and regulation. *Trends Cell Biol,* 12**,** 130-8.

PETAJA-REPO, U. E., HOGUE, M., LAPERRIERE, A., BHALLA, S., WALKER, P. & BOUVIER, M. 2001. Newly synthesized human delta opioid receptors retained in the endoplasmic reticulum are retrotranslocated to the cytosol, deglycosylated, ubiquitinated, and degraded by the proteasome. *J Biol Chem,* 276**,** 4416-23.

PILECKA, I., SADOWSKI, L., KALAIDZIDIS, Y. & MIACZYNSKA, M. 2011. Recruitment of APPL1 to ubiquitin-rich aggresomes in response to proteasomal impairment. *Experimental cell research,* 317**,** 1093-1107.

PLUZNICK, J. L., PROTZKO, R. J., GEVORGYAN, H., PETERLIN, Z., SIPOS, A., HAN, J., BRUNET, I., WAN, L. X., REY, F., WANG, T., FIRESTEIN, S. J., YANAGISAWA, M., GORDON, J. I., EICHMANN, A., PETI-PETERDI, J. & CAPLAN, M. J. 2013. Olfactory receptor responding to gut microbiota-derived signals plays a role in renin secretion and blood pressure regulation. *Proc Natl Acad Sci U S A,* 110**,** 4410-5.

POEKER, S. A., GEIRNAERT, A., BERCHTOLD, L., GREPPI, A., KRYCH, L., STEINERT, R. E., DE WOUTERS, T. & LACROIX, C. 2018. Understanding the prebiotic potential of different dietary fibers using an in vitro continuous adult fermentation model (PolyFermS). *Sci Rep,* 8**,** 4318.

POLIDORI, D., SANGHVI, A., SEELEY, R. J. & HALL, K. D. 2016. How Strongly Does Appetite Counter Weight Loss? Quantification of the Feedback Control of Human Energy Intake. *Obesity (Silver Spring),* 24**,** 2289-2295.

POUTEAU, E., NGUYEN, P., BALLEVRE, O. & KREMPF, M. 2003. Production rates and metabolism of short-chain fatty acids in the colon and whole body using stable isotopes. *Proc Nutr Soc,* 62**,** 87-93.

PRIYADARSHINI, M., KOTLO, K. U., DUDEJA, P. K. & LAYDEN, B. T. 2018. Role of Short Chain Fatty Acid Receptors in Intestinal Physiology and Pathophysiology. *Compr Physiol,* 8**,** 1091-1115.

PRIYADARSHINI, M., VILLA, S. R., FULLER, M., WICKSTEED, B., MACKAY, C. R., ALQUIER, T., POITOUT, V., MANCEBO, H., MIRMIRA, R. G., GILCHRIST, A. & LAYDEN, B. T. 2015. An Acetate-Specific GPCR, FFAR2, Regulates Insulin Secretion. *Mol Endocrinol,* 29**,** 1055-1066.

PSICHAS, A. 2013. *The role of short chain fatty acids in appetite regulation.* Doctoral, Imperial College London.

PSICHAS, A., SLEETH, M. L., MURPHY, K. G., BROOKS, L., BEWICK, G. A., HANYALOGLU, A. C., GHATEI, M. A., BLOOM, S. R. & FROST, G. 2015. The short chain fatty acid propionate stimulates GLP-1 and PYY secretion via free fatty acid receptor 2 in rodents. *Int J Obes (Lond),* 39**,** 424-9.

PUHL, H. L., 3RD, WON, Y.-J., LU, V. B. & IKEDA, S. R. 2015. Human GPR42 is a transcribed multisite variant that exhibits copy number polymorphism and is functional when heterologously expressed. *Scientific reports,* 5**,** 12880-12880.

PUTHENVEEDU, M. A., LAUFFER, B., TEMKIN, P., VISTEIN, R., CARLTON, P., THORN, K., TAUNTON, J., WEINER, O. D., PARTON, R. G. & VON ZASTROW, M. 2010. Sequence-dependent sorting of recycling proteins by actin-stabilized endosomal microdomains. *Cell,* 143**,** 761-73.

QIAN, J., WU, C., CHEN, X., LI, X., YING, G., JIN, L., MA, Q., LI, G., SHI, Y., ZHANG, G. & ZHOU, N. 2014. Differential requirements of arrestin-3 and clathrin for ligand-dependent and -independent internalization of human G protein-coupled receptor 40. *Cell Signal,* 26**,** 2412-23.

RAIBORG, C. & STENMARK, H. 2009. The ESCRT machinery in endosomal sorting of ubiquitylated membrane proteins. *Nature,* 458**,** 445-52.
RAISLEY, B., ZHANG, M., HERELD, D. & HADWIGER, J. A. 2004. A cAMP receptor-like G protein-coupled receptor with roles in growth regulation and development. *Dev Biol,* 265**,** 433-45.
RANJAN, R., GUPTA, P. & SHUKLA, A. K. 2016. GPCR Signaling: beta-arrestins Kiss and Remember. *Curr Biol,* 26**,** R285-8.
RANKOVIC, Z., BRUST, T. F. & BOHN, L. M. 2016. Biased agonism: An emerging paradigm in GPCR drug discovery. *Bioorg Med Chem Lett,* 26**,** 241-250.
RASHID, S., PILECKA, I., TORUN, A., OLCHOWIK, M., BIELINSKA, B. & MIACZYNSKA, M. 2009. Endosomal adaptor proteins APPL1 and APPL2 are novel activators of beta-catenin/TCF-mediated transcription. *The Journal of biological chemistry,* 284**,** 18115-18128.
RASMUSSEN, S. G., DEVREE, B. T., ZOU, Y., KRUSE, A. C., CHUNG, K. Y., KOBILKA, T. S., THIAN, F. S., CHAE, P. S., PARDON, E., CALINSKI, D., MATHIESEN, J. M., SHAH, S. T., LYONS, J. A., CAFFREY, M., GELLMAN, S. H., STEYAERT, J., SKINIOTIS, G., WEIS, W. I., SUNAHARA, R. K. & KOBILKA, B. K. 2011. Crystal structure of the beta2 adrenergic receptor-Gs protein complex. *Nature,* 477**,** 549-55.
REIDELBERGER, R. D., HAVER, A. C., CHELIKANI, P. K. & BUESCHER, J. L. 2008. Effects of different intermittent peptide YY (3-36) dosing strategies on food intake, body weight, and adiposity in diet-induced obese rats. *Am J Physiol Regul Integr Comp Physiol,* 295**,** R449-58.
REIMANN, F., HABIB, A. M., TOLHURST, G., PARKER, H. E., ROGERS, G. J. & GRIBBLE, F. M. 2008. Glucose sensing in L cells: a primary cell study. *Cell Metab,* 8**,** 532-9.
REIMANN, F., TOLHURST, G. & GRIBBLE, F. M. 2012. G-protein-coupled receptors in intestinal chemosensation. *Cell Metabolism,* 15**,** 421-31.
REIMANN, F., WARD, P. S. & GRIBBLE, F. M. 2006. Signaling Mechanisms Underlying the Release of Glucagon-Like Peptide 1. *Diabetes,* 55**,** S78.
REIMER, R. A. 2006. Meat hydrolysate and essential amino acid-induced glucagon-like peptide-1 secretion, in the human NCI-H716 enteroendocrine cell line, is regulated by extracellular signal-regulated kinase1/2 and p38 mitogen-activated protein kinases. *J Endocrinol,* 191**,** 159-170.
REYES-TURCU, F. E., VENTII, K. H. & WILKINSON, K. D. 2009. Regulation and cellular roles of ubiquitin-specific deubiquitinating enzymes. *Annu Rev Biochem,* 78**,** 363-97.
RICHARDSON, M. D., BALIUS, A. M., YAMAGUCHI, K., FREILICH, E. R., BARAK, L. S. & KWATRA, M. M. 2003. Human substance P receptor lacking the C-terminal domain remains competent to desensitize and internalize. *J Neurochem,* 84**,** 854-63.
RINK, J., GHIGO, E., KALAIDZIDIS, Y. & ZERIAL, M. 2005. Rab conversion as a mechanism of progression from early to late endosomes. *Cell,* 122**,** 735-49.
ROBERTSON, M. D., BICKERTON, A. S., DENNIS, A. L., VIDAL, H. & FRAYN, K. N. 2005. Insulin-sensitizing effects of dietary resistant starch and effects on skeletal muscle and adipose tissue metabolism. *Am J Clin Nutr,* 82**,** 559-67.
ROMAN-VENDRELL, C., YU, Y. J. & YUDOWSKI, G. A. 2012. Fast modulation of mu-opioid receptor (MOR) recycling is mediated by receptor agonists. *J Biol Chem,* 287**,** 14782-91.

ROMERO, G., VON ZASTROW, M. & FRIEDMAN, P. A. 2011. Role of PDZ proteins in regulating trafficking, signaling, and function of GPCRs: means, motif, and opportunity. *Adv Pharmacol,* 62**,** 279-314.

ROSCIGLIONE, S., THERIAULT, C., BOILY, M. O., PAQUETTE, M. & LAVOIE, C. 2014. Galphas regulates the post-endocytic sorting of G protein-coupled receptors. *Nat Commun,* 5**,** 4556.

ROSENBLATT, M. 2009. When two keys fit one lock, surprises follow. *Nature Chemical Biology,* 5**,** 707.

ROZENFELD, R. & DEVI, L. A. 2007. Receptor heterodimerization leads to a switch in signaling: beta-arrestin2-mediated ERK activation by mu-delta opioid receptor heterodimers. *Faseb j,* 21**,** 2455-65.

RYU, J., GALAN, A. K., XIN, X., DONG, F., ABDUL-GHANI, M. A., ZHOU, L., WANG, C., LI, C., HOLMES, B. M., SLOANE, L. B., AUSTAD, S. N., GUO, S., MUSI, N., DEFRONZO, R. A., DENG, C., WHITE, M. F., LIU, F. & DONG, L. Q. 2014. APPL1 potentiates insulin sensitivity by facilitating the binding of IRS1/2 to the insulin receptor. *Cell Rep,* 7**,** 1227-38.

SAMAMA, P., COTECCHIA, S., COSTA, T. & LEFKOWITZ, R. J. 1993. A mutation-induced activated state of the beta 2-adrenergic receptor. Extending the ternary complex model. *J Biol Chem,* 268**,** 4625-36.

SASSMANN, A., GIER, B., GRONE, H. J., DREWS, G., OFFERMANNS, S. & WETTSCHURECK, N. 2010. The Gq/G11-mediated signaling pathway is critical for autocrine potentiation of insulin secretion in mice. *J Clin Invest,* 120**,** 2184-93.

SATAKE, H., MATSUBARA, S., AOYAMA, M., KAWADA, T. & SAKAI, T. 2013. GPCR Heterodimerization in the Reproductive System: Functional Regulation and Implication for Biodiversity. *Front Endocrinol (Lausanne),* 4**,** 100-100.

SATO, Y., NENQUIN, M. & HENQUIN, J. C. 1998. Relative contribution of Ca2+-dependent and Ca2+-independent mechanisms to the regulation of insulin secretion by glucose. *FEBS Lett,* 421**,** 115-9.

SAWZDARGO, M., GEORGE, S. R., NGUYEN, T., XU, S., KOLAKOWSKI, L. F. & O'DOWD, B. F. 1997. A cluster of four novel human G protein-coupled receptor genes occurring in close proximity to CD22 gene on chromosome 19q13.1. *Biochem Biophys Res Commun,* 239**,** 543-7.

SCARSELLI, M. & DONALDSON, J. G. 2009. Constitutive internalization of G protein-coupled receptors and G proteins via clathrin-independent endocytosis. *The Journal of biological chemistry,* 284**,** 3577-3585.

SCHEFFZEK, K. & WELTI, S. 2012. Pleckstrin homology (PH) like domains - versatile modules in protein-protein interaction platforms. *FEBS Lett,* 586**,** 2662-73.

SCHENCK, A., GOTO-SILVA, L., COLLINET, C., RHINN, M., GINER, A., HABERMANN, B., BRAND, M. & ZERIAL, M. 2008. The endosomal protein Appl1 mediates Akt substrate specificity and cell survival in vertebrate development. *Cell,* 133**,** 486-97.

SCHEPPACH, W. 1994. Effects of short chain fatty acids on gut morphology and function. *Gut,* 35**,** S35-8.

SCHMIDT, A. & HALL, A. 2002. Guanine nucleotide exchange factors for Rho GTPases: turning on the switch. *Genes Dev,* 16**,** 1587-609.

SCHMIDT, J., SMITH, N. J., CHRISTIANSEN, E., TIKHONOVA, I. G., GRUNDMANN, M., HUDSON, B. D., WARD, R. J., DREWKE, C., MILLIGAN, G., KOSTENIS, E. & ULVEN, T. 2011. Selective orthosteric free fatty acid receptor 2 (FFA2) agonists: identification of

the structural and chemical requirements for selective activation of FFA2 versus FFA3. *J Biol Chem,* 286**,** 10628-40.
SCHOFIELD, Z. V., CROKER, D., ROBERTSON, A. A. B., MASSEY, N. L., DONOVAN, C., TEE, E., EDWARDS, D., WOODRUFF, T. M., HALAI, R., HANSBRO, P. M. & COOPER, M. A. 2018. Characterisation of small molecule ligands 4CMTB and 2CTAP as modulators of human FFA2 receptor signalling. *Scientific reports,* 8**,** 17819.
SCHWARTZ, M. W., SIPOLS, A. J., MARKS, J. L., SANACORA, G., WHITE, J. D., SCHEURINK, A., KAHN, S. E., BASKIN, D. G., WOODS, S. C., FIGLEWICZ, D. P. & ET AL. 1992. Inhibition of hypothalamic neuropeptide Y gene expression by insulin. *Endocrinology,* 130**,** 3608-16.
SEACHRIST, J. L., ANBORGH, P. H. & FERGUSON, S. S. 2000. beta 2-adrenergic receptor internalization, endosomal sorting, and plasma membrane recycling are regulated by rab GTPases. *J Biol Chem,* 275**,** 27221-8.
SEAMAN, M. N. 2012. The retromer complex - endosomal protein recycling and beyond. *J Cell Sci,* 125**,** 4693-702.
SEAMAN, M. N., MCCAFFERY, J. M. & EMR, S. D. 1998. A membrane coat complex essential for endosome-to-Golgi retrograde transport in yeast. *J Cell Biol,* 142**,** 665-81.
SHENG, M. & SALA, C. 2001. PDZ domains and the organization of supramolecular complexes. *Annu Rev Neurosci,* 24**,** 1-29.
SHENOY, S. K. 2007. Seven-transmembrane receptors and ubiquitination. *Circ Res,* 100**,** 1142-54.
SHENOY, S. K., MCDONALD, P. H., KOHOUT, T. A. & LEFKOWITZ, R. J. 2001. Regulation of receptor fate by ubiquitination of activated beta 2-adrenergic receptor and beta-arrestin. *Science,* 294**,** 1307-13.
SHUKLA, A. K., WESTFIELD, G. H., XIAO, K., REIS, R. I., HUANG, L. Y., TRIPATHI-SHUKLA, P., QIAN, J., LI, S., BLANC, A., OLESKIE, A. N., DOSEY, A. M., SU, M., LIANG, C. R., GU, L. L., SHAN, J. M., CHEN, X., HANNA, R., CHOI, M., YAO, X. J., KLINK, B. U., KAHSAI, A. W., SIDHU, S. S., KOIDE, S., PENCZEK, P. A., KOSSIAKOFF, A. A., WOODS, V. L., JR., KOBILKA, B. K., SKINIOTIS, G. & LEFKOWITZ, R. J. 2014. Visualization of arrestin recruitment by a G-protein-coupled receptor. *Nature,* 512**,** 218-222.
SIEHLER, S. 2007. G12/13-dependent signaling of G-protein-coupled receptors: disease context and impact on drug discovery. *Expert Opin Drug Discov,* 2**,** 1591-604.
SIMPSON, A. K., WARD, P. S., WONG, K. Y., COLLORD, G. J., HABIB, A. M., REIMANN, F. & GRIBBLE, F. M. 2007. Cyclic AMP triggers glucagon-like peptide-1 secretion from the GLUTag enteroendocrine cell line. *Diabetologia,* 50**,** 2181-9.
SINA, C., GAVRILOVA, O., FORSTER, M., TILL, A., DERER, S., HILDEBRAND, F., RAABE, B., CHALARIS, A., SCHELLER, J., REHMANN, A., FRANKE, A., OTT, S., HASLER, R., NIKOLAUS, S., FOLSCH, U. R., ROSE-JOHN, S., JIANG, H. P., LI, J., SCHREIBER, S. & ROSENSTIEL, P. 2009. G protein-coupled receptor 43 is essential for neutrophil recruitment during intestinal inflammation. *J Immunol,* 183**,** 7514-22.
SIPOLS, A. J., BASKIN, D. G. & SCHWARTZ, M. W. 1995. Effect of intracerebroventricular insulin infusion on diabetic hyperphagia and hypothalamic neuropeptide gene expression. *Diabetes,* 44**,** 147-51.
SMITH, G. P., JEROME, C., CUSHIN, B. J., ETERNO, R. & SIMANSKY, K. J. 1981. Abdominal vagotomy blocks the satiety effect of cholecystokinin in the rat. *Science,* 213**,** 1036-7.
SMITH, N. J. & MILLIGAN, G. 2010. Allostery at G protein-coupled receptor homo- and heteromers: uncharted pharmacological landscapes. *Pharmacol Rev,* 62**,** 701-25.

SMITH, N. J., WARD, R. J., STODDART, L. A., HUDSON, B. D., KOSTENIS, E., ULVEN, T., MORRIS, J. C., TRANKLE, C., TIKHONOVA, I. G., ADAMS, D. R. & MILLIGAN, G. 2011. Extracellular loop 2 of the free fatty acid receptor 2 mediates allosterism of a phenylacetamide ago-allosteric modulator. *Mol Pharmacol,* 80**,** 163-73.

SMITH, P. M., HOWITT, M. R., PANIKOV, N., MICHAUD, M., GALLINI, C. A., BOHLOOLY, Y. M., GLICKMAN, J. N. & GARRETT, W. S. 2013. The microbial metabolites, short-chain fatty acids, regulate colonic Treg cell homeostasis. *Science,* 341**,** 569-73.

SMITH, S. R., GARVEY, W. T., GREENWAY, F. L., ZHOU, S., FAIN, R., PILSON, R., FUJIOKA, K. & ARONNE, L. J. 2017. Coadministration of lorcaserin and phentermine for weight management: A 12-week, randomized, pilot safety study. *Obesity (Silver Spring),* 25**,** 857-865.

SMITH, S. R., WEISSMAN, N. J., ANDERSON, C. M., SANCHEZ, M., CHUANG, E., STUBBE, S., BAYS, H., SHANAHAN, W. R., BEHAVIORAL, M., LORCASERIN FOR, O. & OBESITY MANAGEMENT STUDY, G. 2010. Multicenter, placebo-controlled trial of lorcaserin for weight management. *N Engl J Med,* 363**,** 245-56.

SMRCKA, A. V. 2008. G protein betagamma subunits: central mediators of G protein-coupled receptor signaling. *Cellular and Molecular Life Sciences,* 65**,** 2191-214.

SPOSINI, S., JEAN-ALPHONSE, F. G., AYOUB, M. A., OQUA, A., WEST, C., LAVERY, S., BROSENS, J. J., REITER, E. & HANYALOGLU, A. C. 2017. Integration of GPCR Signaling and Sorting from Very Early Endosomes via Opposing APPL1 Mechanisms. *Cell Rep,* 21**,** 2855-2867.

SPRECKLEY, E. & MURPHY, K. G. 2015. The L-Cell in Nutritional Sensing and the Regulation of Appetite. *Front Nutr,* 2**,** 23.

SRIVASTAVA, A., GUPTA, B., GUPTA, C. & SHUKLA, A. K. 2015. Emerging Functional Divergence of beta-Arrestin Isoforms in GPCR Function. *Trends Endocrinol Metab,* 26**,** 628-642.

STEGENGA, H., HAINES, A., JONES, K., WILDING, J. & GUIDELINE DEVELOPMENT, G. 2014. Identification, assessment, and management of overweight and obesity: summary of updated NICE guidance. *BMJ,* 349**,** g6608.

STEINERT, R. E., POLLER, B., CASTELLI, M. C., DREWE, J. & BEGLINGER, C. 2010. Oral administration of glucagon-like peptide 1 or peptide YY 3-36 affects food intake in healthy male subjects. *Am J Clin Nutr,* 92**,** 810-7.

STEVENS, R. C., CHEREZOV, V., KATRITCH, V., ABAGYAN, R., KUHN, P., ROSEN, H. & WUTHRICH, K. 2013. The GPCR Network: a large-scale collaboration to determine human GPCR structure and function. *Nat Rev Drug Discov,* 12**,** 25-34.

STUMPEL, F., BURCELIN, R., JUNGERMANN, K. & THORENS, B. 2001. Normal kinetics of intestinal glucose absorption in the absence of GLUT2: evidence for a transport pathway requiring glucose phosphorylation and transfer into the endoplasmic reticulum. *Proc Natl Acad Sci U S A,* 98**,** 11330-5.

SUMITHRAN, P., PRENDERGAST, L. A., DELBRIDGE, E., PURCELL, K., SHULKES, A., KRIKETOS, A. & PROIETTO, J. 2011. Long-term persistence of hormonal adaptations to weight loss. *N Engl J Med,* 365**,** 1597-604.

SUOFU, Y., LI, W., JEAN-ALPHONSE, F. G., JIA, J., KHATTAR, N. K., LI, J., BARANOV, S. V., LERONNI, D., MIHALIK, A. C., HE, Y., CECON, E., WEHBI, V. L., KIM, J., HEATH, B. E., BARANOVA, O. V., WANG, X., GABLE, M. J., KRETZ, E. S., DI BENEDETTO, G., LEZON, T. R., FERRANDO, L. M., LARKIN, T. M., SULLIVAN, M., YABLONSKA, S., WANG, J., MINNIGH, M. B., GUILLAUMET, G., SUZENET, F., RICHARDSON, R. M., POLOYAC, S.

M., STOLZ, D. B., JOCKERS, R., WITT-ENDERBY, P. A., CARLISLE, D. L., VILARDAGA, J. P. & FRIEDLANDER, R. M. 2017. Dual role of mitochondria in producing melatonin and driving GPCR signaling to block cytochrome c release. *Proc Natl Acad Sci U S A,* 114**,** E7997-e8006.

SUZUKI, K., JAYASENA, C. N. & BLOOM, S. R. 2011. The gut hormones in appetite regulation. *J Obes,* 2011**,** 528401.

SZENTMIKLOSI, A. J., GALAJDA, Z., CSEPPENTO, A., GESZTELYI, R., SUSAN, Z., HEGYI, B. & NANASI, P. P. 2015. The Janus face of adenosine: antiarrhythmic and proarrhythmic actions. *Curr Pharm Des,* 21**,** 965-76.

SZIDONYA, L., CSERZO, M. & HUNYADY, L. 2008. Dimerization and oligomerization of G-protein-coupled receptors: debated structures with established and emerging functions. *J Endocrinol,* 196**,** 435-53.

TAELMAN, V. F., DOBROWOLSKI, R., PLOUHINEC, J. L., FUENTEALBA, L. C., VORWALD, P. P., GUMPER, I., SABATINI, D. D. & DE ROBERTIS, E. M. 2010. Wnt signaling requires sequestration of glycogen synthase kinase 3 inside multivesicular endosomes. *Cell,* 143**,** 1136-48.

TAGGART, A. K., KERO, J., GAN, X., CAI, T. Q., CHENG, K., IPPOLITO, M., REN, N., KAPLAN, R., WU, K., WU, T. J., JIN, L., LIAW, C., CHEN, R., RICHMAN, J., CONNOLLY, D., OFFERMANNS, S., WRIGHT, S. D. & WATERS, M. G. 2005. (D)-beta-Hydroxybutyrate inhibits adipocyte lipolysis via the nicotinic acid receptor PUMA-G. *J Biol Chem,* 280**,** 26649-52.

TAKEBE, K., NIO, J., MORIMATSU, M., KARAKI, S., KUWAHARA, A., KATO, I. & IWANAGA, T. 2005. Histochemical demonstration of a Na(+)-coupled transporter for short-chain fatty acids (slc5a8) in the intestine and kidney of the mouse. *Biomed Res,* 26**,** 213-21.

TAN, T., BEHARY, P., THARAKAN, G., MINNION, J., AL-NAJIM, W., ALBRECHTSEN, N. J. W., HOLST, J. J. & BLOOM, S. R. 2017. The Effect of a Subcutaneous Infusion of GLP-1, OXM, and PYY on Energy Intake and Expenditure in Obese Volunteers. *J Clin Endocrinol Metab,* 102**,** 2364-2372.

TANG, C., AHMED, K., GILLE, A., LU, S., GRONE, H. J., TUNARU, S. & OFFERMANNS, S. 2015. Loss of FFA2 and FFA3 increases insulin secretion and improves glucose tolerance in type 2 diabetes. *Nat Med,* 21**,** 173-7.

TANG, W. J. & HURLEY, J. H. 1998. Catalytic mechanism and regulation of mammalian adenylyl cyclases. *Mol Pharmacol,* 54**,** 231-40.

TANOWITZ, M. & VON ZASTROW, M. 2003. A novel endocytic recycling signal that distinguishes the membrane trafficking of naturally occurring opioid receptors. *J Biol Chem,* 278**,** 45978-86.

TAPPE-THEODOR, A., AGARWAL, N., KATONA, I., RUBINO, T., MARTINI, L., SWIERCZ, J., MACKIE, K., MONYER, H., PAROLARO, D., WHISTLER, J., KUNER, T. & KUNER, R. 2007. A molecular basis of analgesic tolerance to cannabinoids. *J Neurosci,* 27**,** 4165-77.

TEMKIN, P., LAUFFER, B., JAGER, S., CIMERMANCIC, P., KROGAN, N. J. & VON ZASTROW, M. 2011. SNX27 mediates retromer tubule entry and endosome-to-plasma membrane trafficking of signalling receptors. *Nat Cell Biol,* 13**,** 715-21.

TERRILLON, S., DURROUX, T., MOUILLAC, B., BREIT, A., AYOUB, M. A., TAULAN, M., JOCKERS, R., BARBERIS, C. & BOUVIER, M. 2003. Oxytocin and vasopressin V1a and V2 receptors form constitutive homo- and heterodimers during biosynthesis. *Mol Endocrinol,* 17**,** 677-91.

TETSUKA, M., SAITO, Y., IMAI, K., DOI, H. & MARUYAMA, K. 2004. The basic residues in the membrane-proximal C-terminal tail of the rat melanin-concentrating hormone receptor 1 are required for receptor function. *Endocrinology,* 145**,** 3712-23.

THANAWALA, V. J., FORKUO, G. S., STALLAERT, W., LEFF, P., BOUVIER, M. & BOND, R. 2014. Ligand bias prevents class equality among beta-blockers. *Curr Opin Pharmacol,* 16**,** 50-7.

THOMPSON, D., MCARTHUR, S., HISLOP, J. N., FLOWER, R. J. & PERRETTI, M. 2014. Identification of a novel recycling sequence in the C-tail of FPR2/ALX receptor: association with cell protection from apoptosis. *J Biol Chem,* 289**,** 36166-78.

THOMSEN, A. R. B., JENSEN, D. D., HICKS, G. A. & BUNNETT, N. W. 2018. Therapeutic Targeting of Endosomal G-Protein-Coupled Receptors. *Trends Pharmacol Sci,* 39**,** 879-891.

THOMSEN, A. R. B., PLOUFFE, B., CAHILL, T. J., 3RD, SHUKLA, A. K., TARRASCH, J. T., DOSEY, A. M., KAHSAI, A. W., STRACHAN, R. T., PANI, B., MAHONEY, J. P., HUANG, L., BRETON, B., HEYDENREICH, F. M., SUNAHARA, R. K., SKINIOTIS, G., BOUVIER, M. & LEFKOWITZ, R. J. 2016. GPCR-G Protein-beta-Arrestin Super-Complex Mediates Sustained G Protein Signaling. *Cell,* 166**,** 907-919.

TIKHONOVA, I. G. 2017. Application of GPCR Structures for Modelling of Free Fatty Acid Receptors. *Handb Exp Pharmacol,* 236**,** 57-77.

TOBIN, A. B., BUTCHER, A. J. & KONG, K. C. 2008. Location, location, location...site-specific GPCR phosphorylation offers a mechanism for cell-type-specific signalling. *Trends Pharmacol Sci,* 29**,** 413-20.

TOBIN, A. B. & WHEATLEY, M. 2004. G-protein-coupled receptor phosphorylation and palmitoylation. *Methods Mol Biol,* 259**,** 275-81.

TOHGO, A., CHOY, E. W., GESTY-PALMER, D., PIERCE, K. L., LAPORTE, S., OAKLEY, R. H., CARON, M. G., LEFKOWITZ, R. J. & LUTTRELL, L. M. 2003. The stability of the G protein-coupled receptor-beta-arrestin interaction determines the mechanism and functional consequence of ERK activation. *J Biol Chem,* 278**,** 6258-67.

TOLHURST, G., HEFFRON, H., LAM, Y. S., PARKER, H. E., HABIB, A. M., DIAKOGIANNAKI, E., CAMERON, J., GROSSE, J., REIMANN, F. & GRIBBLE, F. M. 2012. Short-chain fatty acids stimulate glucagon-like peptide-1 secretion via the G-protein-coupled receptor FFAR2. *Diabetes,* 61**,** 364-71.

TORGERSON, J. S., HAUPTMAN, J., BOLDRIN, M. N. & SJOSTROM, L. 2004. XENical in the prevention of diabetes in obese subjects (XENDOS) study: a randomized study of orlistat as an adjunct to lifestyle changes for the prevention of type 2 diabetes in obese patients. *Diabetes Care,* 27**,** 155-61.

TREJO, J. 2005. Internal PDZ ligands: novel endocytic recycling motifs for G protein-coupled receptors. *Mol Pharmacol,* 67**,** 1388-90.

TROMPETTE, A., GOLLWITZER, E. S., YADAVA, K., SICHELSTIEL, A. K., SPRENGER, N., NGOM-BRU, C., BLANCHARD, C., JUNT, T., NICOD, L. P., HARRIS, N. L. & MARSLAND, B. J. 2014. Gut microbiota metabolism of dietary fiber influences allergic airway disease and hematopoiesis. *Nat Med,* 20**,** 159-66.

TSVETANOVA, N. G., TRESTER-ZEDLITZ, M., NEWTON, B. W., RIORDAN, D. P., SUNDARAM, A. B., JOHNSON, J. R., KROGAN, N. J. & VON ZASTROW, M. 2017. G Protein-Coupled Receptor Endocytosis Confers Uniformity in Responses to Chemically Distinct Ligands. *Mol Pharmacol,* 91**,** 145-156.

TSVETANOVA, N. G. & VON ZASTROW, M. 2014. Spatial encoding of cyclic AMP signaling specificity by GPCR endocytosis. *Nat Chem Biol,* 10**,** 1061-5.
TURNBAUGH, P. J. & GORDON, J. I. 2009. The core gut microbiome, energy balance and obesity. *J Physiol,* 587**,** 4153-8.
UNETT, D. J., GATLIN, J., ANTHONY, T. L., BUZARD, D. J., CHANG, S., CHEN, C., CHEN, X., DANG, H. T., FRAZER, J., LE, M. K., SADEQUE, A. J., XING, C. & GAIDAROV, I. 2013. Kinetics of 5-HT2B receptor signaling: profound agonist-dependent effects on signaling onset and duration. *J Pharmacol Exp Ther,* 347**,** 645-59.
UWADA, J., YOSHIKI, H., MASUOKA, T., NISHIO, M. & MURAMATSU, I. 2014. Intracellular localization of the M1 muscarinic acetylcholine receptor through clathrin-dependent constitutive internalization is mediated by a C-terminal tryptophan-based motif. *J Cell Sci,* 127**,** 3131-40.
VALASSI, E., SCACCHI, M. & CAVAGNINI, F. 2008. Neuroendocrine control of food intake. *Nutr Metab Cardiovasc Dis,* 18**,** 158-68.
VAN KOPPEN, C. J. & JAKOBS, K. H. 2004. Arrestin-independent internalization of G protein-coupled receptors. *Mol Pharmacol,* 66**,** 365-7.
VARSANO, T., TAUPIN, V., GUO, L., BATERINA, O. Y., JR. & FARQUHAR, M. G. 2012. The PDZ protein GIPC regulates trafficking of the LPA1 receptor from APPL signaling endosomes and attenuates the cell's response to LPA. *PLoS One,* 7**,** e49227.
VENKATESAN, S., PETROVIC, A., LOCATI, M., KIM, Y. O., WEISSMAN, D. & MURPHY, P. M. 2001. A membrane-proximal basic domain and cysteine cluster in the C-terminal tail of CCR5 constitute a bipartite motif critical for cell surface expression. *J Biol Chem,* 276**,** 40133-45.
VILLA, S. R., PRIYADARSHINI, M., FULLER, M. H., BHARDWAJ, T., BRODSKY, M. R., ANGUEIRA, A. R., MOSSER, R. E., CARBONEAU, B. A., TERSEY, S. A., MANCEBO, H., GILCHRIST, A., MIRMIRA, R. G., GANNON, M. & LAYDEN, B. T. 2016. Loss of Free Fatty Acid Receptor 2 leads to impaired islet mass and beta cell survival. *Sci Rep,* 6**,** 28159.
VINES, C. M., REVANKAR, C. M., MAESTAS, D. C., LARUSCH, L. L., CIMINO, D. F., KOHOUT, T. A., LEFKOWITZ, R. J. & PROSSNITZ, E. R. 2003. N-formyl peptide receptors internalize but do not recycle in the absence of arrestins. *J Biol Chem,* 278**,** 41581-4.
VINOLO, M. A., RODRIGUES, H. G., NACHBAR, R. T. & CURI, R. 2011. Regulation of inflammation by short chain fatty acids. *Nutrients,* 3**,** 858-76.
VISTEIN, R. & PUTHENVEEDU, M. A. 2013. Reprogramming of G protein-coupled receptor recycling and signaling by a kinase switch. *Proc Natl Acad Sci U S A,* 110**,** 15289-94.
VIZCARRA, J. A., KIRBY, J. D., KIM, S. K. & GALYEAN, M. L. 2007. Active immunization against ghrelin decreases weight gain and alters plasma concentrations of growth hormone in growing pigs. *Domest Anim Endocrinol,* 33**,** 176-89.
VON ENGELHARDT, W., BARTELS, J., KIRSCHBERGER, S., ZU DUTTINGDORF, H. D. & BUSCHE, R. 1998. Role of short-chain fatty acids in the hind gut. *Vet Q,* 20**,** 52-59.
WAGENER, B. M., MARJON, N. A., REVANKAR, C. M. & PROSSNITZ, E. R. 2009. Adaptor protein-2 interaction with arrestin regulates GPCR recycling and apoptosis. *Traffic,* 10**,** 1286-300.
WANG, B., CHANDRASEKERA, P. C. & PIPPIN, J. J. 2014. Leptin- and leptin receptor-deficient rodent models: relevance for human type 2 diabetes. *Curr Diabetes Rev,* 10**,** 131-45.
WANG, C., LI, X., MU, K., LI, L., WANG, S., ZHU, Y., ZHANG, M., RYU, J., XIE, Z., SHI, D., ZHANG, W. J., DONG, L. Q. & JIA, W. 2013. Deficiency of APPL1 in mice impairs

glucose-stimulated insulin secretion through inhibition of pancreatic beta cell mitochondrial function. *Diabetologia,* 56**,** 1999-2009.
WANG, J., CARRILLO, J. J. & LIN, H. V. 2016. GPR142 Agonists Stimulate Glucose-Dependent Insulin Secretion via Gq-Dependent Signaling. *PLoS One,* 11**,** e0154452.
WANG, J., WU, X., SIMONAVICIUS, N., TIAN, H. & LING, L. 2006. Medium-chain fatty acids as ligands for orphan G protein-coupled receptor GPR84. *J Biol Chem,* 281**,** 34457-64.
WANG, Y., JIAO, X., KAYSER, F., LIU, J., WANG, Z., WANSKA, M., GREENBERG, J., WEISZMANN, J., GE, H., TIAN, H., WONG, S., SCHWANDNER, R., LEE, T. & LI, Y. 2010. The first synthetic agonists of FFA2: Discovery and SAR of phenylacetamides as allosteric modulators. *Bioorg Med Chem Lett,* 20**,** 493-8.
WEGNER, C. S., RODAHL, L. M. & STENMARK, H. 2011. ESCRT proteins and cell signalling. *Traffic,* 12**,** 1291-7.
WELCH, H. C., COADWELL, W. J., ELLSON, C. D., FERGUSON, G. J., ANDREWS, S. R., ERDJUMENT-BROMAGE, H., TEMPST, P., HAWKINS, P. T. & STEPHENS, L. R. 2002. P-Rex1, a PtdIns(3,4,5)P3- and Gbetagamma-regulated guanine-nucleotide exchange factor for Rac. *Cell,* 108**,** 809-21.
WELLS, C. A., ZURAWSKI, Z., BETKE, K. M., YIM, Y. Y., HYDE, K., RODRIGUEZ, S., ALFORD, S. & HAMM, H. E. 2012. Gβγ inhibits exocytosis via interaction with critical residues on soluble N-ethylmaleimide-sensitive factor attachment protein-25. *Molecular pharmacology,* 82**,** 1136-1149.
WERTHMANN, R. C., VOLPE, S., LOHSE, M. J. & CALEBIRO, D. 2012. Persistent cAMP signaling by internalized TSH receptors occurs in thyroid but not in HEK293 cells. *Faseb j,* 26**,** 2043-8.
WEST, C. & HANYALOGLU, A. C. 2015. Minireview: Spatial Programming of G Protein-Coupled Receptor Activity: Decoding Signaling in Health and Disease. *Mol Endocrinol,* 29**,** 1095-106.
WHEELER, S. E., STACEY, H. M., NAHAEI, Y., HALE, S. J., HARDY, A. B., REIMANN, F., GRIBBLE, F. M., LARRAUFIE, P., GAISANO, H. Y. & BRUBAKER, P. L. 2017. The SNARE Protein Syntaxin-1a Plays an Essential Role in Biphasic Exocytosis of the Incretin Hormone Glucagon-Like Peptide 1. *Diabetes,* 66**,** 2327-2338.
WHISTLER, J. L., ENQUIST, J., MARLEY, A., FONG, J., GLADHER, F., TSURUDA, P., MURRAY, S. R. & VON ZASTROW, M. 2002. Modulation of postendocytic sorting of G protein-coupled receptors. *Science,* 297**,** 615-20.
WHITNEY, E. N. & ROLFES, S. R. 1996. *Understanding nutrition,* St. Paul, MN, West Publishing.
WOLEVER, T. M., BRIGHENTI, F., ROYALL, D., JENKINS, A. L. & JENKINS, D. J. 1989. Effect of rectal infusion of short chain fatty acids in human subjects. *Am J Gastroenterol,* 84**,** 1027-33.
WOLFE, B. L., MARCHESE, A. & TREJO, J. 2007. Ubiquitination differentially regulates clathrin-dependent internalization of protease-activated receptor-1. *J Cell Biol,* 177**,** 905-16.
WOLLHEIM, C. B., ULLRICH, S., MEDA, P. & VALLAR, L. 1987. Regulation of exocytosis in electrically permeabilized insulin-secreting cells. Evidence for Ca2+ dependent and independent secretion. *Biosci Rep,* 7**,** 443-54.
WOOD, W. G., WACHTER, C. & SCRIBA, P. C. 1981. Experiences using chloramine-T and 1, 3, 4, 6-tetrachloro-3 alpha, 6 alpha-diphenylglycoluril (Iodogen) for radioiodination of materials for radioimmunoassay. *J Clin Chem Clin Biochem,* 19**,** 1051-6.

WOODMAN, P. G. 2000. Biogenesis of the sorting endosome: the role of Rab5. *Traffic,* 1**,** 695-701.
WOODS, S. C., SEELEY, R. J., BASKIN, D. G. & SCHWARTZ, M. W. 2003. Insulin and the blood-brain barrier. *Curr Pharm Des,* 9**,** 795-800.
WORLD HEALTH ORGANISATION. 2018. *Obesity and overweight* [Online]. Available: https://www.who.int/news-room/fact-sheets/detail/obesity-and-overweight [Accessed].
WYNNE, K., PARK, A. J., SMALL, C. J., MEERAN, K., GHATEI, M. A., FROST, G. S. & BLOOM, S. R. 2006. Oxyntomodulin increases energy expenditure in addition to decreasing energy intake in overweight and obese humans: a randomised controlled trial. *Int J Obes (Lond),* 30**,** 1729-36.
WYNNE, K., STANLEY, S., MCGOWAN, B. & BLOOM, S. 2005. Appetite control. *J Endocrinol,* 184**,** 291-318.
XIANG, Y. & KOBILKA, B. 2003. The PDZ-binding motif of the beta2-adrenoceptor is essential for physiologic signaling and trafficking in cardiac myocytes. *Proc Natl Acad Sci U S A,* 100**,** 10776-81.
XIN, X., ZHOU, L., REYES, C. M., LIU, F. & DONG, L. Q. 2011. APPL1 mediates adiponectin-stimulated p38 MAPK activation by scaffolding the TAK1-MKK3-p38 MAPK pathway. *Am J Physiol Endocrinol Metab,* 300**,** E103-10.
XIONG, Y., MIYAMOTO, N., SHIBATA, K., VALASEK, M. A., MOTOIKE, T., KEDZIERSKI, R. M. & YANAGISAWA, M. 2004. Short-chain fatty acids stimulate leptin production in adipocytes through the G protein-coupled receptor GPR41. *Proc Natl Acad Sci U S A,* 101**,** 1045-50.
YAMAUCHI, J., NAGAO, M., KAZIRO, Y. & ITOH, H. 1997. Activation of p38 mitogen-activated protein kinase by signaling through G protein-coupled receptors. Involvement of Gbetagamma and Galphaq/11 subunits. *J Biol Chem,* 272**,** 27771-7.
YANG, J., BROWN, M. S., LIANG, G., GRISHIN, N. V. & GOLDSTEIN, J. L. 2008. Identification of the acyltransferase that octanoylates ghrelin, an appetite-stimulating peptide hormone. *Cell,* 132**,** 387-96.
YANG, Z., LI, H., CHAI, Z., FULLERTON, M. J., CAO, Y., TOH, B. H., FUNDER, J. W. & LIU, J. P. 2001. Dynamin II regulates hormone secretion in neuroendocrine cells. *J Biol Chem,* 276**,** 4251-60.
YANG, Z., YANG, F., ZHANG, D., LIU, Z., LIN, A., LIU, C., XIAO, P., YU, X. & SUN, J. P. 2017. Phosphorylation of G Protein-Coupled Receptors: From the Barcode Hypothesis to the Flute Model. *Mol Pharmacol,* 92**,** 201-210.
YARWOOD, R. E., IMLACH, W. L., LIEU, T., VELDHUIS, N. A., JENSEN, D. D., KLEIN HERENBRINK, C., AURELIO, L., CAI, Z., CHRISTIE, M. J., POOLE, D. P., PORTER, C. J. H., MCLEAN, P., HICKS, G. A., GEPPETTI, P., HALLS, M. L., CANALS, M. & BUNNETT, N. W. 2017. Endosomal signaling of the receptor for calcitonin gene-related peptide mediates pain transmission. *Proc Natl Acad Sci U S A,* 114**,** 12309-12314.
YONEZAWA, T., KOBAYASHI, Y. & OBARA, Y. 2007. Short-chain fatty acids induce acute phosphorylation of the p38 mitogen-activated protein kinase/heat shock protein 27 pathway via GPR43 in the MCF-7 human breast cancer cell line. *Cell Signal,* 19**,** 185-93.
YU, Y. J., DHAVAN, R., CHEVALIER, M. W., YUDOWSKI, G. A. & VON ZASTROW, M. 2010. Rapid delivery of internalized signaling receptors to the somatodendritic surface by sequence-specific local insertion. *J Neurosci,* 30**,** 11703-14.

YUDOWSKI, G. A., PUTHENVEEDU, M. A., LEONOUDAKIS, D., PANICKER, S., THORN, K. S., BEATTIE, E. C. & VON ZASTROW, M. 2007. Real-time imaging of discrete exocytic events mediating surface delivery of AMPA receptors. *J Neurosci,* 27**,** 11112-21.

YUDOWSKI, G. A., PUTHENVEEDU, M. A. & VON ZASTROW, M. 2006. Distinct modes of regulated receptor insertion to the somatodendritic plasma membrane. *Nat Neurosci,* 9**,** 622-7.

ZAIBI, M. S., STOCKER, C. J., O'DOWD, J., DAVIES, A., BELLAHCENE, M., CAWTHORNE, M. A., BROWN, A. J., SMITH, D. M. & ARCH, J. R. 2010. Roles of GPR41 and GPR43 in leptin secretory responses of murine adipocytes to short chain fatty acids. *FEBS Lett,* 584**,** 2381-6.

ZERIAL, M. & MCBRIDE, H. 2001. Rab proteins as membrane organizers. *Nat Rev Mol Cell Biol,* 2**,** 107-17.

ZHANG, X., SUN, N., ZHENG, M. & KIM, K. M. 2016. Clathrin-mediated endocytosis is responsible for the lysosomal degradation of dopamine D3 receptor. *Biochem Biophys Res Commun,* 476**,** 245-251.

ZHANG, Y., SUN, B., FENG, D., HU, H., CHU, M., QU, Q., TARRASCH, J. T., LI, S., SUN KOBILKA, T., KOBILKA, B. K. & SKINIOTIS, G. 2017. Cryo-EM structure of the activated GLP-1 receptor in complex with a G protein. *Nature,* 546**,** 248.

ZHENG, H., LOH, H. H. & LAW, P. Y. 2013. Posttranslation modification of G protein-coupled receptor in relationship to biased agonism. *Methods Enzymol,* 522**,** 391-408.

ZIVKOVIC, A. M., TELIS, N., GERMAN, J. B. & HAMMOCK, B. D. 2011. Dietary omega-3 fatty acids aid in the modulation of inflammation and metabolic health. *Calif Agric (Berkeley),* 65**,** 106-111.

ZONCU, R., PERERA, R. M., BALKIN, D. M., PIRRUCCELLO, M., TOOMRE, D. & DE CAMILLI, P. 2009. A phosphoinositide switch controls the maturation and signaling properties of APPL endosomes. *Cell,* 136**,** 1110-1121.